Western University
Scholarship@Western

Digitized Theses | Digitized Special Collections

1988

The Vibration Of Beams And Plates Studied Using Orthogonal Polynomials

Chan-soo Kim

Follow this and additional works at: https://ir.lib.uwo.ca/digitizedtheses

Recommended Citation
Kim, Chan-soo, "The Vibration Of Beams And Plates Studied Using Orthogonal Polynomials" (1988). *Digitized Theses*. 1705.
https://ir.lib.uwo.ca/digitizedtheses/1705

This Dissertation is brought to you for free and open access by the Digitized Special Collections at Scholarship@Western. It has been accepted for inclusion in Digitized Theses by an authorized administrator of Scholarship@Western. For more information, please contact tadam@uwo.ca, wlswadmin@uwo.ca.

National Library of Canada
Bibliothèque nationale du Canada

Canadian Theses Service
Service des thèses canadiennes

Ottawa, Canada
K1A 0N4

NOTICE

The quality of this microform is heavily dependent upon the quality of the original thesis submitted for microfilming. Every effort has been made to ensure the highest quality of reproduction possible.

If pages are missing, contact the university which granted the degree.

Some pages may have indistinct print especially if the original pages were typed with a poor typewriter ribbon or if the university sent us an inferior photocopy.

Previously copyrighted materials (journal articles, published tests, etc.) are not filmed.

Reproduction in full or in part of this microform is governed by the Canadian Copyright Act, R.S.C. 1970, c. C-30.

AVIS

La qualité de cette microforme dépend grandement de la qualité de la thèse soumise au microfilmage. Nous avons tout fait pour assurer une qualité supérieure de reproduction.

S'il manque des pages, veuillez communiquer avec l'université qui a conféré le grade.

La qualité d'impression de certaines pages peut laisser à désirer, surtout si les pages originales ont été dactylographiées à l'aide d'un ruban usé ou si l'université nous a fait parvenir une photocopie de qualité inférieure.

Les documents qui font déjà l'objet d'un droit d'auteur (articles de revue, tests publiés, etc.) ne sont pas microfilmés.

La reproduction, même partielle, de cette microforme est soumise à la Loi canadienne sur le droit d'auteur, SRC 1970, c. C-30.

NL-339 (r. 88/04)

Canada

THE VIBRATION OF BEAMS AND PLATES STUDIED USING ORTHOGONAL POLYNOMIALS

by

Chan-Soo Kim

Department of Mechanical Engineering

Submitted in partial fulfillment
of the requirements for the degree of
Doctor of Philosophy

Faculty of Graduate Studies
The University of Western Ontario
London, Ontario
April, 1988

© Chan-Soo Kim 1988

Permission has been granted to the National Library of Canada to microfilm this thesis and to lend or sell copies of the film.

The author (copyright owner) has reserved other publication rights, and neither the thesis nor extensive extracts from it may be printed or otherwise reproduced without his/her written permission.

L'autorisation a été accordée à la Bibliothèque nationale du Canada de microfilmer cette thèse et de prêter ou de vendre des exemplaires du film.

L'auteur (titulaire du droit d'auteur) se réserve les autres droits de publication; ni la thèse ni de longs extraits de celle-ci ne doivent être imprimés ou autrement reproduits sans son autorisation écrite.

ISBN 0-315-40782-4

ABSTRACT

The orthogonally generated polynomials proposed by R.B. Bhat as admissible functions for use in the Rayleigh-Ritz method for dynamic and static problems of single-span beams and rectangular plates are generalized for use in the study of various more complicated beam and plate problems. The orthogonal polynomials themselves are discussed in some detail. These functions are then used in the Rayleigh-Ritz method to obtain solutions for the free vibration problems of slender beams, thin rectangular plates, a box-like structure, and thin annular, circular and sectorial plates. Various complicating effects are included.

The approach presented in this thesis is straightforward but more general than the approaches presented previously in the literature. The accuracy and versatility of the approach are demonstrated using various example problems. Numerical results are generated both for new problems and for problems for which comparison results are available in the literature.

For the vibration problem of slender beams, the analysis is presented for beams subject to complicating factors which include the existence of an arbitrary number of concentrated masses (with or without rotary inertia) and/or intermediate simple supports, and subject to any combination of free, simply supported or clamped boundary conditions and/or elastic supports. The effects of constant axial loading

(either constant directional or tangential follower force) and variable cross section are also included.

For thin rectangular plates, the analysis is presented for rectangularly orthotropic plates (which include the isotropic case) with any number of intermediate line supports and point supports. (The Lagrangian multiplier method is used for point supported plates.) The analysis is further extended to one type of box-like structure.

The analysis of annular plates includes the effects of polar orthotropy, intermediate concentric ring supports and radially varying thickness. By permitting the inner radius to become very small, circular plates are also treated, including the case with a central point support.

Finally, annular and circular sectorial plates are treated. Again the analysis includes several complicating effects such as polar orthotropy, intermediate simple supports in both radial and circumferential directions and varying thickness in both directions.

ACKNOWLEDGEMENTS

It is the pleasure of the author to express sincere gratitude to his supervisor, Professor S.M. Dickinson, whose invaluable guidance and encouragement have greatly contributed to the completion of this work. He has also painstakingly corrected and refined the manuscript of this thesis.

The author is deeply grateful to his wife Hong-Im for her consistent confidence and patience throughout the years. Thanks are also extended to his daughter Shinae and his son Jisung, whose love have been priceless.

The author wishes to thank all his friends in London, Ontario for their friendships he is indebted. Thanks are also due to Mrs. Linda McGugan and Ms. Joanne Lemon for their meticulous typing.

TABLE OF CONTENTS

	PAGE
CERTIFICATE OF EXAMINATION	ii
ABSTRACT	iii
ACKNOWLEDGEMENTS	v
TABLE OF CONTENTS	vi
NOMENCLATURE	viii
CHAPTER 1. INTRODUCTION	1
1.1. INTRODUCTORY REMARKS	1
1.2. BEAM VIBRATION PROBLEMS	4
1.3. CONTINUOUS AND POINT SUPPORTED RECTANGULAR PLATE VIBRATION PROBLEMS	7
1.4. ANNULAR AND CIRCULAR PLATE VIBRATION PROBLEMS	13
1.5. SECTORIAL PLATE VIBRATION PROBLEMS	17
CHAPTER 2. ORTHOGONAL POLYNOMIALS	22
2.1. ORTHOGONAL FUNCTIONS	22
2.1.1. Definition of Orthogonality	22
2.1.2. Generation of Orthogonal Functions	23
2.2. ORTHOGONAL POLYNOMIALS	27
2.2.1. Generation of Orthogonal Polynomials	27
2.2.2. Characteristics of Orthogonal Polynomials	36
2.2.3. Beam Characteristic Orthogonal Polynomials	42
CHAPTER 3. VIBRATION OF BEAMS	55
3.1. INTRODUCTORY REMARKS	55
3.2. ANALYSIS	55
3.3. BEAMS WITH NO ELASTIC SPRING	66
3.3.1. Beams of Uniform Cross Section	66
3.3.2. Beams of Non-uniform Cross Section	92

TABLE OF CONTENTS (continued)

	PAGE
3.4. ELASTICALLY RESTRAINED BEAMS	101
3.4.1. Beams of Uniform Cross Section	101
3.4.2. Beams of Non-uniform Cross Section	115
CHAPTER 4. VIBRATION OF RECTANGULAR PLATES	123
4.1. INTRODUCTORY REMARKS	123
4.2. ANALYSIS	127
4.3. PLANE CONTINUOUS PLATES	133
4.4. A BOX-LIKE STRUCTURE	144
4.5. POINT SUPPORTED PLATES	155
CHAPTER 5. VIBRATION OF ANNULAR AND CIRCULAR PLATES	172
5.1. INTRODUCTORY REMARKS	172
5.2. ANALYSIS	173
5.3. ANNULAR PLATES	179
5.3.1. Annular Plates of Uniform Thickness	180
5.3.2. Annular Plates of Variable Thickness	193
5.4. CIRCULAR PLATES	197
CHAPTER 6. VIBRATION OF SECTORIAL PLATES	204
6.1. INTRODUCTORY REMARKS	204
6.2. ANALYSIS	205
6.3. UNIFORM, ISOTROPIC, SINGLE PLATES	214
6.4. PLATES WITH COMPLICATING FACTORS	218
CHAPTER 7. CONCLUDING REMARKS	229
REFERENCES	231
APPENDIX A. VALUES FOR AN ELASTICALLY RESTRAINED BEAM	249
APPENDIX B. EQUATIONS FOR POLAR ORTHOTROPIC PLATES	258
VITA	268

NOMENCLATURE

The following is a list of the main symbols used in this thesis. Other symbols are defined in context.

English Symbols

a	a constant, a side length of rectangular plates in x-direction, or outer radius of annular, circular or sectorial plates
b	a constant, a side length of rectangular plates in y-direction, or inner radius of annular or annular sectorial plates
B_n, C_n	constants in the recurrence formula for orthogonal polynomials
D	flexural rigidity for isotropic plate, $D=Eh^3/12(1-\nu^2)$
D_x	flexural rigidity in x-direction, $D_x=E_xh^3/12(1-\nu_{xy}\nu_{yx})$
D_y	flexural rigidity in y-direction, $D_y=E_yh^3/12(1-\nu_{xy}\nu_{yx})$
D_{xy}	twisting rigidity in Cartesian coordinates, $D_{xy}=G_{xy}h^3/12$

D_r	flexural rigidity in radial direction, $D_r=E_r h^3/12(1-\nu_{r\theta}\nu_{\theta r})$
D_θ	flexural rigidity in circumferential direction, $D_\theta=E_\theta h^3/12(1-\nu_{r\theta}\nu_{\theta r})$
$D_{r\theta}$	twisting rigidity in polar coordinates, $D_{r\theta}=G_{r\theta}h^3/12$
E	Young's modulus
EI	flexural rigidity of a beam
EI_0	flexural rigidity of a beam at $x=0$
E_x, E_y	Young's moduli in x- and y-directions, respectively
E_r, E_θ	Young's moduli in r- and θ-directions, respectively
g, g(x), ...	generating functions for orthogonal polynomials
G_{xy}	shear modulus in Cartesian coordinates
$G_{r\theta}$	shear modulus in polar coordinates
h, h(x,y),...	thickness of plates
J_i	rotary inertia of the i'th concentrated mass

$\bar{J}_i$	non-dimensionalized parameter for J_i, $\bar{J}_i = J_i / m_0 \ell^3$
k_t	t'th translational spring coefficients
K_t	non-dimensionalized parameter for k_t, $K_t = k_t \ell^3 / EI$
ℓ	length of a beam
ℓ_j	location of intermediate supports of a beam
m	mass per unit length
m_0	mass per unit length at $x=0$
M_i	i'th concentrated mass
p	non-dimensionalized parameter for P, $p = P\ell^2 / EI_0$
P	axial load of beam
r	radial directional coordinate (polar coordinates)
s_r	r'th rotational spring constants
S_r	non-dimensionalized parameter for s_r, $S_r = s_r \ell / EI$
T_{max}	maximum kinetic energy

U_{max}	maximum strain energy stored in springs
V_{max}	maximum strain energy
w, $w(x,y)$,...	maximum deflection with respect to time τ
w_f, $w_f(x)$,...	weight function
x, y	Cartesian coordinates
z	a coordinate normal to x-y (cartesian coordinates) or r-θ (polar coordinates) plane

Greek Symbols

δ_{mn}	Kronecker's delta; $\delta_{mn}=1$ for $m=n$, $\delta_{mn}=0$ for $m\neq n$
ξ, η	non-dimensionalized coordinates
θ	angular coordinate
ν	Poisson's ratio for isotropic plate
ν_{xy}, ν_{yx}	Poisson's ratios in Cartesian coordinates
$\nu_{r\theta}$, $\nu_{\theta r}$	Poisson's ratios in polar coordinates
ρ	material density
τ	time

$\Phi_i(\xi)$, $\Psi_j(\eta)$	functions; used as the admissible functions in vibration problems
ω	radian natural frequency
Ω	non-dimensionalized frequency parameter

The author of this thesis has granted The University of Western Ontario a non-exclusive license to reproduce and distribute copies of this thesis to users of Western Libraries. Copyright remains with the author.

Electronic theses and dissertations available in The University of Western Ontario's institutional repository (Scholarship@Western) are solely for the purpose of private study and research. They may not be copied or reproduced, except as permitted by copyright laws, without written authority of the copyright owner. Any commercial use or publication is strictly prohibited.

The original copyright license attesting to these terms and signed by the author of this thesis may be found in the original print version of the thesis, held by Western Libraries.

The thesis approval page signed by the examining committee may also be found in the original print version of the thesis held in Western Libraries.

Please contact Western Libraries for further information:
E-mail: libadmin@uwo.ca
Telephone: (519) 661-2111 Ext. 84796
Web site: http://www.lib.uwo.ca/

CHAPTER 1

INTRODUCTION

1.1 INTRODUCTORY REMARKS

Various approaches have been used to solve the problem of the transverse vibration of slender, straight beams or thin, flat plates. In particular, for uniform, single span beams with any combination of free, simply supported, clamped or sliding boundary conditions, exact solutions to the governing equation of motion can be easily obtained [1-3], and natural frequency parameters and corresponding normal modes of free vibration, which are called '(vibration) characteristic beam functions', have been widely tabulated [1, 2, 4-6]. Also, the formulae for integrals containing characteristic beam functions have been given [6-8] and have proven to be very useful in the analysis of dynamic systems whose modes can be described in terms of the mode shapes of uniform, single span beams. The exact solutions can also be obtained for certain other beam and plate problems. However, the approach for the exact solution is limited to some special cases, particularly for plate problems, and is not possible to be used for general problems. Hence, most of the approaches for the solution of vibration problems are approximate in nature.

Among the various approximate methods presented, the

most widely used method for the vibration (and buckling, equilibrium, etc.) problem is, to the author's knowledge, the Rayleigh method [9] or the Rayleigh-Ritz method [10] (Often, this method is called simply 'Ritz's method' or 'the Ritz method'. However, in this thesis, the term 'the Rayleigh-Ritz method' is used). The well known Rayleigh or Rayleigh-Ritz method is relatively simple but usually gives satisfactory results for numerous problems (for example, see references [11-17]). Both methods require the use of the energy expressions (i.e. strain or elastic energy and kinetic energy) for the system to be solved and the assumption of admissible function(s) which satisfy at least the geometrical boundary conditions (i.e. zero displacement and/or zero slope).

The rate of convergence and accuracy of the Rayleigh-Ritz method depend upon the choice of the admissible functions for use in the series representing the deflection of the system. Probably, the most popular admissible functions used for vibration problems of single rectangular plates (and certain other plates) with any combination of classical boundary conditions (In this thesis, the 'classical boundary condition' means free, simply supported or clamped boundary condition, as is common in the vibration community.) were the products of the characteristic beam functions (for example, see references [15-17]). These functions have very attractive features such as the orthogonality of the

functions, the simplicity of the formulae for necessary integration [6-8], etc.. The use of the characteristic beam functions yields very good results for plates with no free edge, but the results obtained for plates involving one or more free edges are less satisfactory due to the occurrence of over-restraint at free edges. (This will be discussed further in Chapter 4). In order to increase the accuracy of the results, particulary for plates with free edges, various other sets of functions have been used. These include the degenerated beam functions [18, 19], the functions obtained from the modified Bolotin method [20, 21], simply supported plate functions [22-24], and beam characteristic orthogonal polynomials [25-29] and so on. Among these sets of functions, the best set of functions is the beam characteristic orthogonal polynomials; the functions have some advantageous features such as the relative ease of generation and integration, the orthogonality (as in the case of characteristic beam functions and simply supported plate functions), and the excellence of the results, not only for plates with no free edge but also for plates with free edges.

In this thesis, the beam characteristic orthogonal polynomials, suggested by Bhat [25-27, 30] for dynamic and static problems of single span beams or plates, are generalized to be used as the admissible functions in the Rayleigh-Ritz method for various beam and plate problems including several complicating effects. The orthogonal

polynomials are discussed in some detail in Chapter 2, where the generation procedure is given, together with the identification of some important characteristics, and the method of construction of the starting function, etc.. Then, using the polynomials, various vibration problems of beams (Chapter 3), rectangular plates (Chapter 4), annular and circular plates (Chapter 5) and sectorial plates (Chapter 6) are studied.

In the following sections in this chapter, the general scope of the beam and plate problems treated in this thesis are discussed, together with the related work presented in the literature. It may be noted that, though numerous selected references are cited in the following, there still remains a fair amount of related work in the body of the literature. For more related studies, references are made to the excellent review works by Blevins [6] for both beam and plate problems, and by Leissa [31-33] for plate problems.

1.2. BEAM VIBRATION PROBLEMS

The problem of the transverse vibration of straight, slender beams has received substantial attention from researchers, particularly over the past two decades or so. Numerous studies have been conducted in which various complicating factors have been considered, including the existence of concentrated masses with or without rotary inertia of the masses, translational and/or rotational

springs, axial loading, intermediate supports (that is, multi-span beams) and non-uniformity of cross section. There appears, however, to have been no study in which a single approach has been put forward for the treatment of slender beams subject to any or all combinations of these effects and having any combination of the classical boundary conditions and/or elastic supports. Rather, mainly individual beam problems have been considered, either including one or more complicating factor(s) for a particular beam or a single complicating factor for a number of different beams.

The problem of beams with no elastic spring has been treated by a number of investigators. Various methods of solution have been presented for uniform multi-span beams without other complicating effects [38-41] or including the effect of axial load [42-44]. In particular, Gorman [41] presented an exact solution to the governing differential equation from which he generated copious graphical and tabular results for beams for which the solution is applicable. Laura et al. [45] treated a two-span beam with concentrated masses at the mid-point of each span and included the effect of axial load; only the fundamental mode was considered, however. Single-span beams with one concentrated mass (particularly tip loaded cantilevers) have received considerable attention [46-61], the effects of axial load and/or non-uniform cross section being included in some instances. Somewhat fewer researchers have dealt with the

problem of beams with more than one concentrated mass attached [45, 62-65].

Numerous researchers have tackled the vibration problem of beams of non-uniform cross section [51, 60, 66-75] but their attention appears to have been confined to single span beams.

Various uniform beams with elastically restrained ends have been considered by Maltbaek [56] and Gorman [41], who presented exact solutions for single and double span beams and generated copious graphical or tabular results, the effect of a concentrated mass being included in some instances. Several other constrained uniform beams have also been studied, including a translationally restrained cantilever beam with or without a tip mass [46, 55, 64, 76-78], a beam with one end spring-hinged and with or without a mass at the other free end [62, 63, 79-81], a beam with one end spring-hinged and subject to a translational restraint at the other end [82] and so on; each reference includes valuable results obtained. The effect of an intermediate simple support has been considered for the beam with one end spring-hinged and the other end free [83], and with both ends spring-hinged and subject to an axial force and with concentrated masses [45, 84]. In a more general sense, beams with any number of elastic supports and concentrated masses have been studied by Bapat and Bapat [85].

The effect of non-uniformity of cross section, together with that of an axial force, has been considered by Laura and his colleagues [51, 53, 60, 83, 86]. Non-uniform beams, subject to elastic restraints, have been studied also by Goel [87].

In Chapter 3, a simple, unified approach is proposed for the treatment of the vibration problem of non-uniform, continuous, slender beams having an arbitrary number of concentrated masses (with or without rotary inertia) and any combination of classical boundary conditions and/or elastic supports. The effect of constant axial loading, either constant directional force or tangential follower force, is included. The Rayleigh-Ritz method is used for the analysis, with the orthogonally generated polynomials as the admissible functions. Numerical results are presented for particular beam problems, for which comparison values are available in the literature, serving to illustrate the applicability and accuracy of the approach. A selection of results for problems hitherto untreated in the literature is also given.

1.3. CONTINUOUS AND POINT SUPPORTED RECTANGULAR PLATE VIBRATION PROBLEMS.

For single rectangular plates, Bhat [25-27] showed that the use of the orthogonal polynomials as the admissible functions in the Rayleigh-Ritz method yields excellent results for the natural frequencies of several example plates

having various combinations of edge conditions. The applicability of his approach for the determination of nodal patterns is also illustrated by Kaushal and Bhat [28]. The excellence of the functions is further examined by Dickinson and Di Blasio [29] who conducted a convergence study and introduced the effect of special orthotropy and in-plane loading, generating results for critical buckling load, natural frequencies, mode shapes and associated bending moment and shear force distributions. In the present work, the author's generalized orthogonal polynomials are used to study the vibration problem of continuous plates, including one type of box structure, and plates with point supports.

The vibration of continuous plates has been studied by a number of researchers, some treating the intermediate supports as rigid with respect to lateral translation and offering no rotational restraint (referred to in this thesis as line supports) and others including the effects of translational and rotational rigidity and inertia of the supports (often referred to as stringers). Rather less attention has been given to the vibration of box structures.

Much of the work reported in the literature has been concerned with plates continuous only in one direction. Veletsos and Newmark [88] used the Holzer method for the determination of the natural frequencies of plates simply supported along the continuous edges (that is, the edges

perpendicular to the intermediate supports) and presented calculations for two four-span plates. A two-span, simply supported plate was analyzed by Ungar [89] and a semi-graphical approach presented. The Bolotin edge effect method [90] was used by Bolotin [91] and by Moskalenko and Chen [92] for multi-span plates, the method permitting the treatment of clamped, continuous edges. Dickinson and Warburton [93] also used the edge effect method for the study of two-span plates, among other systems, and obtained natural frequencies for such plates involving clamped, simply supported and free edges. More recently, the modified Bolotin method, developed independently by Vijayakumar [94] and Elishakoff [95], was used by Elishakoff and Sternberg [96] to determine the natural frequencies of plates with an arbitrary number of equal spans; numerical values were given for fully clamped two- and six-span plates and for two-span plates having clamped continuous edges with the ends simply supported. The receptance method, perhaps more popular for beam vibration work, was used by Azimi, Hamilton and Soedel [97] for plates simply supported on the ends and results were presented for three- and four-span plates.

The problem of the vibration of line supported plates which are continuous in two directions has received rather less attention. However, Dill and Pister [98] presented a powerful and elegant series solution which is applicable not only to plates continuous in one or two directions but also

to L-shaped configurations, as demonstrated in reference [98], or virtually any configuration which may be built up from rectangular plates. Two such configurations are the five- and six-sided box structures, which were analyzed using this approach by Dickinson and Warburton [99]. The series solution was subsequently extended by Dickinson to apply to specially orthotropic plates and plate systems [100] and to include the effect of uniform in-plane loads [101], although no numerical results were given for plate systems. The application of Bolotin's method to two-way continuous plates and to box-like structures is also discussed in reference [93], numerical results being given for the latter. Takahashi and Chishaki [102] presented a sine series solution for the vibration of simply supported plates continuous over a number of supports in two directions and provided numerical results for a plate having two spans in each direction.

The vibration of point supported rectangular plates has also received considerable attention from researchers, much of the interest likely stemming from the potential application of the analyses to practical problems including the vibration of column supported slabs, printed circuit boards and panels in ships and aircraft, and the selection of optimum hold-down point positions of solar panels. A survey of the literature, however, reveals that the majority of the work concerns plates having particular support conditions, the only general study of which the author is aware being

that by Fan and Cheung [103], who used a spline finite strip approach to treat plates having various combinations of conventional boundary conditions and various numbers of arbitrarily located point supports.

The most widely studied point supported plate problem is that of otherwise fully free plates. Such plates have been considered with four corner point supports [104, 105], with supports at the mid-points of all four edges [106, 107], with multiple point supports along the edges [108, 109], with supports symmetrically located at four points on the diagonals [110-116], with supports more generally symmetrically located [117] and with arbitrary numbers and locations of point supports [118-120].

The problem of plates having one or more edges conventionally supported (simply supported or clamped) and having point supports elsewhere has received less attention. Included in those studies which have dealt with such problems are the cases of a plate having two adjacent edges simply supported and/or clamped, the other two free, with a point support at the otherwise free corner [121-125], a plate with all edges either simply supported or all clamped, with a point support at the centre [107, 114, 125, 126], a fully simply supported plate with a point support on one centreline [127] and cantilever plates with point supports symmetrically distributed along the free edges [128] or at arbitrary

locations within the plate or on its edges [129].

In Chapter 4, a general approach is presented for the solution of the free vibration problem for rectangular isotropic or specially orthotropic plates (that is, plates for which the principal axes of orthotropy are parallel to the edges) and plate systems continuous over line supports lying parallel to the plate edges, having any combination of conventional edge supports, and permitting the treatment of such plates subject to arbitrarily located point supports. Clearly, the finite element and finite strip methods are applicable to the types of problems discussed, as they are to most problems amenable to classical solutions. However, the author believes that there is value in providing what are often simpler, more efficient and/or more accurate solutions to those problems for which such solutions exist. The Rayleigh-Ritz method is employed, in conjunction with Lagrangian multipliers when point supports are included. For plates with no point supports, the formulation of the Rayleigh-Ritz method using the orthogonally generated polynomials as admissible functions is as straightforward for continuous plate problems as it is for the single-span plate problem and yields results of comparable accuracy with little or no more computational difficulty.

Numerical results are presented for a number of different plate problems, including point supported plates

and a particular four-span plate system which forms a cantilevered box. In several instances, comparisons are made with values available in the literature and in all the cases close agreement may be seen to be achieved.

1.4. ANNULAR AND CIRCULAR PLATE VIBRATION PROBLEMS

Annular and circular plates subject to various complicating factors are frequently used in engineering applications where dynamic excitation may be encountered, thus it is important that their vibrational characteristics be known. As a consequence, the lateral vibration of such plates has been the subject of numerous studies [31-37].

For isotropic, circular plates of uniform thickness and subject to the classical boundary conditions of clamped, free or simple support, exact solutions in terms of Bessel functions exist, from which numerical natural frequency parameters and, in some cases, nodal patterns have been determined by several investigators. Among these investigators are Carrington [130], who studied clamped plates, Itao and Crandall [131], who tabulated natural frequency parameters and mode shapes for free plates, and Leissa and Narita [132], who presented natural frequency parameters for simply supported plates. In the case of polar orthotropic circular plates, no closed form, exact solution exists, even when subject to the classical boundary conditions and no other complicating factor, and various

approximate approaches are presented in references [133-140].

For continuous circular plates, Bodine [141, 142] presented an exact solution for the isotropic circular plate continuous over a single rigid ring support, and Singh and Mirza [143] obtained an exact solution for the axisymmetrical vibration of an isotropic plate, elastically supported on two concentric rings. Continuous circular plates were also treated by Laura et al. [144] and Kunukkasseril and Swamidas [145]. The effect of radially varying thickness on the behaviour of isotropic circular plates is studied for the fundamental frequency parameters by Laura and his colleagues [146-149] using the Rayleigh-Ritz method with several terms of simple polynomials, the effect of polar orthotropy being included in some instances.

For isotropic annular plates with various combinations of the classical boundary conditions, Vogel and Skinner [150] obtained exact solutions, from which they generated copious results, both in tabular and graphical forms, for the natural frequency parameters for a wide range of inside to outside radii ratios. In the case of polar orthotropic annular plates, various different methods of analysis have been presented, including those by Vijayakumar and Ramaiah [151, 152] and Narita [153], who used the Rayleigh-Ritz method, Lizarev et al. [154], who used a series solution to the differential equation, Greenberg and Stavsky [155] (both

for annular and circular plates), who used a finite difference method, and Ginesu et al. [156] and Gorman [157], who used the finite element method, copious numerical results being presented in reference [157]. By permitting the inner radius of the annular plate to become very small, Narita [153] presented results for the circular plate as well.

For annular plates continuous over concentric ring supports, rather fewer studies have been reported in the literature. Kunakkasseril and Swamidas [145] developed a series solution for polar orthotropic annular (and circular) plates, elastically or rigidly supported on concentric circles, but numerical examples were presented for the isotropic case only. Narita [158] used the Rayleigh-Ritz method in conjunction with the Lagrangian multipliers (Lagrangian multiplier method) to obtain a frequency equation for polar orthotropic, annular plates continuous over rigid ring supports and presented numerical results for plates of various degrees of orthotropy. Again, by letting the inner radius become very small, results for the circular plate were also generated.

Annular plates having thickness which varies with radius have been treated by several researchers. The axisymmetrical vibration of isotropic plates with linearly varying thickness has been studied by Raju et al. [159], who used the finite element method, and Soni and Amba-Rao [160], who used the

Chebyshev collocation method. The latter work is extended by Gupta and Lal [161], to include the effect of an in-plane force, and by Lal and Gupta [162], to include polar orthotropy. The axisymmetrical vibration of such plates was further considered by Sankaranarayanan et al. [163], using the Rayleigh-Ritz technique, and by Gupta et al. [164], using a spline technique to solve the governing differential equation. The natural frequency parameters for both the axisymmetrical and non-axisymmetrical modes of polar orthotropic, annular plates of linearly varying thickness was obtained by Gorman [165], who used the finite element method. Exact, closed form solutions have been presented by Conway et al. [166] for linearly tapered isotropic plates with Poisson's ratio 1/3, and by Lenox and Conway [167] for isotropic and polar orthotropic plates having parabolic thickness variation.

In Chapter 5, a straightforward, unified approach is given for the solution of the free, lateral vibration problem of thin annular plates which may be of isotropic or polar orthotropic material, may have radially varying thickness and may be continuous over one or more rigid concentric ring supports and subject to the classical boundary conditions. Again, with the orthogonally generated polynomials as the admissible functions, the Rayleigh-Ritz method is used to obtain a frequency equation. From the frequency equation, numerical results are obtained for a number of particular plates, with comparisons being made with values available in

the literature in several cases. By permitting the inner radius to become very small and assuming the inner periphery free, as discussed by Narita [153, 158], solid circular plates are also treated. In addition, plates simply supported or clamped at the centre, which were partly treated in references [168-170], are discussed.

1.5. SECTORIAL PLATE VIBRATION PROBLEMS

The problem of the transverse vibration of circular and annular sectorial plates has received considerable attention in recent years, though far fewer studies have been reported compared with those for beams, rectangular plates, circular plates or annular plates. The study of the problem is of practical importance for a better understanding of the behaviour of sectorial plate components; the components whose geometry are sectorial have been widely used in ships, curved bridge decks and panels, and aeronautical and space structures. Sectorial plates have two straight radial boundaries, and one circumferential (circular) boundary, for circular sectorial plates, or two circumferential boundaries, for annular sectorial plates. In order to avoid the confusion of radial and circumferential boundaries, in this thesis, the term 'edge' is used for a straight, radial edge and the term 'periphery' for a circumferential periphery (circular arc).

For uniform, isotropic plates with both edges simply supported, exact solutions are obtainable regardless of the boundary conditions (provided that they are homogeneous) at the peripheries, as mentioned by Leissa [31, 36]. The frequency determinants, which involve Bessel functions, are of the second order for circular sectorial plates and are of the fourth order for annular sectorial plates. The order of the Bessel functions are, in general, non-integer. In spite of the relative simplicity of the solutions, the results presented in the literature are scanty, and are only those for which the orders of the Bessel functions are integers and which correspond to the higher modes of circular or annular plates. Westmann [171] presented the exact solution for a circular sectorial plate with a free periphery. For annular sectorial plates, Ramakrishnan and Kunukkasseril [172] and Wilson and Garg [173] presented the solution for the case of free peripheries. Ramakrishnan and Kunukkasseril [174] also presented results for plates with both peripheries simply supported or clamped as special cases in their study of stiffened sectorial plates. Plates with both radial edges simply supported have also been treated by using the Rayleigh-Ritz method by Westmann [171] and Ramaiah and Vijayakumar [175], who used simple polynomials as the admissible functions.

Ben-Amoz [176] used an energy method to analyze uniform, isotropic, circular sectorial plates with fully clamped

boundaries. His approach was later extended by Rubin [177] to analyze both circular and annular sectorial plates with clamped edges, subject to other boundary conditions at the peripheries. The plates with clamped edges were also treated by Westmann [171], who used the Rayleigh-Ritz method, by Bhattacharya and Bhowmic [178], who used the Kantorovich method, and by Cheung and Cheung [179], who used the finite strip method. (The finite strip method is applicable to polar orthotropic plates with other boundary conditions as well.) A clamped semicircular plate is a special case of circular segment plates and was treated by Khurasia and Rawtani [180], using a finite element method. Experimentally, Waller [181] observed the lowest two mode shapes (non-rigid body) of a fully free semicircular plate, and Maruyama and Ichinomiya [182] obtained frequencies and mode shapes of fully clamped sectorial plates (both circular and annular). Swaminadham et al. [183] treated plates with inner periphery clamped and the other boundaries free by using the finite element method; the analytical results were verified by an experiment.

Polar orthotropic sectorial plates have been treated by several investigators. The plates with both edges simply supported were treated by Rubin [184], who presented a series solution (Frobenius' method), and by Ramaiah [185], who used the Rayleigh-Ritz method with simple polynomials as the admissible functions. The Rayleigh-Ritz method was also used

for the solution of polar orthotropic plates with any combination of the classical boundary conditions by Irie et al. [186], who used spline functions as the admissible functions. Mukhopadhyay [187] presented a semi-analytic solution (the resulting equation is solved by a finite difference technique) for annular sectorial plates, and Srinivasan and Thiruvenkatachari [188] used an integral equation technique for fully clamped, annular sectorial plates.

Other vibration problems of sectorial plates treated in the literature are those for isotropic annular sectorial plates with rotationally restrained boundaries [189], for laminated annular sectorial plates [190] and for polar orthotropic, sectorial plates resting on point supports [191]. To the author's knowledge, no treatment is given for plates with variable thickness and/or continuous over intermediate supports, though the semi-analytic approach in reference [187] was mentioned to be applicable to plates of variable thickness.

In Chapter 6, a simple approach is proposed for the treatment of the vibration problem of polar orthotropic, sectorial plates which may be continuous over intermediate supports and/or of variable thickness. The classical boundary conditions only are treated. Again, the Rayleigh-Ritz method is used for the analysis, with the orthogonally

generated polynomials as the admissible functions. Results are given for various example plates. In several instances, comparisons are made with results available in the literature, to illustrate the accuracy and convergence of the approach.

CHAPTER 2

ORTHOGONAL POLYNOMIALS

2.1. ORTHOGONAL FUNCTIONS

2.1.1. Definition of Orthogonality [192-194]

Consider a function $w_f(x)$ which is non-negative and integrable on an interval $a \leq x \leq b$ (the interval is denoted by $a \leq x \leq b$ or $[a, b]$). It is also assumed that

$$w_f(x) > 0 \text{ on } a < x < b \tag{2.1a}$$

so that

$$\int_a^b w_f(x)dx > 0. \tag{2.1b}$$

This is the requirement for the weight function for orthogonal functions.

Two functions $\Phi_m(x)$ and $\Phi_n(x)$ are called 'orthogonal' on the interval $a \leq x \leq b$, with respect to the weight function (or weighting function) $w_f(x)$, if

$$\int_a^b w_f(x)\Phi_m(x)\Phi_n(x)dx = 0. \tag{2.2}$$

When each member of a set of functions $\Phi_k(x)$ is orthogonal to every other member of the set, the set of functions is

called 'an orthogonal set of functions', 'an orthogonal series of functions', 'an orthogonal function sequence' or, loosely, 'orthogonal functions' when there is no danger of ambiguity. The orthogonal set of functions may be expressed as

$$\int_a^b w_f(x)\Phi_m(x)\Phi_n(x)dx = c_m\delta_{mn};\ m,\ n = 1,2,3,\ldots, \quad (2.3)$$

where c_m is a constant and δ_{mn}, called 'the Kronecker delta' or 'Kronecker's delta', is defined as 0 if $m \neq n$ and 1 if $m = n$. In equation (2.3), an additional condition

$$\int_a^b w_f(x)\Phi_m^2 dx \neq 0$$

is included, and this condition is automatically satisfied if the weight function is defined by equation (2.1).

In addition, if a set of orthogonal functions $\Phi_k(x)$ has the property

$$\int_a^b w_f(x)\Phi_m(x)\Phi_n(x)dx = \delta_{mn};\ m,n = 1,\ 2,\ 3,\ \ldots, \quad (2.4)$$

the set of functions is called an 'orthonormal' set of functions.

2.1.2. Generation of Orthogonal Functions

If a function $\Phi_1(x)$ is given, say $\Phi_1(x) = f_1(x)$, a series of orthogonal functions $\Phi_k(x)$, starting from $\Phi_1(x)$,

on the given interval $a \leq x \leq b$ with respect to the given weight function $w_f(x)$ can be generated step by step as follows:

Let $\Phi_2(x) = a_1 f_1(x) + a_2 f_2(x)$.

Then applying the orthogonality defined in equation (2.2) yields

$$a_1 \int_a^b w_f(x) f_1^2(x) dx + a_2 \int_a^b w_f(x) f_1(x) f_2(x) dx = 0.$$

Taking one of the two constants a_1 and a_2 arbitrarily, the other constant can be determined, and thus Φ_2 is obtained.

In general, suppose $\Phi_1(x)$, $\Phi_2(x)$, . . ., $\Phi_n(x)$ have been generated, $\Phi_{n+1}(x)$ can be assumed as

$$\Phi_{n+1}(x) = \sum_{i=1}^{n+1} a_i f_i(x).$$

Then applying the orthogonality relation, equation (2.2), gives n simultaneous equations with n+1 constants yet undetermined:

$$\sum_{i=1}^{n+1} a_i \int_a^b w_f(x) \Phi_m(x) f_i(x) dx = 0; \; m=1, 2, \ldots, n. \qquad \text{(a)}$$

Setting one of the non-zero constants a_i to a value arbitrarily, the remaining n constants can be determined and thus $\Phi_{n+1}(x)$ is obtained.

It may be desirable in some instances to obtain normalized functions. In such a case, an orthonormal series of functions is given as

$$\bar{\Phi}_k(x) = c_k\Phi_k(x),$$

where $\bar{\Phi}_k(x)$ and $\Phi_k(x)$ denote normalized and non-normalized functions, respectively, and c_k is chosen such that

$$c_k = (\int_a^b w_f(x)\Phi_k{}^2(x)dx)^{-1/2}.$$

Alternatively, the constants for the orthonormal series of functions can be directly determined from the n simultaneous equations (a) and an additional normalizing equation

$$\int_a^b w_f(x)\Phi_{n+1}^2(x)dx = 1,$$

rather than fixing one of the constants a_i arbitrarily.

For orthonormal functions, a little more convenient method, known as the 'Gram-Schmidt process' or 'Gram-Schmidt orthonormalization procedure', may be used [192] as follows.

The first orthonormal function $\bar{\Phi}_1(x)$ is given as

$$\bar{\Phi}_1(x) = c_1 f_1(x),$$

where c_1 is chosen as $c_1 = (\int_a^b w_f(x)f_1^2(x)dx)^{-1/2}$, so that

$$\int_a^b w_f(x)\bar{\Phi}_1{}^2(x)dx = 1.$$

Next let

$$\Phi_2(x) = f_2(x) - a_1\bar{\Phi}_1(x).$$

Then,

$$\int_a^b w_f(x)\bar{\Phi}_1(x)\Phi_2(x)dx=\int_a^b w_f(x)\bar{\Phi}_1(x)f_2(x)dx-a_1\int_a^b w_f(x)\bar{\Phi}_1^2(x)dx=0,$$

provided that a_1 is chosen as $a_1 = \int_a^b w_f(x)\bar{\Phi}_1(x)f_2(x)dx$, since

$\int_a^b w_f(x)\bar{\Phi}_1^2(x)dx=1$. With this choice of a_1, then, the second orthonormal function is obtained as

$$\bar{\Phi}_2(x)=(\int_a^b w_f(x)\Phi_2^2(x)dx)^{-1/2}\Phi_2(x).$$

In general, suppose $\bar{\Phi}_1(x)$, $\bar{\Phi}_2(x)$, . . ., $\bar{\Phi}_n(x)$ have been generated such that

$$\int_a^b w_f(x)\bar{\Phi}_i(x)\bar{\Phi}_j(x)dx = \delta_{ij};\ i,\ j=1,2,3,\ .\ .\ .,\ n.$$

Let

$$\Phi_{n+1}(x) = f_{n+1}(x) - \sum_{i=1}^{n} a_i\bar{\Phi}_i(x),$$

and the constants a_i are chosen as

$$a_i = \int_a^b w_f(x)\bar{\Phi}_i(x)f_{n+1}(x)dx.$$

Then,

$$\int_a^b w_f(x)\bar{\Phi}_j(x)\Phi_{n+1}(x)dx$$

$$= \int_a^b w_f(x)\bar{\Phi}_j(x)f_{n+1}(x)dx - \sum_{i=1}^{n} a_i \int_a^b w_f(x)\bar{\Phi}_j(x)\bar{\Phi}_i(x)dx$$

$$= a_j - a_j = 0.$$

Therefore $\bar{\Phi}_{n+1}(x) = (\int_a^b w_f(x)\Phi_{n+1}^2(x)dx)^{-1/2}\Phi_{n+1}(x)$

2.2. ORTHOGONAL POLYNOMIALS

2.2.1. Generation of Orthogonal Polynomials

When a set of orthogonal functions is constructed only with polynomials and the difference of the degree (the highest degree of each member) between any two consecutive members of the polynomials is just 1, a number of relationships are known to exist [192, 193]. Among them, one of the most important relationships is the recurrence relation which is

$$\Phi_{n+1}(x)=(A_n x-B_n)\Phi_n(x)-C_n\Phi_{n-1}(x);\ n=1,2,3,\ldots, \qquad (2.5)$$

where A_n, B_n and C_n are constants, and $\Phi_0(x)$ is defined as 0. Further, when A_n is 1 or the coefficient of the term including the highest degree of the member is unity, the polynomial is called a 'monic' polynomial [192]. For monic

polynomials the constants B_n and C_n are given as [192, 193]

$$B_n = \int_a^b w_f(x)x\Phi_n^2(x)dx/\int_a^b w_f(x)\Phi_n^2(x)dx,$$

$$C_n = \int_a^b w_f(x)\Phi_n^2(x)dx/\int_a^b w_f(x)\Phi_{n-1}^2(x)dx.$$

Using the recurrence formula (2.5), such a set of orthogonal polynomials can be generated much more simply than by using the Gram-Schmidt process.

In this thesis, the recurrence formula (2.5) is generalized by replacing the first term in the right hand side of the formula with g(x),

$$\Phi_{n+1}(x) = \{g(x)-B_n\}\Phi_n(x)-C_n\Phi_{n-1}(x);\ n=1,2,3,\ .\ .\ . \qquad (2.6)$$

Here, the function g(x) is termed the 'generating function'. The constants B_n and C_n are given as

$$B_n = \int_a^b w_f(x)g(x)\Phi_n^2(x)dx/\int_a^b w_f(x)\Phi_n^2(x)dx, \qquad (2.7a)$$

$$C_n = \int_a^b w_f(x)\Phi_n^2(x)dx/\int_a^b w_f(x)\Phi_{n-1}^2(x)dx, \qquad (2.7b)$$

and $\Phi_0(x)$ is again defined as zero.

The derivations of the constants B_n and C_n in equation (2.5) are performed in a similar manner to those for g(x)=x. However, for the sake of completeness, the derivation is presented here, in which $\Phi_n(x)$, g(x), $w_f(x)$, . . . are

denoted by Φ_n, g, w_f, . . . when there is no danger of ambiguity.

Considering the orthogonality relation between Φ_{n+1} and Φ_n, using equation (2.6),

$$\int_a^b w_f \Phi_{n+1} \Phi_n dx = \int_a^b w_f g \Phi_n^2 dx - B_n \int_a^b w_f \Phi_n^2 dx - C_n \int_a^b w_f \Phi_{n-1} \Phi_n dx = 0.$$

Due to the orgthogonality,

$$\int_a^b w_f \Phi_{n-1} \Phi_n dx = 0,$$

and thus

$$B_n = \int_a^b w_f g \Phi_n^2 dx / \int_a^b w_f \Phi_n^2 dx.$$

Next, considering the orthogonality relation between Φ_{n+1} and Φ_{n-1},

$$\int_a^b w_f \Phi_{n+1} \Phi_{n-1} dx = \int_a^b w_f g \Phi_n \Phi_{n-1} dx - B_n \int_a^b w_f \Phi_n \Phi_{n-1} dx - C_n \int_a^b w_f \Phi_{n-1}^2 dx = 0$$

Again, due to the orthogonality,

$$\int_a^b w_f \Phi_n \Phi_{n-1} dx = 0,$$

and thus

$$C_n = \int_a^b w_f g \Phi_n \Phi_{n-1} dx / \int_a^b w_f \Phi_{n-1}^2 dx. \qquad (2.7b')$$

Further,

$$\int_a^b w_f \Phi_n^2 dx = \int_a^b w_f \Phi_n \{(g-B_{n-1})\Phi_{n-1} - C_{n-1}\Phi_{n-2}\} dx$$

$$= \int_a^b w_f g \Phi_n \Phi_{n-1} dx - B_{n-1} \int_a^b w_f \Phi_n \Phi_{n-1} dx - C_{n-1} \int_a^b w_f \Phi_n \Phi_{n-2} dx$$

$$= \int_a^b w_f g \Phi_n \Phi_{n-1} dx.$$

Therefore, the constant C_n in equation (2.7b') can be rewritten in the form

$$C_n = \int_a^b w_f \Phi_n^2 dx / \int_a^b w_f \Phi_{n-1}^2 dx.$$

The polynomials generated by the generalized recurrence formula (2.6) still maintain the overall orthogonality relation (equation (2.3)), not only the orthogonality relation between three consecutive polynomials. The proof is given as follows. (The orthogonality between three consecutive polynomials may be regarded as self proved in the derivation of the constants B_n and C_n. However, for the sake of the completeness of the proof itself, it is included in the following proof.)

First, the orthogonality between the starting and the second functions is verified. Since the constant B_1, given in equation (2.7a), is

$$B_1 = \int_a^b w_f g \Phi_1^2 dx / \int_a^b w_f \Phi_1^2 dx,$$

$$\int_a^b w_f \Phi_1 \Phi_2 dx = \int_a^b w_f \Phi_1 \{(g-B_1)\Phi_1\} dx = \int_a^b w_f g \Phi_1^2 dx - B_1 \int_a^b w_f \Phi_1^2 dx = 0. \qquad \text{(b)}$$

Next, consider any two consecutive members of the polynomials,

$$\int_a^b w_f \Phi_k \Phi_{k+1} dx = \int_a^b w_f \Phi_k \{(g-B_k)\Phi_k - C_k \Phi_{k-1}\} dx$$

$$= \int_a^b w_f g \Phi_k^2 dx - B_k \int_a^b w_f \Phi_k^2 dx - C_k \int_a^b w_f \Phi_{k-1} \Phi_k dx. \qquad \text{(c)}$$

Since $B_k = \int_a^b w_f g \Phi_k^2 dx / \int_a^b w_f \Phi_k^2 dx$, the first two terms in the right hand side of equation (c) are identically zero and thus

$$\int_a^b w_f \Phi_k \Phi_{k+1} dx = -C_k \int_a^b w_f \Phi_{k-1} \Phi_k dx. \qquad \text{(d)}$$

Equation (d) shows a recurrence relation (k is an arbitrary natural number), and hence can be rewritten as

$$\int_a^b w_f \Phi_k \Phi_{k+1} dx = -C_k \int_a^b w_f \Phi_{k-1} \Phi_k dx$$

$$= -C_k [-C_{k-1} \int_a^b w_f \Phi_{k-2} \Phi_{k-1} dx] = \ldots\ldots$$

$$= (-1)^{k-1} C_k C_{k-1} \ldots C_2 \int_a^b w_f \Phi_1 \Phi_2 dx.$$

Since $\int_a^b w_f \Phi_1 \Phi_2 dx = 0$, as shown in equation (b),

$$\int_a^b w_f \Phi_k \Phi_{k+1} dx = 0. \qquad \text{(e)}$$

This equation shows that any two consecutive polynomials are orthogonal.

Further,

$$\int_a^b w_f \Phi_k \Phi_{k+2} dx = \int_a^b w_f \Phi_k \{(g-B_{k+1})\Phi_{k+1} - C_{k+1}\Phi_k\} dx$$

$$= \int_a^b w_f g \Phi_k \Phi_{k+1} dx - B_{k+1} \int_a^b w_f \Phi_k \Phi_{k+1} dx - C_{k+1} \int_a^b w_f \Phi_k^2 dx. \qquad \text{(f)}$$

From equation (2.7b'), $C_{k+1} = \int_a^b w_f g \Phi_{k+1} \Phi_k dx / \int_a^b w_f \Phi_k^2 dx$.

Substitution of C_{k+1} and equation (e) into equation (f) yields

$$\int_a^b w_f \Phi_k \Phi_{k+2} dx = 0. \qquad \text{(g)}$$

Equation (g), together with equation (e), shows that any three consecutive polynomials are orthogonal.

Let us now assume that any n consecutive polynomials, where $n \geq 3$, are orthogonal. Then,

$$\int_a^b w_f \Phi_r \Phi_s dx = a_r \delta_{rs}; \qquad k-n+1 \leq r, s \leq k, \qquad \text{(h)}$$

where a_r are constants and δ_{rs} denotes the Kronecker delta. Also, using equation (2.6),

$$\int_a^b w_f \Phi_{k-n+1}\Phi_{k+1}dx = \int_a^b w_f \Phi_{k-n+1}\{(g-B_k)\Phi_k - C_k\Phi_{k-1}\}dx$$

$$= \int_a^b w_f g\Phi_{k-n+1}\Phi_k dx - B_k\int_a^b w_f \Phi_{k-n+1}\Phi_k dx - C_k\int_a^b w_f \Phi_{k-n+1}\Phi_{k-1}dx.$$

From equation (h), $\int_a^b w_f \Phi_{k-n+1}\Phi_k dx = \int_a^b w_f \Phi_{k-n+1}\Phi_{k-1}dx = 0$.

Hence,

$$\int_a^b w_f \Phi_{k-n+1}\Phi_{k+1}dx = \int_a^b w_f g\Phi_{k-n+1}\Phi_k dx.$$

The recurrence formula (2.6) can be rewritten as

$$g\Phi_{k-n+1} = \Phi_{k-n+2} + B_{k-n+1}\Phi_{k-n+1} + C_{k-n+1}\Phi_{k-n}.$$

Thus,

$$\int_a^b w_f \Phi_{k-n+1}\Phi_{k+1}dx = \int_a^b w_f (\Phi_{k-n+2} + B_{k-n+1}\Phi_{k-n+1} + C_{k-n+1}\Phi_{k-n})\Phi_k dx$$

$$= \int_a^b w_f \Phi_{k-n+2}\Phi_k dx + B_{k-n+1}\int_a^b w_f \Phi_{k-n+1}\Phi_k dx + C_{k-n+1}\int_a^b w_f \Phi_{k-n}\Phi_k dx.$$

Again from equation (h),

$$\int_a^b w_f \Phi_{k-n+2}\Phi_k dx = \int_a^b w_f \Phi_{k-n+1}\Phi_k dx = 0,$$

and thus,

$$\int_a^b w_f \Phi_{k-n+1}\Phi_{k+1}dx = C_{k-n+1}\int_a^b w_f \Phi_{k-n}\Phi_k dx.$$

This equation shows a recurrence relation, and, utilizing

the recurrence relation, the equation can be rewritten as

$$\int_a^b w_f \Phi_{k-n+1} \Phi_{k+1} dx = C_{k-n+1} C_{k-n} C_{k-n-1} \cdots C_2 \int_a^b w_f \Phi_1 \Phi_{n+1} \, dx. \tag{i}$$

From the assumption, or taking k=n in equation (h),

$$\int_a^b w_f \Phi_r \Phi_s dx = a_r \delta_{rs}; \qquad 1 \leq r, \; s \leq n. \tag{j}$$

Using equations (2.6) and (j), the right hand integral in equation (i) can be rewritten as

$$\int_a^b w_f \Phi_1 \Phi_{n+1} dx = \int_a^b w_f \Phi_1 \{(g-B_n)\Phi_n - C_n \Phi_{n-1}\} dx$$

$$= \int_a^b w_f g \Phi_1 \Phi_n - B_n \int_a^b w_f \Phi_1 \Phi_n dx - C_n \int_a^b w_f \Phi_1 \Phi_{n-1} dx$$

$$= \int_a^b w_f g \Phi_1 \Phi_n dx = \int_a^b w_f (\Phi_2 + B_1 \Phi_1) \Phi_n dx$$

$$= \int_a^b w_f \Phi_2 \Phi_n dx + B_1 \int_a^b w_f \Phi_1 \Phi_n dx = 0.$$

Therefore,

$$\int_a^b w_f \Phi_{k-n+1} \Phi_{k+1} dx = 0. \tag{k}$$

Equation (k) shows that, when any n consecutive polynomials for $n \geq 3$ are orthogonal, (n+1) consecutive polynomials are orthogonal, too. This, together with the proof of the orthogonality between any three consecutive polynomials, verifies that the polynomials generated by the recurrence

formula (2.6) are altogether orthogonal.

It may be noted that, the proof of

$$\int_a^b w_f \Phi_n^2 dx \neq 0$$

is omitted here, since the relation is automatically satisfied if the weight function is defined by equation (2.1), as mentioned earlier.

When it is required to generate an orthonormal set of polynomials, normalization at each step makes the generation procedure simpler, as follows.

$$\Phi_{n+1}(x) = \{g(x) - B_n\}\bar{\Phi}_n(x) - A_n^{1/2}\bar{\Phi}_{n-1}(x), \tag{2.8a}$$

$$\bar{\Phi}_{n+1}(x) = A_{n+1}^{-(1/2)}\Phi_{n+1}(x), \tag{2.8b}$$

where $A_n = \int_a^b w_f(x)\Phi_n^2(x)dx$, $B_n = \int_a^b w_f(x)g(x)\bar{\Phi}_n^2(x)dx$,

$\bar{\Phi}_n(x)$ and $\Phi_n(x)$ denote normalized and non-normalized polynomials, and $\Phi_0(x)$ is defined as zero. The derivation of the constants in equation (2.8) is shown as follows.

Let $\Phi_{n+1} = (g-B_n)\bar{\Phi}_n - C_n\bar{\Phi}_{n-1}$,

and then,

$$\int_a^b w_f \Phi_{n+1} \bar{\Phi}_n dx = \int_a^b w_f g \bar{\Phi}_n^2 dx - B_n \int_a^b w_f \bar{\Phi}_n^2 dx - C_n \int_a^b \bar{\Phi}_{n-1} \bar{\Phi}_n dx = 0.$$

Since $\int_a^b w_f \bar{\Phi}_n^2 dx = 1$ and $\int_a^b \bar{\Phi}_{n-1} \bar{\Phi}_n dx = 0$,

$$B_n = \int_a^b w_f g \bar{\Phi}_n^2 dx.$$

Further,

$$\int_a^b w_f \Phi_{n+1} \bar{\Phi}_{n-1} dx = \int_a^b w_f g \bar{\Phi}_n \bar{\Phi}_{n-1} dx - B_n \int_a^b w_f \bar{\Phi}_n \bar{\Phi}_{n-1} dx - C_n \int_a^b w_f \bar{\Phi}_{n-1}^2 dx = 0.$$

Since $\int_a^b w_f \bar{\Phi}_n \bar{\Phi}_{n-1} dx = 0$ and $\int_a^b w_f \bar{\Phi}_{n-1}^2 dx = 1$,

thus, $C_n = \int_a^b w_f g \bar{\Phi}_n \bar{\Phi}_{n-1} dx$.

In addition,

$$\int_a^b w_f \Phi_n \bar{\Phi}_n dx = \int_a^b w_f g \bar{\Phi}_{n-1} \bar{\Phi}_n dx - B_{n-1} \int_a^b w_f \bar{\Phi}_{n-1} \bar{\Phi}_n dx - C_{n-1} \int_a^b w_f \bar{\Phi}_{n-2} \bar{\Phi}_n dx$$

$$= \int_a^b w_f g \bar{\Phi}_{n-1} \bar{\Phi}_n dx.$$

Thus C_n can be rewritten as

$$C_n = \int_a^b w_f \Phi_n \bar{\Phi}_n dx = A_n^{1/2} \int_a^b w_f \bar{\Phi}_n^2 dx = A_n^{1/2}.$$

2.2.2. Characteristics of Orthogonal Polynomials

Among the characteristics of orthogonal polynomials, two which may be useful for use in the Rayleigh-Ritz method

are presented here (The following may be documented in the literature, for $g(x) = x$, but the author is not aware of such).

Consider a continuous polynomial $\Phi_1(x)$ defined in an interval $a \leq x \leq b$.

Theorem (1). If

$$\Phi_1 = d\Phi_1/dx = d^2\Phi_1/dx^2 = \ldots = d^r\Phi_1/dx^r = 0 \text{ at } x=x_p, \qquad (l)$$

where x_p is located in the interior of the interval, then the orthogonal polynomials $\Phi_k(x)$ generated by recurrence formula (2.6) (or (2.8)) have the property

$$\Phi_k = d\Phi_k/dx = d^2\Phi_k/dx^2 = \ldots = d^r\Phi_k/dx^r = 0 \text{ at } x=x_p.$$

(Proof)

Let us assume that Φ_{k-1} and Φ_k have the property

$$\Phi_{k-1}=d\Phi_{k-1}/dx=d^2\Phi_{k-1}/dx^2 = \ldots = d^r\Phi_{k-1}/dx^r=0 \text{ at } x=x_p, \qquad (m)$$

$$\Phi_k=d\Phi_k/dx=d^2\Phi_k/dx^2 = \ldots = d^r\Phi_k/dx^r=0 \text{ at } x=x_p. \qquad (n)$$

From equation (2.6);

$$\Phi_{k+1}=(g-B_k)\Phi_k-C_k\Phi_{k-1},$$

and

$$\frac{d\Phi_{k+1}}{dx} = \frac{dg}{dx}\Phi_k + (g-B_k)\frac{d\Phi_k}{dx} - C_k\frac{d\Phi_{k-1}}{dx},$$

$$\frac{d^2\Phi_{k+1}}{dx^2} = \frac{d^2g}{dx^2}\Phi_k + 2\frac{dg}{dx}\frac{d\Phi_k}{dx} + (g-B_k)\frac{d^2\Phi_k}{dx^2} - C_k\frac{d^2\Phi_{k-1}}{dx^2} ,$$

$$\ldots\ldots\ldots\ldots\ldots\ldots\ldots\ldots\ldots\ldots , \qquad (o)$$

$$\ldots\ldots\ldots\ldots\ldots\ldots\ldots\ldots\ldots\ldots ,$$

$$\frac{d^r\Phi_{k+1}}{dx^r} = \frac{d^rg}{dx^r}\Phi_k + r\frac{d^{r-1}g}{dx^{r-1}}\frac{d\Phi_k}{dx} + \ldots + (g-B_k)\frac{d^r\Phi_k}{dx^r} - C_k\frac{d^r\Phi_{k-1}}{dx^r}.$$

At $x = x_p$, substituting equations (m) and (n) into equations (o) yields

$$\Phi_{k+1} = \frac{d\Phi_{k+1}}{dx} = \frac{d^2\Phi_{k+1}}{dx^2} = \ldots = \frac{d^r\Phi_{k+1}}{dx^r} = 0 \text{ at } x=x_p. \qquad (p)$$

Equations (m), (n) and (p) shows that the functions generated by equation (2.6) have the property mentioned consecutively.

Theorem (2). When a starting function $\Phi_1(x)$ has symmetry or anti-symmetry about the centre of the interval $a \leq x \leq b$, then all the members of the orthogonal polynomials generated by recurrence formula (2.6) or (2.8) have symmetry or anti-symmetry under the following conditions.

(i) If the generating function $g(x)$ is symmetrical or can be made symmetrical simply by adding or subtracting a constant, then all the members of the orthogonal

polynomials have the same symmetry (i.e. all members are symmetrical or all are anti-symmetrical).

(ii) If the generating function $g(x)$ is anti-symmetrical or can be made anti-symmetrical simply by adding or subtracting a constant, then all the members of the orthogonal polynomials are symmetrical or anti-symmetrical alternately, provided that the weight function $w_f(x)$ is symmetrical.

(Proof)

(i). Let $g(x) = g_s(x) + c_s$,
where $g_s(x)$ is a symmetrical function and c_s is a constant. Then, recurrence formula (2.6) can be rewritten as

$$\Phi_2 = g_s\Phi_1 + (c_s-B_1)\Phi_1,$$

$$\Phi_{n+1} = g_s\Phi_n + (c_s-B_n)\Phi_n - C_n\Phi_{n-1};\ n = 2, 3, \ldots .$$

Since g_s is symmetrical and c_s-B_1 = constant is again symmetrical, Φ_2 must have the same symmetry as Φ_1. Further, if any two consecutive polynomials (Φ_{n-1} and Φ_n) have the same symmetry, then, the next polynomial (Φ_{n+1}) must have the same symmetry, too, since g_s, (c_s-B_n) and C_n are symmetrical. Therefore, if Φ_1 has a symmetry or anti-symmetry, the same symmetry is retained consecutively.

(ii). Let $g(x) = g_a(x) + c_a$,

where $g_a(x)$ is an anti-symmetrical function and c_a a constant. Then, equation (2.6) can be rewritten as

$$\Phi_2 = g_a\Phi_1 + (c_a-B_1)\Phi_1$$

$$\Phi_{n+1} = g_a\Phi_n + (c_a-B_n)\Phi_n - C_n\Phi_{n-1};\ n = 2, 3, \ldots \qquad (q)$$

Substituting the first of equations (q) into the orthogonality relation yields

$$\int_a^b w_f\Phi_1\Phi_2 dx = \int_a^b w_f g_a \Phi_1^2 dx + (c_a-B_1)\int_a^b w_f\Phi_1^2 dx = 0.$$

Since w_f and Φ_1^2 are symmetrical (Φ_1 is symmetrical or anti-symmetrical), and g_a is anti-symmetrical,

$$\int_a^b w_f g_a \Phi_1^2 dx = 0.$$

Thus $(c_a-B_1) = 0$ $(\int_a^b w_f\Phi_1^2 dx \neq 0)$,

and further, the first of equations (q) yields $\Phi_2 = g_a\Phi_1$. Therefore, if Φ_1 is symmetrical, Φ_2 is anti-symmetrical, or vice versa.

Let us assume that Φ_{n-1} is symmetrical and Φ_n is anti symmetrical, or vice versa. Considering the orthogonality,

$$\int_a^b w_f\Phi_{n+1}\Phi_n dx = \int_a^b w_f g_a \Phi_n^2 dx + (c_a-B_n)\int_a^b w_f\Phi_n^2 dx - C_n\int_a^b w_f\Phi_{n-1}\Phi_n dx = 0.$$

Due to the orthogonality,

$$\int_a^b w_f \Phi_{n-1} \Phi_n \, dx = 0,$$

and also,

$$\int_a^b w_f g_a \Phi_n^2 \, dx = 0,$$

since w_f and Φ_n^2 are symmetrical while g_a is anti-symmetrical. Thus $(c_a - B_n) = 0$ and further, the second of equations (q) yields

$$\Phi_{n+1} = g_a \Phi_n - c_n \Phi_{n-1}.$$

Since Φ_{n-1} is symmetrical and Φ_n is anti-symmetrical, or vice versa, Φ_{n+1} must have the same symmetry as Φ_{n-1}. Therefore, if Φ_1 has a symmetry (symmetrical or anti-symmetrical), the symmetry is changed alternately, provided that the weight function is symmetrical. Additionally, it should be noted that the constant B_n has always the same value for any member of the polynomials, i.e. $B_1 = B_2 = \ldots = c_a$. In particular, if the generating function is anti-symmetrical about the centre of the interval, $B_1 = B_2 = \ldots = 0$.

Theorems (1) and (2) are very important in that they ensure that the generated polynomials satisfy the chosen boundary conditions, both at the extremes of a system and at intermediate positions (such as at internal supports), and preserve the symmetry of the system, if required.

2.2.3. Beam Characteristic Orthogonal Polynomials

Numerous sets of orthogonal polynomials can be obtained by using recurrence formula (2.6) or (2.8), taking different starting function, weight function, generating function and/or the interval. With the generating function $g(x) = x$ and starting function unity, a number of well-known polynomials are obtained. Some such polynomials [192, 193] are: Legendre polynomials, obtained with weight function $w_f(x) = 1$ on the interval $-1 \leq x \leq 1$; Chebyshev polynomials of the first kind, with $w_f(x) = (1-x^2)^{(-1/2)}$ on $-1 \leq x \leq 1$; Chebyshev polynomials of the second kind, with $w_f(x) = (1-x^2)^{1/2}$ on $-1 \leq x \leq 1$; Laguerre polynomials, with $w_f(x)=e^{-x}$ on $0 \leq x \leq \infty$; Hermite polynomials, with

$$w_f(x) = e^{-x^2} \text{ on } -\infty \leq x \leq \infty; \text{ and so on.}$$

In 1985, Bhat [25-27, 30] suggested beam characteristic orthogonal polynomials for use in the Rayleigh-Ritz method as the admissible functions for dynamic and static problems of single span beams or rectangular plates with classical boundary conditions. Again, with the generating function $g(x) = x$, the starting function $\Phi_1(x)$ was suggested to be chosen as the simplest polynomial of the least degree that satisfies both the geometrical and the natural boundary conditions of the beam. In the present work, Bhat's suggestion has been extended and applied to the problem of

the vibration of beams or plates with sliding boundary conditions, multi-span beams or plates, etc.

In this work, the term 'beam characteristic orthogonal polynomials' is used for the orthogonal polynomials which can be used as the admissible functions in the Rayleigh-Ritz method or such methods for beam or plate problems, and thus satisfy at least zero displacement and zero slope conditions. The 'beam characteristic orthogonal polynomials' will be abbreviated 'BCOP'. (It might be mentioned that actual beam functions, derived from the exact solution of slender beam equations have been used with considerable success for the study of plate problems [11-17].)

The starting function $\Phi_1(x)$ is constructed to satisfy both geometrical and natural boundary conditions of the appropriate beam, as suggested by Bhat, and zero displacement conditions at intermediate supports for multi-span beams. The boundary conditions are $\Phi_1'' = \Phi_1''' = 0$ for free, $\Phi_1 = \Phi_1'' = 0$ for simply supported, $\Phi_1 = \Phi_1' = 0$ for clamped ends, and $\Phi_1' = \Phi_1''' = 0$ for sliding ends of uniform beams (The prime denotes the differentiation with respect to x). On the interval $0 \leq x \leq 1$, for beams with no intermediate support, the starting functions satisfying the boundary conditions may be written, for monic polynomials,

$$\Phi_1(x) = \sum_{i=1}^{5} a_i x^{i-1}, \tag{2.9}$$

where the coefficients a_i are given in Table 2.1.

Since the geometrical boundary conditions are the only necessary conditions for the admissible functions in the Rayleigh-Ritz method, alternative starting functions can be constructed. The geometrical boundary conditions are $\Phi_1 = 0$ for simply supported, $\Phi_1 = \Phi_1' = 0$ for clamped and $\Phi_1' = 0$ for sliding ends, and no geometrical boundary condition exists for free end. The starting functions for single span beams may, then, be given as, on the interval $0 \le x \le 1$,

$$\Phi_1(x) = \sum_{i=1}^{4} b_i x^{i-1}, \tag{2.10}$$

except for clamped-clamped beam (which is the same as in equation (2.9), since all the boundary conditions are geometrical), where the coefficients b_i are given in Table 2.2.

For multi-span beams, the starting functions are given, recurrently by multiplying the functions given by equations (2.9) or (2.10) by the factor $(x-x_p)$, where x_p denote the locations of the intermediate supports.

For classical boundary conditions, the generating function can be taken as $g(x) = x$, since all the members of

Table 2.1

Coefficients of starting functions satisfying both geometrical and natural boundary conditions, for single span beams on the interval [0,1]. (F = Free, S = Simply supported, C = Clamped, Sl = Sliding).

Boundary Conditions	Coefficients				
	a_1	a_2	a_3	a_4	a_5
F-F	1	0	0	0	0
F-S	-1	1	0	0	0
F-C	3	-4	0	0	1
S-F	0	1	0	0	0
S-S	0	1	0	-2	1
S-C	0	0.5	0	-1.5	1
C-F	0	0	6	-4	1
C-S	0	0	1.5	-2.5	1
C-C	0	0	1	-2	1
Sl-F	1	0	0	0	0
Sl-S	5	0	-6	0	1
Sl-C	1	0	-2	0	1
F-Sl	1	0	0	0	0
S-Sl	0	8	0	-4	1
C-Sl	0	0	4	-4	1
Sl-Sl	1	0	0	0	0

Table 2.2

Coefficients of starting functions satisfying geometrical boundary conditions only, for single span beams on the interval [0,1]. (F=Free, S=Simply Supported, C=Clamped, Sl=Sliding)

Boundary Conditions	Coefficients			
	b_1	b_2	b_3	b_4
F-F*	1	0	0	0
F-S*	-1	1	0	0
F-C	1	-2	1	0
S-F*	0	1	0	0
S-S	0	1	-1	0
S-C	0	1	-2	1
C-F	0	0	1	0
C-S	0	0	-1	1
Sl-F*	1	0	0	0
Sl-S	1	0	-1	0
Sl-C	0.5	0	-1.5	1
F-Sl	1	0	0	0
S-Sl*	0	-2	1	0
C-Sl	0	0	-1.5	1
Sl-Sl*	1	0	0	0

* The Starting function is the same as that satisfying both geometrical and natural boundary conditions.

the orthogonal polynomials generated with $g(x) = x$ satisfy the geometrical boundary conditions by theorem (1) in the previous section. However, for beams with sliding end(s), it is required to use higher degree generating functions since $\Phi_1 \neq 0$, $\Phi_1' = 0$ at the end and thus theorem (1) is not applicable. To detect the generating function for beams with sliding end(s), it is assumed that Φ_{n-1} and Φ_n satisfy the boundary condition $\Phi_{n-1}' = \Phi_n' = 0$ at the boundary, and then, from recurrence formula (2.6),

$$\Phi_{n+1}' = g'\Phi_n + (g-B_n)\Phi_n' - C_n\Phi_{n-1}' = g'\Phi_n$$

at the boundary. In order to give $\Phi_{n+1}' = 0$ at the boundary, then, $g'=0$ at the boundary, since $\Phi_n \neq 0$. The lowest degree generating functions satisfying $g'(x)=0$ at the boundary are given as, for monic polynomials, $g(x)=x^2$ for beams with a sliding end at $x=0$, $g(x)=x^2-2x$ for beams with a sliding end at $x=1$ and $g(x)=x^3-1.5x^2$ for beams with both ends sliding.

It is possible to choose some other generating functions. Then, with the same starting functions, various other sets of BCOP can be obtained taking different generating functions. Even with the same generating functions, again various other sets of BCOP can be obtained taking different weight functions. The choice of weight function is related to the mass distribution of the beam, and will be explained in the following chapters.

The first five shapes of BCOP, excluding the rigid body modes, are shown in Figures 2.1 and 2.2, for single span beams with classical boundary conditions taking $g(x)=x$ and $w_f(x)=1$ (which corresponds to the uniform beams). Each mode is arranged to make the largest value unity by multiplying (or dividing) by an appropriate constant. In Figure 2.1, the modes are obtained using the starting functions (2.9) and compared to the vibration characteristic beam functions, which are the exact solution of slender beam vibration modes. In Figure 2.2, the BCOP generated with starting function (2.9) and starting function (2.10) are compared. It may be noted that, when symmetry exists, the symmetrical and anti-symmetrical modes appear alternately, as verified in the previous section (theorem (2)). It is also noted that, for the free-free beam, the BCOP are the same as the shifted Legendre polynomials.

Finally, to illustrate the effect of using a higher degree generating function, the first five members of the BCOP were computed using $g(x) = x^3-1.5\ x^2$ and starting function from equation (2.9), for a beam with both ends simply supported. These are compared with the exact characteristic beam function in Figure 2.3. The BCOP generated here satisfy both the geometrical ($\Phi_k=0$) and natural ($\Phi_k''=0$) boundary conditions.

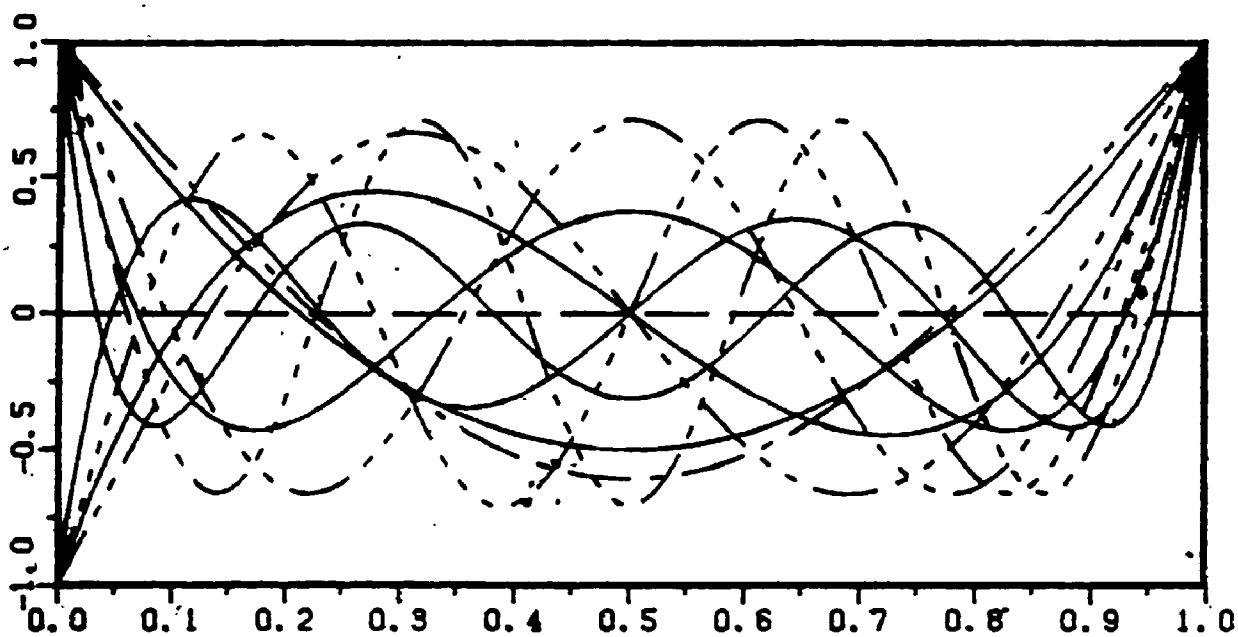

Figure 2.1. (a) A Free-Free Beam

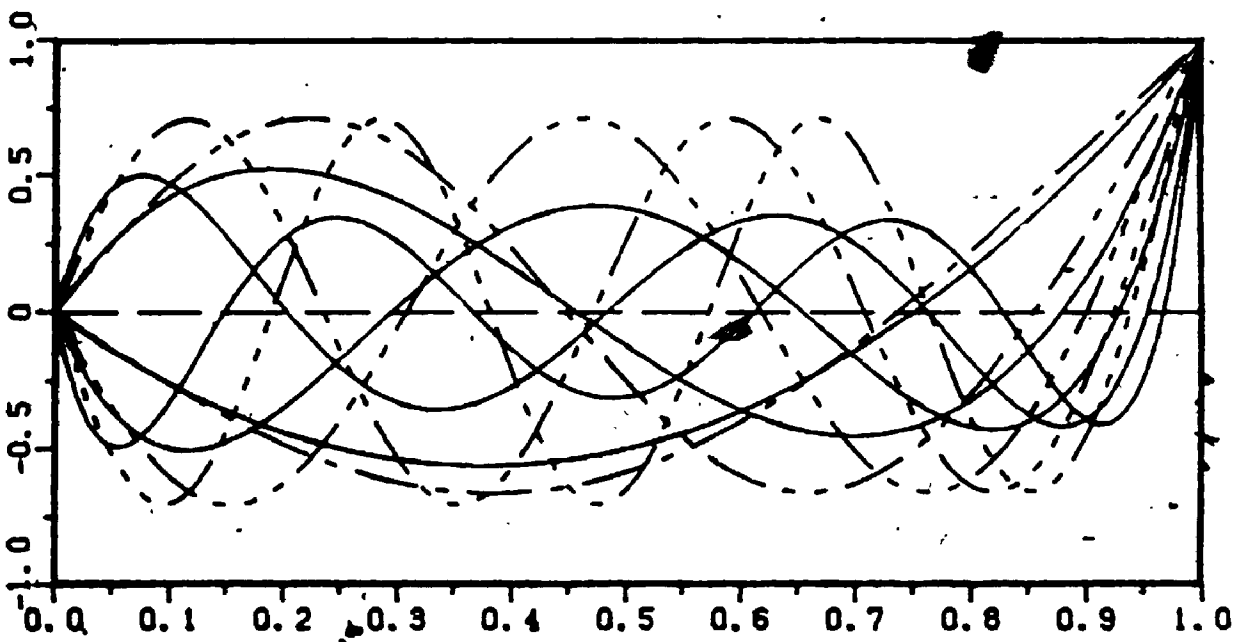

Figure 2.1. (b) A Simply Supported-Free Beam

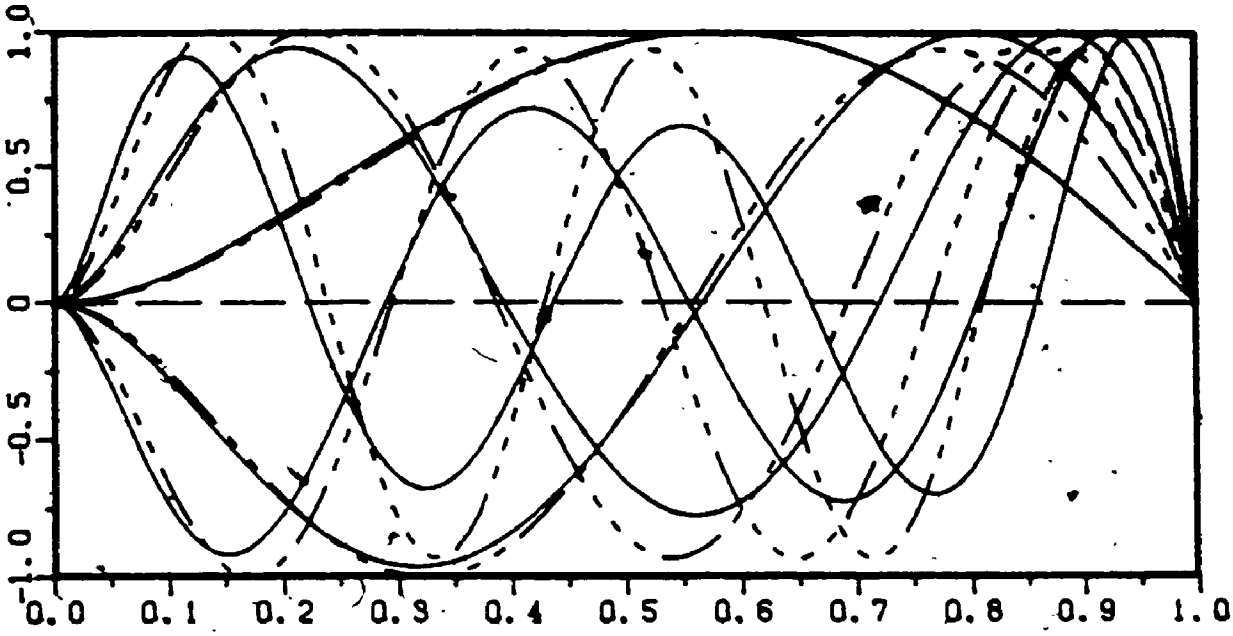

Figure 2.1. (c) A Clamped-Simply Supported Beam

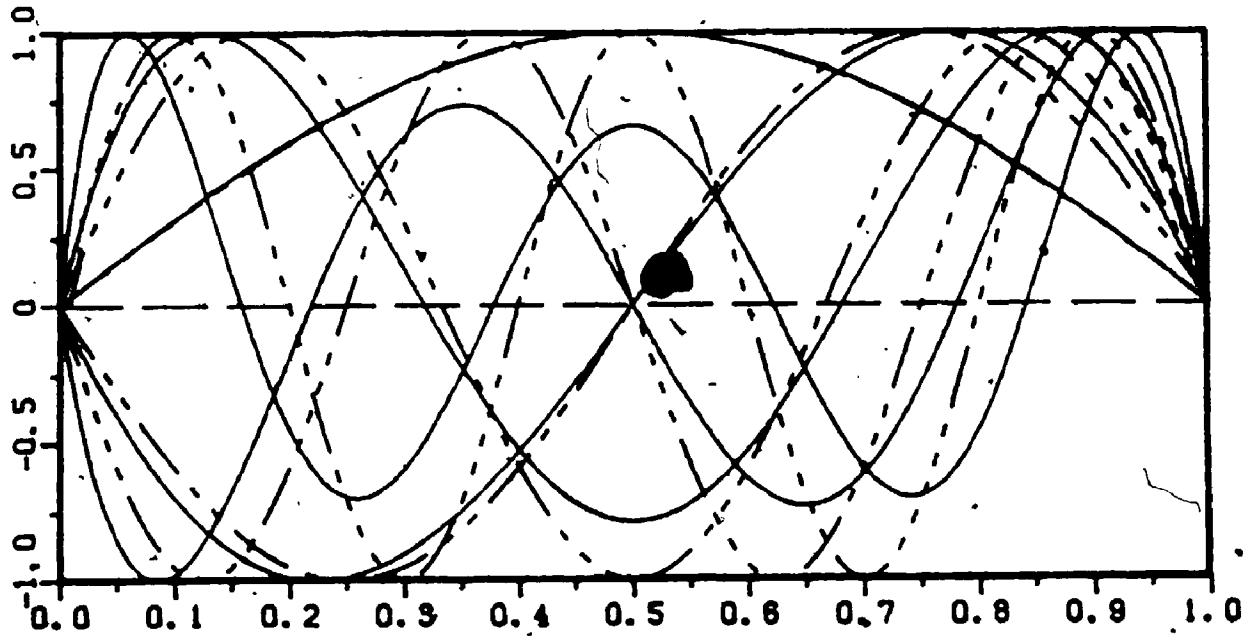

Figure 2.1. (d) A Simply Supported-Simply Supported Beam

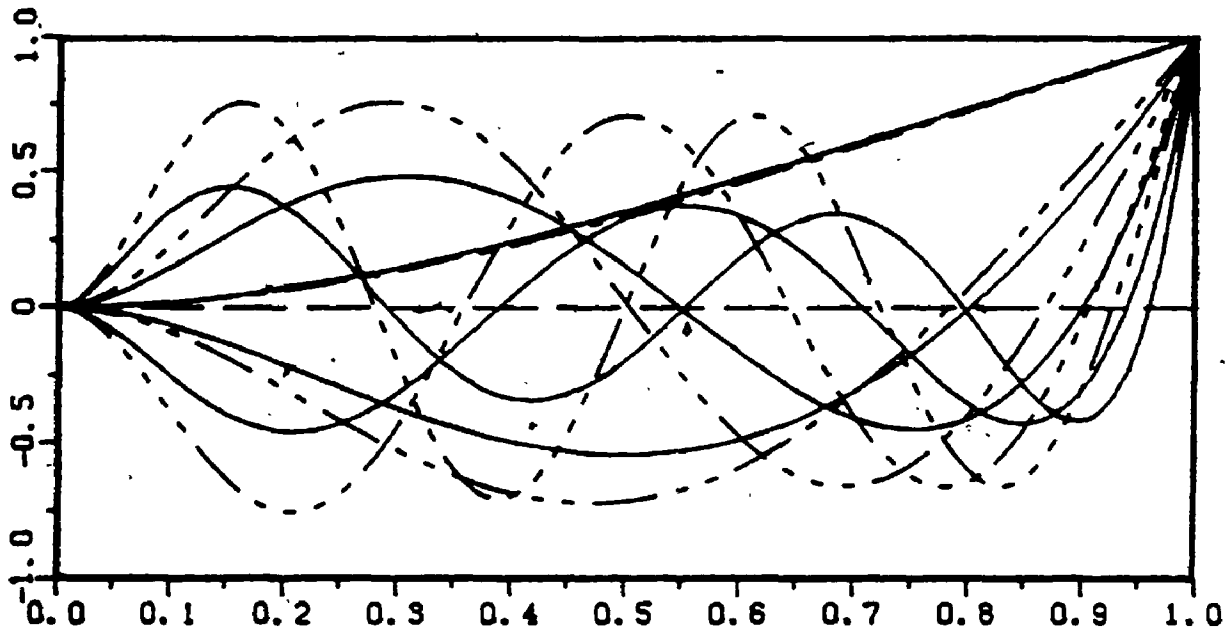

Figure 2.1. (e) A Clamped-Free Beam

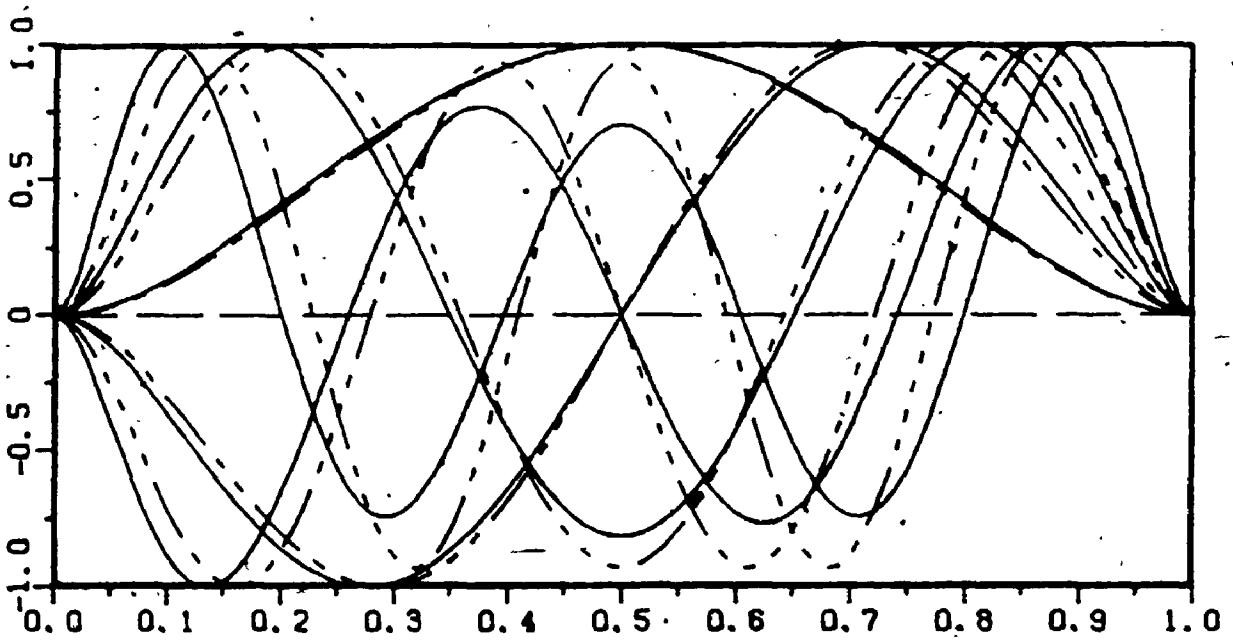

Figure 2.1. (f) A Clamped-Clamped Beam

Figure 2.1. Comparison of the shapes of BCOP (equation (2.9) and g(x) = x) and exact beam function. ——, BCOP; ——·——, ——··——, ——···——, ——····——, ——·····——; 1st, 2nd, 3rd, 4th, 5th modes of exact beam function.

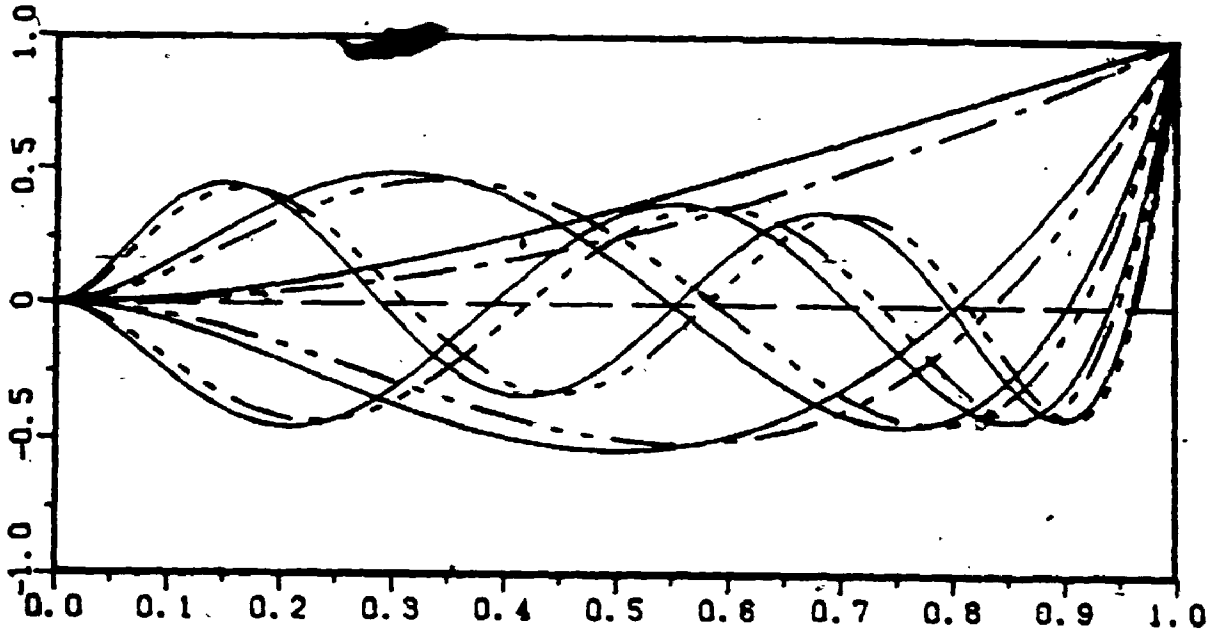

Figure 2.2. (a) A Clamped-Free Beam

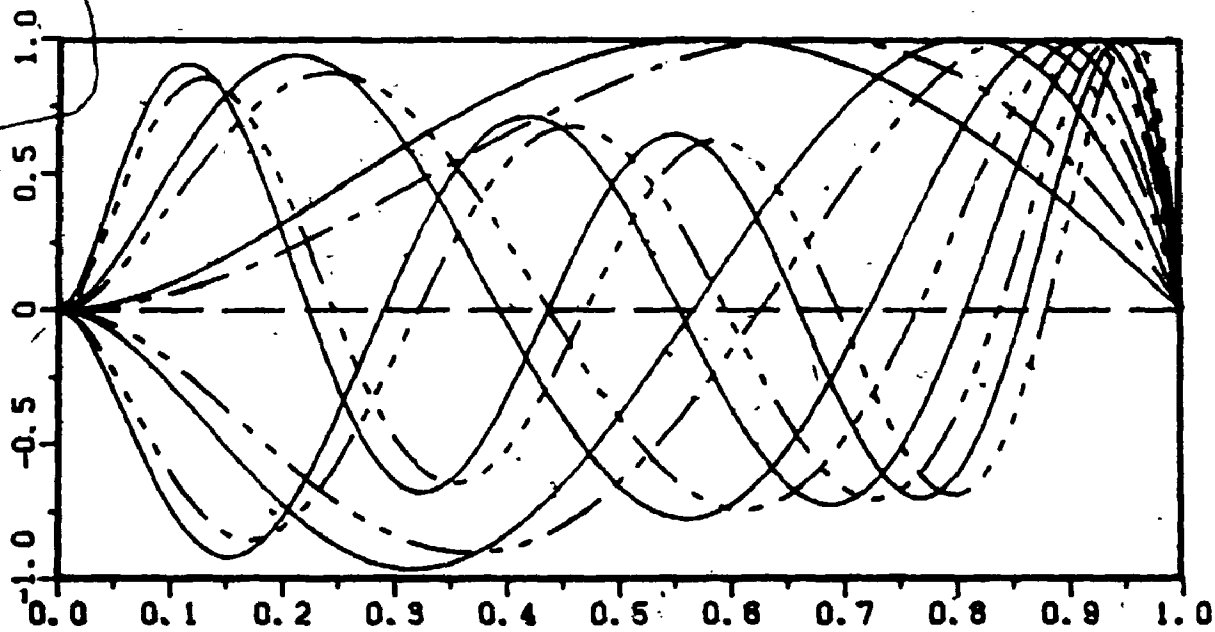

Figure 2.2. (b) A Clamped-Simply Supported Beam

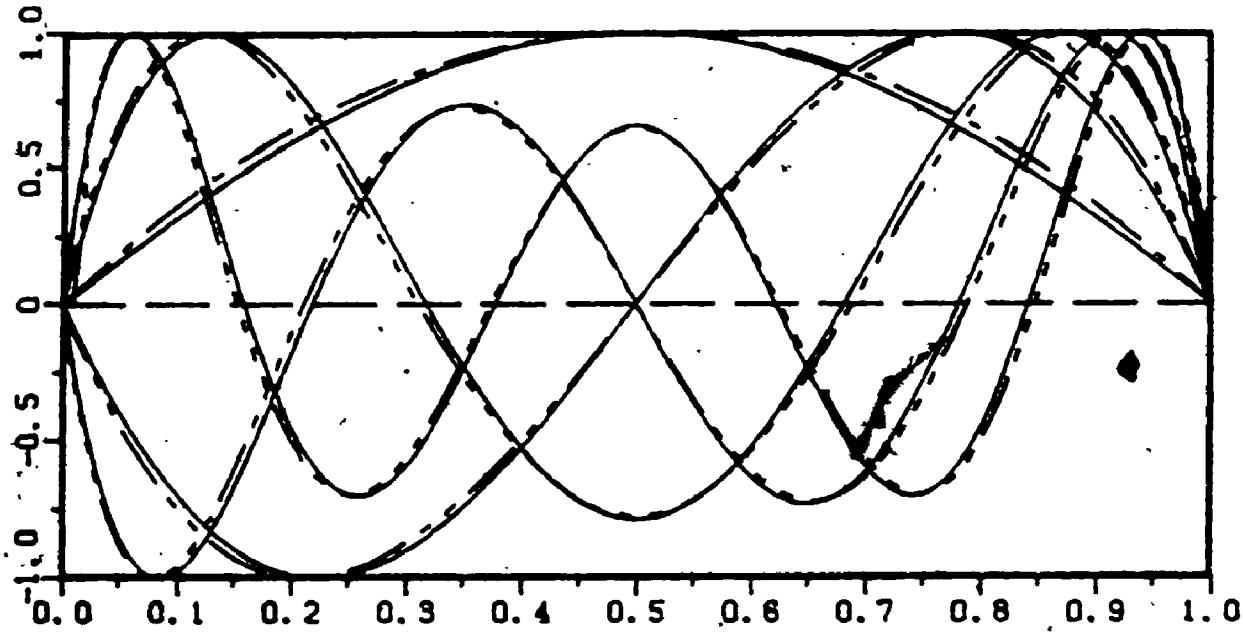

Figure 2.2 (c) A Simply Supported-Simply Supported Beam

Figure 2.2. Comparison of the shapes of BCOP generated with starting function satisfying both geometrical and natural boundary conditions and with starting function satsifying geometrical boundary conditions only (g(x) = x). ——, BCOP with higher degree starting function; —·—, —··—, —···—, —····—, —·····—; 1st, 2nd, 3rd, 4th, 5th modes of BCOP with lower degree starting function.

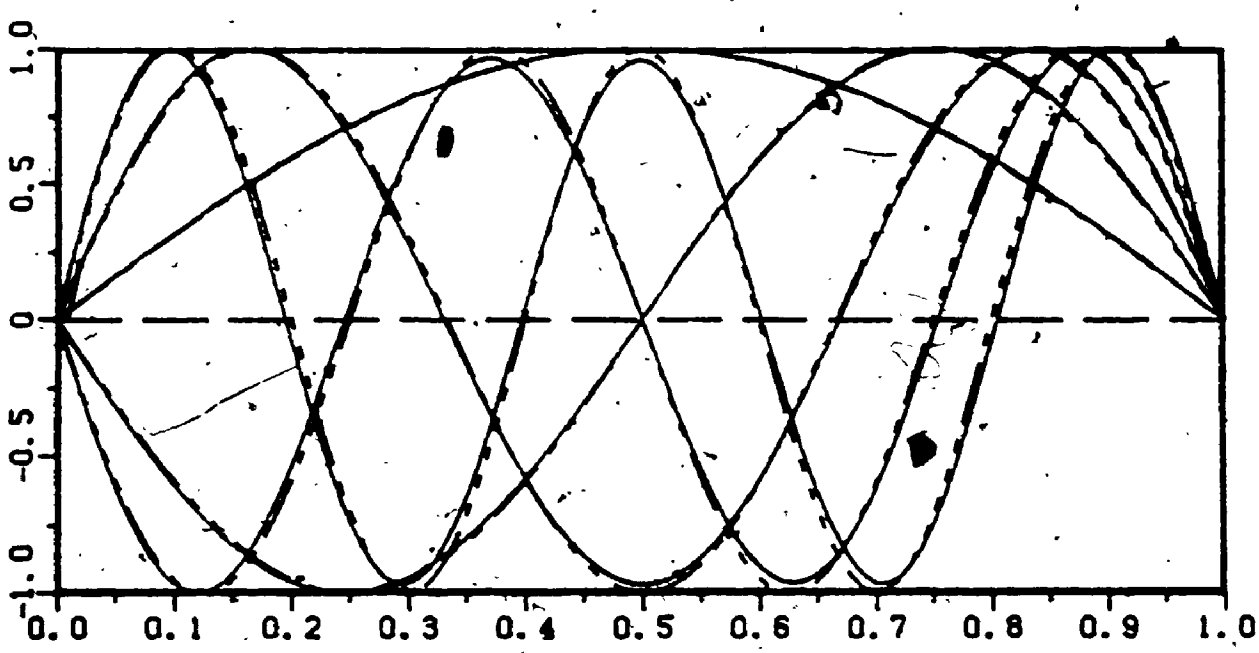

Figure 2.3 Comparison of the shapes of BCOP generated with $g(x) = x^3 - 1.5\ x^2$ and exact characteristic beam function for a beam with both ends simply supported. ——, BCOP; —·—, —··—, —···—, —····—, —·····—; 1st, 2nd, 3rd, 4th 5th modes of characteristic beam function.

CHAPTER 3

VIBRATION OF BEAMS

3.1 INTRODUCTORY REMARKS

As mentioned in Chapter 1, though numerous researchers have tackled the problem of the transverse vibration of straight, slender beams with various complicating factors, their attention appears to have been confined to mainly individual beam problems, and thus there appears to have been no study in which a single approach has been put forward for the treatment of the beams subject to any or all combinations of the factors. In this chapter, a simple, unified approach is presented for the treatment of the beams using the Rayleigh-Ritz method with the BCOP studied in Chapter 2 as the admissible functions. Numerical results are presented for particular beam problems in comparison with those in the literature, where available.

3.2 ANALYSIS

It is assumed that a multi-span, elastically restrained, slender beam, which lies along the x-axis and vibrates in the x-z plane, is subject to a constant, axial, compressive force P and is bounded by $x=0$, $x=\ell$, as shown in Figure 3.1. The intermediate supports at $x=\ell_j$ are assumed to prevent lateral displacement and to offer no resistance to rotation (simple support). The boundary conditions are considered to be

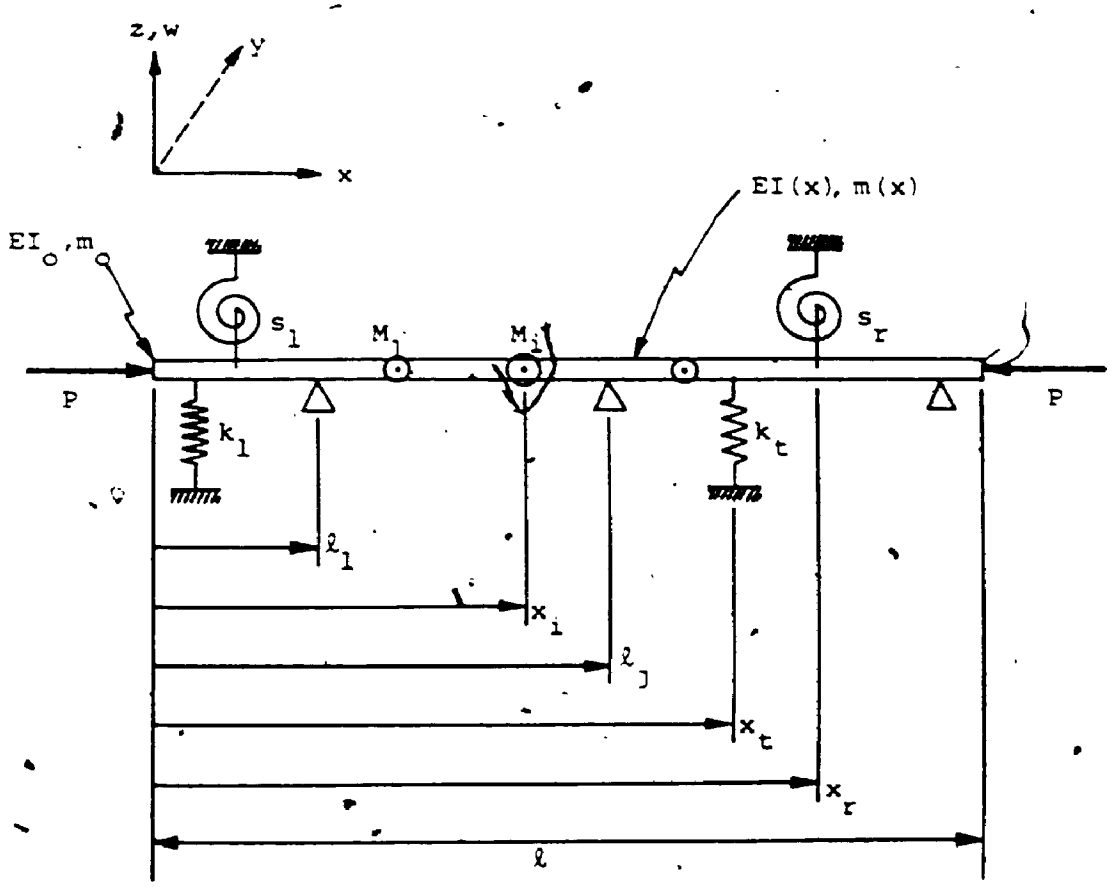

Figure 3.1. A multi-span, elastically restrained beam with arbitrary number of concentrated masses under an axial load.

clamped, simply supported or free (free in the figure) and the flexural rigidity EI and mass per unit length m are functions of x. The concentrated masses M_i, translational springs (spring constants k_t) and rotational springs (spring constants s_r) are attached at points located at x_i, x_t and x_r (i, t, r=1, 2, . . .), respectively. Two types of end load P are considered. The first is that for which each load P acts at all times parallel to the undeformed axis of the beam, regardless of end slope or displacement (Euler column type loading); this constitutes conservative loading. The second is that for which, where an end is permitted lateral displacement and slope, the force acts along the tangent to the elastic curve at the end (a tangential follower force); this constitutes non-conservative loading.

For free vibration of the beam, the deflection may be written as $w(x)\sin\omega\tau$, where ω is the radian natural frequency of vibration and $w(x)$ the maximum deflection with respect to time τ. Then the maximum strain and kinetic energies associated with the beam motion, respectively, are

$$V_{max} = \frac{1}{2}\int_0^{\ell} EI(x)\left(\frac{\partial^2 w}{\partial x^2}\right)^2 dx - \frac{P}{2}\int_0^{\ell}\left(\frac{\partial w}{\partial x}\right)^2 dx, \tag{3.1}$$

$$T_{max} = \frac{\omega^2}{2}\int_0^{\ell} m(x)w^2 dx + \frac{\omega^2}{2}\sum_i \left[M_i w^2 + J_i\left(\frac{\partial w}{\partial x}\right)^2\right]_{x=x_i}, \tag{3.2}$$

where the last term of equation (3.2) represents the effect of rotary inertia of the concentrated masses, J_i being the

moment of inertia of the i'th mass about the y-axis.

Supplementary to the strain energy, for elastically restrained beams, there is an additional strain energy stored in the elastic restraining springs. The energy is given by

$$U_{max} = \sum_t \frac{k_t}{2} w^2 \Big|_{x=x_t} + \sum_r \frac{s_r}{2} \left(\frac{\partial w}{\partial x}\right)^2 \Big|_{x=x_r}. \tag{3.3}$$

The total maximum strain energy is, then, $V_{max} + U_{max}$.

The mathematical expressions for various boundary conditions are $w = dw/dx = 0$ for clamped boundary, $w = d^2w/dx^2 = 0$ for simply supported boundary and $d^2w/dx^2 = d^3w/dx^3 = 0$ for free boundary ($dw/dx = d^3w/dx^3 = 0$ for sliding boundary for uniform beams). When the elastic springs are attached at the ends, the boundary conditions are given by considering the equations relating to the shear force and bending moment at the ends. These conditions can be written as

$$\frac{d}{dx}\left(EI\frac{d^2w}{dx^2}\right)\Big|_{x=0} = k_t\, w\Big|_{x=0}, \quad EI\, d^2w/dx^2\Big|_{x=0} = s_r\, dw/dx\Big|_{x=0}, \tag{3.4 a,b}$$

$$\frac{d}{dx}\left(EI\frac{d^2w}{dx^2}\right)\Big|_{x=\ell} = -k_t w\Big|_{x=\ell}, \quad EI\, d^2w/dx^2\Big|_{x=\ell} = -s_r dw/dx\Big|_{x=\ell}. \tag{3.4 c,d}$$

It may be noted that the classical boundary conditions are special cases for which the spring constants approach zero and/or infinity such as, $k_t = s_r = 0$ for free, $k_t = s_r = \infty$ for clamped, and $k_t = \infty$ and $s_r = 0$ for simply supported ($k_t =$

0, $s_r = \infty$ for sliding). As an example, if $k_t = s_r = \infty$, the boundary conditions (3.4) can be rewritten as

$$w = \frac{1}{k_t}\frac{d}{dx}\left(EI\frac{d^2w}{dx^2}\right) = 0,\ dw/dx = \frac{1}{s_r}\ EI\, d^2w/dx^2 = 0,$$

which are the clamped boundary conditions.

Introducing a non-dimensionalized parameter $\xi = x/\ell$, the flexural rigidity and mass distribution can be expressed as

$$EI(\xi) = EI_0 f(\xi) \text{ and } m(\xi) = m_0 h(\xi), \tag{3.5}$$

where EI_0 and m_0, respectively, denote the stiffness and mass per unit length at $\xi = 0(x=0)$. The deflection w may be expressed as

$$w(\xi) = \sum_k A_k \Phi_k(\xi), \tag{3.6}$$

where $\Phi_k(\xi)$ are appropriate admissible functions for the Rayleigh-Ritz method. Then, equation (3.4) can be written as

$$\left[\frac{1}{f}\frac{df}{d\xi}\frac{d^2w}{d\xi^2} + \frac{d^3w}{d\xi^3}\right]\Big|_{\xi=0} = K_t w\Big|_{\xi=0},\ d^2w/d\xi^2\Big|_{\xi=0} = S_r dw/d\xi\Big|_{\xi=0}, \tag{3.7 a,b}$$

$$\left[\frac{1}{f}\frac{df}{d\xi}\frac{d^2w}{d\xi^2} + \frac{d^3w}{d\xi^3}\right]\Big|_{\xi=1} = -K_t w\Big|_{\xi=1},\ d^2w/d\xi^2\Big|_{\xi=1} = -S_r dw/d\xi\Big|_{\xi=1}, \tag{3.7 c,d}$$

where $K_t = k_t\ell^3/EI_0 f(\xi)$ and $S_r = s_r\ell/EI_0 f(\xi)$.

For the conservative system, substituting equations (3.5) and (3.6) into energy expressions (3.1), (3.2) and

(3.3), equating $V_{max} + U_{max} = -T_{max}$, and minimizing with respect to the coefficients A_k, according to the Rayleigh-Ritz procedure, leads to the eigenvalue equation

$$\sum_j [F_{kj} - \Omega^2 E_{kj}]A_j = 0, \tag{3.8}$$

where the frequency parameter $\Omega = (\omega^2 m_0 \ell^4/EI_0)^{1/2}$,

$$F_{kj} = \int_0^1 f(\xi)\Phi_k''(\xi)\Phi_j''(\xi)d\xi - p\int_0^1 \Phi_k'(\xi)\Phi_j'(\xi)d\xi$$

$$+ \sum_t K_t\Phi_k(\xi_t)\Phi_j(\xi_t) + \sum_r S_r\Phi_k'(\xi_r)\Phi_j'(\xi_r), \text{ and}$$

$$E_{kj} = \int_0^1 h(\xi)\Phi_k(\xi)\Phi_j(\xi) + \sum_i[\bar{M}_i\Phi_k(\xi_i)\Phi_j(\xi_i)$$

$$+ \bar{J}_i\Phi_k'(\xi_i)\Phi_j'(\xi_i)],$$

in which $\xi_i = x_i/\ell$, $\xi_t = x_t/\ell$, $\xi_r = x_r/\ell$, $p = P\ell^2/EI_0$, $\bar{M}_i = M_i/m_0\ell$, $\bar{J}_i = J_i/m_0\ell^3$. The prime denotes the differentiation with respect to ξ. The solution of equation (3.8) yields the natural frequencies of vibration of the beam together with the coefficients for the mode shape (3.6).

For beams for which the end loading P is non-conservative (the follower force case), an additional term accommodating the work done by force P must be included in the Rayleigh-Ritz procedure [195]. This may be written

$$\delta[\text{Work done}) = P[\frac{\partial w}{\partial x}\Big|_{x=\ell}\delta w(\ell) - \frac{\partial w}{\partial x}\Big|_{x=0}\delta_w(0)].$$

Accordingly, the expression F_{kj} in equation (3.8) includes an additional term $p[\Phi_k(1)\Phi_j'(1) - \Phi_k(0)\Phi_j'(0)]$.

It may be noted that, in matrix form, equation (3.8) may be written

$$[F]\{A\} - \Omega^2[E]\{A\} = 0, \tag{3.9}$$

where [F] and [E] are real, symmetrical matrices for conservative systems but that [F] becomes non-symmetrical when a non-conservative, follower force exists. Further, taking appropriate orthogonal or orthonormal functions as the admissible functions, [E] can be reduced to a diagonal or unit matrix, which results in computational advantage.

As mentioned earlier, the rate of convergence and accuracy of the Rayleigh-Ritz method depends upon the choice of the admissible functions. In this work, the BCOP explained in Chapter 2 are used as the functions.

For single-span beams, the starting functions may be written

$$\Phi_1(\xi) = \sum_{i=1}^{5} a_i \xi^{i-1}, \tag{3.10}$$

where, for monic polynomials, the coefficients a_i are given in Table 2.1, and, then, the function $\Phi_1(\xi)$ satisfies both

geometrical and natural boundary conditions of the beam with classical boundary conditions (and sliding boundary condition of uniform beams). As explained in Chapter 2, an alternative set of starting functions, which satisfy the geometrical boundary condition only, can be used as well. However, in this chapter (and also in the following chapters), the starting functions satisfying both geometrical and natural boundary conditions are used, since the satisfaction of the natural boundary condition is a desired property, though it is not a necessary requirement. It may be noted that equation (3.10), with the coefficients given in Table 2.1, can be used as the starting admissible functions not only for beams with classical boundary conditions, but also for beams with elastically restrained ends neglecting the elastic springs, remembering the effect of the springs is included in the energy expression. For beams with elastically restrained ends, though, an alternative starting function may be constructed, considering the boundary conditions including the effect of the springs, as in equations (3.4) or (3.7). Then, the starting function can be expressed again as in equation (3.10), with the coefficients a_i determined from

$$\begin{vmatrix} K_0 & 0 & -2f_0 & -6 \\ 0 & S_0 & -2 & 0 \\ K_\ell & K_\ell & K_\ell+2f_1 & K_\ell+6+6f_1 \\ 0 & S_\ell & 2S_\ell+2 & 3S_\ell+6 \end{vmatrix} \begin{Bmatrix} a_1 \\ a_2 \\ a_3 \\ a_4 \end{Bmatrix} = - \begin{Bmatrix} 0 \\ 0 \\ k_\ell+24+12f_1 \\ 4S_\ell+12 \end{Bmatrix} a_5, \tag{3.11}$$

where $f_0=f'(0)/f(0)$ and $f_1=f'(1)/f(1)$, and

taking one of the non-zero coefficients a_i to be an arbitrary value. The subscripts 0 and ℓ denote the left and the right end of the beam, respectively. It may be noted that the coefficients given in Table 2.I are special cases for which the spring constants in equation (3.11) approach zero and/or infinity, as may be expected from the boundary conditions explained before.

For multi-span beams, the starting functions are given, recurrently, by multiplying the functions given by equation (3.10), with the coefficients given in Table (2.1) or equation (3.11), by the factor $(\xi-\ell_j/\ell)$.

The generating function $g(\xi)$ is chosen such that the polynomials generated satisfy at least the geometrical boundary conditions (In the following sections, the simple polynomial ξ is used for $g(\xi)$ to obtain numerical results, except where indicated). Then using the recurrence formula (2.6) or (2.8), replacing the coordinate x with ξ, taking the weight function $w_f(\xi) = h(\xi)$ (see the following alternative procedure), the desired number of BCOP are generated. It may be noted that, using these BCOP as the admissible functions in equation (3.6), for beams with no concentrated mass, the matrix [E] becomes a diagonal or a unit matrix. Even for beams with concentrated masses, this can be maintained if the following alternative procedure is used for the generation of the subsequent polynomials.

Consider the case of beams with point masses (no rotary inertia), then the orthogonality condition may be expressed, considering the real vibration modes, as

$$\int_0^{\ell} m(x)\Phi_r(x)\Phi_s(x)dx + \sum_i M_i\Phi_r(x_i)\Phi_s(x_i) = c_r\delta_{rs};\ r,s=1,2,3\ldots, \tag{3.12 a}$$

where c_r is a constant and δ_{rs} the Kronecker delta. This equation can be rewritten, in non-dimensionalized form, as

$$\int_0^1 h(\xi)\Phi_r(\xi)\Phi_s(\xi)d\xi + \sum_i \bar{M}_i\Phi_r(\xi_i)\Phi_s(\xi_i) = \bar{c}_r\delta_{rs}, \tag{3.12 b}$$

where $\bar{c}_r$ is a constant ($\bar{c}_r = c_r/m_0\ell$). Using equation (3.12 b), the constants B_n and C_n in the equation

$$\Phi_{n+1}(\xi) = \{g(\xi) - B_n\}\Phi_n(\xi) - C_n\Phi_{n-1}(\xi);\ n=1,2,3,\ldots \tag{3.13}$$

are given as

$$B_n = \frac{[\int_0^1 h(\xi)g(\xi)\Phi_n^2(\xi)d\xi + \sum_i \bar{M}_i g(\xi_i)\Phi_n^2(\xi_i)]}{[\int_0^1 h(\xi)\Phi_n^2(\xi)d\xi + \sum_i \bar{M}_i\Phi_n^2(\xi_i)]},$$

$$C_n = \frac{[\int_0^1 h(\xi)\Phi_n^2(\xi)d\xi + \sum_i \bar{M}_i\Phi_n^2(\xi_i)]}{[\int_0^1 h(\xi)\Phi_{n-1}^2(\xi)d\xi + \sum \bar{M}_i\Phi_{n-1}^2(\xi_i)]}.$$

The admissible functions so generated differ from those described earlier but lead to a new [F] matrix (symmetrical for conservative systems) and a new diagonal [E] matrix (again the latter is a unit matrix, if appropriate normalization is used). The solution obtained from the new eigenvalue problem is identical to that obtained using the original approach. In the event that rotary inertia of the concentrated masses (and/or the beam) is to be included, conceptually the same sort of procedure may be used. However, the simple recurrence formula (3.13) then yields a set of functions in which each function is orthogonal only to its immediate neighbors, the overall orthogonality not being maintained. For such cases, then, there is no advantage in using this formulation over the straightforward relationships (2.6) and (2.8) (replacing x with ξ), in which the concentrated masses are neglected in the recurrence formula, since both approaches yield symmetrical matrices [E] and identical numerical results. The overall orthogonality may be maintained by using the procedure explained in section 2.1.2 but at the expense of considerably more work, which makes this alternative approach unattractive for such problems.

In the following sections, in order to demonstrate the applicability and accuracy of the approach presented, a number of different beam problems have been considered for which comparison results are available in the literature. In

addition, a selection of results for problems not previously treated is presented, further serving to illustrate the versatility of the method and to provide new information which may be of interest to other workers in the field.

3.3. BEAMS WITH NO ELASTIC SPRING

3.3.1 Beams of Uniform Cross Section

The first problem considered in this section is the vibration problem of single span beams without any complicating factors. These beams were treated as the starting step for the investigation of the accuracy of the present approach. The values for frequency parameters, displacement (w), slope ($\ell dw/dx$), bending moment ($\ell^2 d^2w/dx^2$) and shear force ($\ell^3 d^3w/dx^3$) for the lowest four non-rigid body modes, for two sample cases, are shown in Table 3.1-3.4, in comparison with the exact solutions. The frequency parameters obtained agreed with the 'exact' parameters to the number of figures given, except where shown. For the cantilever beam, the values were obtained using 10 terms in the deflection series (3.6), while those for the free beam were obtained using 12 terms including the two rigid body modes. The values for displacement are normalized ($\int_0^\ell w(x)dx=\ell$ or $\int_0^1 w(\xi)d\xi = 1$) and the remaining values are based on this normalization. It may be seen that the present values for displacements and slopes are, for all the modes presented, in excellent agreement with those from the

Table 3.1

The values for displacement and slope for a cantilever beam.

x/ℓ	Present w	Present $\ell dw/dx$	Exact w	Exact $\ell dw/dx$
(1) First mode: Ω = 3.51602				
0.00	0.000000	0.000000	0.000000	0.000000
0.10	0.033547	0.654812	0.033547	0.654812
0.20	0.127742	1.213035	0.127742	1.213035
0.30	0.272966	1.675665	0.272966	1.675665
0.40	0.459769	2.045180	0.459769	2.045180
0.50	0.679046	2.326109	0.679046	2.326109
0.60	0.922269	2.525491	0.922269	2.525491
0.70	1.181753	2.653224	1.181753	2.653224
0.80	1.450955	2.722313	1.450955	2.722313
0.90	1.724799	2.749032	1.724799	2.749032
1.00	2.000000	2.753011	2.000000	2.753011
(2) Second mode: Ω = 22.0345				
0.00	0.000000	0.000000	0.000000	0.000000
0.10	0.185259	3.355119	0.185259	3.355119
0.20	0.602110	4.648094	0.602110	4.648093
0.30	1.052266	4.070100	1.052266	4.070102
0.40	1.366939	2.022843	1.366939	2.022841
0.50	1.427332	-0.906285	1.427332	-0.906284
0.60	1.178952	-4.038799	1.178952	-4.038798
0.70	0.634104	-6.741868	0.634104	-6.741870
0.80	-0.140072	-8.575275	-0.140072	-8.575273
0.90	-1.047504	-9.419051	-1.047504	-9.419051
1.00	-2.000000	-9.561557	-2.000000	-9.561557
(3) Third mode: Ω = 61.6972				
0.00	0.000000	0.000000	0.000000	0.000000
0.10	0.456158	7.531075	0.456138	7.531061
0.20	1.208980	6.236149	1.209012	6.236236
0.30	1.512511	-0.709505	1.512479	-0.710149
0.40	1.051852	-8.120782	1.051849	-8.119800
0.50	0.039392	-11.103559	0.039375	-11.103998
0.60	-0.947492	-7.581857	-0.947530	-7.582407
0.70	-1.314850	0.712641	-1.314852	0.713595
0.80	-0.789774	9.471486	-0.789747	9.470843
0.90	0.457037	14.676546	0.457015	14.676934
1.00	2.000000	15.697335	2.000000	15.697332
(4) Fourth mode: Ω = 120.903 (Exact = 120.902)				
0.00	0.000000	0.000000	0.000000	0.000000
0.10	0.769579	11.123304	0.770016	11.126808
0.20	1.508392	1.218760	1.507581	1.211337
0.30	0.867084	-13.013771	0.867739	-12.991616
0.40	-0.631547	-13.978973	-0.631119	-14.005636
0.50	-1.412769	-0.095520	-1.414237	-0.090075
0.60	-0.654046	13.680260	-0.652990	13.705161
0.70	0.794366	12.202196	0.794781	12.169426
0.80	1.287229	-3.670921	1.286075	-3.653560
0.90	0.103303	-18.442543	0.104067	-18.451499
1.00	-2.000147	-21.993476	-2.000000	-21.991819

Table 3.2

The values for bending moment and shear force for a cantilever beam.

	Present		Exact	
x/ℓ	$\ell^2 d^2w/dx^2$	$\ell^3 d^3w/dx^3$	$\ell^2 d^2w/dx^2$	$\ell^3 d^3w/dx^3$
(1) First mode				
0.00	7.032031	-9.679701	7.032031	-9.679629
0.10	6.064420	-9.665638	6.064420	-9.665638
0.20	5.101581	-9.571694	5.101581	-9.571693
0.30	4.155060	-9.328772	4.155060	-9.328774
0.40	3.242712	-8.879667	3.242712	-8.879664
0.50	2.387537	-8.178633	2.387537	-8.178634
0.60	1.616554	-7.190883	1.616554	-7.190885
0.70	0.959752	-5.891668	0.959752	-5.891664
0.80	0.449142	-4.265045	0.449142	-4.265049
0.90	0.117952	-2.302332	0.117952	-2.302329
1.00	0.000001	0.000052	0.000000	0.000000
(2) Second mode				
0.00	44.069143	-210.702966	44.068983	-210.684043
0.10	23.081258	-207.543945	23.081208	-207.544009
0.20	3.086366	-188.951948	3.086409	-188.951788
0.30	-13.972122	-148.552984	-13.972150	-148.553675
0.40	-25.977599	-88.993708	-25.977605	-88.992852
0.50	-31.450564	-19.969183	-31.450528	-19.969507
0.60	-30.119771	44.572784	-30.119804	44.572267
0.70	-23.186142	89.681672	-23.186142	89.682618
0.80	-13.267219	102.419175	-13.267187	102.418373
0.90	-4.082035	73.927489	-4.082079	73.928343
1.00	0.000161	0.016380	0.000000	0.000000
(3) Third mode				
0.00	123.310660	-958.570320	123.394429	-968.481664
0.10	28.170233	-905.549222	28.196564	-905.525943
0.20	-48.702294	-584.254329	-48.725212	-584.324649
0.30	-81.138184	-44.382555	-81.122696	-44.026821
0.40	-58.4[illegible]321	468.273060	-58.459991	467.813366
0.50	2.448258	684.890951	2.429340	685.085750
0.60	64.878504	500.723145	64.896169	500.969025
0.70	93.316597	44.298281	93.315724	43.814224
0.80	74.607284	-385.184459	74.592669	-384.758377
0.90	28.121932	-464.191217	28.142432	-464.645490
1.00	0.075285	7.493549	0.000000	0.000000
(4) Fourth mode				
0.00	243.372168	-2825.382916	241.803832	-2658.853096
0.10	-12.045367	-2224.720623	-12.581857	-2230.821535
0.20	-156.000046	-448.341298	-155.488968	-441.722447
0.30	-95.827032	1483.781153	-96.090574	1471.306980
0.40	79.211899	1644.779423	78.947736	1656.980200
0.50	170.325919	-9.326997	170.983998	-10.890197
0.60	76.763297	-1681.352099	76.303507	-1693.308222
0.70	-104.739894	-1587.476133	-104.911314	-1570.711281
0.80	-182.932269	158.266739	-182.269773	146.459005
0.90	-92.278915	1332.986501	-93.096430	1345.252379
1.00	2.863190	299.323044	0.000000	0.000000

Table 3.3

The values for displacement and slope for a free beam.

x/ℓ	Present w	Present $\ell dw/dx$	Exact w	Exact $\ell dw/dx$
(1) First mode: Ω = 22.3733				
0.00	2.000000	-9.294551	2.000000	-9.294551
0.10	1.074329	-9.147073	1.074329	-9.147073
0.20	0.195454	-8.268756	0.195453	-8.268757
0.30	-0.544009	-6.341737	-0.544009	-6.341735
0.40	-1.040495	-3.453261	-1.040495	-3.453263
0.50	-1.215644	0.000000	-1.215644	0.000000
0.60	-1.040495	3.453261	-1.040495	3.453263
0.70	-0.544009	6.341737	-0.544009	6.341735
0.80	0.195454	8.268756	0.195453	8.268757
0.90	1.074329	9.147073	1.074329	9.147073
1.00	2.000000	9.294551	2.000000	9.294551
(2) Second mode: Ω = 61.6728				
0.00	2.000000	-15.718618	2.000000	-15.718618
0.10	0.454856	-14.699323	0.454859	-14.699364
0.20	-0.794494	-9.502577	-0.794499	-9.502515
0.30	-1.324030	-0.775263	-1.324024	-0.775260
0.40	-0.966053	7.446761	-0.966058	7.446655
0.50	0.000000	10.800564	0.000000	10.800724
0.60	0.966053	7.446761	0.966058	7.446655
0.70	1.324030	-0.775263	1.324024	-0.775260
0.80	0.794494	-9.502577	0.794499	-9.502515
0.90	-0.454856	-14.699323	-0.454859	-14.699364
1.00	-2.000000	-15.718618	-2.000000	-15.718618
(3) Third mode: Ω = 120.906 (Exact = 120.903)				
0.00	2.000169	-21.992493	2.000000	-21.990478
0.10	-0.103083	-18.443048	-0.103929	-18.449989
0.20	-1.287153	-3.666267	-1.285727	-3.650426
0.30	-0.793037	12.217337	-0.793862	12.178967
0.40	0.656716	13.697934	0.655687	13.734831
0.50	1.420287	0.000000	1.422381	0.000000
0.60	0.656716	-13.697934	0.655687	-13.734831
0.70	-0.793037	-12.217337	-0.793862	-12.178967
0.80	-1.287153	3.666267	-1.285727	3.650426
0.90	-0.103083	18.443048	-0.103929	18.449989
1.00	2.000169	21.992493	2.000000	21.990478
(4) Fourth mode: Ω = 199.886 (Exact = 120.859)				
0.00	2.001236	-28.293500	2.000000	-28.274372
0.10	-0.585793	-19.665436	-0.588020	-19.613393
0.20	-1.205772	8.316857	-1.200922	8.240041
0.30	0.458726	18.816970	0.451357	18.810297
0.40	1.394323	-3.308794	1.400097	-3.180009
0.50	0.000000	-19.830637	0.000000	-20.017060
0.60	-1.394323	-3.308794	-1.400097	-3.180009
0.70	-0.458726	18.816970	-0.451357	18.810297
0.80	1.205772	8.316857	1.200922	8.240041
0.90	0.585793	-19.665436	0.588020	-19.613393
1.00	-2.001236	-28.293500	-2.000000	-28.274372

Table 3.4

The values for bending moment and shear force for a free beam.

	Present		Exact	
x/ℓ	$\ell^2 d^2w/dx^2$	$\ell^3 d^3w/dx^3$	$\ell^2 d^2w/dx^2$	$\ell^3 d^3w/dx^3$
(1) First mode				
0.00	0.000189	-0.020702	0.000000	0.000[illegible]
0.10	4.230927	76.889318	4.230869	76.888[illegible]
0.20	13.857790	108.304251	13.857837	108.304878
0.30	24.521137	98.777722	24.521118	98.776659
0.40	32.563224	57.910740	32.563199	57.911637
0.50	35.532001	0.000000	35.532050	0.000000
0.60	32.563224	-57.910740	32.563199	-57.911637
0.70	24.521137	-98.777722	24.521118	-98.776659
0.80	13.857790	-108.304251	13.857837	-108.304878
0.90	4.230927	-76.889318	4.230869	-76.888724
1.00	0.000189	0.020702	0.000000	0.000000
(2) Second mode				
0.00	0.014566	-1.901500	0.000000	0.000000
0.10	28.110984	463.812294	28.106656	463.871279
0.20	74.419749	382.812444	74.423387	382.762291
0.30	92.852392	-48.022956	92.848608	-48.025449
0.40	63.801799	-509.913574	63.804493	-509.854219
0.50	0.000000	-704.226669	0.000000	-704.311515
0.60	-63.801799	-509.913574	-63.804493	-509.854219
0.70	-92.852392	-48.022956	-92.848608	-48.025449
0.80	-74.419749	382.812444	-74.423387	382.762291
0.90	-28.110984	463.812294	-28.106656	463.871279
1.00	-0.014566	-1.901500	0.000000	0.000000
(3) Third mode				
0.00	-3.143230	337.737863	0.000000	0.000000
0.10	92.135321	1334.132939	93.101989	1345.384372
0.20	183.151712	158.712601	182.301341	146.892318
0.30	104.683772	-1589.606438	105.020676	-1569.463822
0.40	-76.465184	-1672.643420	-75.971081	-1689.661179
0.50	-169.066751	0.000000	-169.989983	0.000000
0.60	-76.465184	1672.643420	-75.971081	1689.661179
0.70	104.683772	1589.606438	105.020676	1569.463822
0.80	183.151712	-158.712601	182.301341	-146.892318
0.90	92.135321	-1334.132939	93.101989	-1345.384372
1.00	-3.143230	-337.737863	0.000000	0.000000
(4) Fourth mode				
0.00	-14.055400	1800.779411	0.000000	0.000000
0.10	210.517832	2600.840094	214.746965	2545.394656
0.20	267.730254	-2034.883338	263.659873	-1981.251850
0.30	-88.909382	-3847.065256	-84.475804	-3841.022446
0.40	-275.383345	686.764068	-278.506117	614.603915
0.50	0.000000	3889.610422	0.000000	3990.975688
0.60	275.383345	686.764068	278.506117	614.603915
0.70	88.909382	-3847.065256	84.475804	-3841.022446
0.80	-267.730254	-2034.883338	-263.659873	-1981.251850
0.90	-210.517832	2600.840094	-214.746965	2545.394656
1.00	14.055400	1800.779411	0.000000	0.000000

exact solutions, but the values for bending moment and shear force are relatively less satisfactory, particularly for higher modes. The trend is similar for beams with other boundary conditions, as may be expected. The accuracy will be increased by using increased number of terms in the series.

The second problem treated is that of two-span continuous beams, again with no other complicating factor. The positions of the intermediate supports are considered to be located at ℓ_1/ℓ = 0.25, 0.5 or 0.75. The first five natural frequency parameters for the simply supported-simply supported-free beam with ℓ_1/ℓ = 0.5, as an example, are shown in Table 3.5, as computed using different numbers of terms in the series (3.6). Comparison values from the work of Greif and Mittendorf [38] (who used a component mode analysis) are given together with 'exact' results calculated by the writer directly from the solution of the slender beam differential equation. It may be seen that the convergence of the present results is reasonably rapid with quite close agreement with the comparison values being achieved. In Figures 3.2-3.5, the first five mode shapes (for the beam with both ends free, the rigid body rotation mode is excluded) are shown in graphical form, the results being obtained using 16 terms in the series. In addition, for the clamped-simply supported-free beam with ℓ_1/ℓ = 0.5, the values for displacement (normalized), slope, bending moment and shear force for the lowest four modes are presented in Table 3.6 in comparison

Table 3.5

Frequency parameters $(\omega^2 m_o \ell^4/EI_o)^{\frac{1}{2}}$ for a two-span beam, simply supported at $x = 0$ and $x = \ell/2$ and free at $x = \ell$.

No. of terms in ϕ_1	Mode Sequence Number				
	1	2	3	4	5
6	9.0905	46.817	83.863	185.51	471.61
8	9.0801	46.692	80.000	173.34	264.64
10	9.0756	46.646	79.333	172.09	238.43
12	9.0737	46.625	79.083	171.73	233.73
14	9.0728	46.615	78.961	171.59	232.37
16	9.0723	46.610	78.902	171.50	231.83
Ref. [38]	9.0714	46.597	78.757	-	-
Exact	9.0711	46.597	78.758	171.32	230.60

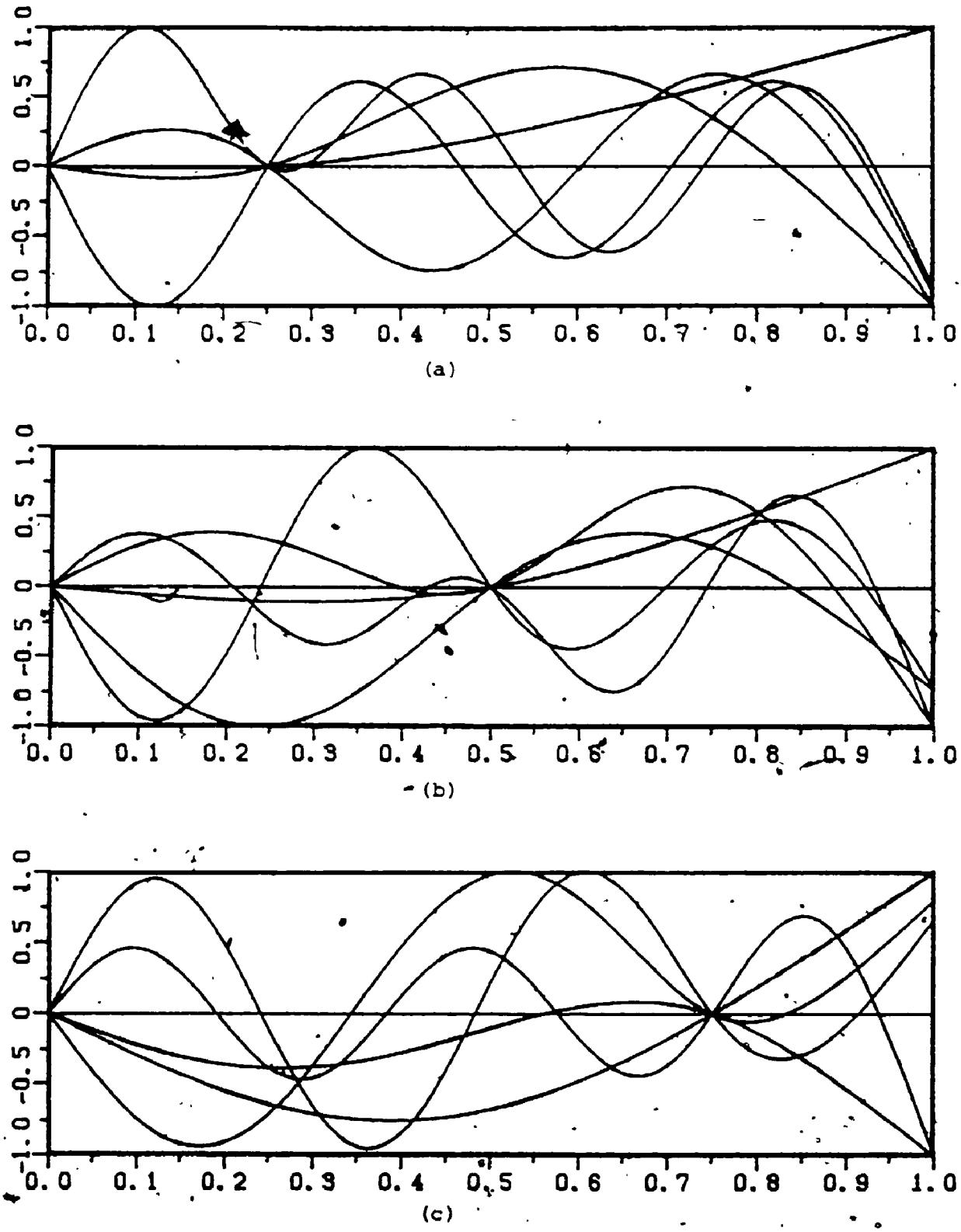

Figure 3.2. Mode shapes for two span beams with ends simply supported and free, and the intermediate support at (a) $\ell_1/\ell = 0.25$; (b) $\ell_1/\ell = 0.5$; (c) $\ell_1/\ell = 0.75$.

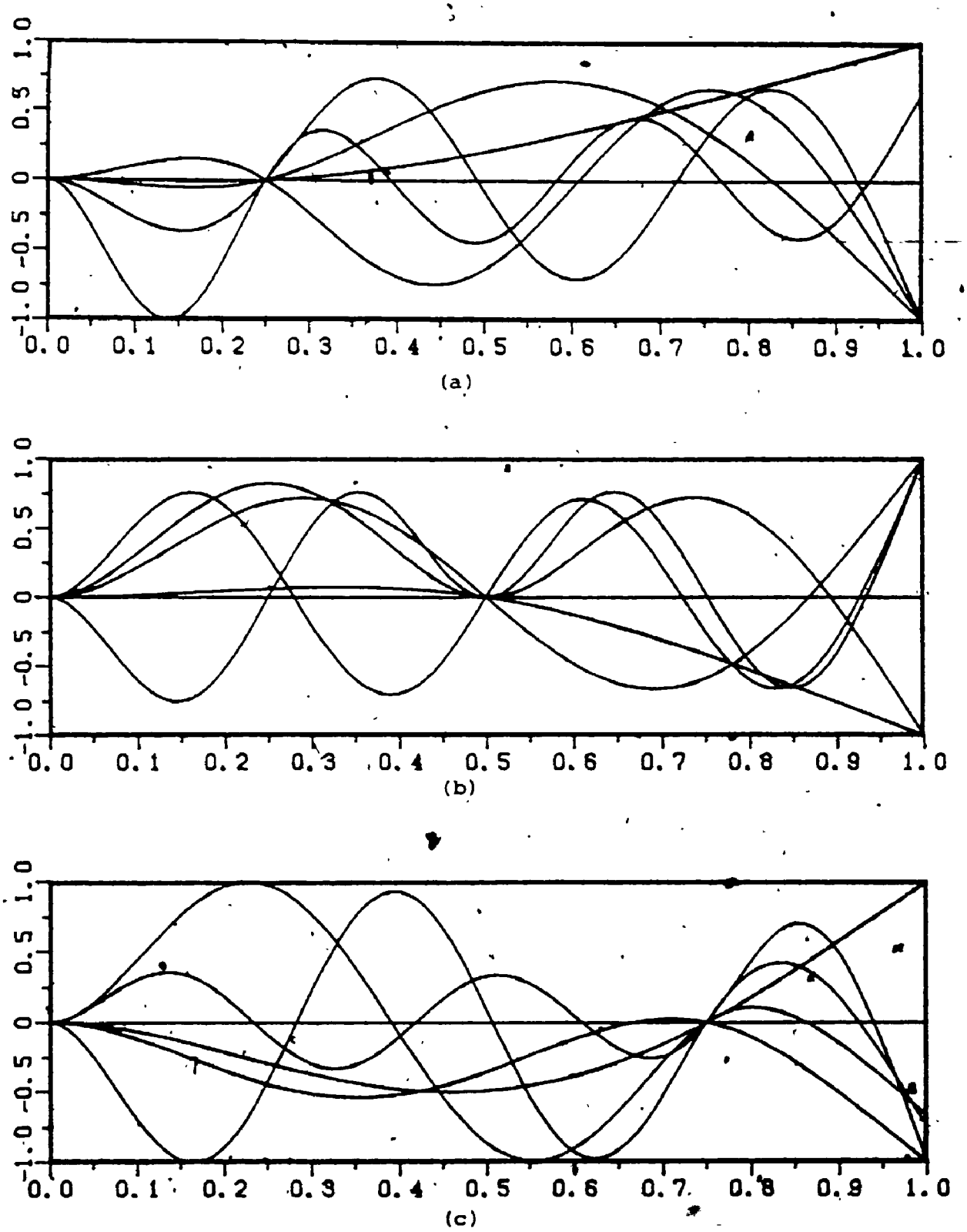

Figure 3.3. Mode shapes for two span beams with ends clamped and free, and the intermediate support at (a) $\ell_1/\ell = 0.25$; (b) $\ell_1/\ell = 0.5$; (c) $\ell_1/\ell = 0.75$.

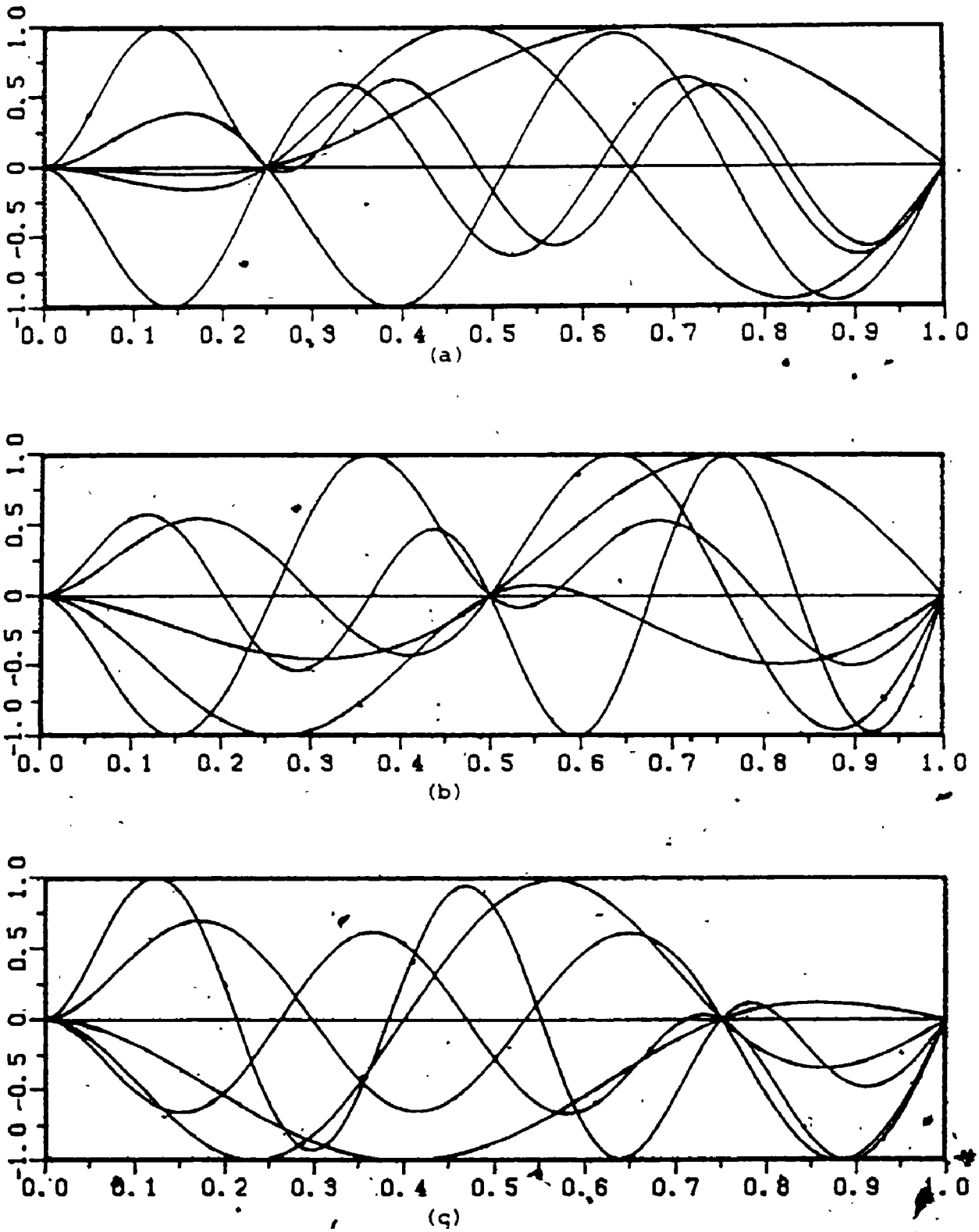

Figure 3.4. Mode shapes for two span beams with ends clamped and simply supported, and the intermediate support at (a) $\ell_1/\ell = 0.25$; (b) $\ell_1/\ell = 0.5$; (c) $\ell_1/\ell = 0.75$.

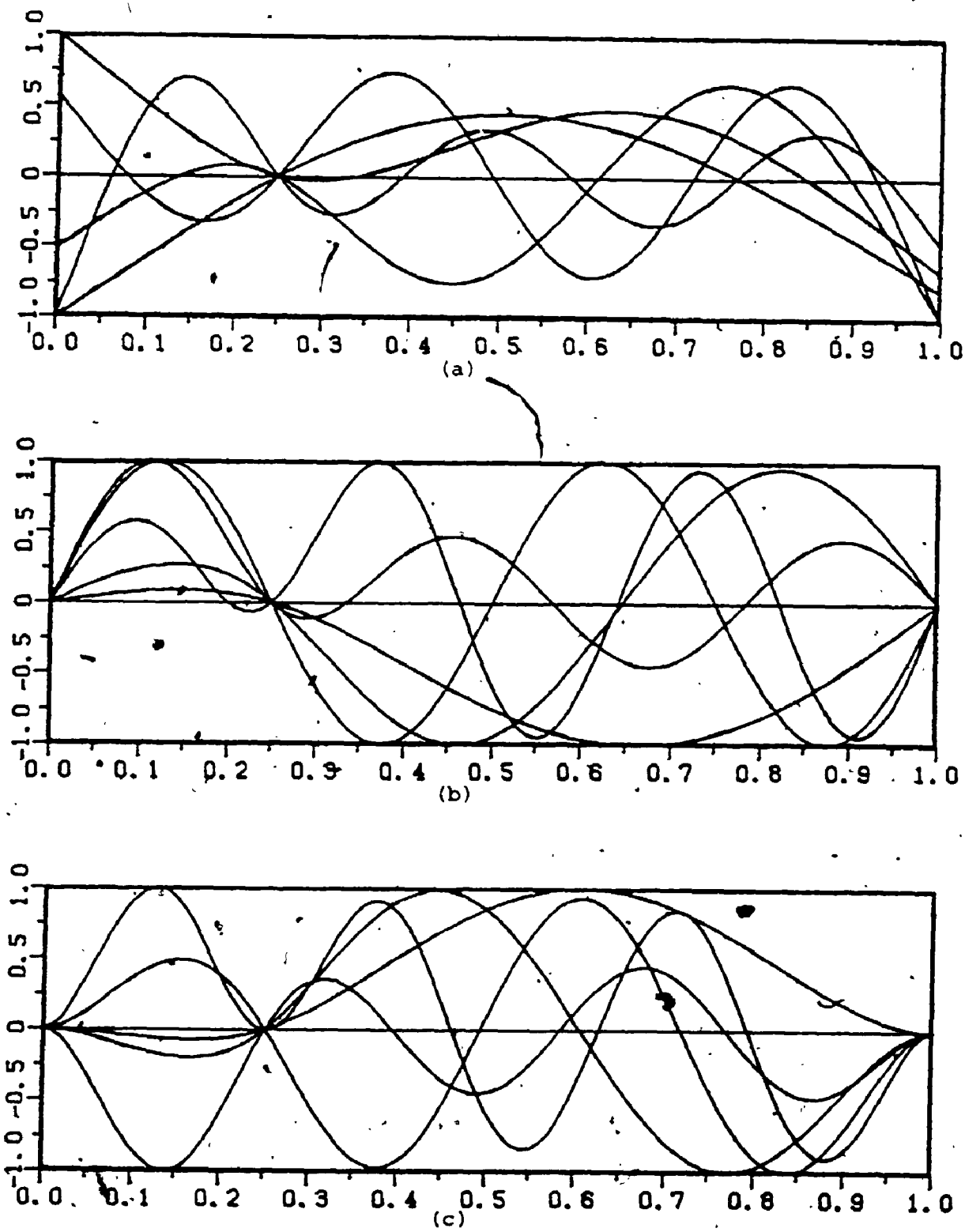

Figure 3.5. Mode shapes for two span beams with both ends the same boundary conditions and the intermediate support at $\ell_1/\ell = 0.25$, (a) free ends; (b) simply supported ends; (c) clamped ends.

Table 3.6

The values for displacement, slope, bending moment and shear force for a two span beam; clamped at x=0, simply supported at x=0.5ℓ and free at x=ℓ.

	Present		Exact	
x/ℓ	w	ℓdw/dx	w	ℓdw/dx
(1) First mode: Ω = 9.8713 (Exact = 9.8696)				
0.00	0.00000	0.00000	0.00000	0.00000
0.10	0.04087	0.71624	0.04085	0.71372
0.20	0.12217	0.81006	0.12213	0.80928
0.30	0.18260	0.29185	0.18236	0.29463
0.40	0.16152	-0.80802	0.16121	-0.81540
0.50	0.00000	-2.50474	0.00000	-2.50408
0.60	-0.33932	-4.20092	-0.33965	-4.19480
0.70	-0.82037	-5.33342	-0.82057	-5.33532
0.80	-1.39015	-5.98363	-1.39020	-5.98217
0.90	-2.00412	-6.24528	-2.00408	-6.24301
1.00	-2.63155	-6.28447	-2.63138	-6.28319
(2) Second mode: Ω = 61.673 (Exact = 61.673)				
0.00	0.00000	0.00000	0.00000	0.00000
0.10	0.44292	7.31141	0.44286	7.30899
0.20	1.17279	6.03198	1.17265	6.03099
0.30	1.46325	-0.75890	1.46297	-0.75671
0.40	1.00560	-8.02939	1.00534	-8.03352
0.50	0.00000	-11.09801	0.00000	-11.09748
0.60	-0.99234	-7.65468	-0.99260	-7.65126
0.70	-1.36017	0.79805	-1.36040	0.79656
0.80	-0.81623	9.76200	-0.81633	9.76360
0.90	0.46731	15.10053	0.46736	15.10324
1.00	2.05469	16.14832	2.05495	16.15050
(3) Third mode: Ω = 88.988 (Exact = 88.826)				
0.00	0.00000	0.00000	0.00000	0.00000
0.10	0.62851	9.77334	0.62674	9.81045
0.20	1.48166	5.30987	1.47739	5.31946
0.30	1.48486	-5.08642	1.48716	-5.14376
0.40	0.63723	-10.09104	0.64502	-9.84321
0.50	0.00000	-0.31638	0.00000	-0.33863
0.60	0.56903	9.35755	0.57685	9.14366
0.70	1.33645	4.07321	1.33739	4.10756
0.80	1.16745	-7.85383	1.16370	-7.86923
0.90	-0.12999	-16.88994	-0.13098	-16.88474
1.00	-1.96689	-18.89385	-1.96375	-18.84956
(4) Fourth mode: Ω = 199.86 (Exact = 199.86)				
0.00	0.00000	0.00000	0.00000	0.00000
0.10	1.07575	12.75115	1.07578	12.75125
0.20	1.32076	-9.92481	1.32081	-9.92516
0.30	-0.42316	-19.24161	-0.42318	-19.24175
0.40	-1.39512	3.08010	-1.39519	3.07888
0.50	0.00000	19.99281	0.00000	19.99294
0.60	1.39848	3.17521	1.39841	3.17618
0.70	0.45083	-18.78785	0.45081	-18.78763
0.80	-1.19952	-8.23047	-1.19947	-8.23011
0.90	-0.58733	19.59028	-0.58731	19.58976
1.00	1.99766	28.24128	1.99759	28.24031

Table 3.6 (continued).

x/ℓ	Present $\ell^2 d^2w/dx^2$	Present $\ell^3 d^3w/dx^3$	Exact $\ell^2 d^2w/dx^2$	Exact $\ell^3 d^3w/dx^3$
(1) First mode				
0.00	9.82263	68.94051	10.23706	-62.01255
0.10	4.09312	-68.53000	4.03946	-61.87152
0.20	-1.98156	-60.30914	-2.11507	-61.08547
0.30	-8.26002	-54.70642	-8.15235	-59.56067
0.40	-14.03291	-68.53104	-14.01861	-57.79721
0.50	-18.70039	0.83438	-19.73921	-56.87496
0.60	-14.13368	64.48150	-14.09992	55.35794
0.70	-8.87130	46.08518	-8.80293	49.79964
0.80	-4.23401	38.95710	-4.31242	39.08453
0.90	-1.16501	25.94725	-1.17963	22.57382
1.00	-0.15384	-49.61264	0.00000	0.00000
(2) Second mode				
0.00	119.59650	-854.49107	119.86084	-942.02339
0.10	27.29762	-885.50078	27.25987	-880.93909
0.20	-47.53173	-569.03054	-47.61463	-569.48974
0.30	-79.42922	-43.17876	-79.34930	-46.46167
0.40	-57.90628	439.22267	-57.89625	446.28115
0.50	0.71044	686.03976	0.00000	647.29192
0.60	65.53493	529.84340	65.55757	523.86287
0.70	95.34627	46.81854	95.39970	49.34499
0.80	76.51278	-393.32911	76.46823	-393.27899
0.90	28.88542	-474.30827	28.87891	-476.61651
1.00	-0.10285	-33.17485	0.00000	0.00000
(3) Third mode				
0.00	193.80601	-5551.63720	180.81577	-1674.33894
0.10	16.66552	-1300.99926	18.22790	-1491.40943
0.20	-97.95686	-654.88278	-93.60170	-630.83317
0.30	-91.86865	468.86446	-94.76493	608.87867
0.40	16.06228	1803.15721	15.43391	1481.90485
0.50	147.42641	-24.99001	177.65288	1674.06873
0.60	15.70172	-1782.58393	14.54245	-1508.68216
0.70	-100.35135	-613.77458	-101.99718	-719.51086
0.80	-122.35795	351.26358	-119.49293	847.13175
0.90	-53.52908	718.76585	-52.83010	814.35552
1.00	4.53508	1463.19202	0.00000	0.00000
(4) Fourth mode				
0.00	400.11343	-5634.89174	400.19991	-5657.70062
0.10	-117.65032	-3925.64971	-117.66285	-3924.63913
0.20	-240.27325	1648.90728	-240.30441	1648.83180
0.30	90.29610	3764.66435	90.31660	3763.93957
0.40	280.14994	-638.07984	280.15926	-636.31968
0.50	0.18275	-3995.62303	0.00000	-4005.41276
0.60	-278.18356	-612.42095	-278.17056	-613.86342
0.70	-84.38626	3835.90016	-84.37402	3836.39463
0.80	263.36399	1978.93041	263.34220	1978.86476
0.90	214.49744	-2541.90024	214.48823	-2542.32786
1.00	-0.02156	-7.06428	0.00000	0.00000

with the exact values calculated by the author. The values for displacement and slope are in close agreement; the agreement for bending moment and shear force is somewhat poorer in some instances, especially in the region of the boundaries. The bending moment and shear force are represented graphically in Figures 3.6 and 3.7.

The third problem treated is that of a three-span continuous beam, again carrying neither concentrated mass nor axial load, the support conditions at $x=0$ and $x=\ell$ being either both simply supported or both clamped, with various combinations of the location of the two intermediate simple supports. The first three frequency parameters for each case are given in Table 3.7, together with 'exact' results from the excellent work of Gorman [41]. It may be seen that the agreement between Gorman's results and those of the present work, which were computed using ten terms in the deflection series, is again reasonably good; it could be improved by taking more terms in the series (3.6).

The fourth problem considered is that of a cantilever beam with one or more attached concentrated mass(es), with or without rotary inertia. The case where the mass is located at the tip has been studied fairly extensively, with 'exact' results being given by To [48], amongst others. It was therefore considered appropriate to use the present analysis to calculate some frequency parameters for this case for comparison with exact values. Such a comparison is made in

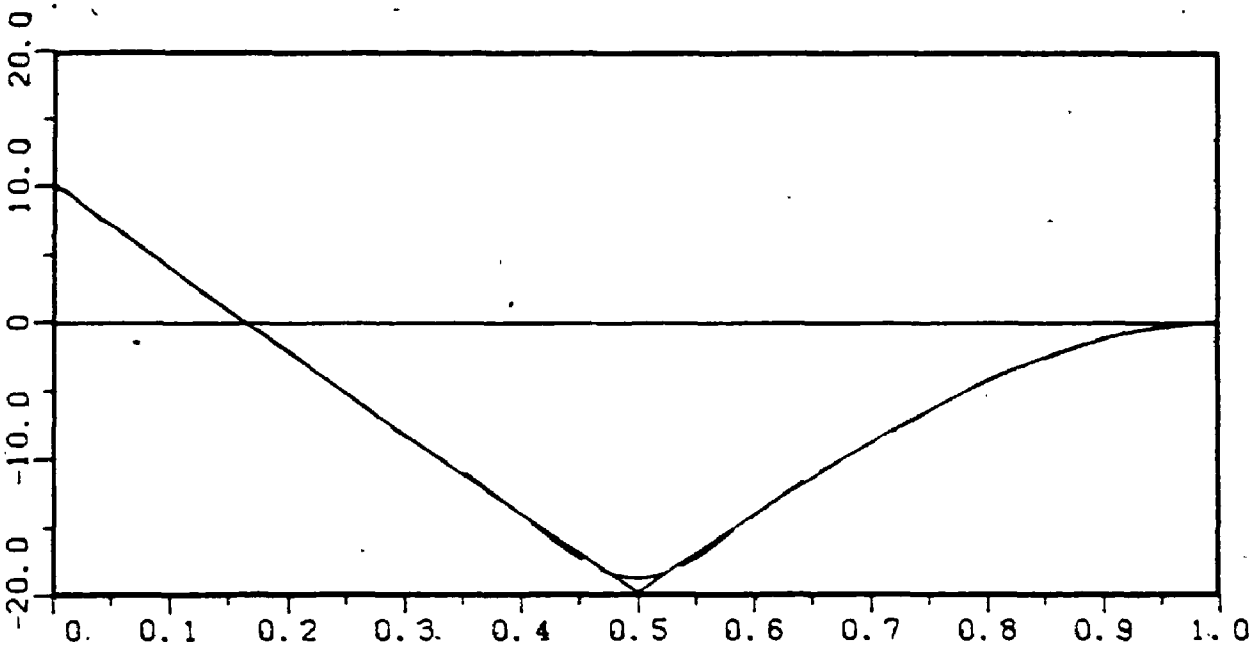

Figure 3.6. (a) First Mode

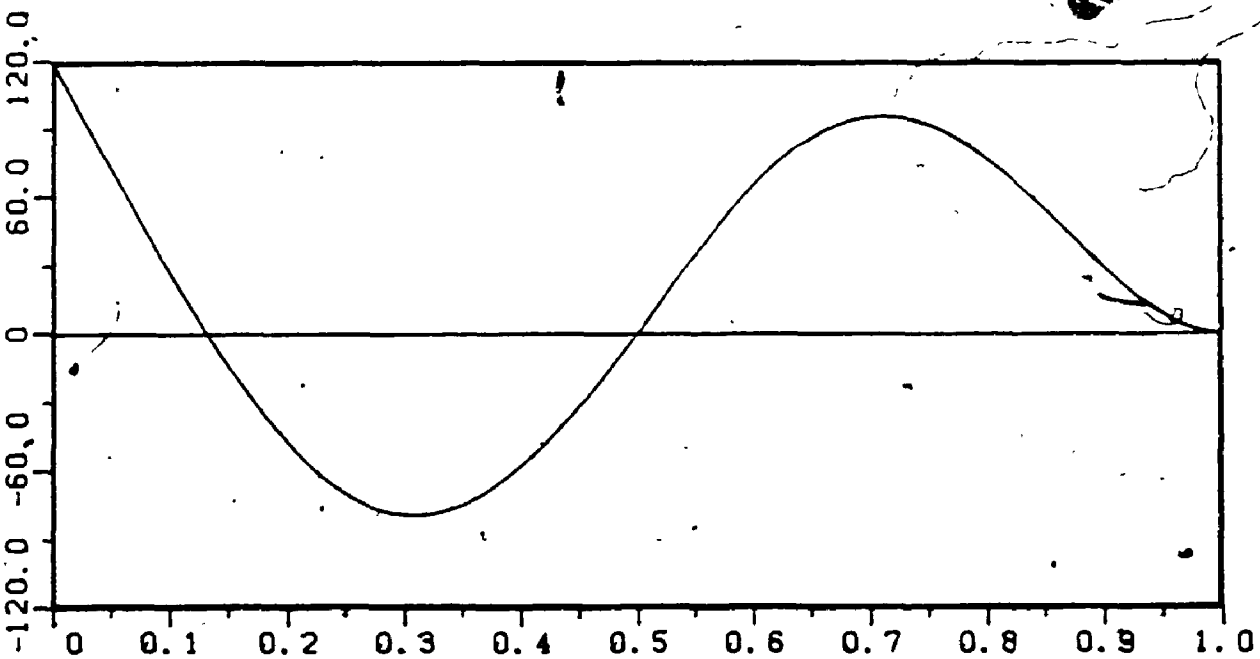

Figure 3.6. (b) Second Mode

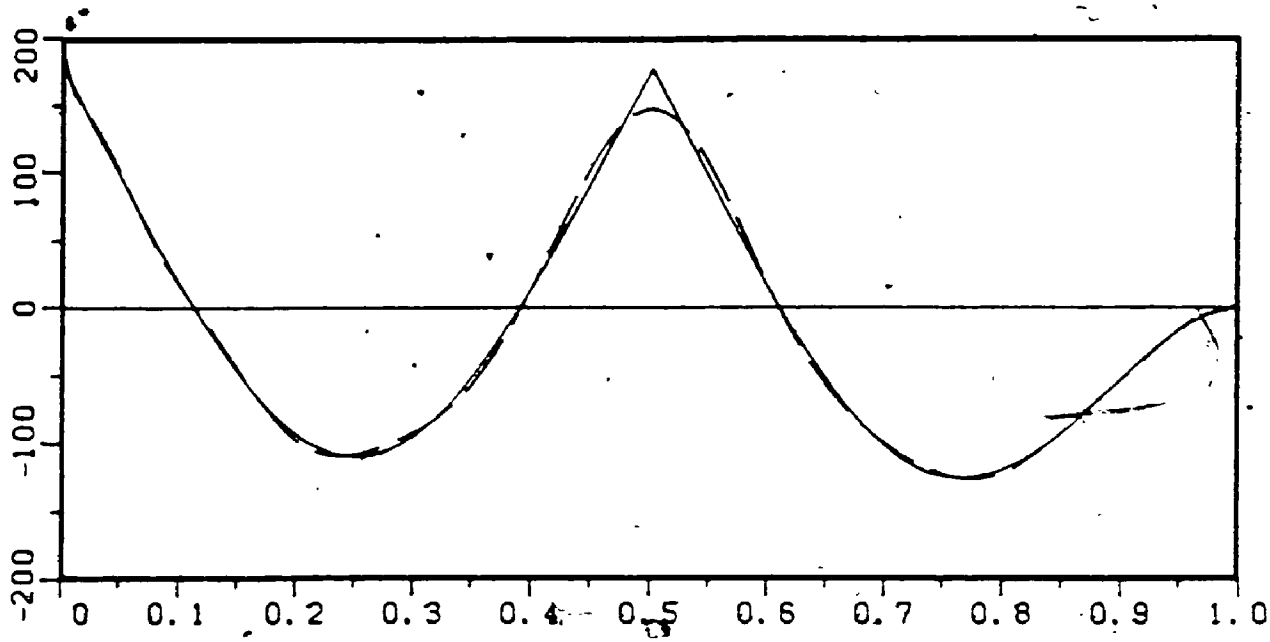

Figure 3.6. (c) Third Mode

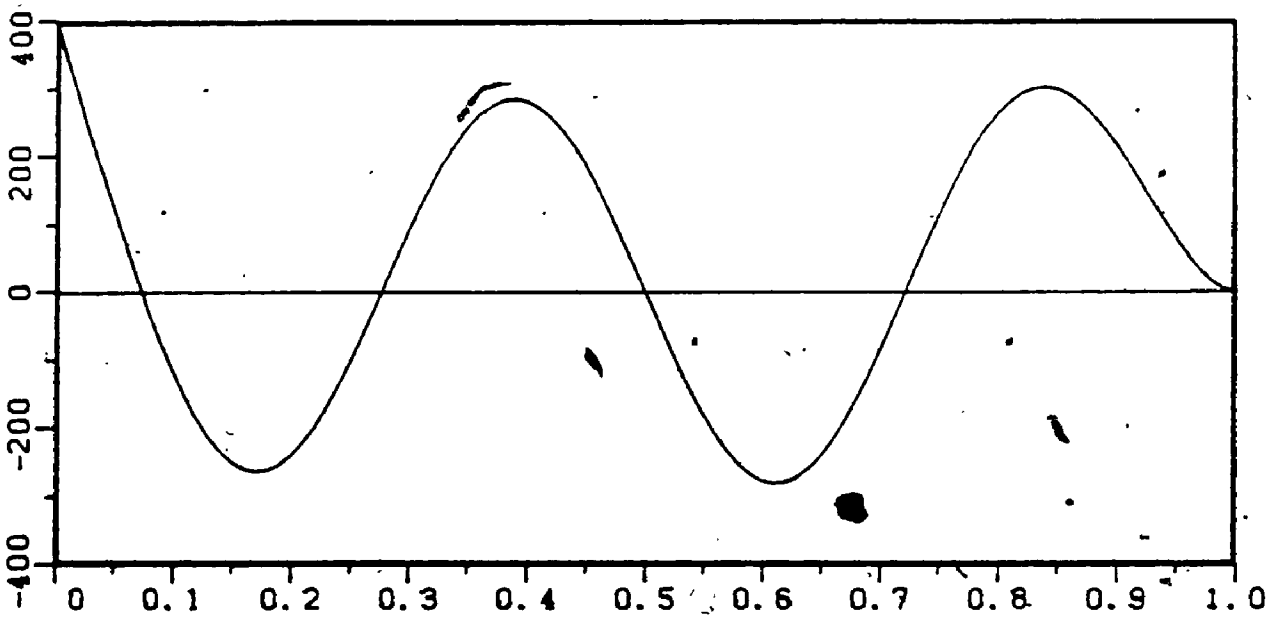

Figure 3.6. (d) Fourth Mode

Figure 3.6. Comparison of the bending moment ($\ell^2 d^2w/dx^2$) for a two span beam clamped at $x=0$, simply supported at $x/\ell=0.5$ and free at $x/\ell=1$.
——, exact; —— ——, present approximation.

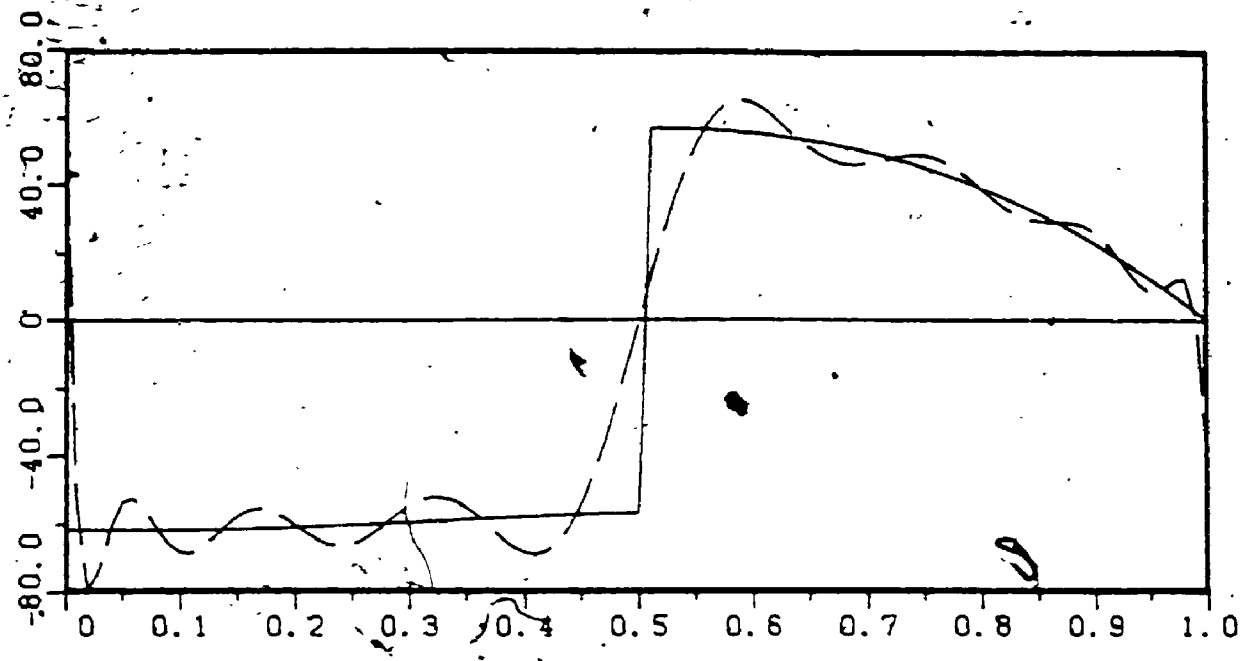

Figure 3.7. (a) First Mode

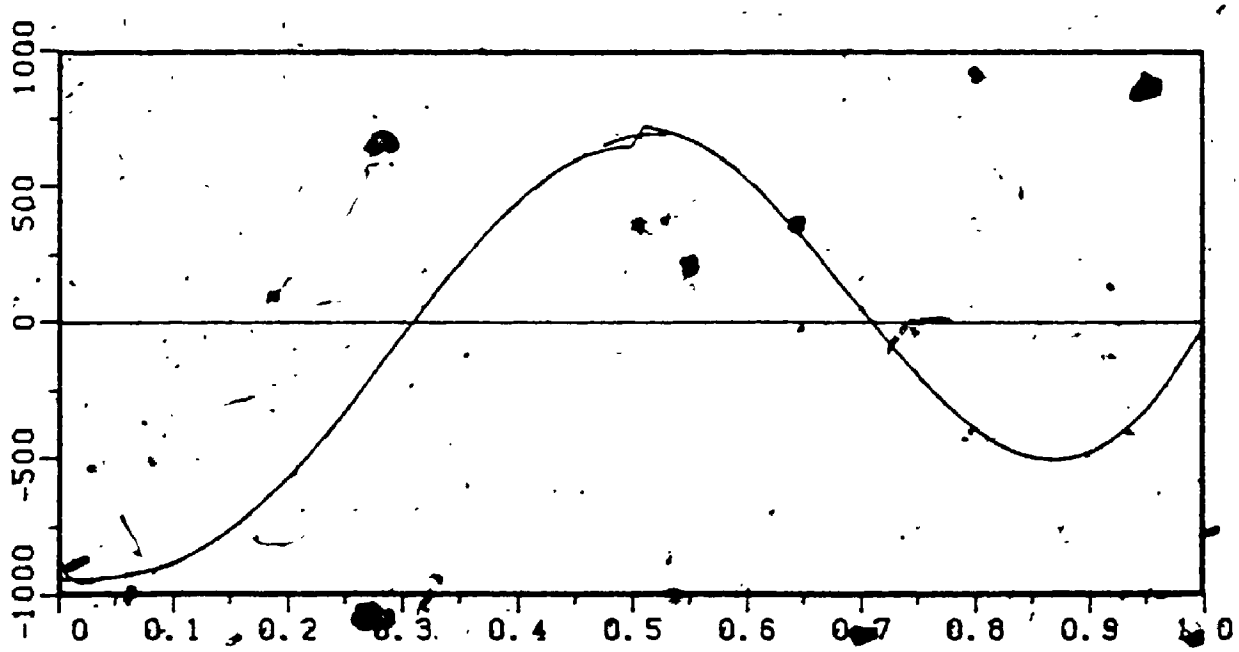

Figure 3.7. (b) Second Mode

2

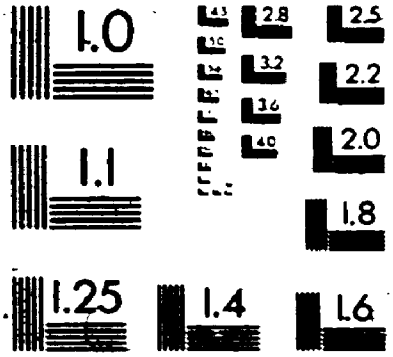

MICROCOPY

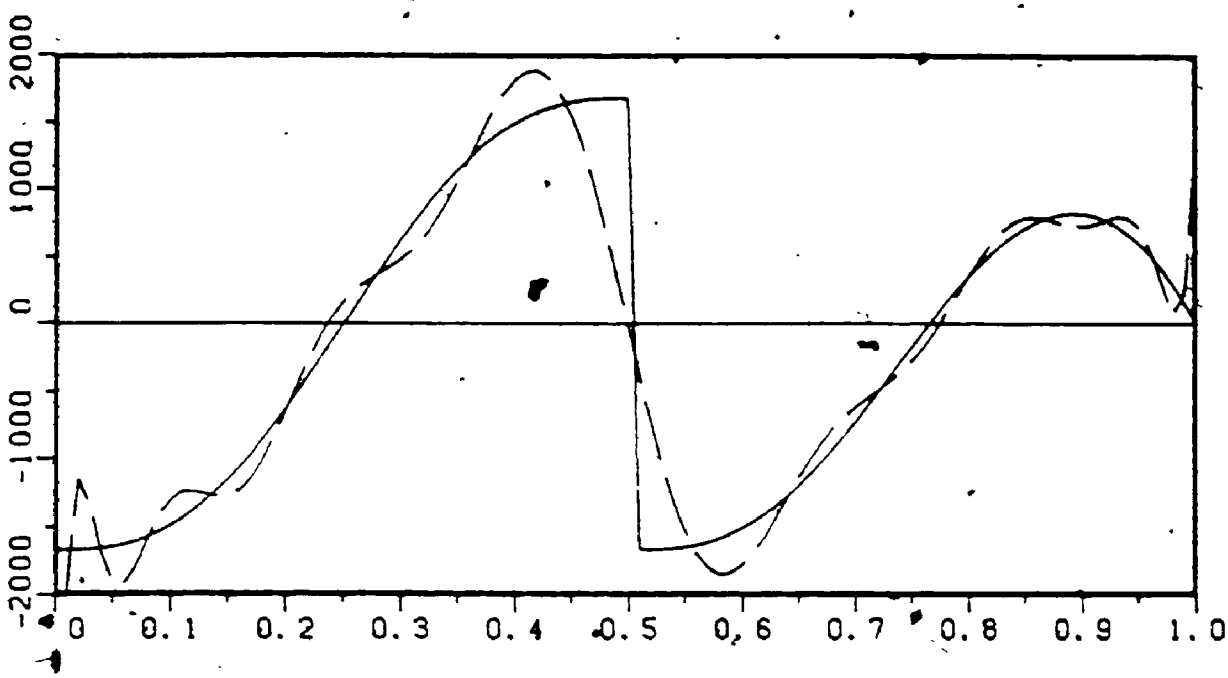

Figure 3.7. (c) Third Mode

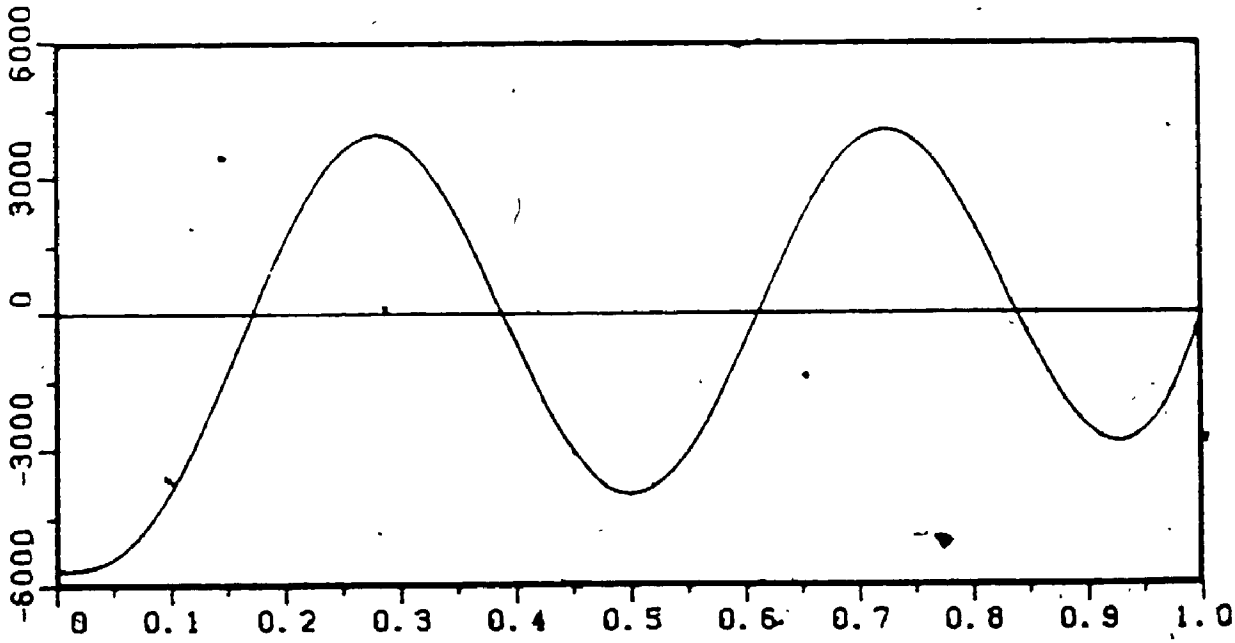

Figure 3.7. (d) Fourth Mode

Figure 3.7. Comparison of the shear force ($\ell^3 d^3w/dx^3$) for a two span beam clamped at $x=0$, simply supported at $x/\ell=0.5$ and free at $x/\ell=1$.
——, exact; — —, present approximation.

Table 3.7

Comparison of frequency parameters $(\omega^2 m_o \ell^4/EI_o)^{\frac{1}{2}}$ for a three-span uniform beam ($p=0$, number of terms in $\Phi_i=10$).

ℓ_2/ℓ	Source of Results	Boundary Conditions S — S			C — C		
(1) $\ell_1/\ell=0.125$							
0.25	Present	25.35	82.97	174.4	36.90	102.6	202.6
	Exact [41]	25.30	82.76	174.0	36.86	102.4	202.2
0.375	Present	34.04	112.5	218.4	49.83	139.1	241.1
	Exact [41]	33.98	112.1	218.2	49.73	138.8	240.3
0.5	Present	48.90	114.0	184.6	70.60	123.3	224.0
	Exact [41]	48.85	113.2	183.1	70.54	122.3	222.6
0.625	Present	59.65	96.78	200.8	66.07	132.7	211.7
	Exact [41]	59.60	96.33	199.4	65.93	132.3	209.7
0.75	Present	44.37	124.4	198.6	46.54	131.5	249.5
	Exact [41]	44.29	124.3	197.4	46.44	131.1	249.0
0.875	Present	33.59	94.55	188.1	34.81	97.24	193.0
	Exact [41]	33.55	94.40	187.7	34.74	97.06	192.4
(2) $\ell_1/\ell=0.25$							
0.375	Present	36.05	118.3	207.3	52.47	146.4	282.9
	Exact [41]	35.84	117.5	204.5	52.26	145.7	282.2
0.5	Present	51.54	157.9	191.2	75.52	193.2	249.5
	Exact [41]	51.42	158.0	189.6	75.34	192.9	246.8
0.625	Present	76.75	118.3	204.0	97.42	148.1	277.4
	Exact [41]	76.67	117.5	202.5	97.24	146.9	276.2
0.75	Present	61.82	157.9	201.4	66.05	184.6	282.5
	Exact [41]	61.67	158.0	199.9	65.90	184.1	281.9
(3) $\ell_1/\ell=0.375$							
0.5	Present	55.21	96.85	184.5	80.50	140.8	228.0
	Exact [41]	54.77	95.43	181.7	80.00	139.2	225.3
0.625	Present	81.85	94.91	226.9	118.7	138.7	251.8
	Exact [41]	81.74	94.40	224.1	118.6	137.8	247.7

Table 3.8, where a brief convergence study is also given for two particular tip mass characteristics. The convergence may be seen to be very rapid, with excellent agreement with the 'exact' results being achieved. Also given is a set of results for a cantilever with tip mass and subject to (a) a conservative (constant directional) axial load and (b) a non-conservative (tangential) axial load. To engender confidence in the results for the non-conservative system, values are included for the cantilever beam with no tip mass but acted upon by a tangential follower force. The values given agree with results computed by the authors from the exact solution given by Timoshenko and Gere [196] (page 155), to the number of figures presented, except for those modes for which the rounded 'exact' decimal figures are given in parentheses.

In Table 3.9, sets of results are presented for three more cantilever problems, this time with the mass(es) located at positions other than at the tip. The comparison values are from the work of Kounadis [62, 63] and from calculations by the present author using a commercially available finite element package, PAFEC [197]. (The element used in the calculations was the conventional four degree of freedom, cubic displacement, beam bending element which, it is believed, yields upper bounds for the frequencies. Twenty elements were used and the resulting frequencies are expected to be accurate to the number of figures given.) The first set of values, those for $\bar{M}_1=0.5$, $\bar{J}_1=0$, show that whilst the

Table 3.8

Comparison of frequency parameters $(\omega^2 m_o \ell^4/EI_o)^{\frac{1}{2}}$ for a uniform cantilever beam with a tip mass.

$\bar{M}_1^*$	$\bar{J}_1$	p/π^2	No. of terms	Mode Sequence Number 1	2	3	4	5
0.5	0	0	6	2.0163	16.901	51.765	107.88	206.44
			8	2.0163	16.901	51.701	106.09	182.22
			10	2.0163	16.901	51.701	106.06	180.18
		Exact	[48]	2.0163	16.901	51.701	106.06	180.12
0.5	0.5	0	6	1.1997	4.3307	25.144	64.956	130.81
			8	1.1997	4.3307	25.143	64.861	124.49
			10	1.1997	4.3307	25.143	64.860	124.28
		Exact	[48]	1.1997	4.3306	25.143	64.860	124.28
1.0	0	0	10	1.5573	16.250	50.896	105.20	179.29
		Exact	[48]	1.5573	16.250	50.857	105.20	179.23
1.0	1.0	0	10	0.86790	3.3906	24.019	63.463	122.74
		Exact	[48]	0.86790	3.3906	24.019	63.463	122.74
(a) Constant directional axial force (conservative loading)								
0.5	0	-1.0	10	4.3410	20.886	55.983	110.52	184.75
		-0.5	10	3.4159	19.003	53.884	108.31	182.48
		0.1	10	1.5705	16.448	51.253	105.60	179.72
		0.2	10	0.91229	15.982	50.802	105.14	179.26
		0.25	10	0.00000	15.744	50.574	104.91	179.02
(b) Tangential follower force (non-conservative loading)								
0.5	0	0.5	10	2.5651	15.064	49.611	103.85	177.91
		1.0	10	3.4288	12.846	47.429	101.59	175.61
		1.5	10	5.2786	9.5708	45.140	99.276	173.28
		1.62737	10	7.2217	7.2524	44.539	98.678	172.68
		1.62738	10	- *	- *	44.538	98.678	172.68
0	0	0	10	3.5160	22.034	61.697	120.90	199.94(86)
		1.0	10	5.1461	18.640	57.905	116.79	195.66(58)
		2.0	10	9.8283	12.255	53.841	112.53	191.29(20)
		2.03158	10	10.998	11.033	53.707	112.39	191.15(06)
		2.03159	10	- *	- *	53.707	112.39	191.15(06)

* Flutter has occurred.

Table 9.9

Comparison of frequency parameters $(\omega^2 m_o \ell^4/EI_o)^{\frac{1}{2}}$ for uniform cantilever beams with concentrated masses (p=0).

	Source of results	Mode Sequence Number 1	2	3	4	5
0 0.3 1	Ref [62,63]	3.451	17.430	47.302		
	Present					
$\bar{M}_1=0.5, \bar{J}_1=0$	6 terms	3.4512	17.448	47.504	122.35	219.14
	8 "	3.4512	17.441	47.436	114.50	197.23
	10 "	3.4512	17.435	47.368	113.98	196.48
	12 "	3.4512	17.432	47.333	113.89	196.44
	14 "	3.4512	17.432	47.323	113.87	196.41
	PAFEC	3.4512	17.430	47.302	113.83	196.35
0 0.3 1	Ref [62,63]	2.128	8.302	22.911		
	Present					
$\bar{M}_1=\bar{J}_1=0.5$	6 terms	2.167	9.584	28.68	55.35	168.1
	8 "	2.154	9.119	25.92	51.93	142.1
	10 "	2.150	8.971	25.16	51.48	138.5
	12 "	2.148	8.890	24.86	51.18	136.8
	14 "	2.144	8.781	24.47	50.86	135.1
	PAFEC	2.1276	8.3020	22.911	49.913	130.02
0 0.3 0.6 1	Ref [62,63]	1.407	4.034	14.560		
	Present					
$\bar{M}_1=\bar{M}_2=0.5$	6 terms	1.421	4.521	24.20	32.13	78.91
	8 "	1.418	4.295	20.81	28.73	51.93
$J_1=J_2=0.5$	10 "	1.415	4.266	18.62	27.78	45.63
	12 "	1.413	4.260	17.43	27.48	44.02
	14 "	1.412	4.219	16.90	27.13	43.72
	PAFEC	1.4066	4.0340	14.560	25.331	41.655

convergence of the present solution is still rapid, it is slower than for the tip mass problem, more terms being needed in the series to obtain equivalent accuracy. Also, the agreement between the results of Kounadis, PAFEC and the present solution is excellent. When the mass is permitted to have rotary inertia ($\bar{M}_1 = 0.5$, $\bar{J}_1 = 0.5$), the rate of convergence drops off significantly, although the final results appear likely to be similar to that given by Kounadis and PAFEC. The author believes that the drop in the rate of convergence of the present solution is primarily due to the discontinuity in the shear force (and bending moment) introduced by the presence of concentrated masses (and moments of inertia) not being adequately modelled by the continuously differentiable assumed functions. The effect of the discontinuity in bending moment, which requires a discontinuity in second derivative, is much more drastic than that due to the shear force, which requires a discontinuity in third derivative, as may be seen from the first two sets of results in Table 3.9. It should be noted, however, that the value of $\bar{J}_1$ used (0.5) with the particular value of $\bar{M}_1$ (0.5) requires the concentrated mass to have a radius of gyration equal to the length of the beam; which is both severe and unrealistic. These values were used by earlier researchers, with whose work the present results were to be compared. It may also be noted that the discontinuity in shear force occasioned by the presence of a concentrated mass

is similarly present when an intermediate support exists. Fortunately, the effect upon the frequencies predicted for such a case is small. Should a rotational spring stiffness be introduced at an intermediate point along a beam (which will be treated later), then the resulting discontinuity in bending moment may well significantly reduce the rate of convergence of the solution.

The next problem treated is that of a beam with various combinations of end conditions and carrying two intermediate concentrated masses, with and without rotary inertia, one at $x=0.3\ell$, the other at $x=0.7\ell$. Results for this problem are given in Table 3.10, as obtained using ten terms in the deflection series, where no account has been taken of symmetry, despite its existence for four of the configurations. Rigid body modes - i.e. zero frequencies - for beams with one end free and the other simply supported or free are not included in the table. Some comparison values calculated using PAFEC are also given in Table 3.10.

The final problem considered in this section is that of a two-equal-span beam with a concentrated mass attached at the centre of each span, in the presence of a constant axial force. Numerical results for this beam, for the three possible combinations of clamped and simply supported ends, are given in Table 3.11, as computed using ten terms in the deflection series, with no regard to symmetry considerations.

Table 3.10

Frequency parameters $(\omega^2 m_o \ell^4/EI_o)^{\frac{1}{2}}$ for beams with various concentrated masses ($\bar{M}_i$=0.5, No. of terms = 10).

	$\bar{J}_i$	Source of results	Mode Sequence Number 1	2	3
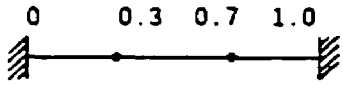	0	Present	15.01	33.93	103.1
	0.005	Present	14.42	33.91	63.92
		PAFEC	14.41	33.88	58.90
	0	Present	10.16	29.31	92.87
	0.005	Present	9.947	28.74	57.78
		PAFEC	9.945	28.68	53.97
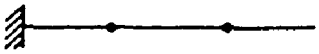	0	Present	2.665	17.23	38.25
	0.005	"	2.629	15.72	37.25
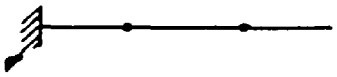	0	"	1.815	12.19	30.54
	0.005	"	1.793	11.02	26.98
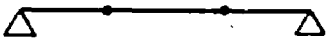	0	"	6.491	23.41	84.96
	0.005	"	6.399	23.14	52.62
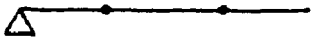	0	"	11.73	34.44	94.33
	0.005	"	11.04	31.98	62.57
	0	"	8.369	25.16	86.31
	0.005	"	7.796	22.31	43.89
	0	"	20.87	41.62	107.4
	0.005	"	17.92	40.59	74.69
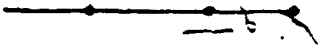	0	"	14.17	35.36	96.64
	0.005	"	12.28	29.48	50.23
	0	Present	10.31	26.67	88.05
	0.005	Present	9.066	21.72	39.47
		PAFEC	9.062	21.67	38.61

Table 3.11

Comparison of frequency-parameters $(\omega^2 m_0 \ell^4/EI_0)^{1/2}$ for two-equal-span beams with concentrated masses attached at the centre of each span ($\bar{M}_1=\bar{M}_2=0.2$).

$p = \frac{P\ell^2}{EI_0}$	Source of results	Boundary Conditions C - C			C - S			S - S		
-10	Present	47.99	65.06	197.1	37.39	59.60	172.8	32.89	48.13	162.8
	Ref.[45]	48.66			38.31			33.23		
- 5	Present	46.70	64.09	194.9	35.84	58.52	170.5	31.19	46.83	160.4
	Ref.[45]	47.42			36.76			31.52		
- 1	Present	45.63	63.31	193.2	34.55	57.64	168.6	29.76	45.76	158.4
	Ref.[45]	46.41			35.47			30.09		
0	Present	45.36	63.11	192.8	34.22	57.42	168.1	29.39	45.49	157.9
	Ref.[45]	46.16			35.14			29.72		
0.5	Present	45.23	63.01	192.5	34.05	57.30	167.9	29.20	45.35	157.7
	Ref.[45]	46.03			34.97			29.53		
1	Present	45.09	62.91	192.3	33.89	57.19	167.6	29.01	45.22	157.4
	Ref.[45]	45.90			34.80			29.34		

Comparison values for the fundamental frequency parameters are available from the work of Laura et al. [45] and are shown in the table.

3.3.2 Beams of Non-uniform Cross Section

In the three examples treated in this section, the beams are considered to be of rectangular cross section of breadth b (in the y-direction) and depth d (in the z-direction); the flexural rigidity of relevance (vibration in the x-z plane) thus varies with bd^3 and the mass per unit length with bd. Based upon the earlier convergence studies, it was considered adequate to use ten terms in the deflection series for the computation of the frequency parameters presented in this section.

The first problem treated is that of a beam of length ℓ, simply supported at each end, having constant breadth but varying linearly in depth from d_0 at $x=0$ to d_1 at $x=\ell$; thus $d(x) = d_0(1+cx/\ell)$, where slope $c=(d_1-d_0)/d_0$. The flexural rigidity and mass per unit length are then given by

$$EI(x) = EI_0(1+cx/\ell)^3 \text{ and } m(x) = m_0(1+cx/\ell)$$

and the functions $f(\xi)$ and $h(\xi)$ in equation (3.5) by

$$f(\xi) = (1+c\xi)^3 \text{ and } h(\xi) = (1+c\xi).$$

Frequency parameters for the first five modes of vibration for such beams are presented in Table 3.12 for various values

Table 3.12

Frequency parameters $(\omega^2 m_o \ell^4/EI_o)^{1/2}$ for a simply supported beam with linearly varying cross-sectional height.

Slope (c)	Source of results	Mode Sequence Number 1	2	3	4	5
0.2	Ref.[66]	10.828	-	-	-	-
	Ref.[67]	10.827	43.357	97.541	-	-
	Present	10.827	43.357	97.535	173.38	271.41
0.4	Ref.[66]	11.738	-	-	-	-
	Ref.[67]	11.734	47.118	105.98	-	-
	Present	11.734	47.117	105.95	188.30	294.45
0.6	Ref.[66]	12.616	-	-	-	-
	Ref.[67]	12.602	50.790	114.22	-	-
	Present	12.601	50.785	114.13	202.78	316.85
0.8	Ref.[66]	13.471	-	-	-	-
	Ref.[67]	13.436	54.390	122.31	-	-
	Present	13.436	54.376	122.12	216.89	338.81
1.0	Ref.[66]	14.311	-	-	-	-
	Ref.[67]	14.245	57.932	130.30	-	-
	Present	14.243	57.904	129.96	230.71	360.44

of slope c. Comparison results from references [66, 67] are also given and it may seem that close agreement is achieved.

The second example treated is the cantilever beam with linear taper and with parabolic taper, as shown in Figure 3.8. The cross-sectional depth d can be expressed as $d = d_0\{1-(1-d_1/d_0)x/\ell\}$, for a linear taper, and $d=d_0\{1-(1-d_1/d_0)\sqrt{x/\ell}\}$, for a parabolic taper. The breadth of the cross-section b can ge given similarly. The stiffness and mass functions $f(\xi)$ and $h(\xi)$, in equation (3.5), then become:

(a) linearly tapered beam

i) beam with linearly tapered breadth, constant depth,

$$f(\xi) = \{1-(1-b_1/b_0)\xi\}, \quad h(\xi) = \{1-(1-b_1/b_0)\xi\}, \tag{3.14a, b}$$

ii) beam with linearly tapered depth, constant breadth,

$$f(\xi) = \{1-(1-d_1/d_0)\xi\}^3, \quad h(\xi) = \{1-(1-d_1/d_0)\xi\}, \tag{3.15a, b}$$

iii) beam with linearly tapered breadth and depth,

$$f(\xi) = \{1-(1-b_1/b_0)\xi\}\{1-(1-d_1/d_0)\xi\}^3; \tag{3.16a}$$

$$h(\xi) = \{1-(1-b_1/b_0)\xi\}\{1-(1-d_1/d_0)\xi\}, \tag{3.16b}$$

(b) parabolically tapered beam

i) beam with parabolically tapered breadth, constant depth,

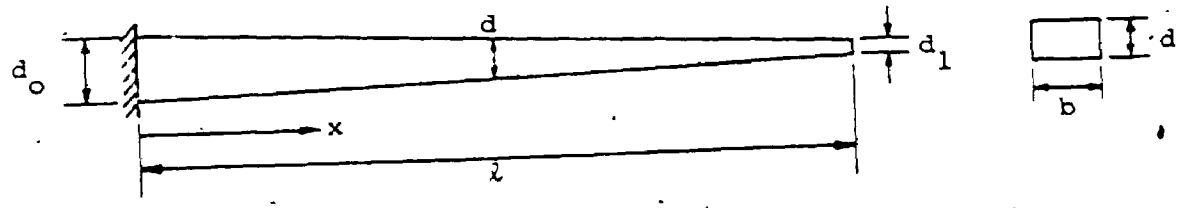

(a) linearly tapered beam

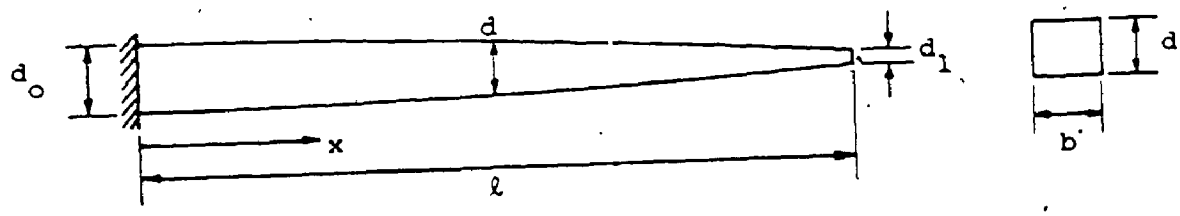

(b) parabolically tapered beam

Figure 3.8. Cantilever beams with linear and parabolic tapers.

$$f(\xi)=\{1-(1-b_1/b_0)\xi^{1/2}\}, \quad h(\xi) = \{1-(1-b_1/b_0)\xi^{1/2}\},$$

ii) beam with parabolically tapered depth, constant breadth,

$$f(\xi)=\{1-(1-d_1/d_0)\xi^{1/2}\}^3, \quad h(\xi) = \{1-(1-d_1/d_0)\xi^{1/2}\},$$

iii) beam with parabolically tapered breadth and depth,

$$f(\xi)=\{1-(1-b_1/b_0)\xi^{1/2}\}\ \{1-(1-d_1/d_0)\xi^{1/2}\}^3,$$

$$h(\xi)=\{1-(1-b_1/b_0)\xi^{1/2}\}\ \{1-(1-d_1/d_0)\xi^{1/2}\}.$$

In each case the subscripts 0 and 1 denote the values at the left- and right-hand end of the beam, respectively. Results for the particular case of b_1/b_0 and/or $d_1/d_0 = 0.2$ are presented in Table 3.13. For linearly tapered beams, comparison is made with values from references [68, 71] and again good agreement may be seen to have been achieved. (It may be noted that the results presented for the doubly tapered cantilever - that is, both breadth and depth varying - are also applicable to beams with certain other cross sections, such as circular, elliptical and diamond shaped.)

Finally, the three span uniform and parabolically tapered beams shown in Figure 3.9 are considered. For the tapered cases, the breadth and/or depth each vary symmetrically about the centre of the beam (ξ=1/2), with the central dimension being half that of the respective dimension at the ends. The stiffness and mass functions $f(\xi)$ and $h(\xi)$

Table 3.13

Frequency parameters $(\omega^2 m_o \ell^4/EI_o)^{1/2}$ for cantilever beams with linear and parabolic taper.

$\frac{b_1}{b_0}$	$\frac{d_1}{d_0}$	Source of results	Mode Sequence Number 1	2	3	4	5
(a) Linearly tapered beams							
0.2	1	Ref.[68]	5.3969	25.656	-	-	-
		Ref.[71]	5.3977	25.656	67.54	125.2	204.4
		Present	5.3976	25.656	65.747	125.26	204.55
1	0.2	Ref.[68]	4.2926	15.742	-	-	-
		Ref.[71]	4.2915	15.736	36.866	68.1	109.58
		Present	4.2925	15.743	36.886	68.144	110.06
0.2	0.2	Ref.[68]	6.1972	18.384	-	-	-
		Ref.[71]	6.1954	18.379	39.818	71.22	112.82
		Present	6.1964	18.386	39.837	71.288	113.33
(b) Parabolically tapered beams							
0.2	1	Present	5.3301	25.435	65.487	125.03	204.45
1	0.2	Present	3.1790	12.085	28.832	53.554	86.731
0.2	0.2	Present	4.4454	13.933	30.993	55.961	89.673

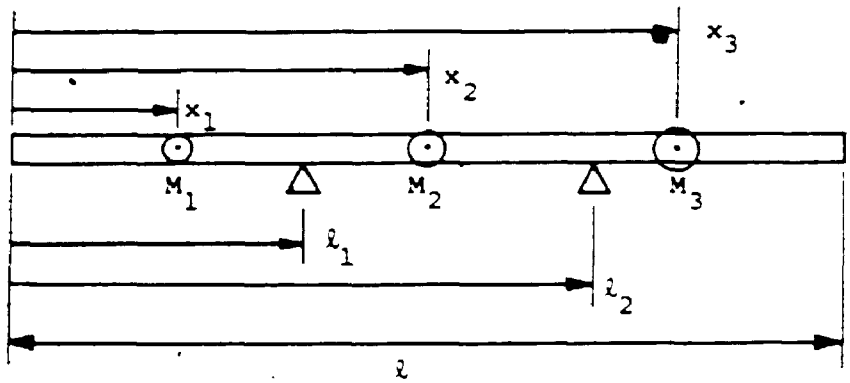

(a) uniform beam

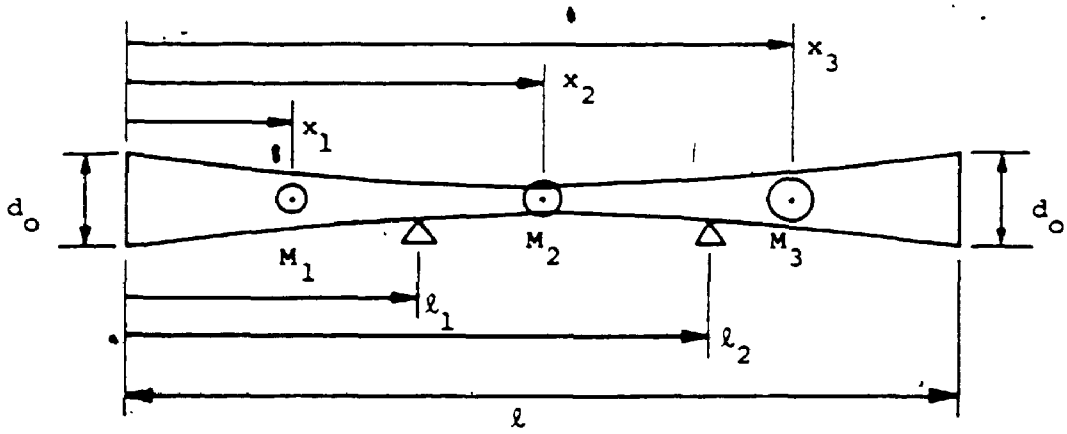

(b) parabolically tapered beam

Figure 3.9. Three-span beams with concentrated masses.

then may be written:

Case (1) for a uniform beam

$$f(\xi) = 1, \quad h(\xi) = 1,$$

Case (2) for a beam with parabolically tapered breadth, uniform depth

$$f(\xi) = 1-2\xi + 2\xi^2, \quad h(\xi) = 1-2\xi + 2\xi^2, \qquad (3.17a, b)$$

Case (3) for a beam with parabolically tapered depth, uniform breadth

$$f(\xi) = (1-2\xi + 2\xi^2)^3, \quad h(\xi) = 1-2\xi + 2\xi^2, \qquad (3.18a, b)$$

Case (4) for a beam with parabolically tapered breadth and depth

$$f(\xi) = (1-2\xi + 2\xi^2)^4, \quad h(\xi) = (1-2\xi + 2\xi^2)^2. \qquad (3.19a, b)$$

Numerical results were computed for three combinations of clamped (C) and simply supported (S) end conditions for concentrated masses $\bar{M}_1 = 0.1$, $\bar{M}_2 = 0.2$ and $\bar{M}_3 = 0.3$ located at $\xi = 0.2$, 0.5 and 0.8, respectively, concentrated moments of inertia $\bar{J}_i = 0$ and with the two intermediate supports located at $\xi = 0.35$ and 0.70. The values of the lowest three frequency parameters for all four cases of cross-sectional uniformity and/or taper are given in Table 3.14, where it should be noted that in the case of the C-S beam, the

Table 3.14

Frequency parameters $(\omega^2 m_0 \ell^4/EI_0)^{1/2}$ for three-span uniform and parabolically tapered beams with concentrated masses as shown in Figure 3.7

Cases	Boundary Conditions								
	C - C			C - S			S - S		
(1)	76.63	134.6	164.5	71.68	116.2	136.2	64.20	99.65	135.8
(2)	67.03	126.0	149.4	62.16	106.8	121.6	56.37	90.61	120.5
(3)	40.39	90.28	105.0	35.98	73.36	83.58	34.44	61.01	80.47
(4)	34.21	84.43	96.85	29.17	65.65	76.68	29.36	54.74	71.66

clamping occurs at the left hand end ($\xi = 0$).

3.4 ELASTICALLY RESTRAINED BEAMS

3.4.1. Beams of Uniform Cross Section

The first set of problems considered in this section is the vibration of single-span beams with both ends elastically restrained against rotation and no translation, and with neither concentrated mass nor axial load. These problems were chosen mainly to show the effect of the use of several sets of orthogonal polynomials, explained in section 3.2, for the admissible functions in the Rayleigh-Ritz method. Four sets of polynomials were generated:

(A) The starting function was chosen to satisfy only the zero deflection condition at each end, the effect of the rotational spring being neglected; thus $\Phi_1(\xi)$ is given by equation (3.10), with the coefficients as given in Table 2.1. The simple generating function $g(\xi) = \xi$ was used.

(B) The starting function was chosen to satisfy both the slope and zero deflection conditions at the ends; thus $\Phi_1(\xi)$ is given by equation (3.10), with the coefficients as given by equation (3.11). The generating function was again simply $g(\xi) = \xi$.

(C) As (B) but with generating function $g(\xi) = \xi^2$.

(D) As (B) but with generating function $g(\xi) = -3\xi^2/2 + \xi^3$.

It may be recognized that each member of the polynomials in case (A) satisfies only the zero deflection conditions at the ends, while in case (D), each member satisfies not only the zero deflection conditions but also the slope conditions at the ends. Further, each member of the polynomials in case (B) satisfy only the zero deflection conditions at the ends (except the starting function), and in case (C), each member satisfies both slope and deflection conditions at $\xi = 0$ and only the zero deflection condition at $\xi = 1$. Table 3.15 shows the results for $S_1 = S_2 = 10$ and $S_1 = 10$, $S_2 = 100$ (subscripts 1 and 2 denote the position of $\xi = 0$ and $\xi = 1$, respectively), in comparison with the exact values computed by the author from the frequency equation given by Gorman [41]. It may be seen that all the sets of polynomials give excellent results and the polynomials generated with higher degree generating function yield a faster rate of convergence for the beam treated. This trend may well be retained for any beam when the shape of the starting function approximates the fundamental mode shape. However, since the starting function, equation (3.10) with the coefficients given by equation (3.11), is constructed to satisfy the end deflection and slope conditions only, the intermediate shape may not be necessarily approximate to the fundamental mode and thus the trend may not be retained, in general. Therefore, in the following problems, the simplest polynomials (case (A): $g(\xi)$

Table 3.15

Comparison of frequency parameters $(\omega^2 m_o \ell^4/EI_o)^{\frac{1}{2}}$ for uniform, single span beams with both ends rotationally restrained and no translation ($M = \bar{J} = p = 0$).

Source of Number of Results	Terms	Mode Sequence Number 1	2	3	4	5
(1) $S_1=S_2=10$						
case (A)	6 terms	17.2699	49.9616	102.561	177.769	555.146
	8 "	17.2695	49.9601	101.338	171.930	280.215
	10 "	17.2695	49.9601	101.318	171.750	262.496
	12 "	17.2695	49.9601	101.318	171.748	261.546
case (B)	6 terms	17.2699	49.9616	101.483	173.155	385.979
	8 "	17.2696	49.9603	101.330	171.812	267.760
	10 "	17.2695	49.9602	101.318	171.748	261.844
	12 "	17.2695	49.9601	101.318	171.748	261.529
case (C)	6 terms	17.2713	49.9664	101.418	174.745	321.367
	8 "	17.2703	49.9635	101.365	171.995	263.866
	10 "	17.2699	49.9619	101.343	171.861	261.905
	12 "	17.2697	49.9611	101.331	171.808	261.712
case (D)	6 terms	17.2702	49.9615	101.347	171.825	261.666
	8 "	17.2698	49.9607	101.330	171.782	261.662
	10 "	17.2696	49.9604	101.323	171.764	261.590
Exact [41]		17.2695	49.9601	101.318	171.748	261.527
(2) $S_1=10$, $S_2=100$						
case (A)	6 terms	19.2728	54.5146	110.558	191.209	661.309
	8 "	19.2722	54.5099	108.811	182.555	298.763
	10 "	19.2722	54.5099	108.773	182.184	276.315
	12 "	19.2722	54.5099	108.773	182.180	274.921
case (B)	6 terms	19.2723	54.5111	108.960	183.516	348.901
	8 "	19.2722	54.5100	108.781	182.239	280.083
	10 "	19.2722	54.5100	108.773	182.181	275.169
	12 "	19.2722	54.5099	108.773	182.181	274.892
case (C)	6 terms	19.2742	54.5154	108.867	184.673	323.351
	8 "	19.2730	54.5131	108.817	182.413	276.881
	10 "	19.2726	54.5117	108.796	182.291	275.232
	12 "	19.2724	54.5109	108.786	182.240	275.062
case (D)	6 terms	19.2734	54.5136	108.844	182.407	275.357
	8 "	19.2727	54.5119	108.809	182.306	275.329
	10 "	19.2724	54.5111	108.793	182.254	275.145
Exact [41]		19.2722	54.5099	108.773	182.180	274.889

= ξ and both starting and subsequent functions neglect the effect of the springs) are used to generate numerical results.

The most widely studied beams subject to elastic spring(s) seem to be cantilever beams and thus it is natural to consider such beams here. First, a cantilever beam with a tip mass with no rotary inertia and subject to a translational spring at the free end is treated using ten terms in the series (3.6), and the frequency parameters for the lowest five modes are given in Table 3.16 for various values of tip mass and spring constant. The values presented are the same as those computed by the author from the exact frequency equation given by Stephen [76] to the number of figures given, except for two cases of the fourth modes and all the fifth modes, for which the rounded exact values are given in parentheses.

The second cantilever beam treated is that subject to both translational and rotational springs positioned at the same point, with no concentrated mass or rotary inertia. The frequency parameters obtained are presented in Table 3.17 in comparison with the exact solution given by Lau [77]. Close agreement may be seen to be achieved for all the spring positions, although, the rate of convergence is significantly reduced when the springs are positioned other than at the tip. Included in the table is a brief convergence study

Table 3.16

Frequency parameters $(\omega^2 m_o \ell^4/EI_o)^{\frac{1}{2}}$ for uniform cantilever beams with tip mass (no rotary inertia) and translational spring at the free end.

$\bar{M}_1$	K_1	Mode sequence number 1	2	3	4	5	
0	0	3.5160	22.034	61.697	120.90	199.94	(199.86)
	1	4.0401	22.126	61.730	120.92	199.95	(199.87)
	10	6.9639	22.980	62.026	121.07	200.04	(199.96)
	100	13.254	31.539	65.354	122.65	200.97	(200.89)
	1000	15.193	47.283	91.251	142.83	212.69	(212.6[illegible])
	10000	15.396	49.712	103.12	174.87	264.03	(263.35)
					(174.82)		
0.2	1	3.0125	18.233	53.563	108.19	182.50	(182.43)
	10	5.3565	18.469	53.604	108.21	182.50	(182.44)
	100	12.431	22.181	54.054	108.33	182.55	(182.48)
	1000	15.182	45.314	66.252	110.06	183.08	(183.02)
	10000	15.396	49.699	102.81	169.45	212.38	(212.35)
					(169.41)		
0.4	1	2.5017	17.187	52.065	106.46	180.61	(180.54)
	10	4.4811	17.292	52.079	106.46	180.61	(180.55)
	100	11.432	19.012	52.237	106.50	180.62	(180.56)
	1000	15.170	41.389	56.104	106.98	180.78	(180.71)
	10000	15.396	49.684	102.27	147.85	185.04	(184.98)
0.6	1	2.1844	16.707	51.446	105.78	179.89	(179.83)
	10	3.9235	16.766	51.453	105.78	179.90	(179.83)
	100	10.455	17.678	51.532	105.80	179.90	(179.84)
	1000	15.157	36.856	53.064	106.02	179.97	(179.91)
	10000	15.395	49.668	101.19	127.04	181.31	(181.25)
0.8	1	1.9632	16.431	51.108	105.42	179.52	(179.46)
	10	3.5309	16.469	51.113	105.42	179.52	(179.46)
	100	9.6096	17.015	51.160	105.43	179.53	(179.49)
	1000	15.142	33.138	51.942	105.56	179.57	(179.51)
	10000	15.395	49.650	98.665	114.65	180.21	(180.15)
1.0	1	1.7979	16.253	50.896	105.20	179.29	(179.23)
	10	3.2358	16.279	50.899	105.20	179.29	(179.23)
	100	8.9058	16.637	50.930	105.21	179.29	(179.23)
	1000	15.126	30.258	51.400	105.29	179.32	(179.26)
	10000	15.395	49.629	93.678	108.97	179.70	(179.64)
2.0	1	1.3373	15.862	50.448	104.74	178.82	(178.76)
	10	2.4097	15.869	50.449	104.74	178.82	(178.76)
	100	6.7426	15.961	50.457	104.74	178.82	(178.76)
	1000	15.008	22.325	50.560	104.76	178.83	(178.77)
	10000	15.395	49.466	69.965	105.12	178.91	(178.85)

Table 3.17

Comparison of frequency parameters $(\omega^2 m_o \ell^4/EI_o)^{\frac{1}{4}}$ for uniform, constrained cantilever beams with a translational spring and a rotational spring positioned at the same point.

Position of Springs (ξ_1)	Number of Terms	Mode Sequence Number 1	2	3	4	5
(1) $K_1=S_1=10$						
0.2	8 terms	2.1470	5.0847	8.0496	11.008	14.356
	10 "	2.1408	5.0715	8.0403	11.002	14.217
	12 "	2.1396	5.0689	8.0388	11.002	14.211
	14 "	2.1373	5.0642	8.0360	11.002	14.211
	16 "	2.1358	5.0613	8.0342	11.002	14.210
	Exact [77]	2.1268	5.0431	8.0236	11.002	14.206
0.4	14 terms	2.5377	4.8106	8.1113	11.324	14.147
	Exact [77]	2.5093	4.8054	8.0925	11.295	14.146
0.6	14 terms	2.7722	4.9919	8.0871	11.311	14.147
	Exact [77]	2.7462	4.9737	8.0698	11.283	14.146
0.8	14 terms	2.7463	5.6351	8.2882	11.023	14.190
	Exact [77]	2.7386	5.5942	8.2564	11.021	14.187
1.0	14 terms	2.71468	5.33488	8.36607	11.43754	14.52711
	Exact [77]	2.71468	5.33488	8.36607	11.43754	14.52711
(2) $K_1=10$, $S_1=100$						
0.2	14 terms	2.3338	5.6594	8.5975	11.011	14.415
	Exact [77]	2.3015	5.5280	8.4238	11.008	14.355
0.4	14 terms	2.9894	4.9339	8.5724	12.443	14.186
	Exact [77]	2.8955	4.9005	8.4459	12.033	14.168
0.6	14 terms	3.1313	5.3893	8.5465	12.394	14.187
	Exact [77]	3.0673	5.2917	8.4175	12.001	14.169
0.8	14 terms	2.8487	6.3681	9.5994	11.159	14.365
	Exact [77]	2.8361	6.2609	9.2429	11.103	14.309
1.0	14 terms	2.73095	5.50295	8.60673	11.72908	14.85527
	Exact [77]	2.73095	5.50295	8.60673	11.72908	14.85527
(3) $K_1=100$, $S_1=10$						
0.2	14 terms	2.1484	5.1091	8.1030	11.042	14.224
	Exact [77]	2.1389	5.0894	8.0906	11.041	14.219
0.4	14 terms	2.6696	5.1701	8.1583	11.330	14.162
	Exact [77]	2.6483	5.1642	8.1399	11.300	14.161
0.6	14 terms	3.4008	5.2275	8.1267	11.317	14.163
	Exact [77]	3.3779	5.2130	8.1096	11.289	14.162
0.8	14 terms	3.8843	5.6776	8.3056	11.052	14.201
	Exact [77]	3.8831	5.6356	8.2746	11.050	14.198
1.0	14 terms	3.78882	5.75618	8.48887	11.48760	14.55237
	Exact [77]	3.78882	5.75618	8.48887	11.48760	14.55237

showing the rate of convergence. It is believed that the drop in convergence rate is, as in the case of beams with concentrated masses, primarily due to the discontinuity in the bending moment and shear force introduced by the presence of springs not being adequately modelled by the continuously differentiable assumed functions.

The last cantilever beam problem treated is single and multi-span, constrained beams with tip masses subject to axial load. The translational and rotational springs are assumed to be located at the tip, and the values are taken as $K_1 = S_1 = \bar{M}_1 = 1$ and $\bar{J}_1 = 0.2$. The results are presented in Table 3.18, where the convergence of the solution is also illustrated.

The next problem considered is that of a beam with one end rotational spring-hinged and the other end elastically restrained against translation, as shown in Figure 3.10. The frequency parameters were obtained using fourteen terms in the series (3.6) and are presented in Table 3.19 for various combinations of spring constants. The values presented are the same as those computed by the author from the exact frequency equation given by Maurizi et al. [82], to the number of figures given. For the rotational spring constant $S_1 = 100$ at $\xi = 0$ and the translational spring constant $K_1 = 1, 100, 10{,}000$ at $\xi = 1$, the lowest five mode shapes are presented in Figure 3.11, where the amplitudes are arranged to

Table 3.18

Frequency parameters $(\omega^2 m_o \ell^4/EI_o)^{\frac{1}{2}}$ for uniform, constrained cantilever beams with a tip mass, subject to an axial load and translational and rotational springs at the free end ($K_1=S_1=\bar{M}_1=1$, $\bar{J}_1=0.2$)

p	Number of Terms	Mode Sequence Number 1	2	3	4	5
(1) Single span beams						
-1	14 terms	2.0937	5.3329	24.632	63.963	123.22
-0.5	14 "	2.0063	5.2947	24.489	63.776	123.01
0	8 "	1.91449	5.25590	24.3460	63.5890	122.994
	10 "	1.91449	5.25590	24.3460	63.5879	122.809
	12 "	1.91449	5.25590	24.3460	63.5879	122.807
	14 "	1.91449	5.25590	24.3460	63.5879	122.807
	Exact [78]	1.91449	5.25590	-	-	-
0.5	14 terms	1.8175	5.2165	24.202	63.400	122.60
1	"	1.7146	5.1765	24.057	63.211	122.40
2	"	1.4859	5.0947	23.764	62.831	121.98
4	"	0.84982	4.9223	23.168	62.064	121.15
(2) Double span beams ($\ell_1/\ell=0.5$)						
-1	8 terms	3.0483	8.9801	63.861	92.887	203.26
	10 "	3.0479	8.9755	63.860	92.314	202.17
	12 "	3.0477	8.9732	63.859	92.072	202.14
	14 "	3.0476	8.9720	63.859	91.945	202.14
-0.5	14 terms	2.9815	8.9273	63.672	91.803	201.92
0	"	2.9133	8.8824	63.485	91.662	201.71
0.5	"	2.8427	8.8375	63.297	91.520	201.49
1	"	2.7695	8.7925	63.109	91.378	201.28
2	"	2.6148	8.7021	62.730	91.093	200.85
4	"	2.2625	8.5203	61.966	90.521	199.98
8	"	1.2104	8.1521	60.407	89.365	198.24
(3) Triple span beams ($\ell_1/\ell=0.4$, $\ell_2/\ell=0.7$)						
-10	14 terms	4.5553	17.714	110.98	167.55	239.84
-5	"	4.2490	17.231	109.17	165.75	238.29
0	"	3.8940	16.736	107.31	163.94	236.72
5	"	3.4707	16.230	105.42	162.11	235.14
10	"	2.9439	15.712	103.49	160.26	233.55
15	"	2.2315	15.181	101.52	158.39	231.94
20	8 terms	0.97380	14.661	99.630	158.36	239.73
	10 "	0.97355	14.658	99.627	157.03	231.83
	12 "	0.97009	14.650	99.576	156.64	230.73
	14 "	0.96543	14.638	99.499	156.50	230.32

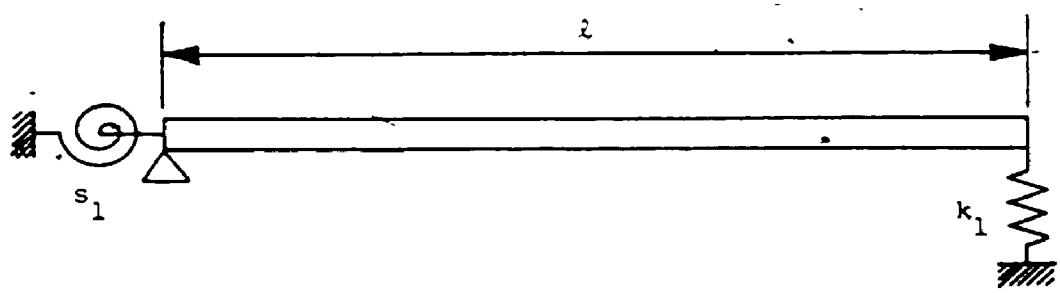

Figure 3.10. A beam with one end rotational spring-hinged, the other end elastically restrained against translation.

Table 3.19

Frequency parameters $(\omega^2 m_o \ell^4/EI_o)^{\frac{1}{2}}$ for uniform beams with one end rotational spring-hinged and the other end elastically restrained against translation.

S_1	K_1	Mode sequence number				
		1	2	3	4	5
0	1	1.7156	15.549	50.005	104.27	178.28
	10	4.9788	16.772	50.372	104.44	178.38
	100	8.9320	26.504	54.571	106.30	179.43
	1000	9.7724	37.849	79.594	128.79	192.90
	10000	9.8599	39.322	88.017	155.24	239.75
1	0	1.5573	16.250	50.896	105.20	179.23
	1	2.3587	16.371	50.935	105.22	179.24
	10	5.4125	17.511	51.292	105.39	179.34
	100	9.6625	27.026	55.378	107.22	180.38
	1000	10.606	38.705	80.367	129.51	193.74
	10000	10.704	40.236	88.950	156.18	240.67
10	0	2.9678	19.356	55.518	110.71	185.35
	1	3.5318	19.455	55.553	110.73	185.36
	10	6.4457	20.394	55.874	110.89	185.45
	100	11.842	29.268	59.526	112.60	186.45
	1000	13.266	42.660	84.579	133.90	199.16
	10000	13.413	44.526	94.181	161.97	246.77
100	0	3.4477	21.620	60.570	118.76	196.42
	1	3.9758	21.712	60.603	118.77	196.43
	10	6.8967	22.576	60.902	118.93	196.52
	100	13.056	31.171	64.271	120.53	197.46
	1000	14.911	46.487	89.952	140.87	209.36
	10000	15.104	48.804	101.31	171.87	259.14
1000	0	3.5090	21.991	61.575	120.66	199.47
	1	4.0335	22.082	61.607	120.68	199.48
	10	6.9570	22.937	61.904	120.83	199.57
	100	13.233	31.500	65.235	122.42	200.50
	1000	15.163	47.197	91.108	142.61	212.25
	10000	15.365	49.615	102.92	174.48	262.86
10000	0	3.5153	22.030	61.685	120.88	199.82
	1	4.0395	22.121	61.717	120.89	199.83
	10	6.9632	22.976	62.014	121.04	199.92
	100	13.251	31.535	65.341	122.63	200.85
	1000	15.190	47.275	91.236	142.80	212.58
	10000	15.393	49.703	103.10	174.78	263.30

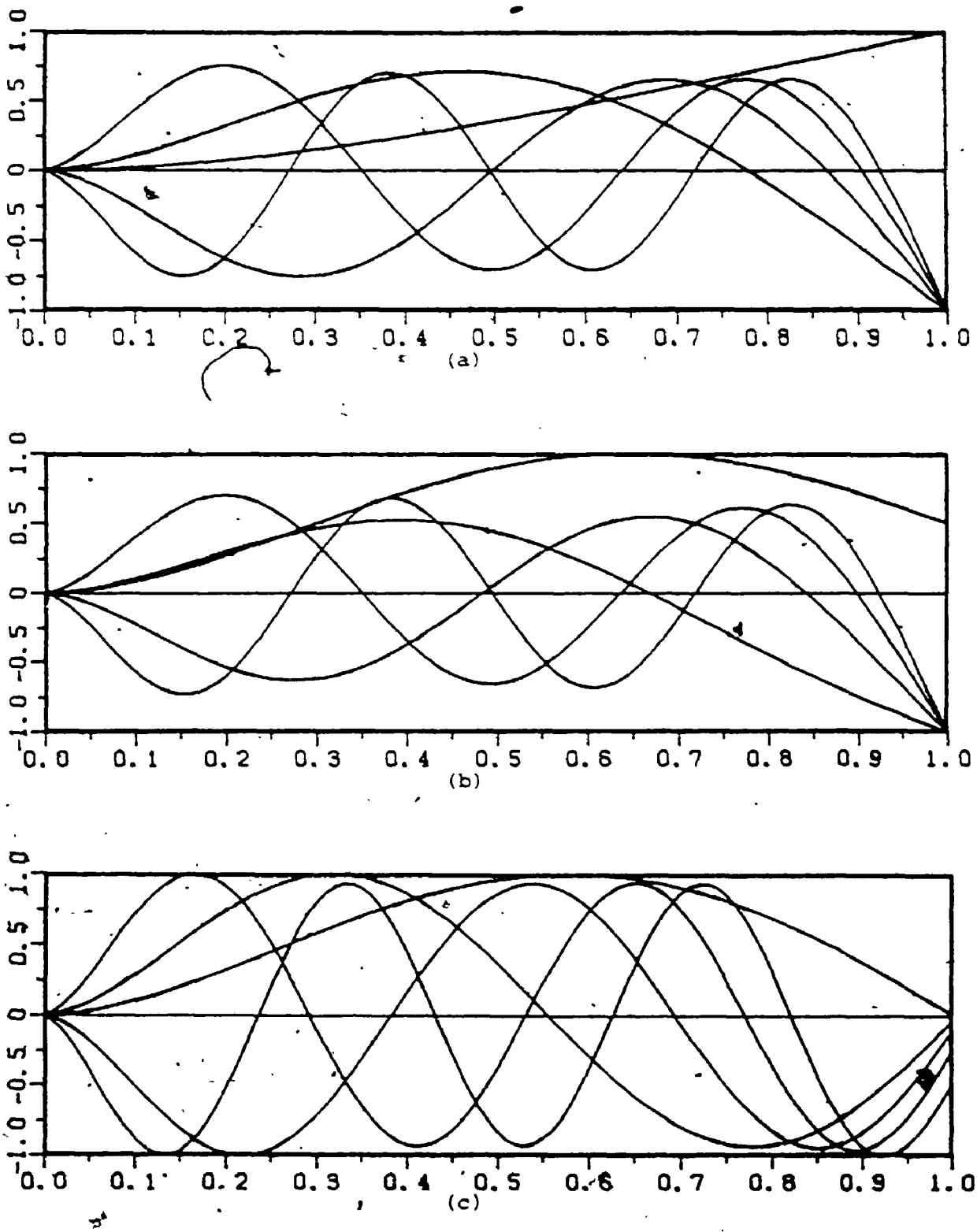

Figure 3.11. Mode shapes for beams with one end rotationally restrained-hinged and the other end translationally restrained; S_1 = 100, (a) K_1 = 1; (b) K_1 = 100; (c) K_1 = 10000.

have maximum values of unity. It should be mentioned that the mode shapes for beams with other values of rotational spring constant (S_1), with the same translational spring constant (K_1), are similar to those given in the figure, and it was not considered appropriate to include further illustrations. Additionally, the values for displacement (normalized), slope, bending moment and shear force for the lowest four modes are presented, for some sample cases, in Appendix A; the values are obtained using sixteen terms rather than fourteen terms in order to increase the accuracy, and may be of interest to other workers in the field.

From the convergence study, when the elastic springs or concentrated masses are attached at the interior of the beam rather than at the ends, and/or the other complicating effects, such as the existence of intermediate support (multi-span beam) etc., exist, the rate of convergence is diminished. Hence, in the following problems treated in this chapter, all the results were obtained using sixteen terms in the series (3.6).

The penultimate problem treated in this section is that of beams with both ends simply supported and subject to one or two intermediate translational spring(s). The frequency parameters for the lowest five modes are presented in Table 3.20 for the beam with one intermediate spring and in Table 3.21 for the beam with two intermediate springs where the two

Table 3.20

Frequency parameters $(\omega^2 m_o \ell^4/EI_o)^{\frac{1}{2}}$ for uniform, simply supported beams subject to an intermediate translational spring.

Spring Constant (K_1)	Location of Spring (ξ_1)	Mode sequence number 1		2	3	4	5
1	0.1	9.8793		39.487	88.834	157.92	246.74
	0.2	9.9045		39.501	88.837	157.92	246.74
	0.3	9.9356		39.501	88.828	157.92	246.74
	0.4	9.9608		39.487	88.830	157.92	246.74
	0.5	9.9704		39.478	88.838	157.91	246.74
10	0.1	9.9652	(9.9652)	39.566	88.900	157.97	246.78
	0.2	10.209	(10.209)	39.707	88.929	157.94	246.74
	0.3	10.504	(10.504)	39.709	88.837	157.94	246.78
	0.4	10.742	(10.741)	39.567	88.865	157.97	246.74
	0.5	10.833	(10.833)	39.478	88.939	157.91	246.78
100	0.1	10.730	(10.730)	40.326	89.557	158.49	247.15
	0.2	12.535	(12.534)	41.723	89.870	158.14	246.74
	0.3	14.554	(14.553)	41.865	88.938	158.13	247.15
	0.4	16.314	(16.313)	40.436	89.223	158.49	246.74
	0.5	17.071	(17.070)	39.478	89.968	157.91	247.15
1000	0.1	14.245	(14.243)	45.861	95.490	163.63	250.95
	0.2	18.600	(18.595)	55.424	100.90	160.56	246.74
	0.3	23.445	(23.439)	62.217	90.445	160.24	250.98
	0.4	30.032	(30.020)	52.736	93.402	164.18	246.74
	0.5	39.478	(39.466)	39.575	101.15	157.91	250.98
10000	0.1	17.268	(17.264)	55.598	114.78	193.01	286.59
	0.2	21.003	(20.997)	68.628	142.82	220.26	246.74
	0.3	26.033	(26.025)	85.272	125.68	182.11	294.36
	0.4	33.159	(33.150)	74.313	119.15	226.83	246.74
	0.5	39.478	(39.478)	58.722	157.91	166.50	298.84

Table 3.21

Frequency parameters $(\omega^2 m_o \ell^4 / EI_o)^{\frac{1}{2}}$ for uniform, simply supported beams subject to two intermediate translational springs ($K_2 = K_1$, $\xi_2 = 1 - \xi_1$)

Spring Constant (K_1)	Location of Spring (ξ_1)	Mode Sequence Number				
		1	2	3	4	5
1	0.1	9.8889	39.496	88.841	157.93	246.75
	0.2	9.9393	39.524	88.847	157.92	246.74
	0.3	10.001	39.524	88.829	157.92	246.75
	0.4	10.051	39.496	88.834	157.93	246.74
10	0.1	10.060	39.653	88.974	158.03	246.82
	0.2	10.543	39.934	89.030	157.96	246.74
	0.3	11.116	39.934	88.848	157.96	246.82
	0.4	11.555	39.653	88.905	158.03	246.74
100	0.1	11.579	41.160	90.282	159.06	247.55
	0.2	15.137	43.788	90.870	158.36	246.74
	0.3	18.869	43.789	89.047	158.36	247.55
	0.4	21.265	41.161	89.637	159.06	246.74
1000	0.1	19.104	52.080	101.83	169.07	254.99
	0.2	31.503	69.821	109.07	162.81	246.74
	0.3	48.838	69.841	91.586	162.82	255.04
	0.4	52.099	53.891	100.12	169.09	246.74
10000	0.1	28.159	76.235	145.44	230.28	322.97
	0.2	44.551	123.28	215.67	223.51	246.74
	0.3	79.427	123.39	130.10	224.04	331.76
	0.4	73.780	76.392	215.79	231.07	246.74

springs are assumed to have the same spring constants and are located symmetrically. In Table 3.20, the values in the parentheses for the fundamental modes are those given by Bapat and Bapat [85], who used the transfer matrix method. Excellent agreement may be seen to exist.

The final problem treated in this section is that of a two-equal-span beam with the ends simply supported and/or clamped, subject to translational springs at the centre of each span. The results are given in Table 3.22 for various combinations of the two spring constants.

3.4.2 Beams of Non-uniform Cross Section

In the three examples treated in this section, the beams are, as in section 3.3.2, considered to be of rectangular cross section of breadth b (in the y-direction) and depth d (in the z-direction); the flexural rigidity of relevance (vibration in the x-z plane) thus varies with bd^3 and the mass per unit length with bd.

The first problem treated is that of a cantilever beam with linear taper, subject to translational and rotational springs at the free end. The breadth b can be expressed as

$$b = b_0 \{1-(1-b_1/b_0)x/\ell\}$$

and the depth d of the cross section can be given similarly. The functions $f(\xi)$ and $h(\xi)$ in equation (3.5) for the

Table 3.22

Frequency parameters $(\omega^2 m_o \ell^4/EI_o)^{\frac{1}{4}}$ for uniform, two-equal-span beams subject to translational springs at the centre of each span.

Spring Constants K_1	K_2	Mode Sequence Number 1	2	3	4	5
(1) Both ends simply supported						
10	10	39.982	62.082	157.91	200.64	355.36
	100	41.989	63.685	157.91	200.72	355.62
	1000	49.017	83.274	157.91	201.52	358.13
	10000	51.569	157.91	166.81	216.49	377.58
100	100	44.239	65.023	157.91	200.79	355.87
	1000	52.334	83.453	157.91	201.60	358.39
	10000	54.997	157.91	166.81	216.58	377.95
1000	1000	73.577	88.351	157.91	202.42	361.04
	10000	80.842	157.91	166.88	217.55	381.67
10000	10000	157.91	165.00	170.30	232.07	418.14
(2) Both ends clamped						
10	10	62.010	89.886	199.88	247.57	417.03
	100	63.424	91.192	199.95	247.57	417.21
	1000	70.499	106.64	200.78	247.57	419.02
	10000	75.066	181.71	227.63	247.58	433.92
100	100	64.956	92.376	200.02	247.57	417.40
	1000	72.780	107.05	200.85	247.57	419.21
	10000	77.681	181.83	227.63	247.58	434.20
1000	1000	88.310	113.93	201.63	247.57	421.12
	10000	99.302	183.18	227.67	247.58	436.99
10000	10000	164.87	220.57	230.99	247.59	463.57
(3) Clamped at $\xi = 0$ and simply supported at $\xi = 1$						
10	10	46.500	80.060	171.50	231.32	375.92
	100	49.658	80.464	171.51	231.39	376.29
	1000	67.731	88.861	171.70	232.09	380.01
	10000	74.991	163.92	181.98	241.94	417.69
100	10	47.025	82.239	171.59	231.33	375.99
	100	50.236	82.579	171.61	231.40	376.35
	1000	69.454	89.791	171.80	232.10	380.08
	10000	77.601	163.93	182.09	241.94	417.85
1000	10	49.536	101.88	172.76	231.44	376.65
	100	52.936	101.98	172.78	231.51	377.02
	1000	77.465	103.64	172.99	232.21	380.79
	10000	99.166	164.07	183.38	241.95	419.44
10000	10	51.626	160.38	213.99	235.80	382.45
	100	55.053	160.38	214.06	235.83	382.85
	1000	80.900	160.38	214.77	236.12	386.86
	10000	160.13	168.89	223.44	242.29	431.47

stiffness and mass per unit length of the beam are, then, given as in equations (3.14)-(3.16). The results for the particular cases of b_1/b_0 and/or $d_1/d_0 = 0.2$ are presented in Table 3.23.

The next example treated is that of two-equal-span, simply supported beams with linearly varying cross sectional depth (constant breadth), subject to rotational springs at the left hand end. The functions $f(\xi)$ and $h(\xi)$ in equation (3.5) are then given by $f(\xi) = (1+c\xi)^3$ and $h(\xi) = (1 + c\xi)$, where the slope c is given by $c = (d_1-d_0)/d_0$. The first five frequency parameters are presented in Table 3.24 for various combinations of slope (c) and spring constant (S_1).

Finally, three span parabolically tapered beams with both ends translationally and rotationally restrained, as shown in Figure 3.12, are considered. The breadth and/or depth are assumed to vary symmetrically about the centre of the beam, with the central dimension being half of the respective dimension at the ends. The stiffness and mass distribution function $f(\xi)$ and $h(\xi)$ are then given as équations (3.17) - (3.19). The intermediate supports are assumed to be located at $\ell_1/\ell = 0.35$ and $\ell_2/\ell = 0.70$. The results are tabulated in Table 3.25 for various combinations of the spring constants K_1 and S_1, considering the spring constants at each end to be the same as those of the other end.

Table 3.23

Frequency parameters $(\omega^2 m_o \ell^4/EI_o)^{\frac{1}{2}}$ for cantilever beams with linear taper subject to translational and rotational springs at the free end.

Spring Constants K_1	S_1	Mode Sequence Number 1	2	3	4	5
(1) $b_1/b_o=0.2$, $d_1/d_o=1$						
0	10	6.9377	31.123	74.829	137.94	220.52
	100	7.0375	31.655	76.042	140.09	223.83
	1000	7.0482	31.714	76.180	140.34	224.23
10	0	10.775	28.869	67.164	126.03	204.90
	10	10.780	32.646	75.549	138.36	220.79
	100	10.781	33.033	76.667	140.44	224.05
	1000	10.781	33.076	76.794	140.68	224.45
100	0	15.566	43.321	80.344	133.85	209.58
	10	18.113	43.656	82.492	142.37	223.37
	100	18.492	43.712	82.830	143.82	226.15
	1000	18.537	43.719	82.869	143.99	226.49
1000	0	16.410	50.221	102.20	170.13	251.02
	10	20.403	56.386	108.55	173.64	251.18
	100	21.065	57.879	110.54	174.87	251.23
	1000	21.143	58.068	110.81	175.04	251.24
(2) $b_1/b_o=1$, $d_1/d_o=0.2$						
0	10	4.7425	17.906	41.189	74.758	118.64
	100	4.7456	17.924	41.234	74.841	118.77
	1000	4.7459	17.926	41.238	74.850	118.79
10	0	8.5865	21.641	40.942	70.481	111.07
	10	9.2093	21.688	43.171	75.864	119.34
	100	9.2161	21.688	43.195	75.932	119.46
	1000	9.2168	21.688	43.198	75.939	119.47
100	0	9.6597	27.342	53.559	86.667	125.82
	10	11.474	30.282	55.837	86.843	126.82
	100	11.497	30.333	55.885	86.898	126.83
	1000	11.500	30.338	55.889	86.898	126.84
1000	0	9.7854	28.150	56.553	94.909	143.05
	10	11.778	32.185	62.628	102.69	151.86
	100	11.804	32.257	62.765	102.91	152.16
	1000	11.807	32.264	62.779	102.93	152.19
(3) $b_1/b_o=0.2$, $d_1/d_o=0.2$						
0	10	6.5152	20.071	43.481	77.125	121.07
	100	6.5158	20.074	43.490	77.142	121.10
	1000	6.5158	20.075	43.491	77.143	121.10
10	0	10.362	27.371	51.230	81.391	120.21
	10	11.419	28.430	51.280	82.452	124.55
	100	11.422	28.434	51.280	82.456	124.56
	1000	11.422	28.434	51.280	82.456	124.56

continued

Table 3.23 (cont'd)

100	0	10.752	29.417	57.721	95.502	142.34
	10	12.270	32.660	62.497	101.04	147.20
	100	12.275	32.660	62.522	101.08	147.23
	1000	12.275	32.661	62.524	101.08	147.23
1000	0	10.794	29.638	58.444	97.348	146.40
	10	12.365	33.146	64.131	105.26	156.47
	100	12.371	33.161	64.160	105.31	156.54
	1000	12.371	33.162	64.163	105.31	156.55

Table 3.24

Frequency parameters $(\omega^2 m_o \ell^4/EI_o)^{\frac{1}{4}}$ for two equal-span, simply supported beams with linearly varying cross-sectional height, subject to a rotational spring at $\xi=0$.

Slope (C)	Spring Constant (S_1)	Mode sequence number 1	2	3	4	5
-1.0	1	10.832	28.248	38.647	64.911	104.58
	10	11.097	30.381	45.252	65.898	106.17
	100	11.215	31.060	51.316	67.542	107.56
	1000	11.231	31.138	52.308	67.968	107.80
	10000	11.233	31.146	52.412	68.017	107.82
-0.5	1	29.141	48.009	109.46	158.28	240.91
	10	30.821	55.565	111.13	168.13	242.65
	100	31.685	63.854	113.20	184.93	246.40
	1000	31.806	65.501	113.65	189.29	247.64
	10000	31.818	65.681	113.70	189.79	247.80
0	1	40.360	62.763	158.86	201.61	356.27
	10	43.594	68.857	163.95	208.72	362.34
	100	45.713	77.534	170.12	225.28	372.88
	1000	46.028	79.528	171.34	230.62	375.55
	10000	46.061	79.752	171.47	231.26	375.85
0.5	1	49.748	78.072	192.62	255.75	427.14
	10	54.204	82.877	201.31	259.60	438.31
	100	57.964	91.147	215.53	270.73	465.14
	1000	58.587	93.308	218.94	275.21	474.21
	10000	58.653	93.557	219.32	275.78	475.29
1.0	1	58.208	93.648	219.84	313.79	483.01
	10	63.432	97.581	229.94	316.54	495.40
	100	68.862	105.23	249.82	324.40	529.19
	1000	69.879	107.46	255.67	327.76	542.75
	10000	69.989	107.72	256.36	328.20	544.47

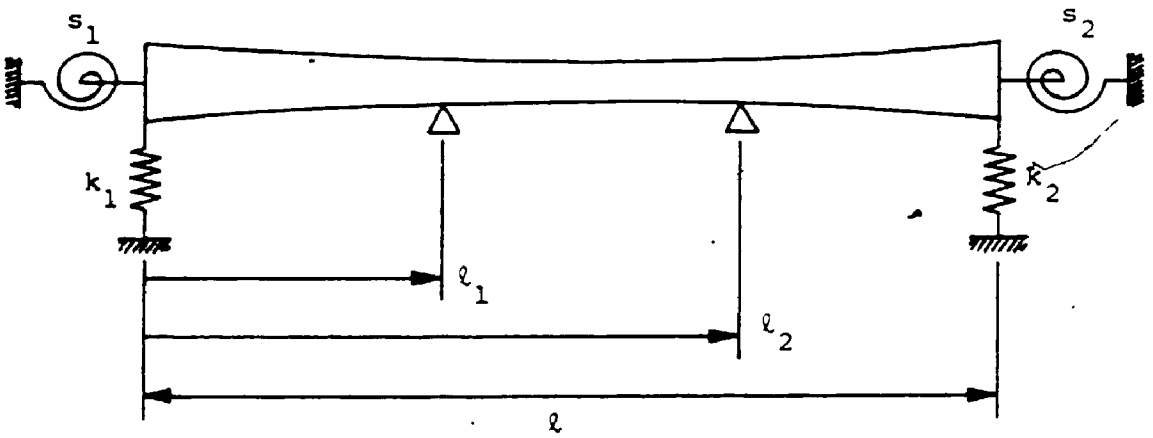

Figure 3.12. A parabolically tapered, three-span-beam with elastically restrained ends.

Table 3.25

Frequency parameters $(\omega^2 m_o \ell^4/EI_o)^{\frac{1}{2}}$ for three-span parabolically tapered beams with both ends translationally and rotationally restrained, as shown in Figure 3.10 ($K_2=K_1$, $S_2=S_1$, $\ell_1/\ell=0.35$, $\ell_2/\ell=0.70$).

Spring constants		Mode Sequence Number				
K_1	S_1	1	2	3	4	5
(1) Beams with parabolically tapered breadth, uniform depth						
0	10	24.600	34.506	121.88	185.70	244.36
	100	28.007	39.581	127.31	209.35	277.07
	1000	28.481	40.329	128.10	213.78	283.58
10	0	17.485	24.439	110.10	156.54	209.25
	10	26.234	35.896	122.01	185.92	244.55
	100	29.264	40.621	127.38	209.49	277.18
	1000	29.691	41.324	128.17	213.89	283.68
100	0	34.844	40.997	112.52	159.37	211.57
	10	37.452	46.301	123.21	187.91	246.31
	100	38.573	48.882	128.09	210.69	278.22
	1000	38.740	49.284	128.81	214.96	284.58
1000	0	72.489	90.373	135.49	193.34	239.39
	10	76.348	91.864	136.44	209.86	265.31
	100	78.925	92.873	137.08	223.95	289.24
	1000	79.383	93.054	137.20	226.74	294.14
(2) Beams with parabolically tapered depth, uniform breadth						
0	10	17.850	25.217	71.667	129.33	172.83
	100	19.743	28.321	73.795	145.12	192.90
	1000	19.976	28.723	74.077	147.54	195.96
10	0	12.730	16.640	64.874	100.51	138.77
	10	19.793	26.881	71.805	129.59	173.05
	100	21.319	29.617	73.894	145.28	193.01
	1000	21.510	29.975	74.170	147.68	196.06
100	0	30.940	35.611	67.700	104.76	142.20
	10	31.572	38.252	73.172	132.06	175.05
	100	31.754	39.148	74.879	146.69	194.04
	1000	31.778	39.272	75.108	148.95	196.95
1000	0	51.279	69.168	91.327	151.82	181.87
	10	57.443	74.857	92.991	158.33	195.99
	100	60.537	78.349	94.094	162.75	205.09
	1000	61.019	78.944	94.289	163.52	206.62
(3) Beams with parabolically tapered breadth and depth						
0	10	16.825	23.640	73.997	129.73	172.66
	100	18.372	26.293	76.002	146.20	194.20
	1000	18.555	26.622	76.250	148.60	197.37
10	0	12.483	15.381	65.528	96.272	132.90
	10	19.156	25.607	74.122	130.00	172.89
	100	20.335	27.877	76.088	146.35	194.32
	1000	20.477	28.162	76.331	148.74	197.47

continued

Table 3.25 (cont'd)

100	0	32.352	36.555	68.850	100.87	136.64
	10	32.600	38.515	75.370	132.54	174.99
	100	32.659	39.080	76.953	147.77	195.37
	1000	32.666	39.154	77.153	150.01	198.38
1000	0	51.860	69.321	92.442	153.81	181.94
	10	60.875	77.613	95.243	160.33	197.54
	100	64.643	82.263	97.029	164.53	207.08
	1000	65.184	83.024	97.334	165.25	208.64

CHAPTER 4

VIBRATION OF RECTANGULAR PLATES

4.1. INTRODUCTORY REMARKS

As mentioned in Chapter 1, the most widely used method for the solution of vibration problems of rectangular plates is the Rayleigh-Ritz (or Rayleigh) method. The formulation of the method requires the assumption of the admissible functions, which satisfy at least the geometrical boundary conditions (i.e. zero displacement and/or zero slope conditions) of the plate concerned. The natural boundary conditions (that is, zero bending moment and/or zero Kirchhoff shear force) can be neglected in the consideration of the admissible functions; the minimization procedure causes convergence towards the satisfaction of these boundary conditions.

For uniform, single, rectangular plates with classical boundary conditions, many researchers, including Ritz himself, have used the products of vibration characteristic beam functions as the admissible functions (for example, see references [15-17]). The use of the beam functions gives, for plates with no free edge, very good results for the natural frequencies, and associated mode shapes, bending moments and shear forces. However, when one or more free edges are involved, the results are less satisfactory for the

frequencies and mode shapes, and are unsatisfactory for bending moments and shear forces. This is due to the fact that the natural boundary conditions of plates at the free edges include the effect of Poisson's ratio and thus the use of the beam functions, which are free from Poisson's ratio, results in the imposition of an over-restraining effect, as shown mathematically in the following.

Consider here an isotropic plate lying in the x-y plane, with the edges parallel or perpendicular to the coordinates. The boundary conditions at the free edges are given at zero bending moment (M_B) and zero Kirchhoff shear force (Q_K). In x-direction, for an example, the conditions are expressed as

$$M_B = -D\left(\frac{\partial^2 w}{\partial x^2} + \nu \frac{\partial^2 w}{\partial y^2}\right) = 0, \tag{4.1a}$$

$$Q_K = -D\left\{\frac{\partial^3 w}{\partial x^3} + (2-\nu)\frac{\partial^3 w}{\partial x\, \partial y^2}\right\} = 0, \tag{4.1b}$$

where D is the plate flexural rigidity and ν is Poisson's ratio. When the admissible functions for the displacement w are assumed as the products of the characteristic beam functions satisfying the equivalent beam boundary conditions, the displacement can be expressed as

$$w = \sum_i \sum_j A_{ij}\Phi_i(x)\Psi_j(y), \tag{4.2}$$

where $\Phi_i(x)$ and $\Psi_j(y)$ denote the beam functions in x- and y-

directions, respectively, and

$$\frac{d^2\Phi_i}{dx^2} = \frac{d^3\Phi_i}{dx^3} = 0. \tag{4.3}$$

Substituting equation (4.2), together with equation (4.3), into the expressions for M_B and Q_K yields

$$M_B = -D\nu \frac{\partial^2 w}{\partial y^2}, \qquad Q_K = -D(2-\nu) \frac{\partial^3 w}{\partial x \partial y^2},$$

which cannot be zero along the edges except for some special points. Hence, the use of the beam functions results the inclusion of additional constrained conditions ($M_B + D\nu\,\partial^2 w/\partial y^2 = 0$, $Q_K + D(2-\nu)\,\partial^3 w/\partial x\,\partial y^2 = 0$). These conditions cause greater stiffness and higher frequencies to be generated. (The effect of the terms including Poisson's ratio is, in fact, very small and thus the frequencies and mode shapes obtained are reasonably accurate.)

It may be noted that, an alternative to the beam functions used are simply supported plate functions [23, 24], which are the mode shapes of plates having two parallel edges simply supported. The results obtained are very similar to those obtained with the beam functions. Also, for clamped plates, the products of functions obtained from the modified Bolotin's method [20, 21] have been used.

In order to release the over-restraining effect involved in the beam functions, Bassily and Dickinson [18, 19]

introduced the concept of 'degenerated beam functions'. The concept is based on the relaxation of the unnecessary beam end conditions imposed. The degenerated beam functions, then, permit the treatment of plates with free edges with equivalent accuracy to that obtained for plates with no free edge using the characteristic beam functions. Other functions, which are free from the over-restraining effect, proposed for the admissible functions in the literature are polynomial functions. Such include simple polynomials used by Narita [118, 129], who studied free and cantilever plates (with point supports), by Laura and Grossi [198, 199], who studied plates with free edges while the remaining edges are elastically restrained against rotation, and by McIntyre and Woodhouse [200], who studied fully free, orthotropic plates, and orthogonal polynomials by Bhat [25-27] as explained earlier. Since the degenerated beam functions are not orthogonal, and are trigonometric and hyperbolic, polynomial functions are more attractive considering the evaluation of integrals involved in the Rayleigh-Ritz procedure. In particular, the BCOP studied in Chapter 2 have more attractive features, which include their orthogonality, superiority of the results for lower modes, and their applicability to plates with various complicating effects.

In the following sections, the BCOP are used to study the vibration problem of continuous plates with any combination of classical boundary conditions, including one

type of box-like structure constructed with rectangular plates, and plates with arbitrary numbers of point supports. Similar to vibrating beam problems, various complicating effects can be included without any formal difficulty; for the sake of brevity, however, these complicating effects are omitted here.

4.2. ANALYSIS

It is assumed that the plate under consideration lies in the x-y plane, is bounded by edges x=0, x=a, y=0 and y=b, and is of uniform thickness, rectangularly orthotropic material with the symmetry axes of the material lying orthogonal to the plate edges. The intermediate line supports are also assumed to lie orthogonal to the plate edges and to prevent motion in the z-direction but to offer no resistance to normal rotations.

For small amplitude, simple harmonic vibration of the plate, the deflection may be expressed as $w(x, y)\sin \omega\tau$, where ω is the radian natural frequency of free vibration and $w(x, y)$ the maximum deflection with respect to time τ. Then, the maximum strain and kinetic energies for the plate during vibration are given, respectively, by [201,202]

$$V_{max} = \frac{1}{2}\int_0^a\int_0^b [D_x(\frac{\partial^2 w}{\partial x^2})^2 + 2\nu_{xy}D_y(\frac{\partial^2 w}{\partial x^2})(\frac{\partial^2 w}{\partial y^2}) + D_y(\frac{\partial^2 w}{\partial y^2})^2$$

$$+ 4\, D_{xy}(\frac{\partial^2 w}{\partial x\, \partial y})^2]dy\, dx, \qquad (4.4)$$

$$T_{max} = \frac{\rho h \omega^2}{2} \int_0^a \int_0^b w^2 dy dx, \tag{4.5}$$

where ρ is the material density, h the plate thickness, ν_{xy} and ν_{yx} Poisson's ratios, and $D_x = E_x h^3/12(1-\nu_{xy}\nu_{yx})$, $D_y = D_x E_y/E_x$ and $D_{xy} = G_{xy} h^3/12$ are flexural rigidities, in which E_x and E_y are Young's moduli in the x- and y-directions, respectively, and G_{xy} is the shear modulus. The isotropic case is obtained by writing $\nu_{xy} = \nu_{yx} = \nu$, $D_x = D_y = Eh^3/12(1-\nu^2) = D$ and $D_{xy} = (1-\nu)D/2$.

Introducing non-dimensionalized parameters, $\xi = x/a$ and $\eta = y/b$, the deflection w may be expressed

$$w = \sum_i \sum_j A_{ij} \Phi_i(\xi) \Psi_j(\eta), \tag{4.6}$$

in which $\Phi_i(\xi)$ and $\Psi_j(\eta)$ denote appropriate shape functions in ξ- and η-directions (x- and y-directions), respectively. Typical shape functions used in the literature for single plates are characteristic beam functions, simply supported plate functions and polynomial functions, as discussed before. Among these functions, the BCOP usually yield the best results for the lower modes.

For continuous plates, it is worth briefly discussing the choice of functions. Consider a plate, as an example, bounded by clamped edges at x=0, a and y=0, b and passing over a line support at $x=\alpha a$, where $\alpha<1$. The functions of concern are those for the x-direction or ξ-direction in non-

dimensionalized form, $\Phi_i(\xi)$. Appropriate admissible functions might be the vibration mode shapes of a uniform beam of length a, clamped at each end and passing over a knife edge support at $x = \alpha a(\xi=\alpha)$. Such functions would satisfy the required boundary conditions for the plate and are relatively easily determined. However, the subsequent use of these functions in the Rayleigh-Ritz procedure would require the tedious and error-prone evaluation of integrals involving products of trigonometric and hyperbolic functions. For plates involving more than two spans, the appropriate beam functions themselves become rather more difficult to determine. (The simply supported plate functions are much more difficult to determine.) In these respects, the BCOP are much more attractive, compared with the beam functions, for continuous plates than for single plates.

The generating procedure for $\Phi_i(\xi)$ and $\Psi_j(\eta)$ is the same as that in Chapter 2, the functions being obtained simply by replacing x by ξ and y by η, and taking the weight function $w_f = 1$, since the plate is of uniform thickness. The choice of the generating function depends upon the type of plate being considered and is given with the discussion of each system. The starting functions for plane plates are chosen as those satisfying both geometrical and natural boundary conditions of the equivalent beams (equation (2.9) for single span plates). For a box-like structure, the starting function will be given in section 4.4.

After substituting equation (4.6) into equations (4.4) and (4.5), and equating energies, the Rayleigh-Ritz procedure requires the minimization of the functional (V_{max}-T_{max}) with respect to the undetermined coefficients A_{ij}, for plates with no point support. However, when point supports are involved, equation (4.6) must also satisfy the constraint conditions at the supported points (x_p, y_p). These constraints may take the form of $w=0$ at $\xi=\xi_p$, $\eta=\eta_p$, for a simple point support which offers no resistance to slope, or may include slope constraints such as $\partial w/\partial\xi = 0$ and/or $\partial w/\partial\eta = 0$, in which $\xi_p = x_p/a$ and $\eta_p = y_p/b$. These may be expressed:

$$\sum_i \sum_j A_{ij}\Phi_i(\xi_p)\Psi_j(\eta_p) = 0, \tag{4.7a}$$

for a simple point support, plus

$$\sum_i \sum_j A_{ij}\Phi_i'(\xi_p)\Psi_j(\eta_p)=0 \text{ and/or } \sum_i \sum_j A_{ij}\Phi_i(\xi_p)\Psi_j'(\eta_p)=0, \tag{4.7b,c}$$

for point supports offering slope restraints in the x-and y-direction, respectively. Although the analysis given here can easily accommodate any or all of the constraints mentioned, the numerical results for point supported plates have been confined to simple point supports, thus only constraint equation (4.7a) is retained in the formulation of the frequency equation. The minimization procedure is performed after the introduction of Lagrangian multipliers into the constraint equation (4.7a) and yields the following

expression:

$$\sum_m \sum_n C_{mnij} - \Omega^2 E_{ii}^{(0,0)} F_{jj}^{(0,0)} A_{ij} + \sum_p \lambda_p \Phi_i(\xi_p)\Psi_j(\eta_p)=0, \tag{4.8}$$

where $\Omega = (\rho h \omega^2 a^4/H)^{\frac{1}{2}}$ and

$$C_{mnij} = \frac{D_x}{H} E_{mi}^{(2,2)} F_{nj}^{(0,0)} + \frac{D_y}{H} \left(\frac{a}{b}\right)^4 E_{mi}^{(0,0)} F_{nj}^{(2,2)}$$

$$+ \left(\frac{a}{b}\right)^2 \left(1-2\frac{D_{xy}}{H}\right)\{E_{mi}^{(0,2)} F_{nj}^{(2,0)} + E_{mi}^{(2,0)} F_{nj}^{(0,2)}\}$$

$$+ 4\frac{D_{xy}}{H}\left(\frac{a}{b}\right)^2 E_{mi}^{(1,1)} F_{nj}^{(1,1)},$$

in which, $H = \nu_{xy} D_y + 2D_{xy}$ (=D in the isotropic case);

$$E_{mi}^{(r,s)} = \int_0^1 (d^r\Phi_m/d\xi^r)(d^s\Phi_i/d\xi^s)d\xi,$$

and

$$F_{nj}^{(r,s)} = \int_0^1 (d^r\Psi_n/d\eta^r)(d^s\Psi_j/d\eta^s)d\eta.$$

The first two terms of equation (4.8) yield, for the plate with no point support (the third term then does not exist), a standard eigenvalue equation, whose solution gives the natural frequencies of the plate. For the plate with point supports, equations (4.8) and (4.7a) yield an eigenvalue determinant, the zeros of which give the natural frequencies of the plate. Then, back substitution of the values for the frequencies yields the coefficient vector, substitution of

which into equation (4.6) gives the plate mode shapes.

For plates with point supports, the direct solution of equations (4.8) and (4.7a) by seeking the frequency parameters for which the determinant becomes zero can be hazardous, since the detection and extraction of multiple, or even close, eigenvalues is very difficult. The algorithm presented by Sehmi [203], which permits the detection and extraction of the zeros of the determinant systematically and infallibly, was therefore used in the computation of the present numerical results for point supported plates. The order of the matrix equation (4.8 and 4.7a), in general, is the product of the number of terms considered for the assumed shape function in the ξ- and η-directions plus the number of constraint conditions; where symmetry exists, however, this may be used to reduce the order of the matrix equation.

It may be noted that, for the calculations of the numerical results, the functions $\Phi_i(\xi)$ and $\Psi_j(\eta)$ in equation (4.6) were both normalized (orthonormal polynomials); the second term in equation (4.8) then reducing to $\Omega^2 A_{ij}$. This gives some computational advantages, as discussed in reference [204], for the solution of the standard eigenvalue problem which is utilized in Sehmi's algorithm [203].

4.3. PLANE CONTINUOUS PLATES

The generating functions used for the problems treated in this section, for plates with no point support, are $g(\xi) = \xi$ and $g(\eta) = \eta$. For plates with simply supported edges, higher degree generating functions may be of interest, which will be discussed briefly in section 4.5, for point supported plates.

The first problem treated is the three-span, continuous plate shown in figure 4.1. The plate is simply supported along edges y=0, y=b, passes over line supports at x=a/4 and 3a/4 and has aspect ratio a/b=4. Three combinations of boundary conditions on edges x=0 and x=a are considered: both edges simply supported (S-S), both edges clamped (C-C) and one edge clamped, the other simply supported (C-S). Exact solutions for this problem have been given by Azimi et al. [97]. The frequency parameters for the lowest six modes of vibration are presented in Table 4.1 and are compared with the exact solutions. When describing the mode type for the S-S and C-C cases, the first S or A indicates symmetry or antisymmetry, respectively, about the x=a/2 axis and the second the symmetry or antisymmetry about the y=b/2 axis. (This convention is used in later tables in this chapter also, except for box-like structure.) For the C-S case, only symmetry or antisymmetry about the y=b/2 axis can exist. It may be seen that for all three cases, the present results are

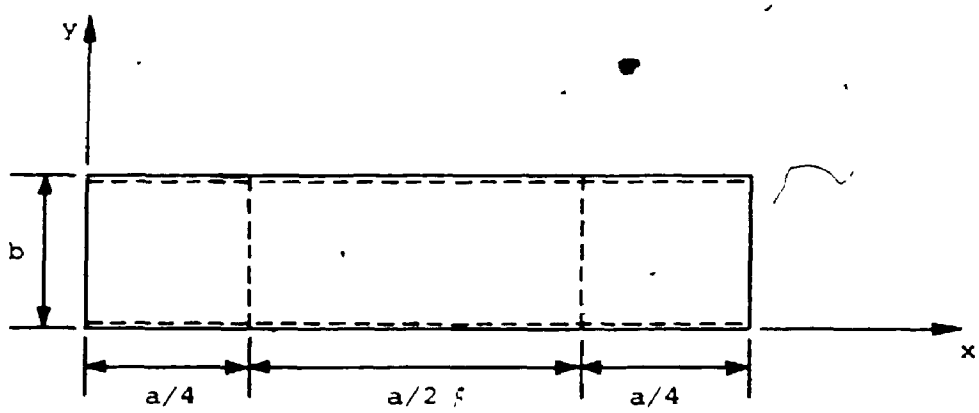

Figure 4.1. Three-span continuous rectangular plate, simply supported along each of the two continuous edges.

Table 4.1. Frequency parameters $(\rho h\omega^2 b^4/D)^{\frac{1}{2}}$ for the three-span plate shown in Figure 4.1.

Edge Condition	No. of terms in series (4.6) i x j	Mode Type					
		SS-1	AS-1	SS-2	AS-2	SS-3	SA-1
S-S	4 x 4	12.990	19.739	21.907	24.145	40.007	42.371
	5 x 5	12.953	19.739	21.714	24.140	36.213	42.308
	6 x 6	12.940	19.739	21.639	23.914	35.529	42.289
	8 x 4	12.931	19.739	21.595	23.813	35.404	42.268
	9 x 4	12.930	19.739	21.594	23.812	35.401	42.268
	Exact [97]	12.92	19.74	21.53	23.65	35.21	42.24
		S-1	S-2	S-3	S-4	S-5	A-1
C-S	9 x 4	12.972	20.118	22.916	26.915	36.628	42.307
	Exact [97]	12.94	20.10	22.64	26.50	35.59	42.24
		SS-1	AS-1	SS-2	AS-2	SS-3	SA-1
C-C	6 x 6	12.982	20.834	25.746	27.328	36.440	42.296
	9 x 4	12.967	20.828	25.684	27.262	36.170	-
	Exact [97]	12.96	20.81	25.64	27.12	35.97	42.25

in close agreement with the exact solutions and the partial convergence study for the S-S case suggests that the rate of convergence is reasonably rapid.

The second problem treated is the two-way, two-span plate shown in Figure 4.2 which is simply supported on edges $x = 0$, a and $y = 0$, b and passes over line supports at $x = \alpha a$ and $y = \gamma b$. Results for a plate of aspect ratio $a/b = 1.5$ with $\alpha = \gamma = 1/\sqrt{3}$ and for a square plate with various values of α and γ are given in Table 4.2, as computed using six terms in each of the series $\Phi_i(\xi)$ and $\Psi_j(\eta)$, without regard to symmetry, even though it exists for the case of $\alpha = \gamma = 1/2$. For the rectangular plate, comparison results obtained by Takahashi and Chishaki [102] are given and reasonably close agreement may be seen to exist. For the case of $\alpha = \gamma = 0$, the system essentially becomes a plate clamped along $x = 0$, $y = 0$ and simply supported along $x = a$, $y = b$, and unsupported elsewhere. When $\alpha = \gamma = 1/2$, the system may be treated as a plate bounded by $x = 0$, $a/2$ and $y = 0$, $b/2$, the $x = 0$, $y = 0$ edges being simply supported while the $x = a/2$, and the $y = b/2$ edges are either clamped or simply supported, depending upon the symmetry or antisymmetry of the mode of vibration of the original plate. Comparison results, from the work of Leissa [17], are therefore given for the square plate, where appropriate. It may be seen that close agreement is obtained for the case of $\alpha = \gamma = 1/2$ but poorer agreement is achieved for $\alpha = \gamma = 0$. The latter may

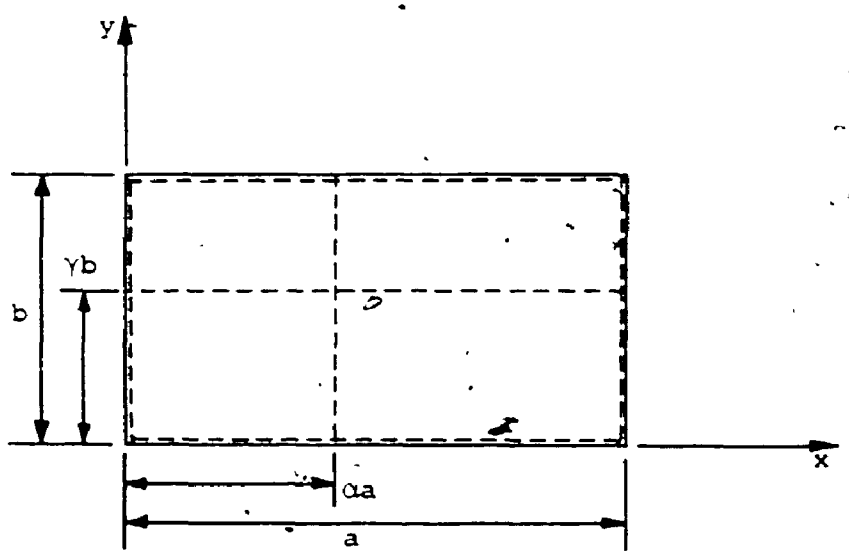

Figure 4.2. Two-way, two-span plate, simply supported all around.

Table 4.2. Frequency parameters $(\rho h\omega^2 b^4/D)^{1/2}$ for the two-way continuous plate shown in Figure 4.2.

Side ratio a/b	Support location α	Support location γ	Source of result	Mode Sequence Number 1	2	3	4	5	6
1.5	$1/\sqrt{3}$	$1/\sqrt{3}$	Present	49.293	63.925	85.322	94.445	98.712	128.15
			Ref [102]	49.305	62.907	83.892	91.301	96.295	123.41
1	0	0	Ref [17]	27.056	60.544	60.791	92.865	114.57	114.72
	0	0	Present	27.887	62.484	62.723	95.995	118.41	118.54
	1/4	1/4	Present	42.844	97.437	97.531	152.58	178.59	178.59
	1/4	1/2	Present	79.040	116.48	130.58	178.91	198.70	210.20
	1/2	1/2	Present	78.958	95.911	95.911	110.81	199.02	199.02
	1/2	1/2	Ref [17]+	78.957	94.585	94.585	108.22*	197.39	197.39

+ Exact solution

* Upper bound

be explained by the fact that as α and γ tend to zero, the assumed starting functions $\Phi_1(\xi)$ and $\Psi_1(\eta)$ satisfy the zero deflection and second derivative conditions of the simple support plus a zero normal slope condition enforced by the proximity and ultimate coincidence of the line support and edge. Thus, instead of satisfying only the zero slope and deflection conditions of the clamped edge, a third, zero curvature, constraint is applied.

As a third problem, the first six frequency parameters for the square, two-way continuous plate shown in Figure 4.3 are presented in Table 4.3. The line support positions are given by $\alpha = 0.35$ and $\beta = 0.7$, thus no symmetry exists. Three combinations of edge conditions are considered: all edges clamped (CCCC); two adjacent edges clamped, the other two simply supported (CCSS); and two opposite edges clamped, the other two simply supported (CSCS). For the fully clamped case, results are given for an orthotropic plate and a brief convergence study is presented for the isotropic plate; the convergence may be seen to be reasonably rapid.

Table 4.4 shows the first six natural frequency parameters for the six-equal-span, clamped plate shown in Figure 4.4, for which $a/b = 6$. Comparison results, obtained by Elishakoff and Sternberg [96] using the modified Bolotin method, which tends to yield lower bounds, are also given. The agreement achieved between the present results (upper

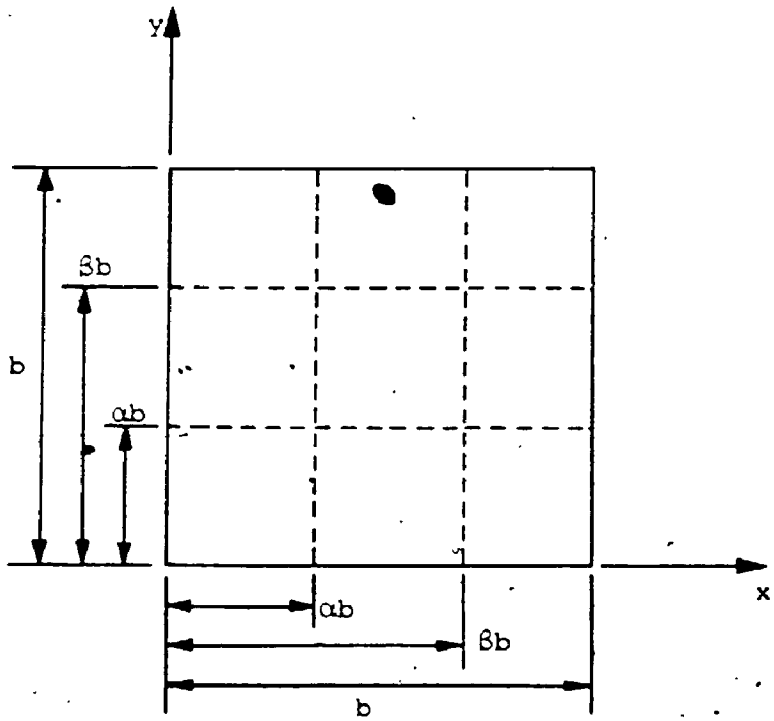

Figure 4.3. Two-way, three-span square plate.

Table 4.3. Frequency parameters $(\rho h\omega^2 b^4/H)^{1/2}$ for the square plate shown in Figure 4.3 for $\alpha = 0.35$ and $\beta = 0.7$.

Material Properties D_x/H ; D_y/H	Boundary Conditions	No. of Terms i x j	Mode Sequence Number 1	2	3	4	5	6
1 ; 1	CCCC	4 x 4	202.40	249.31	249.47	290.71	344.19	344.38
		5 x 5	199.07	244.48	244.54	284.09	299.96	299.96
		6 x 6	198.55	243.27	243.32	282.31	297.20	297.20
	CCSS	6 x 6	190.69	226.87	227.18	259.99	265.88	265.93
	CSCS	6 x 6	184.34	212.77	231.39	256.24	262.44	286.99
1.543 ; 4.810*	CCCC	6 x 6	301.03	345.36	401.76	414.92	449.04	494.99

* The values given for plywood by Hearmon [12]

Table 4.4. Frequency parameters $(\rho h \omega^2 b^4/D)^{\frac{1}{2}}$ for the six-equal-span plate shown in Figure 4.4($i \times j = 6 \times 6$).

Source of Result	Mode Type					
	AS-1	SS-1	AS-2	SS-2	AS-3	SS-3
Present	29.322	30.411	32.157	34.377	35.986	36.898
Reference [96]	29.244	30.102	31.438	33.045	34.494	35.112

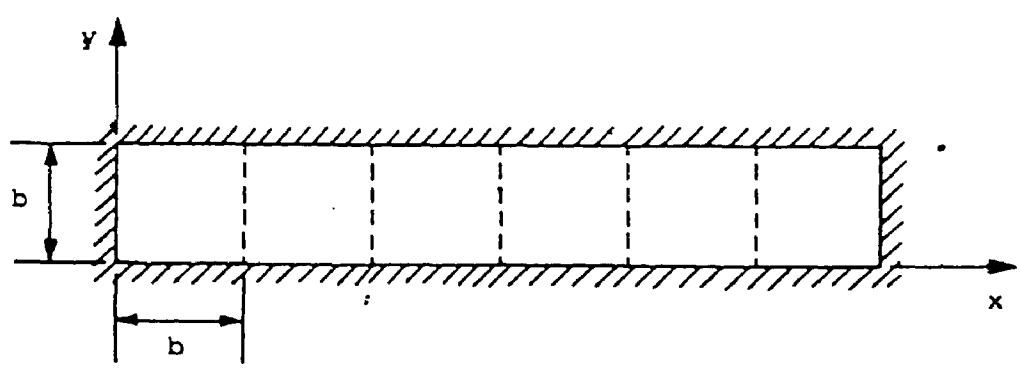

Figure 4.4. Six-equal-span, clamped rectangular plate.

Table 4.5. Frequency parameters $(\rho h\omega^2 b^4/D)^{1/2}$ for a square plate with six equal spans in each direction ($i \times j = 6 \times 6$)

Boundary Conditions	Mode Type	Mode Sequence Number 1	2	3	4	5	6
CCCC	AA	747.42	880.94	880.96	1000.67	1052.08	1052.09
	AS(SA)	799.81	927.43	980.89	1091.97	1092.21	1092.54
	SS	849.64	1023.72	1023.86	1131.15	1131.15	1177.67
SSSS	AA	710.61	786.04	786.04	856.56	966.69	966.69
	AS(SA)	730.10	804.16	869.12	935.00	982.35	1092.01
	SS	749.20	885.98	885.98	1008.88	1106.32	1106.32

bound) and those of the reference (possibly lower bounds) is again very good.

The last problem treated in this section is a square plate having six equal spans in both the x- and y-directions and either clamped on all four edges or simply supported on all four edges. The lowest six frequency parameters in each symmetry group are presented in Table 4.5, as obtained by using six terms in the series for each of $\Phi_i(\xi)$ and $\Psi_j(\eta)$. Confidence in the results may be engendered by recognizing that the frequency of the first mode of the simply supported plate can be obtained by considering that mode of a single span, simply supported plate having six half-waves in each direction. The 'exact' value that results for the frequency parameter is thus $36 \times 2\pi^2$ which is 710.6115, whereas the present approach gives 710.6144.

4.4 A BOX-LIKE STRUCTURE

The open box structure shown in Figure 4.5 is considered. It has side lengths a, b and c and is clamped at its base and free at the top. If in-plane stretching of the constituent plates is neglected, as is permissible for lower modes of vibration, the vertical corners act essentially as line supports since the lateral motion is then restrained, while continuity of normal slope is preserved, through the corners remaining right angles. Since the box is symmetrical about the two planes X = a/2 and Y = b/2, the structure can

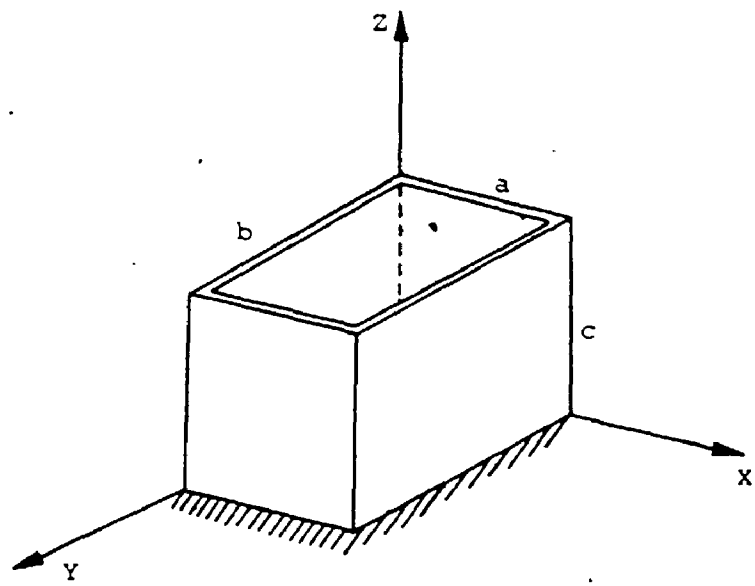

Figure 4.5. Box-like structure.

be considered to vibrate in four families of modes:

Type 1: Modes symmetrical about both $X = a/2$ and $Y = b/2$, the lowest of which is illustrated in Figure 4.6(a), where the box is viewed from above;

Type 2: Modes symmetrical about $X = a/2$ and antisymmetrical about $Y = b/2$, as illustrated in figure 4.6(b),

Type 3: Modes antisymmetrical about $X = a/2$ and symmetrical about $Y = b/2$; and

Type 4: Modes antisymmetrical about both $X = a/2$ and $Y = b/2$.

It is tempting to describe the displacement variation in the X- and Y-directions in terms of polynomials in a coordinate x which is zero at $X = 0$, $Y = 0$, and follows around the perimeter of the box, arriving back at the origin when $x = 2(a + b)$. the conditions to be satisfied by the starting and subsequent functions are zero deflection at each corner and continuity of slope at the origin, the form of the starting function being illustrated in the top part of Figure 4.6(a). Considering x to follow the perimeter in a clockwise direction, it is required that $\Phi_1(\xi) = 0$ at $\xi = 0$, $a/(2a + 2b)$, $1/2$, $(2a + b)/(2a + 2b)$ and 1, and $\Phi_1'(0) = \Phi_1'(1)$, in which $\xi = x/(2a + 2b)$. It should be noted that such a function does not give a deflection shape which is symmetrical about the $X = a/2$, $Y = b/2$ axes; even satisfaction of equal or opposite slopes at the corners does

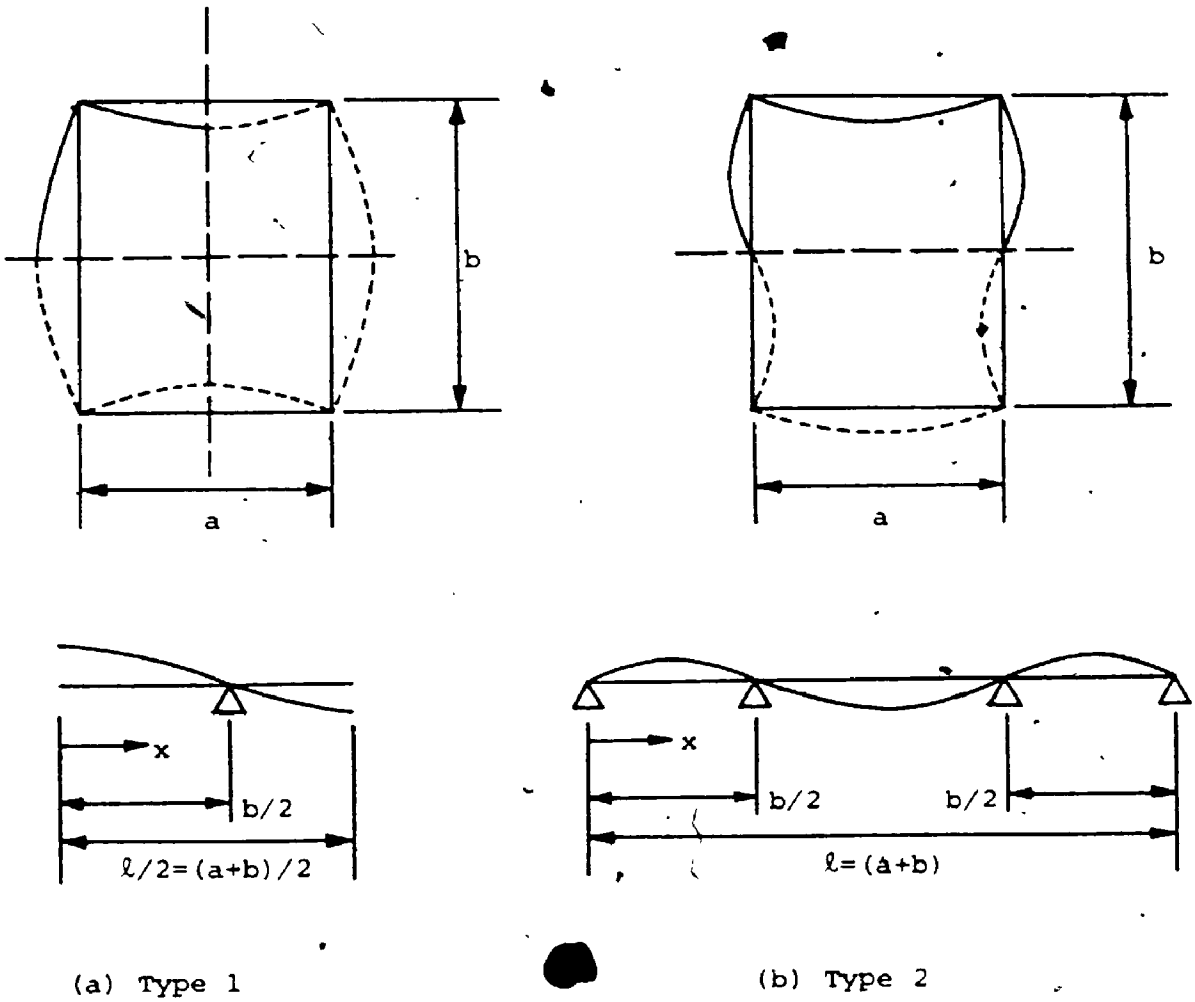

Figure 4.6. Starting functions for box-like structure.

not enforce this symmetry condition. While the satisfaction of symmetry is not a requirement for the method of solution, it is a desired property for the shape functions. Also, the use of the generating function $g(\xi) = \xi$ does not preserve the slope continuity condition at the origin. A higher degree generating function can be taken so that this condition will be preserved but the symmetry (or antisymmetry) of the subsequent functions generated will be further diminished. Instead, it is advantageous to consider only sections of the box and to include its properties of symmetry in the conditions to be satisfied by the polynomial starting and subsequent functions.

For modes of type 1, it is necessary to consider only one quarter of the box, bounded by $X = 0, a/2$, $Y = 0, b/2$ and $Z = 0, c$. In choosing the admissible functions for the X- and Y-directions, it is convenient to consider the two constituent half plates as folded out to form a plane plate, passing over a line support (the corner) and to introduce the coordinate x, as shown in the bottom part of Figure 4.6(a). The starting function Φ_1 is chosen to satisfy zero slope at $x = 0$ and $\ell/2$ and zero deflection at $x = b/2$, where $\ell = a + b$. This gives, for a monic polynomial,

$$\Phi_1(\xi) = \sum_{i=1}^{4} a_i \xi^{i-1},$$

where $\xi = 2x/\ell$, $a_1 = 3b^2/2\ell^2 - b^3/\ell^3$, $a_2 = 0$, $a_3 = -3/2$ and $a_4 = 1$. The use of the simple generating function $g(\xi) = \xi$ for the subsequent polynomials does not preserve the zero slope condition at $x = 0$ and $x = \ell/2$ (theorem (1) in Chapter 2), and thus, in this case, a higher degree generating function $g(\xi) = \xi^3 - 3\xi^2/2$ is used.

For modes of type 2, one half of the box is considered, as illustrated in Figure 4.6(b). The function Φ_1 is chosen to satisfy zero deflection at the axes of antisymmetry ($x = 0, \ell$) and at the line supports ($x = b/2$ and $x = \ell - b/2$), together with symmetry about $x = \ell/2$. A similar starting function is used for modes of type 3, this time with the line supports (corners) located at $x = a/2$ and $x = \ell - a/2$. Assuming the line supports to be at $x = \alpha\ell$ and $x = \ell(1-\alpha)$, the starting function may be written

$$\Phi_1 = (\xi^2 - \xi)(\xi - a)(\xi - 1 + \alpha) = \sum_{i=1}^{5} a_i \xi^{i-1},$$

where $\xi = x/\ell$, $a_2 = -\alpha + \alpha^2$, $a_3 = 1 + \alpha - \alpha^2$, $a_4 = -2$ and $a_5 = 1$. For modes of type 2, $\alpha = b/2\ell$ and for type 3, $\alpha = a/2\ell$. The subsequent polynomials generated with $g(\xi) = \xi$ are antisymmetrical or symmetrical about $x = \ell/2$ alternately (theorem (2) in Chapter 2). The functions $\Phi_i(\xi)$ for the modes of type 2 and 3 are obtained retaining only the odd numbered functions, $\Phi_1(\xi)$, $\Phi_3(\xi)$, $\Phi_5(\xi)$, etc.. The even numbered functions, $\Phi_2(\xi)$, $\Phi_4(\xi)$, $\Phi_6(\xi)$, etc., generated

using either starting function, are the appropriate functions for modes of type 4.

The starting function $\Psi_1(\eta)$ for the Z-direction is that for the clamped-free beam, taking $\eta = Z/c$, and the subsequent functions are generated with $g(\eta) = \eta$.

Natural frequencies for modes of type 1 for a cantilevered open box of dimensions a = 203 mm, b = 152 mm, c = 305 mm, h = 1.5 mm and made of aluminum having properties E = 68.95 GPa, ρ = 2710 kg/m^2 and ν = 0.32 have been reported in the literature [205-207]. The reported values are summarized in Table 4.6, together with results calculated using the present analysis. The values given by Dickinson [206] were obtained using Bolotin's method and are likely to be lower bounds. Those given by Irie, Yamada and Kobayashi [207] were obtained using a Rayleigh-Ritz solution but including membrane stretching effects; thus they may not be upper bounds for the idealization used in this work. Also, it should be mentioned that Irie et al. obtained three extra frequencies (158, 226 and 375 Hz) which were not obtained by the present or other authors. The agreement between the earlier and present results is excellent.

For completeness, the first six frequencies for the other three types of modes for this box are given in Table 4.7, as computed using six terms in the series for each of $\Phi_i(\xi)$ and $\Psi_j(\eta)$.

Table 4.6. Natural frequencies (Hz) for modes of type 1 for the cantilevered open box experimentally tested by Ueng and Nickels [205]

Mode Sequence Number	Source of reported frequency				
	Ueng and Nickels [205]	Dickinson [206]	Irie et al. [207]	Present, i x j 6 x 6	4 x 9
1	-	119	121	120	120
2	-	201	203	202	202
3	290	292	294	296	298
4	360	354	356	356	358
5	-	359	361	360	360
6	510	490	492	499	496
7	-	594	-	623	595
8	750	710	-	740	717
9	-	910	-	936	915
10	1090	1015	-	1013	957

Table 4.7. Natural frequencies (Hz) for modes of types 2, 3 and 4 for the open box of Ueng and Nickels, i x j = 6 x 6

Mode Type	Mode Sequence Number 1	2	3	4	5	6
2	156	225	372	630	717	735
3	232	309	462	506	575	718
4	430	511	669	841	913	932

Further, the frequency parameters for the lowest six modes of each type for cantilevered open boxes of side ratio a:b:c = 1:1:1 and 1:1.5:1.25, with ν = 0.3, are presented in Table 4.8, as obtained using six terms for each of $\Phi_1(\xi)$ and $\Psi_j(\eta)$. For a = b, modes of types 1 and 4 can be obtained from consideration of single plates having the vertical edges both simply supported or both clamped; results for such plates, as obtained from Leissa's work [17], are included for comparison. Also included in Table 4.8 are results for a five-sided, open box of side ratio 1:1.5:1.25, requiring continuity of slope between the vertical sides and a bottom plate of the same thickness, the base no longer being clamped. These values were computed using the series solution of Dill and Pister [98] and are reported, in part, in references [99] and [208]; the values in parentheses have not hitherto been reported. The values are not strictly comparable with the results from the present analysis but they are included for interest. Reasonably close correspondence may be seen to exist, although in two cases, two frequencies are given for the five-sided box where only one exists for the cantilevered box. This is believed to be due to the existence of modes for which the bottom plate vibration is predominant.

Table 4.8. Frequency parameters $(\rho h\omega^2 b^4/D)^{\frac{1}{2}}$ for cantilevered open boxes of two side ratios as computed using $\nu = 0.3$ and $i \times j = 6 \times 6$

		Mode Sequence Number					
a:b:c = 1:1:1		1	2	3	4	5	6
Mode Type	1 Single plate [17]	12.687+	24.020	33.065+	40.039	72.398+	76.761
	1 Present	12.689	24.014	33.066	40.145	72.516	77.055
	2,3 Present	17.577	36.104	52.069	71.463	74.579	107.13
	4 Present	41.703	63.016	64.130	81.820	103.29	118.57
	4 Single plate [17]	41.702+	63.015+	63.439	80.713	103.16+	116.80
a:b:c = 1:1.5:1.25							
Mode Type	1 Present	11.624	28.219	31.142	45.571	70.223	75.048
	1 5-sided box [99,208]	11.154	25.954	27.856 33.967	43.836	(65.353)	(73.926)
	2 Present	13.818	31.937	63.684	70.590	85.026	92.913
	2 5-sided box [99, 208]	13.423	29.160	61.800	63.545	(83.414)	(86.654)
	3 Present	22.810	42.316	42.789	60.051	81.616	97.489
	3 5-sided box [99,208]	22.505	40.404	41.253	51.280 59.769	(76.530)	(91.956)
	4 Present	35.622	55.589	79.109	94.562	98.746	131.42
	4 5-sided box [99,208]	35.276	53.387	(77.967)	(87.205)	(95.494)	(108.04)

+ exact value

4.5. POINT SUPPORTED PLATES

In this section, a number of plates with point supports and having various combinations of classical edge conditions are treated. In those cases where symmetry exists about one or both centrelines, this has been used in the computations and thus the number of terms indicated as being taken in the series $\Phi_i(\xi)$ and $\Psi_j(\eta)$ are only those contributing. Also, with the exception of the convergence studies, six terms were taken in all cases for each of $\Phi_i(\xi)$ and $\Psi_j(\eta)$. The order of each matrix equation to be solved was thus 36 plus the number of contributing point supports. The latter will vary depending upon the symmetry of the plate (for example, half the total number of point supports will contribute in the event of symmetry about one centreline only) and the symmetry or antisymmetry of the modes under consideration. Should a simple point support lie on a centreline of symmetry, then, for those modes antisymmetrical about that line, it makes no contribution and is thus not included in the order of the matrix.

It should be noted that the analyses by Narita [118, 129] for point supported plates of otherwise fully free and cantilever plates are particular cases of the present analysis, since the same Lagrangian multiplier method is used and the simple polynomials used by Narita for the two particular plates combine to be equivalent to the BCOP with

the starting functions satisfying the geometrical boundary conditions only.

The first set of problems considered is that of centrally point supported, square isotropic plates having various combinations of simply supported and clamped edges. These problems were chosen primarily to illustrate the effect of using the first and higher degree generating functions ($g(\xi) = \xi$, ξ^2, $\xi^3 - 3\xi^2/2$ and $g(\eta) = \eta$, η^2, $\eta^3 - 3\eta^2/2$ when dealing with plates involving simply supported edges; comparisons are also made with those results available in the literature which are applicable to these problems. Table 4.9 shows sample results (first six frequency parameters for doubly symmetrical modes) from a convergence study conducted on a fully simply supported plate (SSSS) with and without a central point support. It may be seen, remembering the upper bound characteristics of the method employed, that in both cases the trend is for the higher order generating function to yield more accurate results than the first order function; this is especially pronounced for the higher modes when using small numbers of terms in the series (4.6). Similar results were obtained for the first six symmetrical/antisymmetrical and doubly antisymmetrical modes of such plates. Also shown in Table 4.9 are sample results computed for a plate simply supported along two adjacent edges and clamped along the other two, with and without a central point support. For this case, symmetry about $x = a/2$ or $y = b/2$ does not exist.

Table 4.9

Comparison of frequency parameters $(\rho h\omega^2 a^4/D)^{1/2}$ for square, isotropic plates as obtained by using single degree and higher degree generating functions

Generating function $g(\xi)$, $g(\eta)$	No. of terms in each of ϕ_i, ψ_j	Mode sequence number 1	2	3	4	5	6
SSSS-plate with no point support							
ξ, η	3	19.7392	99.3042	99.3042	178.532	461.779	461.779
	4	19.7392	98.7013	98.7013	177.660	270.153	270.153
	5	19.7392	98.6961	98.6961	177.653	257.193	257.193
	6	19.7392	98.6960	98.6960	177.653	256.620	256.620
$\xi^3-3\xi^2/2$, $\eta^3-3\eta^2/2$	3	19.7392	98.7022	98.7022	177.661	257.776	257.776
	4	19.7392	98.6971	98.6971	177.654	256.633	256.633
	5	19.7392	98.6963	98.6963	177.653	256.614	256.614
	6	19.7392	98.6962	98.6962	177.653	256.611	256.611
Exact	[17]	19.7392	98.6960	98.6960	177.653	256.610	256.610
SSSS-plate with central point support							
ξ, η	3	58.7130	99.3042	161.056	402.156	461.779	501.666
	4	55.6246	98.7013	155.308	234.330	270.153	322.802
	5	54.4766	98.6961	151.923	216.963	257.193	307.225
	6	53.8896	98.6960	150.212	213.078	256.620	303.762
$\xi^3-3\xi^2/2$, $\eta^3-3\eta^2/2$	3	54.8579	98.7022	153.127	220.163	257.776	309.936
	4	53.8807	98.6971	150.119	212.718	256.633	303.626
	5	53.4126	98.6963	148.887	210.887	256.614	301.146
	6	53.1700	98.6962	148.201	209.816	256.611	299.980
SSCC-plate with no point support							
ξ, η	6	27.054	60.539	60.787	92.838	114.85	115.00
ξ^2, η^2	6	27.055	60.540	60.787	92.837	114.56	114.71
Leissa	[17]	27.056	60.544	60.791	92.865	114.57	114.72
SSCC-plate with central point support							
ξ, η	6	53.113	60.539	78.367	92.986	114.85	144.98
ξ^2, η^2	6	52.881	60.540	77.316	92.970	114.56	144.71

Again the trend is for the higher degree generating functions, ξ^2 and η^2 in this case, to yield slightly better results, particularly for the point supported case. The higher degree generating functions were therefore used where applicable throughout the remainder of the problems treated in this section.

In Table 4.10, frequency parameters calculated using the present analysis are given for several centrally point supported, square plates being clamped (C) or simply supported (S) along edges x = 0, y = 0, x = a, y = a, respectively, together with those values available from the literature. For those plates for which symmetry exists about x = a/2 or y = a/2, or about a diagonal, certain modes of vibration will occur which are antisymmetrical about a line or lines passing through the central point supports, whereupon the plate behaves in exactly the same manner as one without the central support. This permits comparisons with appropriate frequency parameters for non-point supported plates, such as those given by Leissa [17]. To the authors' knowledge, the only point supported plate results available in the literature which are appropriate for comparison with the values in Table 4.10 are those by Nowacki [126, 127], obtained using an energy approach, those by Johns and Nataraja [107], using the finite difference method and those by Venkateswara Rao et al. [114], using the finite element method. All apply to the fully simply supported plate with a

Table 4.10

Frequency parameters $(\rho h\omega^2 a^4/D)^{1/2}$ for square, isotropic, central point supported plates with clamped and/or simply supported edges along x=0, y=0, x=a, y=b

Edge conditions and sources of results	Mode type					
SSSS	SA(AS)-1	SS-1	AA-1	SS-2	SA(AS)-2	SS-3
Nowacki [126]	52.6					
Nowacki [127]	49.3					
Johns and Nataraja [107]	53.4					
Venkateswara Rao et al [114]		52.6277				
Present	49.3480	53.1700	78.9568	98.6962	128.3049	148.2006
Leissa [17]*	49.3480		78.9568		128.3049	
SSSC	A-1	S-1	S-2	A-2	S-3	S-4
Present	51.6744	51.9598	67.0362	86.1351	107.562	133.128
Leissa [17]*	51.6743			86.1345		
SSCC	1	2	3	4	5	6
Present	62.881	60.540	77.316	92.970	114.56	144.71
Leissa [17]		60.544			114.57	
SCCC	S-1	A-1	S-2	A-2	S-3	A-3
Present	59.020	71.076	79.235	100.79	123.26	151.90
Leissa [17]		71.084		100.83		
CCCC	SA(AS)-1	SS-1	AA-1	SS-2	SA(AS)-2	SS-3
Present	73.394	80.301	108.22	131.58	165.00	189.97
Leissa [17]	73.413		108.27	131.64		

*exact solution

central point support and each purports to give the fundamental (lowest) frequency parameter. This occurs for the mode with one nodal line through the centre of the plate, as pointed out in reference [107], which corresponds to the second mode of vibration of a simply supported plate without a point support and for which the exact value is known. The value given by Venkateswara Rao et al. [114] is for a mode with no nodal line, which is thus not the fundamental but rather the first fully symmetrical mode. The agreement of the present results with those from references [114, 127 and 17] is excellent.

The second set of problems considered is that of square isotropic plates having point supports at various locations on the edges, all edges being otherwise free. The problem in this category which has received the most attention from researchers is that of the plate having four point supports, one located at each corner of the plate. This problem has been treated in references [103-105, 107-110, 113-115, 118 and 119] and is one of the two for which the present solution yields an equivalent frequency equation to that given by Narita [118] and thus, for like numbers of terms in the series, identical frequencies result. Numerical values for this problem are summarized in Table 4.11. Two further problems considered in this set are those of an otherwise free plate, point supported at the mid-points of all four sides, and a plate point supported at all four corners and at

Table 4.11

Frequency parameters $(\rho h\omega^2 a^4/D)^{\frac{1}{4}}$ for a square, isotropic plate with four corner point supports, otherwise free (ν=0.3)

Source of Results	Mode Type					
	SS-1	SA(AS)-1	SS-2	AA-1	SS-3	AS(SA)-2
Fan and Cheung [103]	7.11	15.77	19.58	38.43	44.37	-
Cox and Boxer [104]	7.117	15.73	19.13	38.42	43.55	-
Reed [105]	7.12	15.77	19.60	38.44	44.4	50.3
Johns and Nataraja [107]	7.11	15.43	17.10	-	43.91	-
Drake et al. [109]						
Experiment	8.65	16.88	21.1	40.5	45.48	-
Theoretical	7.1	15.6	19.4	38.4	44.2	48.4
Tso [110]	7.115	-	-	-	-	-
Petyt and Mirza [113]	7.143	15.59	19.60	38.73	44.79	-
Venkateswara Rao et al. [114,115]	7.11088	15.7702	19.5961	-	-	-
Kerstens [119]	7.15	15.64	19.49	38.62	43.89	-
Narita [118], and Present	7.11089	15.7702	19.5961	38.4361	44.3696	50.3767

the mid-point of each side. Comparison results are available in the literature, for both problems, and are given in Table 4.12, together with results from the present analysis. Close agreement may be seen to exist between the present results and those of the other authors, the methods of solution used by the latter being the finite difference method by Cox [106] and, for the first mode, by Johns and Nataraja [107], the finite element method by Venkateswara Rao [108], the finite strip method by Fan and Cheung [103] and the Lagrangian multiplier method by Drake et al. [109]. The frequency for the mode SA(AS)-1 by Johns and Nataraja was obtained using the Rayleigh-Ritz method. Included in Table 4.12 are results illustrating the rate of convergence of the present solution, which may be seen to be fairly rapid for both types of support conditions. convergence studies on other problems showed similar results.

The third set of problems is that of square, isotropic plates having two adjacent edges simply supported and/or clamped, the remaining two free, with a point support located at the otherwise free corner. For such plates, symmetry about $x = a/2$ or $y = a/2$ does not exist. Results computed for the three possible combinations are shown in Table 4.13, together with comparison results from the literature. The results by Cox [121], obtained by using the finite difference method, appear to be somewhat low, while those by Kerstens et al. [122], from the modal constraint method (computed with

Table 4.12

Frequency parameters $(\rho h\omega^2 a^4/D)^{1/2}$ for a square isotropic plate point supported (a) at the mid-points of all four sides and (b) at all four corners and at the mid-points of all four sides, otherwise free (ν=0.3).

Source of results	Mode Type					
(a)	AA-1	SS-1	SA(AS)-1	SS-2	SA(AS)-2	AA-2
Cox [106]		18.002*				
Johns and Nataraja [107]	13.56		18.7**			
Fan and Cheung [103]	13.47	17.85	18.79	26.92	51.13	
Present						
3x3 terms	13.4687	19.0314	20.1626	29.6818	52.9188	71.2079
4x4 terms	13.4682	18.4029	19.2256	27.3609	52.0821	69.2786
5x5 terms	13.4682	18.1488	19.0262	27.1406	51.6367	69.2655
6x6 terms	13.4682	18.0307	18.9339	27.0488	51.4406	69.2654
(b)	SS-1	SA(AS)-1	AA-1	SS-2	SA(AS)-2	AA-2
Venkateswara Rao [108]	18.20					
Drake et al. [109]						
Experiment	19.6	36.4	39.9	58.0	-	69.1
Theoretical	18.15	34.4	39.8	62.6(63.1)	-	65.5(69.4)
Fan and Cheung [103]	17.852	34.89	38.43	60.12	68.51	
Present						
3x3 terms	19.1541	37.5649	38.4586	68.9786	71.8720	71.2079
4x4 terms	18.4120	35.7681	38.4322	62.3082	70.3901	69.2786
5x5 terms	18.1495	35.3571	38.4316	60.9439	69.5511	69.2655
6x6 terms	18.0307	35.1727	38.4316	60.5821	69.1440	69.2654

*: indicated as the first mode in the reference

**: indicated as the second mode in the reference

Table 4.13

Frequency parameters $(\rho h\omega^2 a^4/D)^{1/2}$ for square, isotropic plates having two adjacent edges simply supported and/or clamped, and a point support at opposite corner (ν=0.3).

Source of results	Mode sequence number 1	2	3	4	5	6
(a) Simply supported - Simply supported						
Cox [121]	8.998					
Kerstens et al. [122]	11.02*					
Laura et al. [123]	9.70	16.81	30.44			
Utjes et al. [125]	9.700	16.81	30.44			
Fan and Cheung [103]	9.61	17.32	30.60	43.66	51.09	64.40
Present	9.6079	17.316	30.596	43.652	51.041	64.364
(b) Clamped - Clamped						
Cox [121]	13.683					
Kerstens et al. [122]	17.43*					
Laura et al. [123]	15.38	23.29	39.29			
Laura & Cortinez [124]	17.85					
Utjes et al. [125]	15.380	23.29	39.29			
Fan and Cheung [103]	15.17	23.93	39.40	54.16	62.83	77.46
Present	15.172	23.923	39.392	54.157	62.850	77.418
(c) Simply supported - Clamped						
Kerstens et al. [122]	13.28*					
Laura & Cortinez [124]	13.83					
Utjes et al. [125]	12.030					
Present	11.940	21.175	35.015	47.398	58.144	70.827

* ν=0.33

= 0.33?), and by Laura and Cortinez [124], from a Rayleigh-Ritz solution, are rather high. The remainder of the results, calculated using the finite element method [123 and 125] and the finite strip method [103], and those from the present analysis are in close agreement and are thus believed to be more accurate.

The fourth set of problems considered is that of rectangular cantilever plates bounded by x = 0, a and y = 0, b, with the clamped edge at x = 0, with point supports located

(a) at x = a/2, y = 0 and at x = a/2, y = b, or

(b) x = a, y = b/4 and at x = a, y = 3b/4, or

(c) at x = a/2, y = 0 and y = b and at x = a, y = b/4 and y = 3b/4.

Frequency parameters for isotropic plates are given in Table 4.14, together with comparison values available from the literature, and for orthotropic plates, for which no comparison results are available, in Table 4.15. The values given by Saliba [128] were calculated using the superposition method pioneered by Gorman [117] and those by Narita [129] were obtained using the Lagrangian multiplier method, which again gives an equivalent frequency equation to that of the present analysis (with starting function satisfying geometrical boundary conditions only) for the above conditions. Narita used eight terms in the series for the x-

Table 4.14

Frequency parameters $(\rho h\omega^2 a^4/D)^{1/2}$ for isotropic, point supported, cantilever plates

Support Case	Source of results	ν	a/b	Mode Type S-1	S-2	S-3	A-1	A-2	A-3
(a)	[128]	0.333	1.0	6.082	25.42	38.64	16.03	50.76	68.80
	[129]	0.333	1.0	6.117	25.44	39.03	16.16	51.53	68.98
		0.333	1.0	6.144	25.46	39.32	16.25	52.16	69.38
	Present	0.3	1.0	6.262	25.38	39.97	16.60	52.13	70.13
		0.3	0.5	4.417	14.[illegible]	24.71	8.615	22.14	33.82
		0.3	2.0	8.450	50.96	60.37	30.17	88.83	121.9
(b)	[128]	0.333	1.0	14.44	27.02	45.17	17.33	43.45	69.42
	[129]	0.333	1.0	14.48	27.02	45.56	17.38	43.62	69.45
		0.333	1.0	14.48	27.02	45.60	17.39	43.63	69.51
	Present	0.3	1.0	14.60	27.18	45.96	17.65	44.20	69.58
		0.3	0.5	9.945	13.53	28.02	10.97	23.09	35.02
		0.3	2.0	14.95	48.19	91.96	28.92	67.63	119.4
(c)		0.333	1.0	21.55	34.60	49.30	36.04	52.23	73.15
	Present	0.3	1.0	21.49	35.28	49.47	36.72	52.22	73.51
		0.3	0.5	12.80	18.85	28.02	19.24	23.33	46.59
		0.3	2.0	39.28	54.14	67.09	61.44	95.17	169.1

Table 4.15

Frequency parameters $(\rho h\omega^2 a^4/H)^{1/2}$ for orthotropic, square, point supported, cantilever plates.

$(D_x/H = 1.543,\ D_y/H = 4.810,\ D_{xy}/H = 0.407)$

Support Case	Mode Type S-1	S-2	S-3	A-1	A-2	A-3
(a)	9.527	36.26	60.72	20.07	84.00	88.51
(b)	18.92	51.18	60.53	22.48	60.15	104.9
(c)	30.66	54.67	65.68	51.66	84.56	108.6

direction and six for the y-direction, thus his results are slightly more accurate than the present results which were obtained using only six terms in each direction.

The final problem considered is that of the plate shown in Figure 4.7. It is free along all four edges, point supported at each corner and is continuous over two perpendicular line supports, as illustrated. The line supports provide restraint in the transverse direction ($w = 0$) but offer no resistance to normal slope. The starting function for the x-direction for this plate is $\Phi_1(\xi) = (\xi-\alpha)$ (see Chapter 2) and the subsequent functions are constructed using recurrence formula (2.6) with the generating function $g(\xi) = \xi$. The functions for the y-direction are obtained simply by replacing ξ with η. In Figure 4.8, the nodal patterns and frequency parameters $(\rho h\omega^2 a^4/D)^{\frac{1}{2}}$ for square isotropic plates with $\nu = 0.3$ are shown for several values of α. It should be noted that for $\alpha = 1/2$, the pairs of modes symmetrical about one central axis and antisymmetrical about the other (SA-1, AS-1 and SA-2, AS-2) are identical in frequency and their nodal patterns are simply rotated through 90°; only one nodal pattern is shown for each pair (3x3 terms in each type are used in calculation). For $\alpha = 0$, at first sight, the problem appears to become that of a square plate simply supported along two adjacent edges, free along the other two and point supported at the otherwise free corner, for which frequency parameters are given under case (a),

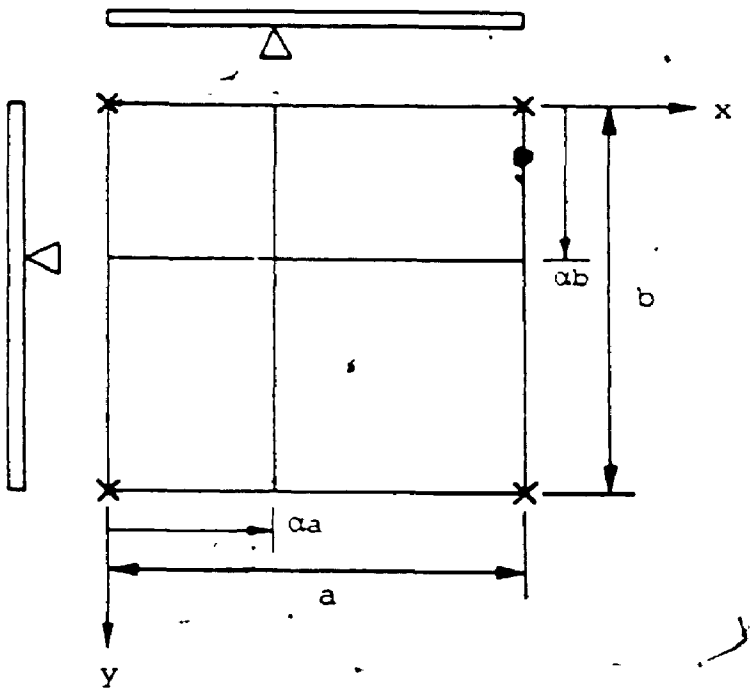

Figure 4.7. Corner supported two-way, two-span isotropic plate.

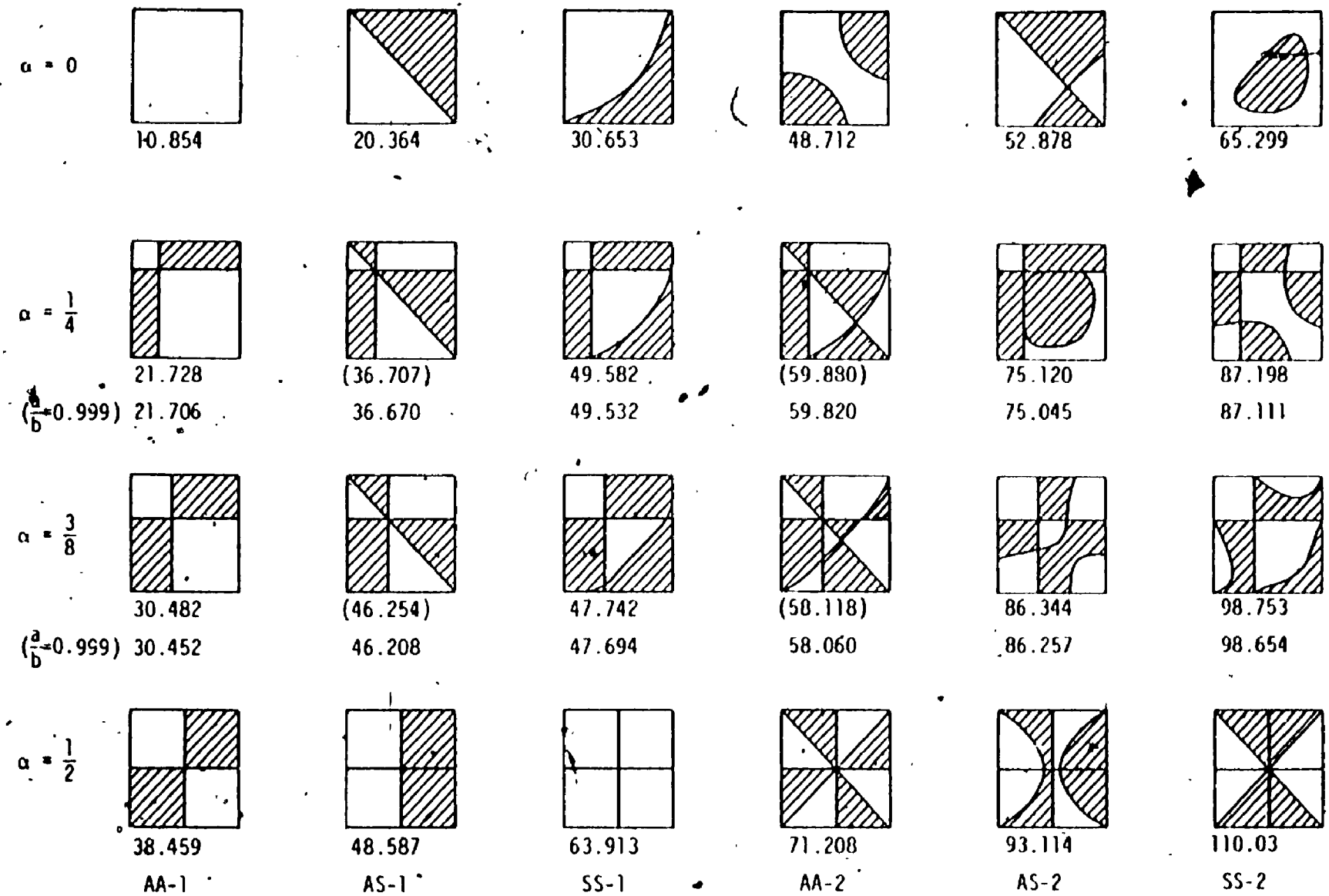

Figure 4. Nodal lines and frequency parameters $(\rho h \omega^2 a^4/D)^{1/2}$ for corner supported, two-way, two-span, square, isotropic plates (ν=0.3).

Table 4.13. However, it must be recognized that the coincidence of the line supports with the point supports as α tends to zero causes the extra restraint of zero normal slope at corners $x = 0$, $y = a$ and $x = a$, $y = 0$. The frequency parameters are thus somewhat higher than the corresponding values given in table 4.13. Also, for the square plate with $\alpha = 1/4$ and $\alpha = 3/8$, the poles and zeros of the frequency determinant obtained using Sehmi's algorithm become coincident for certain modes (values in parentheses) and, while the frequency parameters may be obtained, the mode shapes, and thus nodal patterns, are not readily determinable. Instead, the nodal patterns shown for the modes were obtained for the almost square plate of aspect ratio $a/b = 0.999$, for which the poles and zeros are distinct; the corresponding frequency parameters are also given.

CHAPTER 5

VIBRATION OF ANNULAR AND CIRCULAR PLATES

5.1. INTRODUCTORY REMARKS

As discussed in section 1.4, exact solutions for circular and annular plates exist for isotropic cases. No exact solutions exist for polar orthotropic plates with the only exception of the annular plate with parabolically varying thickness in radius, even when subject to the classical boundary conditions and no other complicating factor, and researchers have used various different methods of analysis for such plates. Nevertheless, the works in the literature are limited to some individual plate problems and no general approach has been presented for polar orthotropic, continuous plates with radially varying thickness.

In this chapter, a simple, unified approach is presented for the solution of the free, lateral vibration problem of thin annular plates which may be of isotropic or polar orthotropic material, may have thickness which varies with radius and may be continuous over one or more rigid concentric ring supports and subject to any (combination) of the classical boundary conditions. The Rayleigh-Ritz method is used, with the BCOP as the admissible functions. To illustrate the versatility and accuracy of the present approach, numerical results are presented for a number of example plates, in comparison with the values given in the

literature, where available.

Although the present approach is primarily concerned with annular plates, the case of the solid circular plate is briefly treated by permitting the inner radius to become very small. If the very small inner periphery is treated as free, this is essentially equivalent to a solid plate with no central support. If it is treated as simply supported, then this approximates a clamped point at the centre.

5.2 ANALYSIS

Consider a thin annular plate with concentric ring supports and a combination of classical boundary conditions. It is assumed that the material of the plate is of variable thickness along the radius, uniform in the circumferential direction and is polar orthotropic. The intermediate ring supports are assumed to prevent transverse displacement but to offer no resistance to normal rotation (simple supports).

For free vibration, the displacement may be written as $w(r,\theta)\sin\omega\tau$, where ω is the radian natural frequency and w the maximum deflection with respect to time τ. The maximum strain and kinetic energies expressed in polar coordinates are, respectively (see Appendix B):

$$V_{max} = \frac{1}{2}\int_b^a\int_0^{2\pi}\left[D_r\left(\frac{\partial^2 w}{\partial r^2}\right)^2 + 2\nu_{\theta r}D_r\frac{\partial^2 w}{\partial r^2}\left(\frac{1}{r}\frac{\partial w}{\partial r} + \frac{1}{r^2}\frac{\partial^2 w}{\partial\theta^2}\right)\right. \tag{5.1}$$

$$+ D_\theta\left(\frac{1}{r}\frac{\partial w}{\partial r} + \frac{1}{r^2}\frac{\partial^2 w}{\partial \theta^2}\right)^2 + 4D_{r\theta}\left\{\frac{\partial}{\partial r}\left(\frac{1}{r}\frac{\partial w}{\partial \theta}\right)\right\}^2\Big] r\,d\theta\,dr,$$

$$T_{max} = \frac{1}{2}\,\omega^2\int_b^a\int_0^{2\pi}\rho h(r)w^2 r\,d\theta\,dr, \tag{5.2}$$

where a and b denote the radii of the outer and inner periphery of the plate, ρ the material density (assumed to be constant), h(r) the thickness of the plate, $D_r = E_r h^3/12(1-\nu_{r\theta}\nu_{\theta r})$, $D_\theta = D_r E_\theta/E_r$ and $D_{r\theta} = G_{r\theta}h^3/12$, in which E_r and E_θ are Young's moduli in the r and θ direction, respectively, $G_{r\theta}$ is the shear modulus, and $\nu_{r\theta}$ and $\nu_{\theta r}$ are Poisson's ratios.

Introducing a non-dimensionalized parameter $\xi = r/a$, the thickness h can be expressed

$$h(\xi) = h_a f_r(\xi), \tag{5.3}$$

where h_a denotes the thickness at the outer periphery and $f_r(\xi)$ describes the variation in thickness. It may be noted that for plates with uniform thickness, function $f_r(\xi)$ becomes unity. For plates for which the thickness varies with some power, p, of the radius, $f_r(\xi)$ may be written

$$f_r(\xi) = 1-(1-h_b/h_a)(1-\xi^p)/\{1-(b/a)^p\}, \tag{5.4}$$

where h_b denotes the thickness at the inner periphery. For linear variation, p = 1 and for parabolic variation, p = 2, etc..

The deflection w may be expressed in the form

$$w(\xi,\theta) = W_n(\xi) \cos n\theta; \quad n = 0, 1, 2, \ldots\ldots, \tag{5.5}$$

where n denotes the number of nodal diameters (circumferential wave number). The mode shape $W_n(\xi)$ in the radial direction is taken as

$$W_n(\xi) = \sum_i A_{in}\Phi_i(\xi), \tag{5.6}$$

where Φ_i are the assumed admissible functions which satisfy at least the geometrical boundary conditions of the plate.

Substituting equations (5.3) and (5.5), together with equation (5.6), into the energy expressions (5.1) and (5.2), and minimizing with respect to the coefficients A_{mn}, according to the Rayleigh-Ritz procedure, leads to the eigenvalue equation (frequency equation)

$$\sum_i [C_{mi} - \Omega^2 G_{mi}]A_{in} = 0, \tag{5.7}$$

where $\Omega^2 = \omega^2\rho h_a a^4/D_{ra}$, m,i = 1, 2, 3, ... ,

$$C_{mi} = E_{mi}^{(1,22)} + \frac{D_\theta}{D_r}\{E_{mi}^{(-1,11)} - n^2(E_{mi}^{(-2,01)} + E_{mi}^{(-2,10)})$$

$$+ n^4E_{mi}^{(-3,00)}\} + \nu_{\theta r}\{E_{mi}^{(0,12)} + E_{mi}^{(0,21)} - n^2(E_{mi}^{(-1,02)}$$

$$+ E_{mi}^{(-1,20)})\} + 4\frac{D_{r\theta}}{D_r}n^2\{E_{mi}^{(-3,00)} - (E_{mi}^{(-2,01)} + E_{mi}^{(-2,10)})$$

$$+ E_{mi}^{(-1,11)}\},$$

$$E_{mi}^{(p,qs)} = \int_{b/a}^{1} \xi^p f^3(\xi)(d^q\Phi_m/d\xi^q)(d^s\Phi_i/d\xi^s)d\xi,$$

$$G_{mi} = \int_{b/a}^{1} \xi f(\xi)\Phi_m\Phi_i d\xi,$$

and D_{ra} denotes the values for D_r at the outer periphery. For axisymmetrical modes, there are no nodal diameters, thus $n = 0$ and the eigenvalue equation becomes independent of the parameter $D_{r\theta}/D_r$. Since the isotropic plate is a particular case of the orthotropic plate, equation (5.7) also applies to the isotropic plate, for which $\nu_{r\theta} = \nu_{\theta r} = \nu$, $D_r = D_\theta = D$ and $D_{r\theta} = (1-\nu)D/2$.

The solution of equation (5.7) yields the natural frequencies of vibration of the plate, together with the coefficients for the mode shape (5.6). The validity and accuracy of the solution depends upon the choice of the admissible functions $\Phi_i(\xi)$. In this work, the BCOP explained in the following are used.

The starting functions $\Phi_i(\xi)$ are chosen so as to satisfy both the geometrical and natural boundary conditions of the equivalent beam, and zero displacement conditions at intermediate supports where such exist. In addition, where simply supported and/or free peripheries are involved, slightly simpler starting functions, neglecting the natural boundary conditions, could be used; it is anticipated that

very similar results would be obtained, as was demonstrated for rectangular plates [29]. The present functions are used simply for consistency. Since the interval is $b/a \leq \xi \leq 1$ ($b \leq r \leq a$), the starting functions for plates with no intermediate support may be written

$$\Phi_1(\xi) = \sum_{j=1}^{5} a_j \xi^{j-1}, \tag{5.8}$$

where a_j are given in Table 5.1. In the table, C, S and F denote clamped, simply supported and free boundary conditions, respectively, the first denoting the condition on the inner periphery and the second the condition on the outer. (This designation is used hereafter in this chapter.) For plates with concentric ring supports, the starting functions are obtained by multiplying the appropriate functions given by equation (5.8) by the factor $(\xi-\xi_r)$, recurrently, where ξ_r denotes the location of the intermediate supports. The subsequent polynomials are generated by the recurrence formula, such as equation (2.6). The equation is rewritten here:

$$\Phi_{k+1}(\xi) = \{g(\xi)-B_k(\xi)\}\Phi_k(\xi)-C_k\Phi_{k-1}(\xi);\ k=1,2,3,\ \ldots, \tag{5.9}$$

where

$$B_k = \int_{b/a}^{1} w_f(\xi)g(\xi)\Phi_k^2(\xi)d\xi/\int_{b/a}^{1} w_f(\xi)\Phi_k^2(\xi)d\xi,$$

$$C_k = \int_{b/a}^{1} w_f(\xi)\Phi_k(\xi)d\xi/\int_{b/a}^{1} w_f(\xi)\Phi_{k-1}^2(\xi)d\xi.$$

Table 5.1

The coefficients of starting functions for plates with no intermediate support (c=b/a)

Boundary Conditions	coefficients				
	a_1	a_2	a_3	a_4	a_5
C-C	c^2	$-2c(1+c)$	$1+4c+c^2$	$-2(1+c)$	1
C-S	$c^2(3-c)$	$-c(6+3c-c^2)$	$3(1+3c)$	$-(5+3c)$	2
C-F	$c^2(6-8c+3c^2)$	$-4c(3-3c+c^2)$	6	-4	1
S-C	$-c(1-3c)$	$1-3c-6c^2$	$3c(3+c)$	$-(3+5c)$	2
S-S	$-c(1-3c+c^2)$	$(1+c)(1-4c+c^2)$	$6c$	$-2(1+c)$	1
S-F	$-c$	1	0	0	0
F-C	$3-8c+6c^2$	$-4(1-3c+3c^2)$	$6c^2$	$-4c$	1
F-S	1	-1	0	0	0
F-F	1	0	0	0	0

The weight function $w_f(\xi)$ is determined by considering the orthogonality of the vibration modes. Recalling the kinetic energy expression (5.2), the orthogonality can be expressed, in terms of the non-dimensionalized parameter, as

$$\int_{b/a}^{1} \xi f_r(\xi)\Phi_m(\xi)\Phi_i(\xi)d\xi = G_{mi}\delta_{mi}, \qquad (5.10)$$

where G_{mi} is a constant and δ_{mi} the Kronecker delta. Therefore, the weight function is $w_f(\xi) = \xi f_r(\xi)$. The generating function is chosen as $g(\xi) = \xi$, which makes the subsequent polynomials ($k > 1$) generated satisfy only the geometrical boundary conditions. (As discussed in the previous chapters, the higher degree generating function may be used, but it has not been used to obtain the results presented in this chapter.)

It is worth noting that, as in Chapters 3 and 4, the first and second terms of frequency equation (5.7) yield symmetrical and diagonal matrices, respectively. When the polynomials generated by equation (5.9) are appropriately normalized, the second term of equation (5.7) yields an identity matrix; this gives some computational advantage.

5.3. ANNULAR PLATES

In order to demonstrate the applicability and accuracy of the approach presented, equation (5.7) was used to generate numerical values for some illustrative plates which may be of polar orthotropic material, have radially varying

3 of/de 3

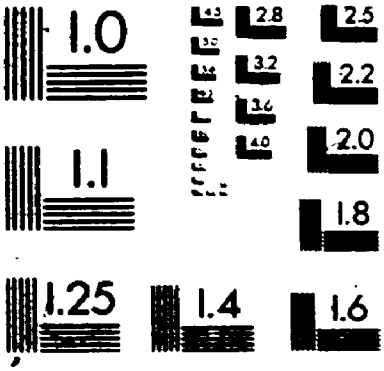

MICRO

thickness and be continuous over concentric ring supports. With the exception of the convergence studies, seven or eight terms of series (5.6), depending upon the rate of convergence, were taken for each of the nodal diameters, and thus the frequency equation (5.7) yields 7x7 or 8x8 matrices. For isotropic plates, Poisson's ratio is taken as 0.3 except for one comparative study. Throughout the tables for the results, the heading of the values (the numbers in the parentheses) denotes the number of nodal diameters (n) and nodal circles (s), excluding the supports at the peripheries and intermediate rings where such exist. As mentioned before, for axisymmetrical modes, there are no nodal diameters (n=0) and the frequency parameters appear to be independent of the parameter $D_{r\theta}/D_r$. Hence, in the case of polar orthotropic plates, the frequency parameters presented for n=0 are applicable to any value of $D_{r\theta}/D_r$ rather than only the values indicated. In other words, the values given for $D_{r\theta}/D_r$ apply only to the non-axisymmetrical modes.

5.3.1. Annular Plates of Uniform Thickness

The first problem considered in this section is isotropic annular plates of uniform thickness with no intermediate support, in order to show the accuracy of the present approach. The frequency parameters were obtained using seven terms in series (5.6) for each of the nodal diameters, for plates with inner periphery clamped and outer

periphery having each of three different boundary conditions, clamped (C), simply supported (S) and free (F). The frequency parameters for the lowest nine modes are presented in Table 5.2 for the hole size (b/a) 0.1, 0.5 and 0.7, in comparison with those of exact analysis by Vogel and Skinner [150]. Close agreement may be seen to exist between the present results and those of the exact solution. However, it may be noted that, the present results obtained by using the Rayleigh-Ritz method are upper bounds and thus the smaller quoted values of the exact solution, in some cases, seem to include numerical round-off errors; this is believed to be due to the conversion of the parameter given in the reference to that used in this work.

The second problem considered is that of orthotropic plates of uniform thickness with no intermediate support. The boundary conditions are chosen to be inner periphery simply supported and outer periphery clamped (S-C), both peripheries simply supported (S-S), and inner periphery free and outer periphery simply supported (F-S). The orthotropy is chosen to be that given by $D_\theta/D_r = 5$, $D_{r\theta}/D_r = 0.35$ and $\nu_{\theta r} = 0.3$, and the hole size (b/a) is taken as 0.5. The lowest ten frequency parameters are presented in Table 5.3, together with those obtained by Gorman [157], who used the finite element method, and those by Narita [158], who used the Lagrangian multiplier method. The agreement achieved between the present results and those by other researchers is

Table 5.2

Comparison of frequency parameters $(\omega^2 \rho h a^4/D)^{\frac{1}{2}}$ for isotropic annular plates of uniform thickness with no intermediate support ($\nu = 0.3$)

Boundary conditions	source of results	No. of nodal diameters and nodal circles (n,s)								
(1) b/a = 0.1		(0,0)	(1,0)	(2,0)	(3,0)	(4,0)	(0,1)	(1,1)	(2,1)	(5,0)
C-C	Present	27.281	28.918	36.622	51.221	69.679	75.369	78.642	90.463	90.740
	Exact [150]	27.3	28.4	36.7	51.2	-	75.3	78.2	90.5	-
C-S	Present	17.790	19.397	26.722	40.064	56.848	60.148	63.252	74.649	76.203
	Exact [150]	17.8	19.0	26.8	40.0	-	60.1	62.8	74.7	-
C-F	Present	4.2378	3.4801	5.6253	12.451	21.836	25.267	27.683	36.957	33.495
	Exact [150]	4.23	3.14	5.62	12.4	-	25.3	27.3	37.0	-
(2) b/a = 0.5		(0,0)	(1,0)	(2,0)	(3,0)	(4,0)	(5,0)	(6,0)	(7,0)	(8,0)
C-C	Present	89.251	90.230	93.321	98.928	107.57	119.70	135.60	155.33	178.82
	Exact [150]	89.2	90.2	93.4	99.0	-	-	-	-	-
C-S	Present	59.820	60.987	64.631	71.107	80.802	93.988	110.75	131.07	154.68
	Exact [150]	59.8	70.0	64.6	71.0	-	-	-	-	-

Table 5.2 (continued)

Comparison of frequency parameters $(\omega^2 \rho h a^4/D)^{\frac{1}{2}}$ for isotropic annular plates of uniform thickness with no intermediate support (ν = 0.3)

Boundary conditions	source of results	No. of nodal diameters and nodal circles (n,s)								
(2) b/a = 0.5 (continued)										
		(0,0)	(1,0)	(2,0)	(3,0)	(4,0)	(5,0)	(6,0)	(7,0)	(8,0)
C-F	Present	13.024	13.290	14.704	18.562	25.596	35.730	48.673	64.185	82.106
	Exact [150]	13.0	13.3	14.7	18.5	-	-	-	-	-
(3) b/a = 0.7										
		(0,0)	(1,0)	(2,0)	(3,0)	(4,0)	(5,0)	(6,0)	(7,0)	(8,0)
C-C	Present	248.40	249.16	251.48	255.44	261.20	268.92	278.82	291.10	305.96
	Exact [150]	247.8	249.5	251.1	256.1	-	-	-	-	-
C-S	Present	168.52	169.49	172.41	177.38	184.51	193.95	205.85	220.35	237.55
	Exact [150]	168.5	170.2	171.8	176.8	-	-	-	-	-
C-F	Present	36.953	37.498	39.277	42.654	48.071	55.880	66.270	79.291	94.912
	Exact [150]	37.5	37.0	39.3	42.6					

Table 5.3

Comparison of frequency parameters $(\omega^2 \rho h a^4/D_r)^{\frac{1}{2}}$ for polar orthotropic annular plates of uniform thickness with no intermediate support ($D_\theta/D_r = 5$, $D_{r\theta}/D_r = 0.35$, $\nu_{\theta r} = 0.3$; $b/a = 0.5$)

Source of results	No. of nodal diameters and nodal circles (n,s)									
(1) S-C	(0,0)	(1,0)	(2,0)	(3,0)	(4.0)	(5,0)	(6,0)	(0,1)	(1,1)	(2,1)
Gorman [157]	67.145	68.446	73.883	86.829	-	-	-	205.71	207.41	213.15
Narita [158]	67.14	68.45								
Present										
3 terms	67.1491	68.4512	73.8988	86.8729	109.668	142.047	182.349	214.578	216.150	221.379
4 terms	67.1479	68.4491	73.8904	86.8382	109.558	141.792	181.910	205.778	207.476	213.108
5 terms	67.1445	68.4452	73.8846	86.8282	109.542	141.775	181.903	205.750	207.454	213.102
6 terms	67.1443	68.4450	73.8844	86.8279	109.542	141.775	181.903	205.676	207.379	213.022
7 terms	67.1443	68.4450	73.8844	86.8279	109.542	141.775	181.902	205.676	207.379	213.022
8 terms	67.1443	68.4450	73.8844	86.8279	109.542	141.775	181.902	205.676	207.378	213.022
(2) S-S	(0,0)	(1,0)	(2,0)	(3,0)	(4,0)	(5,0)	(6,0)	(0,1)	(1,1)	(2,1)
Gorman [157]	43.720	45.165	51.320	65.546	-	-	-	162.56	164.38	170.48
Narita [158]	43.72	45.16								
Present 7 terms	43.720	45.164	51.320	65.547	89.068	120.79	159.10	162.55	64.37	170.47

Table 5.3 (continued)

Comparison of frequency parameters $(\omega^2\rho h a^4/D_r)^{1/2}$ for polar orthotropic annular plates of uniform thickness with no intermediate support $(D_\theta/D_r = 5,\ D_{r\theta}/D_r = 0.35,\ \nu_{\theta r} = 0.3,\ b/a = 0.5)$

Source of results	No. of nodal diameters and nodal circles (n,s)									
	(1,0)	(1,0)	(2,0)	(3,0)	(0,1)	(1,1)	(4,0)	(2,1)	(5,0)	(3,1)
(3) F-S Gorman [157]	11.30	18.05	33.80	56.521	73.462	78.439	-	93.794	-	120.08
Narita [158]	11.30	18.05								
Present 7 terms	11.305	18.045	33.795	56.522	73.459	78.436	85.450	93.790	119.72	120.08

excellent. For the S-C case, a convergence study is also included in the table, which shows that the rate of convergence is fairly rapid. Similar trends of convergence were observed in the other cases.

The third problem treated is that of polar orthotropic plates of uniform thickness with one intermediate ring support. Five different composite materials, whose properties have been given in reference [155], are considered: the orthotropic parameters D_θ/D_r, $D_{r\theta}/D_r$ and $\nu_{\theta r}$ are 0.02, 0.01323 and 0.0052, for ultra-high modulus graphite epoxy [UHMG]; 0.04, 0.02158 and 0.012, for high-modulus graphite epoxy (HMG); 0.0517, 0.02648 and 0.01551, for PRD 49-III epoxy (PRD); 0.08306, 0.04435 and 0.02243, for high-strength graphite epoxy (HSG); and 50, 0.66129 and 0.26, for ultra-high modulus graphite epoxy inverted (UHMGI). The hole size (b/a) is assumed to be 0.3 and the intermediate ring support is chosen to be located at $\xi_r = 0.5$ (half the outer radius). With the exception of the convergence study, the numerical results were obtained using seven terms in the series (5.6) for three different boundary conditions of both peripheries free (F-F), clamped (C-C) and simply supported (S-S). For the F-F case, the lowest six frequency parameters and the second axisymmetrical frequency parameter (the lowest seven frequency parameters for UHMGI) are presented in Table 5.4, in comparison with those given by Narita [158], who used the Lagrangian multiplier method. Excellent agreement may be

Table 5.4

Comparison of frequency parameters $(\omega^2 \rho h a^4/D_r)^{\frac{1}{2}}$ for polar orthotropic annular paltes of uniform thickness with free peripheries and an intermediate ring support (b/a = 0.3, ξ_w = 0.5)

Source of Results	No. of nodal diameters and nodal circles (n,s)						
(1) UHMG	(0,0)	(1,0)	(2,0)	(3,0)	(4,0)	(5,0)	(0,1)
Narita [158]	0.802	1.559	2.880	4.417	-	-	47.30
Present							
3 terms	0.80238	1.5627	2.8970	4.4679	6.2493	8.2267	54.612
5 terms	0.80226	1.5607	2.8838	4.4246	6.1516	8.0538	47.502
7 terms	0.80225	1.5605	2.8825	4,4207	6.1439	8.0423	47.305
(2) HMG	(0,0)	(1,0)	(2,0)	(3,0)	(4,0)	(5,0)	(0,1)
Narita [158]	1.134	2.044	3.685	5.590	-	-	47.35
Present	1.1341	2.0468	3.6905	5.5981	7.7257	10.105	47.357
(3) PRD	(0,0)	(1,0)	(2,0)	(3,0)	(4,0)	(5,0)	(0,1)
Narita [158]	1.289	2.278	4.062	6.117	-	-	47.38
Present	1.2891	2.2815	4.0701	6.1285	8.4239	11.026	47.389
(4) HSG	(0,0)	(1,0)	(2,0)	(3,0)	(4,0)	(5,0)	(0,1)
Narita [158]	1.633	2.903	5.067	7.440	-	-	47.48
Present	1.6333	2.9093	5.0787	7.4560	10.117	13.260	47.487
(5) UHMGI	(2,0)	(1,0)	(0,0)	(3,0)	(4,0)	(0,1)	(1,1)
Narita [158]	18.70	25.68	32.25	44.89	-	115.0	-
Present	18.798	25.789	32.321	44.905	91.607	115.26	117.02

seen to be achieved. (It may be mentioned that, though the present results and those by Narita are for the same orthotropic material, the numerical values used for the orthotropy are not exactly the same as each other due to the round-off involved in different parameters used.) Included in Table 5.4 are results illustrating a rate of convergence of the present approach, which again shows that the rate of convergence is fairly rapid. For the remaining two cases of boundary conditions, for which no comparable results are available in the literature, the lowest seven frequency parameters are presented in Table 5.5.

The last problem considered in this section is that of isotropic and orthotropic annular plates of uniform thickness with one to three intermediate ring supports. The results were obtained for the hole size of b/a = 0.2, using eight terms in series (5.6) for each of the circumferential modes. For isotropic plates, the frequency parameters for the lowest seven modes are presented in Table 5.6, for the cases of the inner periphery free and the outer periphery clamped, simply supported or free. The locations of the rings are those given in the table. For plates with both peripheries free, the lowest six frequency parameters and the second axisymmetrical frequency parameter are presented in Table 5.7 for polar orthotropic material of high-modulus graphite epoxy (HMG). The locations of the rings were assumed to be the same as those for the isotropic plates.

Table 5.5

Frequency parameters $(\omega^2 \rho h a^4/D_r)^{\frac{1}{2}}$ for polar orthotropic annular plates of uniform thickness with an intermediate ring support ($b/a = 0.3$, $\xi_r = 0.5$)

Material	No. of nodal diameters and nodal circles (n,s)						
(1) C-C	(0,0)	(1,0)	(2,0)	(3,0)	(4,0)	(5,0)	(0,1)
UHMG	77.562	77.601	77.724	77.949	78.305	78.833	218.[illegible]4
HMG	77.575	77.643	77.858	78.256	78.893	79.846	218.36
PRD	77.582	77.687	77.934	78.430	79.226	80.418	218.37
HSG	77.603	77.739	78.172	78.971	80.243	82.129	218.40
UHMGI	(0,0)	(1,0)	(2,0)	(3,0)	(4,0)	(0,1)	(1,1)
	104.01	104.46	115.79	156.19	227.04	258.64	268.40
(2) S-S	(0,0)	(1,0)	(2,0)	(3,0)	(4,0)	(5,0)	(0,1)
UHMG	49.123	49.172	49.327	49.612	50.064	50.735	169.38
HMG	49.154	49.239	49.510	50.012	50.817	52.019	169.41
PRD	49.171	49.277	49.613	50.237	51.240	52.737	169.43
HSG	49.212	49.383	49.925	50.925	52.512	54.841	169.47
UHMGI	(0,0)	(1,0)	(2,0)	(3,0)	(4,0)	(0,1)	(1,1)
	79.500	79.928	91.106	133.16	201.11	215.01	216.80

Table 5.6

Frequency parameters $(\omega^2\rho h a^4/D)^{\frac{1}{2}}$ for isotropic annular plates of uniform thickness with several intermediate ring supports ($b/a = 0.2$, $\nu = 0.3$)

Boundary Conditions	No. of nodal diameters and nodal circles (n,s)						
(1) plates with one ring support at $\xi_r = 0.6$							
F-C	(0,0)	(1,0)	(2,0)	(0,1)	(3,0)	(1,1)	(2,1)
	25.553	44.711	75.194	103.88	108.41	111.47	124.07
F-S	(0,0)	(1,0)	(2,0)	(0,1)	(1,1)	(3,0)	(2,1)
	23.920	42.274	67.194	74.408	79.645	84.683	94.653
F-F	(0,0)	(1,0)	(2,0)	(3,0)	(0,1)	(4,0)	(5,0)
	7.7058	12.492	16.312	21.409	28.496	28.770	38.711
(2) plates with two ring supports at $\xi_r = 0.5$ and 0.75							
F-C	(0,0)	(1,0)	(2,0)	(3,0)	(0,1)	(1,1)	(4,0)
	41.760	65.210	108.88	163.25	189.27	200.09	220.60
F-S	(0,0)	(1,0)	(2,0)	(3,0)	(0,1)	(1,1)	(2,1)
	41.566	64.983	108.36	160.13	165.45	170.02	179.29
F-F	(0,0)	(1,0)	(2,0)	(3,0)	(0,1)	(4,0)	(5,0)
	32.672	35.632	38.848	43.657	44.227	50.490	59.563
(3) plates with three ring supports at $\xi_r = 0.4$, 0.6 and 0.8							
F-C	(0,0)	(1,0)	(2,0)	(3,0)	(0,1)	(1,1)	(2,1)
	80.162	107.88	168.17	245.32	293.14	297.64	309.33

Table 5.6 (continued)

Frequency parameters $(\omega^2\rho h a^4/D)^{\frac{1}{2}}$ for isotropic annular plates of uniform thickness with several intermediate ring supports ($b/a = 0.2$, $\nu = 0.3$)

Boundary Conditions	No. of nodal diameters and nodal circles (n,s)						
(3) plates with three ring suports at $\xi_r = 0.4$, 0.6 and 0.8 (continued)							
F-S	(0,0) 80.140	(1,0) 107.86	(2,0) 168.08	(3,0) 243.75	(0,1) 257.47	(1,1) 259.88	(2,1) 266.56
F-F	(0,0) 55.976	(1,0) 57.047	(2,0) 59.873	(3,0) 64.576	(4,0) 71.307	(5,0) 80.179	(0,1) 80.631

Table 5.7

Frequency parameters $(\omega^2 \rho h a^4/D_r)^{\frac{1}{2}}$ for polar orthotropic annular plates of uniform thickness with free peripheries and several intermediate ring supports ($b/a = 0.2$, $D_\theta/D_r = 0.04$, $D_{r\theta}/D_r = 0.02158$, $\nu_{\theta r} = 0.012$

No. of rings (ξ_r)	No. of nodal diameters and nodal circles (n,s)						
	(0,0)	(1,0)	(2,0)	(3,0)	(4,0)	(5,0)	(0,1)
1 (0.6)	1.5838	4.3667	7.8599	10.417	12.428	14.308	25.636
2 (0.5, 0.75)	29.846	30.474	31.813	33.011	34.010	35.056	41.093
3 (0.4,0.6, 0.8)	53.489	53.579	53.841	54.255	54.824	55.577	77.004

5.3.2. Annular Plates of Variable Thickness

The first problem considered in this section is a set of plates with linear variation in thickness along the radius. The lowest six frequency parameters and the second frequency parameter for the axisymmetrical vibration (0,1), or the lowest seven frequency parameters when the second axisymmetrical frequency parameter is not greater than the seventh frequency parameter, are presented in Table 5.8 for isotropic material and in Table 5.9 for orthotropic material. The values for the hole size (b/a) and the thickness ratio (h_b/h_a) are those given in the tables. For isotropic plates, the results for the axisymmetrical modes are compared to the exact solution for $\nu = 1/3$, from the work of Conway et al. [166], those by Sankaranarayanan et al. [163], who used the Rayleigh-Ritz method with simple polynomials, and those by Raju et al. [159], who used the finite element method. Though the rate of convergence is relatively slower for small values of hole size and thickness ratio ($b/a = h_b/h_a = 0.1$), as shown in the table, the agreement between the present results and those by others is very good. In some cases, the values of the exact solution are larger than the present upper bound results, and this may be due to the round-off errors in conversion of the parameter used in the reference to the present parameter and/or, as pointed out by Sankaranarayanan et al. [163], possibly due to numerical errors in the evaluation of the Bessel functions in the exact

Table 5.8

Frequency parameters $(\omega^2 \rho h_a^4/D_a)^{\frac{1}{2}}$ for isotropic annular plates of linear variable thickness with clamped peripheries and no intermediate ring support

Source of Results	No. of nodal diameters and nodal circles (n,s)						
(1) $\nu = 1/3$, $b/a = h_b/h_a = 0.1$							
Present	(0,0)	(1,0)	(2,0)	(3,0)	(0,1)	(1,1)	(2,1)
4 terms	14.769	16.597	22.425	32.244	40.983	42.797	48.621
5 terms	14.105	16.059	22.166	32.186	37.941	40.105	46.611
6 terms	13,732	15.762	22.028	32.152	36.461	38.693	45.733
7 terms	13.522	15.595	21.950	32.132	35.686	38.004	45.278
8 terms	13.406	15.501	21.904	32.119	35.274	37.633	45.023
Exact[166]	13.28	-	-	-	34.84	-	-
Ref[163]	13.36	-	-	-	35.12	-	-
(2) $\nu = 1/3$, $b/a = h_b/h_a = 0.5$							
Present (7 or 8 terms)	(0,0) 65.916	(1,0) 66.727	(2,0) 69.265	(3,0) 73.806	(4,0) 80.704	(5,0) 90.281	(0,1) 180.70
Exact[166]	66.0	-	-	-	-	-	180.8
Ref [163]	65.92	-	-	-	-	-	180.72
(3) $\nu = 0.3$, $b/a = h_b/h_a = 0.1$							
Present	(0,0)	(1,0)	(2,0)	(3,0)	0,1)	(1,1)	(2,1)
7 terms	13.587	15.689	22,086	32.283	35.781	38.115	45.426
8 terms	13.472	15.597	22.042	32.270	35.370	37.746	45.173
Ref [163]	13.42	-	-	-	35.21	-	-
Ref [159]	14.23	-	-	-	38.12	-	-

Table 5.8 (continued)

Frequency parameters $(\omega^2 \rho h_a^4/D_a)^{\frac{1}{2}}$ for isotropic annular plates of linear variable thickness with clamped peripheries and no intermediate ring support

Source of nodal circles Results	No. of nodal diameters and (n,s)						
(4) $\nu = 0.3$, $b/a = h_b/h_a = 0.5$							
Present (7 or 8 terms)	(0,0) 65.954	(1,0) 66.767	(2,0) 69.312	(3,0) 73.863	(4,0) 80.773	(5,0) 90.361	(0,1) 180.76
Ref [163]	65.954	-	-	-	-	-	180.7
Ref [159]	66.06	-	-	-	-	-	181.6

Table 5.9

Frequency parameters $(\omega^2 \rho h_a^4/D_a)^{\frac{1}{2}}$ for polar orthotropic annular plates of linear variable thickness with clamped peripheries and no intermediate support ($D_\theta/D_r = 50$, $D_{r\theta}/D_r = 0.66129$, $\nu_{\theta r} = 0.26$)

Source of Results	No. of nodal diameters and nodal circles (n,s)						
(1) $b/a = h_b/h_a = 0.1$							
Present (8 terms)	(0,0) 30.667	(1,0) 38.942	(0,1) 65.577	(2,0) 70.108	(1,1) 70.893	(0,2) 107.40	(2,1) 108.21
(2) $b/a = h_b/h_a = 0.5$							
Present (8 terms)	(0,0) 82.268	(1,0) 84.400	(2,0) 96.623	(3,0) 129.55	(4,0) 186.36	(0,1) 204.51	(1,1) 206.45
(3) $b/a = 0.5$, $h_b/h_a = 2$							
Present (8 terms)	(1,0) 160.84	(0,0) 163.42	(2,0) 166.09	(3,0) 208.91	(4,0) 295.71	(0,1) 405.66	(1,1) 406.38

solution. In Table 5.9, the orthotropy has been taken as the one for the ultra-high modulus graphite epoxy inverted (UHMGI).

The next problem considered is that of polar orthotropic annular plates of parabolic variation in thickness with and without intermediate ring supports. The orthotropy taken is again the one for the ultra-high modulus graphite epoxy inverted (UHMGI). The hole size (b/a) and thickness ratio (h_b/h_a) are chosen to be 0.3 and 2, respectively. The power p in equation (5.4) for the thickness variation is given as 2 for the parabolic variation. The results were obtained using eight terms in series (5.6) and are presented in Table 5.10 for the lowest six frequencies and the second frequency for the axisymmetrical mode. The boundary conditions were considered to be both peripheries clamped and the locations of the intermediate supports chosen are given in the table.

5.4. CIRCULAR PLATES

As mentioned before, by letting the inner radius become very small, the present approach for annular plates can be applied to the solid circular plates. To show the validity of the approach, several example plates are treated in this section.

First, isotropic, solid circular plates with uniform thickness are considered taking the values for the hole size

Table 5.10

Frequency parameters $(\omega^2 \rho h_a^4/D_{ra})^*$ for polar orthotropic, clamped annular plates of parabolic variable thickness with and without intermediate ring supports ($D_\theta/D_r = 50$, $D_{r\theta}/D_r = 0.66129$, $\nu_{\theta r} = 0.26$, $b/a = 0.3$, $h_b/h_a = 2$, $p = 2$)

	No. of nodal diameters and nodal circles (n,s)						
(1) plate with no ring support							
	(2,0) 2196.3	(1,0) 2637.6	(0,0) 3101.8	(3,0) 3470.8	(4,0) 5091.4	(1,1) 6593.5	(0,1) 6856.0
(2) plate with one ring support at $\xi_r = 0.65$							
	(2,0) 4281.5	(3,0) 4429.9	(1,0) 4449.7	(0,0) 4554.9	(4,0) 5223.4	(5,0) 6645.8	(0,1) 11771
(3) plate with two ring supports at $\xi_r = 0.5$ and 0.75							
	(2,0) 6121.7	(1,0) 6180.4	(3,0) 6198.7	(0,0) 6219.5	(4,0) 6569.0	(5,0) 7335.4	(0,1) 15586
(4) plate with three ring supports at $\xi_r = 0.45$, 0.65 and 0.8							
	(2,0) 8004.8	(1,0) 8025.2	(0,0) 8039.5	(3,0) 8044.1	(4,0) 8237.3	(5,0) 8683.2	(0,1) 21877

$b/a = 0.001$. The inner periphery is assumed to be free, which then approximates very closely the solid circular plate with no central support. The results were obtained for three different classical boundary conditions of the outer peripheries and are presented in Table 5.11, together with those of the exact solutions [130-132]. Excellent agreement may be seen to be achieved for all the cases of the boundary conditions. It should be mentioned here that, for the clamped circular plate, the frequency parameters of the exact solution do not depend upon Poisson's ratio, though the present results were obtained for $\nu = 0.3$.

The second example considered is uniform, isotropic solid circular plates simply supported or clamped at the centre with classical boundary conditions on the periphery. As mentioned by Leissa [31], it is obvious that for two or more nodal diameters ($n \geq 2$) the resultant frequencies and the mode shapes for plates simply supported or clamped at the centre are identical to those for plates with no constraint at the centre. This is due to the fact that, at the intersection of two nodal lines, the slopes in all directions, as well as the deflection, are zero. In the case of one nodal diameter ($n=1$), the frequencies and mode shapes for central point supported plates are, as shown by Southwell [168] for a plate with the free periphery, identical to those for the plates with no central point support, since the displacement on the nodal line is zero. For axisymmetrical

Table 5.11

Comparison of frequency parameters $(\omega^2 \rho h a^4/D)^*$ for isotropic circular plates of uniform thickness

Source of Results	No. of nodal diameters and nodal circles (n,s)						
(1) Clamped (ν = 0.3)							
	(0,0)	(1,0)	(2,0)	(0,1)	(3,0)	(1,1)	(4,0)
Exact [130]	10.2158	21.26	34.88	39.771	51.04	60.82	69.6659
7 terms	10.2158	21.260	34.877	39.771	51.030	60.829	69.674
(2) Simply supported (ν = 0.3)							
	(0,0)	(1,0)	(2,0)	(0,1)	(3,0)	(1,1)	(4,0)
Exact [132]	4.93515	13.8982	25.6133	29.7200	39.9573	48.4789	56.8416
7 terms	4.93515	13.8982	25.6134	29.7203	39.9575	48.4810	56.8547
8 terms	4.93515	13.8982	25.6133	29.7200	39.9575	48.4796	56.8425
(3) Free (ν = 0.330)							
	(2,0)	(0,1)	(3,0)	(1,1)	(4,0)	(5,0)	(2,1)
Exact [131]	5.2620	9.0689	12.244	20.513	21.527	33.062	35.243
7 terms	5.2620	9.0689	12.244	20.513	21.529	33.079	35.246
8 terms	5.2620	9.0689	12.244	20.513	21.527	33.062	35.244

modes (n=0), the plates simply supported at the centre behave in exactly the same manner as the plates clamped at the centre. This is due to the fact that the continuity of the axisymmetrical modes at the centre constitutes zero slope, as well as the zero displacement. Then, from the above discussion, it is necessary only to that for the central clamped plates for n = 0 and n = 1. Such can be treated by assuming the inner periphery to be simply supported with very small value of the radius, since the simply supported condition satisfies the zero displacement condition at the centre and the very small value of the radius approximates the zero slope. The numerical results were obtained, however, only for the axisymmetrical modes (n = 0) for ν = 0.3, taking b/a = 0.001 and seven terms in series (5.6). The lowest four frequency parameters are presented in Table 5.12, in comparison with those by Southwell [168] for an otherwise free plate and by Sakharov [170] for the plates with simply supported and clamped peripheries. It may be seen that close agreement is achieved between the present results and those obtained by others.

Finally, in addition, the frequency parameters for the axisymmetrical modes of uniform, polar orthotropic circular plates subject to either central point clamped or no central constraint are presented in Table 5.13. The outer periphery is assumed to be clamped. The orthotropy is that for the ultra-high modulus graphite epoxy inverted (UHMGI). The

Table 5.12

Compairson of frequency parameters $(\omega^2 \rho h a^4/D)^{\frac{1}{2}}$ for axisymmetrical modes of uniform, isotropic circular plates simply supported or clamped at the centre (ν = 0.3)

Source of results	Number of nodal circles 0	1	2	3
(1) plate with free periphery				
present	3.7525	20.927	60.703	120.78
Southwell [168]	3.752	20.91	60.68	119.7
(2) plate with simply supported periphery				
present	14.820	49.519	103.88	179.66
Sakharov [170]	14.8	49.4	-	-
(3) plate with clamped periphery				
present	22.744	61.993	121.30	201.29
Sakharov [170]	22.7	61.9	-	-

results were obtained taking b/a = 0.001 and eight terms in series (5.6), and may be of interest to the other researchers.

Table 5.13

Frequency parameters $(\omega^2\rho h a^4/D_r)^{\frac{1}{2}}$ for polar orthotropic circular plates of uniform thickness clamped at the periphery ($D_\theta/D_r = 50$, $D_{r\theta}/D_r = 0.66129$, $\nu_{\theta r} = 0.26$)

Conditions at the centre	Number of nodal circles 0	1	2	3
No constraint	28.972	93.691	174.90	276.69
point clamped	59.717	131.81	222.19	335.83

CHAPTER 6

VIBRATION OF SECTORIAL PLATES

6.1 INTRODUCTORY REMARKS

As mentioned in section 1.5, the problem of the transverse vibration of circular and annular sectorial plates has received considerable attention in recent years. However, the study of the problem is limited to single plates with uniform thickness; it appears that no study has been performed for sectorial plates which are continuous over intermediate simple supports or of non-uniform thickness.

In this chapter, a straightforward, general approach is presented for the solution of the vibration problem of polar orthotropic sectorial plates which may be of continuous over radial and/or circumferential intermediate supports, and of variable thickness. The boundary conditions are considered to be any combination of classical boundary conditions. The Rayleigh-Ritz method is used for the analysis with the BCOP as the admissible functions. Numerical results are presented for a number of example plates. Though the analysis is given for polar orthotropic plates, the majority of the results presented are for the isotropic case; it was not considered practical to present copious results for varying degrees of orthotropy. In several instances, convergence of the solution is demonstrated and, where possible, comparisons are

made with results available in the literature. The present approach is essentially for annular sectorial plates, and circular sectorial plates are treated by allowing the inner radius to become very small.

6.2 ANALYSIS

Consider a thin, annular sectorial plate with radial and concentric supports, bounded by two radial edges $\theta = 0$, α (radian) and two circumferential peripheries $r = b, a$, as shown in Figure 6.1. It is assumed that the material of the plate is of variable thickness both in radial and circumferential directions, and is polar orthotropic. the intermediate radial and circumferential supports are assumed to prevent transverse displacement but to offer no resistance to normal rotation (simple supports), and the boundary conditions are classical (i.e. any combination of free, simply supported and/or clamped).

For free vibration, the displacement may be written as $w(r,\theta)\sin\omega\tau$, where ω is the radian natural frequency and w the maximum deflection with respect to time τ. The maximum strain and kinetic energies in polar coordinates are, respectively (as in Chapter 5, see Appendix B):

$$V_{max} = \frac{1}{2}\int_b^a\int_0^\alpha \left[D_r\left(\frac{\partial^2 w}{\partial r^2}\right)^2 + 2\nu_{\theta r}D_r \frac{\partial^2 w}{\partial r^2}\left(\frac{1}{r}\frac{\partial w}{\partial r} + \frac{1}{r^2}\frac{\partial^2 w}{\partial \theta^2}\right)\right.$$

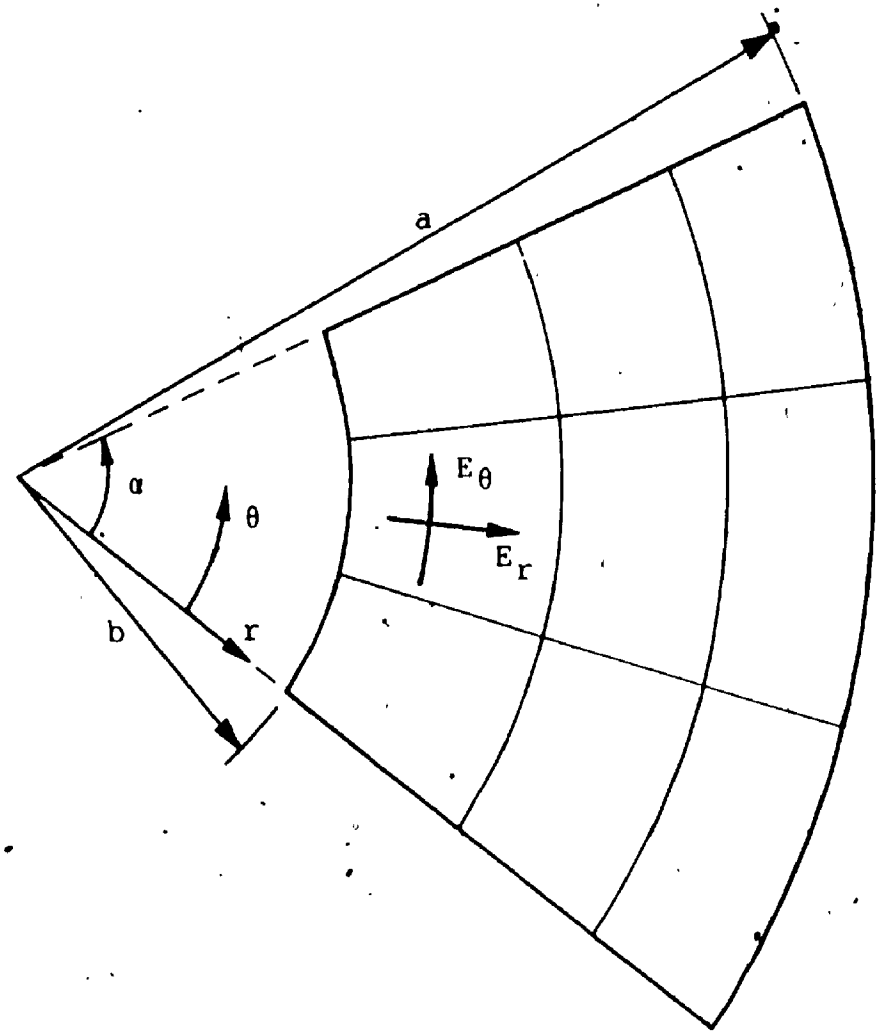

Figure 6.1. A polar orthotropic circular sectorial plate continuous over intermediate supports.

$$+ D_\theta\left(\frac{1}{r}\frac{\partial w}{\partial r} + \frac{1}{r^2}\frac{\partial^2 w}{\partial \theta^2}\right)^2 + 4D_{r\theta}\left\{\frac{\partial}{\partial r}\left(\frac{1}{r}\frac{\partial w}{\partial \theta}\right)\right\}^2\Big] r d\theta dr, \qquad (6.1)$$

$$T_{max} = \tfrac{1}{2}\omega^2 \int_b^a\int_0^\alpha \rho h(r,\theta) w^2 r d\theta dr, \qquad (6.2)$$

where $h(r,\theta)$ is the thickness of the plate and all the other parameters are the same as those given in Chapter 5, respectively.

Introducing non-dimensionalized parameters $\xi = r/a$ and $\eta = \theta/\alpha$ (θ and α (radians) are non-dimensional values), the thickness h can be expressed

$$h(\xi, \eta) = h_{ao} f_r(\xi) f_\theta(\eta), \qquad (6.3)$$

where h_{ao} denotes the thickness at $r=a$, $\theta=0$ ($\xi=1$, $\eta=0$) and $f_r(\xi)f_\theta(\eta)$ describes the variation in thickness. It should be noted that the thickness variation treated in this work is only for the case where the variables are separable. It may also be noted that for plates with uniform thickness, both functions $f_r(\xi)$ and $f_\theta(\eta)$ become unity, respectively. For plates for which the thickness varies with some power, p, of the radius, and q, of the angle, $f_r(\xi)$ and $f_\theta(\eta)$ may be written, respectively,

$$f_r(\xi) = 1 - (1 - h_b/h_a)(1 - \xi^p)/\{1 - (b/a)^p\} \qquad (6.4)$$

$$f_\theta(\theta) = 1 - (1 - h_\alpha/h_o)\eta^q, \qquad (6.5)$$

where h_b/h_a denotes the ratio of the thickness at the inner

periphery to that at the outer periphery on any radial line and h_α/h_o the ratio of the thickness at $\theta = \alpha$ to that at $\theta = 0$ along any concentric circular arc. For linear variation in radial direction and uniform in circumferential direction, p = 1 and q = 0; for linear variation in each direction, p = q = 1; for parabolic variation in each direction, p = q = 2, etc..

The deflection w may be expressed in the form

$$w(\xi,\eta) = \sum_i \sum_j A_{ij}\Phi_i(\xi)\Psi_j(\eta) \tag{6.6}$$

where Φ_i and Ψ_j are the assumed admissible functions in the radial and circumferential directions, respectively.

Substituting equations (6.3) and (6.6), together with equations (6.4) and (6.5), into the energy expressions (6.1) and (6.2), and minimizing with respect to the coefficients A_{mn}, according to the Rayleigh-Ritz procedure, leads to the eigenvalue equation (frequency equation),

$$\sum_i \sum_j [C_{mnij} - \Omega^2 G_{mi} H_{nj}] A_{ij} = 0, \tag{6.7}$$

where $\Omega^2 = \omega^2 \rho h_{ao} a^4 / D_{rao}$, m, n, i, j = 1, 2, 3, ...,

$$C_{mnij} = E_{mi}^{(1,22)} F_{nj}^{(00)} + \frac{D_\theta}{D_r} \{E_{mi}^{(-1,11)} F_{nj}^{(00)} + \frac{1}{\alpha^2} (E_{mi}^{(-2,01)} F_{nj}^{(20)}$$

$$+ E_{mi}^{(-2,10)} F_{nj}^{(02)}) + \frac{1}{\alpha^4} E_{mi}^{(-3,00)} F_{nj}^{(22)}\}$$

$$+ \nu_{\theta r}\{E_{mi}^{(0,12)}F_{nj}^{(00)} + E_{mi}^{(0,21)}F_{nj}^{(00)} + \frac{1}{\alpha^2}(E_{mi}^{(-1,02)}F_{nj}^{(20)}$$

$$+ E_{mi}^{(-1,20)}F_{nj}^{(02)})\}$$

$$+ \frac{4}{\alpha^2}\frac{D_{r\theta}}{D_r}\{E_{mi}^{(-3,00)} - (E_{mi}^{(-2,01)} + E_{mi}^{(-2,10)})$$

$$+ E_{mi}^{(-1,11)}\}F_{nj}^{(11)},$$

$$E_{mi}^{(p,qs)} = \int_{b/a}^{1}\xi^p f_r^3(\xi)(d^q\Phi_m/d\xi^q)(d^s\Phi_i/d\xi^s)d\xi,$$

$$F_{nj}^{(qs)} = \int_0^1 f_\theta^3(\eta)(d^q\Psi_n/d\eta^q)(d^s\Psi_j/d\eta^s)s\eta,$$

$$G_{mi} = \int_{b/a}^{1}\xi f_r(\xi)\Phi_m\Phi_i d\xi,$$

$$H_{nj} = \int_0^1 f_\theta(\eta)\Psi_n\Psi_j d\eta,$$

and D_{rao} denotes the values for D_r at $r = a$, $\theta = 0$. As in Chapter 5, the isotropic plate is a particular case of the orthotropic plate and thus equation (6.7) also applies to the isotropic plate, for which $\nu_{r\theta} = \nu_{\theta r} = \nu$, $D_r = D_\theta = D$ and $D_{r\theta} = (1-\nu)D/2$.

For plates with both radial edges simply supported, with no intermediate radial support and of uniform thickness in circumferential direction, the exact solution can be expressed in the form

$$w(\xi,\eta) = W_n(\xi) \sin n\pi\eta, \tag{6.8}$$

where n denotes the mode sequence number in circumferential direction (i.e. (n-1) is the number of nodal radii excluding the supports). In this case, when using the Rayleigh-Ritz approach, the exact variation in displacement with θ(or η) may be retained and $W_n(\xi)$ can be expressed as

$$W_n(\xi) = \sum_i A_{in}\Phi_i(\xi), \tag{6.9}$$

where $\Phi_i(\xi)$ are the assumed admissible functions. Remembering the uniformity of thickness in circumferential direction, the thickness h can be expressed as

$$h(\xi) = h_a f_r(\xi), \tag{6.10}$$

where h_a denotes the thickness at $r = a(\xi = 1)$. Using equations (6.8) - (6.10) the Rayleigh-Ritz procedure gives an alternative eigenvalue equation

$$\sum_i [C_{mi} - \Omega^2 G_{mi}] A_{mn} = 0, \tag{6.11}$$

where $\Omega^2 = \omega^2 \rho h_a a^4 / D_{ra}$, m, i = 1, 2, 3, ...,

$$C_{mi} = E_{mi}^{(1,22)} + \frac{D_\theta}{D_r}\{E_{mi}^{(-1,11)} - (\frac{n\pi}{\alpha})^2(E_{mi}^{(-2,01)} + E_{mi}^{(-2,10)})$$

$$+ (\frac{n\pi}{\alpha})^4 E_{mi}^{(-3,00)}\}$$

$$+ \nu_{\theta r}\{E_{mi}^{(0,12)} + E_{mi}^{(0,21)} - (\frac{n\pi}{\alpha})^2(E_{mi}^{(-1,02)} + E_{mi}^{(-1,20)})\}$$

$$+ 4 \frac{D_{r\theta}}{D_r}\left(\frac{n\pi}{a}\right)^2 \{E_{mi}^{(-3,00)} - (E_{mi}^{(-2,01)} + E_{mi}^{(-2,10)})$$

$$+ E_{mi}^{(-1,11)}\}$$

and D_{ra} denotes the value for D_r at $r = a$ ($\xi = 1$). This alternative equation allows better estimation with smaller matrices.

The solution of equation (6.7) (or equation (6.11) for plates with both edges simply supported) yields the natural frequencies of vibration of the plate, together with the coefficients for the mode shape (6.6) (or (6.8) for plates with both edges simply supported). The validity and accuracy of the solution depend upon the choice of the admissible functions in each direction, $\Phi_i(\xi)$ and $\Psi_j(\eta)$. In this work, again the BCOP are used. The BCOP $\Phi_i(\xi)$ in the radial direction are exactly the same as those given in Chapter 5 for annular plates, and thus, only the BCOP in the circumferential direction $\Psi_j(\eta)$ are explained in the following.

The starting functions in the circumferential direction $\Psi_i(\eta)$ are chosen so as to satisfy the equivalent beam boundary conditions, both geometrical and natural; and zero displacement conditions at intermediate supports where such exist. The starting functions for plates with no intermediate support may be written

$$\Psi_1(\eta) = \sum_{j=1}^{5} a_j \eta^{j-1} \tag{6.12}$$

where a_j are the same as those given in Table 2.1, in which the first F, S or C denotes the condition at $\theta = 0$ and the second the condition at $\theta = \alpha$. Again, the lower degree starting function, such as those in equation (2.10), which satisfy only the geometrical boundary conditions could be used and would yield very similar results. The present functions are used simply for consistency. For plates with radial supports, the starting functions are obtained by multiplying appropriate functions given by equation (6.12) by the factor $(\eta - \eta_\theta)$, recurrently, where η_θ denotes the location of the intermediate radial supports. The subsequent polynomials are generated by the recurrence formula, such as equation (2.6). The equation is rewritten here:

$$\Psi_{k+1}(\eta) = \{g(\eta) - B_k\}\Psi_k(\eta) - C_k\Psi_{k-1}(\eta); \quad k = 1,2,3,\ldots, \tag{6.13}$$

$$B_k = \int_0^1 w_f(\eta) g(\eta) \Psi_k^2(\eta) d\eta / \int_0^1 w_f(\eta) \Psi_k^2(\eta) d\eta,$$

$$C_k = \int_0^1 w_f(\eta) \Psi_k^2(\eta) d\eta / \int_0^1 w_f(\eta) \Psi_{k-1}^2(\eta) d\eta,$$

The weight function $w_f(\eta)$ is determined considering the orthogonality of the vibration modes. Recalling the kinetic energy expression (6.2) and the orthogonality condition in the radial direction, equation (5.10), the orthogonality of circumferential modes may be expressed

$$\alpha \int_0^1 f_\theta(\eta)\Psi_n(\eta)\Psi_j(\eta)d\eta = H_{nj}\delta_{nj}, \tag{6.14}$$

where H_{nj} is a constant and δ_{nj} the Kronecker delta. Therefore, the weight function is $w_f(\eta) = f_\theta(\eta)$. the generating function is chosen as $g(\eta) = \eta$, which makes the subsequent polynomials ($k > 1$) generated satisfy only the geometrical boundary conditions. Again, higher degree generating functions may be used for plates with simply supported edge(s) (as in rectangular plate problem), but such have not been used to obtain the results presented in this chapter. It may also be noted that, when both edges have the same boundary conditions and the thickness along any circular arc is constant, the BCOP are symmetrical and antisymmetrical about $\eta = 1/2$ ($\theta = \alpha/2$) alternately, by the theorem (2) in Chapter 2.

It is worth noting again that, the first and second terms of frequency equation (6.7) or (6.11) yield symmetrical and diagonal matrices, respectively. When appropriately normalized polynomials are used as the admissible functions in equation (6.6) or (6.9), the second term of equation (6.7) or (6.11) yields an identity matrix: this gives some computational advantage.

In order to illustrate the accuracy and utility of the approach described, numerical results are presented in the following sections for a number of specific plates. Where

possible, comparisons are made with previously published results. Although the calculations were performed making use of symmetry, where it existed, the number of terms indicated in the following sections denotes the whole number of terms used; when symmetry exists, only half the number of terms indicated actually contribute to the solution.

6.3 UNIFORM, ISOTROPIC, SINGLE PLATES

The first problem treated in this section is that of uniform, isotropic, annular sectorial plates with both radial edges simply supported. Two cases of the boundary conditions are considered for the circumferential peripheries; both free and both simply supported. The lowest six frequency parameters for $b/a = 0.5$, $\alpha = \pi/4$, obtained by using equations (6.11) and (6.7) respectively, are presented in Table 6.1, in comparison with the exact solution by Ramakrishnan and Kunukkasseril [174]. Poisson's ratio is taken as 0.3. In the table, the heading of the values denotes the number of nodal radii (k) and nodal circular arcs(s), excluding the boundary supports. Close agreement may be seen to exist. However, remembering the upper bound characteristics of the Rayleigh-Ritz method employed in the present analysis, the cases where the present results are lower than those in the reference requires some comment. Where the approximate solution is only very slightly lower than the exact result (eg. case (2), mode (0,0)), this may be

Table 6.1

Comparison of frequency parameters $(\omega^2 \rho h a^4/D)^{\frac{1}{2}}$ for uniform, isotropic, annular sectorial plates with radial edges simply supported ($b/a = 0.5$, $\alpha = \pi/4 = 45°$, $\nu = 0.3$)

Source of Results	No. of nodal diameters and nodal arcs (k,s)					
(1) Both peripheries free						
	(0,0)	(0,1)	(1,0)	(0,2)	(2,0)	(1,1)
Ref. [174]	21.066	66.746	81.602	146.63	176.14	176.84
Eqn. (6.11)						
4 terms	21.075	68.398	81.715	164.97	176.50	183.60
5 terms	21.074	67.162	81.712	149.70	176.50	177.44
6 terms	21.067	66.725	81.624	148.73	176.32	177.35
Eqn. (6.7)						
4 x 4 terms	21.080	68.404	81.782	164.97	183.70	226.26
5 x 5 terms	21.074	67.162	81.779	149.70	177.54	177.70
6 x 6 terms	21.067	66.725	81.624	148.73	177.35	177.52
(2) Both Peripheries simply supported						
	(0,0)	(1,0)	(0,1)	(2,0)	(1,1)	(0,2)
Ref. [174]	68.380	150.96	189.61	278.46	283.59	387.73
Eqn. (6.11)						
4 terms	68.396	150.99	189.75	278.50	285.13	485.74
5 terms	68.379	150.98	189.75	278.39	283.85	390.28
6 terms	68.379	150.98	189.60	278.39	283.62	390.02
Eqn. (6.7)						
4 x 4 terms	68.399	151.06	189.75	285.20	337.47	485.74
5 x 5 terms	68.379	151.06	189.75	279.82	283.92	390.28
6 x 6 terms	68.379	150.98	189.60	279.82	283.62	390.02

attributable to the conversion of the parameter used in the reference to that in the present table. For the larger discrepancies (eg. case (1), mode (0,1)), the author can only offer the explanation that he suspects that the quoted 'exact' values include some numerical errors which may have occurred in the evaluation of Bessel functions or that there is some slight error in the present results which he has been unable to discover. Included in the table are brief convergence studies which show fairly rapid rate of convergence.

The second problem considered is that of uniform, isotropic, circular sectorial plates with fully clamped boundaries. As mentioned before, the present analysis is essentially for annular sectorial plates and circular sectorial plates are treated by taking a very small value of inner radius. The lowest five frequency parameters are presented in Table 6.2 taking b/a = 0.00001. For $\alpha = \pi/2$, $\nu = 0.3$, the results obtained with 4, 5 and 6 terms in each direction in the series (6.6) are compared with those by Srinivasan and Thiruvenkatachari [188], who used an integral equation technique. It may be seen that close agreement is achieved between the present results and those in the reference for both cases, and the rate of convergence of the present analysis is fairly rapid. For $\nu = 0.33$, taking six terms in each direction in equation (6.6), the results were obtained for various values of the angle subtended and are

Table 6.2

Comparison of frequency parameters $(\omega^2\rho h a^4/D)^{\frac{1}{2}}$ for uniform, isotropic, fully-clamped, circular sectorial plates.

α	Source of Results	Mode sequence numbers 1	2	3	4	5
(1) $\nu = 0.3$						
$\pi/2$ (90°)	Ref. [188]	48.70	88.13	105.06	138.33	165.31
	Eqn. (6.7)					
	4 x 4 terms	48.824	88.122	106.63	141.52	171.71
	5 x 5 terms	48.787	87.824	105.18	137.25	166.64
	6 x 6 terms	48.786	87.785	104.89	137.10	164.95
(2) $\nu = 0.33$						
$\pi/6$ (30°)	Exp. [182]	184.6	295.2	422.6	430.6	571.8
	6 x 6 terms	188.4	308.0	418.6	466.7	612.7
	8 x 6 terms	188.2	300.8	417.6	433.2	603.7
		(2.0)	(1.9)	(-1.2)	(0.6)	(5.6)
$\pi/3$ (60°)	Exp. [182]	72.74	143.1	147.0	234.5	237.8
	6 x 6 terms	75.63	145.6	148.8	237.2	244.1
		(4.0)	(1.7)	(1.2)	(1.2)	(2.6)
$\pi/2$ (90°)	Exp. [182]	51.51	91.76	108.9	141.1	168.9
	6 x 6 terms	48.79	87.79	104.9	137.1	164.9
		(-5.3)	(-4.3)	(-3.7)	(-2.8)	(-2.4)
$2\pi/3$ (120°)	Exp. [182]	37.30	62.04	-	92.50	-
	6 x 6 terms	37.54	62.82	86.94	94.62	127.0
		(0.6)	(1.3)		(2.3)	
$5\pi/6$ (150°)	Exp. [182]	30.46	49.85	70.90	76.25	107.8
	6 x 6 terms	31.62	49.69	71.77	78.00	98.07
		(3.8)	(-0.32)	(1.2)	(2.3)	(-9.0)
π (180°)	Exp. [182]	23.63	38.96	55.02	64.25	-
	6 x 6 terms	28.12	41.73	58.73	71.91	78.61
	6 x 8 terms	28.12	41.73	58.68	71.91	78.38
		(19.0)	(7.1)	(6.7)	(11.9)	

compared with experimental results by Maruyama and Ichinomiya [182]. For $\alpha = \pi/6$ and π, the values obtained with 8 x 6 and 6 x 8 terms, respectively, are also included in the table; the results with 8 x 8 terms were identical up to the figure presented. In addition, the error percentages based on the experimental results are given in parentheses. The agreement, while not being excellent, is typical of that which may be expected between experimental and theoretical results.

The last problem treated in this section is that of uniform, isotropic, annular sectorial plates with fully clamped boundaries. The problem immediately preceding this is a special case of this problem. The results are presented in Table 6.3. For a plate with $\nu = 0.3$, $b/a = 0.5$ and $\alpha = \pi/2$, the present results are compared again with those by an integral equation technique [188]. The agreement achieved is very good. For $\nu = 0.33$ and $\alpha = \pi/3$, the results are presented for various values of b/a in comparison with those from experiment [182]. Again, error percentages are given in parentheses. With the exception of a few of the lower modes, the agreement between the theoretical and experimental results is quite good.

6.4 PLATES WITH COMPLICATING FACTORS

In order to demonstrate the versatility of the present analysis, several example plates with complicating factors

Table 6.3

Comparison of frequency parameters $(\omega^2\rho h a^4/D)^{\frac{1}{2}}$ for uniform, isotropic, fully-clamped, annular sectorial plates.

b/a	Source of Results	Mode sequence numbers 1	2	3	4	5
(1) $\nu = 0.3$, $\alpha = \pi/2 = 90°$						
0.5	Ref. [188]	95.04	114.52	151.24	204.41	253.74
	Eqn. (6.7)					
	4 x 4 terms	95.233	114.97	152.58	211.46	253.39
	5 x 5 terms	95.221	114.96	150.63	211.44	253.29
	6 x 6 terms	95.221	114.94	150.63	201.96	253.22
(2) $\pi = 0.33$; $\alpha = \pi/3 = 60°$						
	Exp. [182]	63.14	127.0	137.2	214.5	229.1
	6 x 6 terms	75.63	145.2	148.8	235.1	243.8
0.1	8 x 8 terms	75.63	145.2	148.8	234.1	243.5
		(19.8)	(14.3)	(8.5)	(9.1)	(6.3)
	Exp. [182]	69.05	133.5	144.7	227.6	234.3
0.2	6 x 6 terms	75.69	146.4	148.8	241.8	243.9
		(9.6)	(9.7)	(2.8)	(6.2)	(4.1)
	Exp. [182]	74.59	143.5	151.2	240.2	247.6
0.3	6 x 6 terms	77.30	148.8	159.0	243.8	251.9
		(3.6)	(3.7)	(5.2)	(1.5)	(1.7)
	Exp. [182]	79.57	148.1	185.4	239.3	259.6
0.4	6 x 6 terms	85.25	150.1	194.2	243.9	266.0
		(7.1)	(1.4)	(4.7)	(1.9)	(2.5)
	Exp. [182]	98.41	157.9	244.6	256.4	312.9
0.5	6 x 6 terms	106.1	159.4	246.2	263.9	317.5
		(7.8)	(0.9)	(0.7)	(2.9)	(1.5)
	Exp. [182]	133.1	185.9	258.5	358.4	380.2
0.6	6 x 6 terms	152.0	192.9	266.0	369.9	398.7
		(14.2)	(3.8)	(2.9)	(3.2)	(4.9)

such as polar orthotropy, intermediate supports or varying thickness are considered. The complicating factors can all be included simultaneously, however, in the following examples, each factor is considered individually since, with the exception of one case, there exist no comparable results in the literature. From the earlier convergence study, it was decided to take 6 x 6 terms for equation (6.7) and six terms for equation (6.11) to obtain the results presented.

The first problem treated in this section is uniform, polar orthotropic, sectorial plates with fully simply supported boundaries. In Table 6.4, the lowest five frequency parameters for b/a = 0.05, the angle subtended 100°, $\nu_{\theta r} = 0.3$ and three combinations of D_θ/D_r and $D_{r\theta}/D_r$ are presented in comparison with those by Irie et al. [186] and Ramaiah [185], who used the Rayleigh-Ritz method with spline functions and simple polynomials, respectively, as the admissible functions. The analysis in reference [185] is in fact equivalent to that of equation (6.11). While the present results were obtained with 6 x 6 or 6 terms, those in reference [186] were obtained with five terms and in reference [185] with eight terms. Excellent agreement may be seen to exist for all the modes presented.

The second problem treated is that of uniform, polar orthotropic sectorial plates with both circumferential peripheries simply supported. The lowest six frequency

Table 6.4

Comparison of frequency parameters $(\omega^2 \rho h a^4/D_r)^{\frac{1}{2}}$ for uniform, polar orthotropic, sectorial plates with fully simply supported boundaries
($b/a = 0.05$, $\alpha = 100°$, $\nu_{\theta r} = 0.3$)

$\frac{D_\theta}{D_r}$	$\frac{D_{r\theta}}{D_r}$	Source of Results	Number of nodal radii and arcs (k,s)				
			(0,0)	(1,0)	(2,0)	(0,1)	(3,0)
0.1	0.35	Ref. [186]	20.3	35.9	55.0	61.6	
		Ref. [185]	20.142	35.497	54.595	61.514	-
		Eqn. (6.7)	20.148	35.497	54.746	61.525	77.667
		Eqn. (6.11)	20.148	35.497	54.595	61.525	76.808
			(0,0)	(1,0)	(0,1)	(2,0)	(1,1)
1.0	0.35	Ref. [186]	23.5	[illegible]9	66.5	84.6	-
		Ref. [185]	23.220	[illegible]788	66.203	84.631	-
		Eqn. (6.7)	23.225	49.788	66.213	85.017	110.86
		Eqn. (6.11)	23.225	49.788	66.213	84.653	110.86
			(0,0)	(0,1)	(1,0)	(0,2)	(2,0)
10	4.85	Ref. [186]	56.8	130.9	136.7	-	243.8
		Ref. [185]	56.276	129.71	136.55	-	243.77
		Eqn. (6.7)	56.276	129.93	136.55	224.43	244.84
		Eqn. (6.11)	56.276	129.93	136.55	224.43	243.78

parameters obtained by using equation (6.7) are presented in Table 6.5 for all the combination of classical boundary conditions for radial edges. The values for D_θ/D_r are considered to be 0.1, 1 and 10, while the other values are taken as constants ($b/a = 0.3$, $\alpha = \pi/3$, $D_{r\theta}/D_r = 0.35$, $\nu_{\theta r} = 0.3$). There is no comparable results in the open literature. In the table, the edge condition F, S and C denote free, simply supported and clamped boundary conditions at $\theta = 0$ or α. For the plate with both edges simply supported, the results obtained with equation (6.11) are also given in the parentheses.

The third problem is that of uniform, isotropic, sectorial plates with or without intermediate simple supports. For plates with both radial edges simply supported, the lowest six frequency parameters obtained by using equation (6.11) are presented in Table 6.6 for all the combinations of classical boundary conditions at circumferential peripheries. For plates with $b/a = 0.2$, $\alpha = \pi/3$ and $\nu = 0.3$, three cases of support conditions are considered;

(A) a plate with no intermediate support,

(B) a plate with one intermediate support at $r = 0.6a$, and

(C) a plate with two intermediate supports at $r = 0.5a$ and $0.8a$.

In the table, the first F, S and C in the first column denote

Table 6.5

Frequency parameters $(\omega^2 \rho h a^4/D_r)^{\frac{1}{2}}$ for uniform, polar orthotropic, sectorial plates with both circumferential peripheries simply supported.
$(a/b = 0.3,\ \alpha = \pi/3,\ D_{r\theta}/D_r = 0.35,\ \nu_{\theta r} = 0.3)$

Edge conditions	$\frac{D_\theta}{D_r}$	Mode sequence number 1	2	3	4	5	
F-F	0.1	17.884	32.997	62.519	77.374	96.786	99.966
	1	20.482	34.076	76.527	80.842	100.06	149.31
	10	25.187	35.285	87.508	102.66	139.23	190.66
F-S	0.1	23.226	48.341	81.331	83.132	123.10	128.06
	1	24.804	58.127	86.346	120.96	133.08	187.97
	10	28.217	90.039	104.36	182.49	199.06	253.42
F-C	0.1	23.930	51.484	83.410	86.378	126.60	133.12
	1	27.485	68.679	88.496	134.77	147.52	189.47
	10	40.254	98.994	133.06	198.87	228.10	296.71
S-S	0.1	36.558	66.569	103.96	104.94	152.78	153.19
		(36.558)	(66.569)	(103.96)	(104.64)	(150.88)	(153.19)
	1	41.910	98.061	108.20	178.50	185.43	212.35
		(41.910)	(98.061)	(108.20)	(177.63)	(185.43)	(212.35)
	10	71.525	142.06	203.52	243.07	320.79	387.33
		(71.525)	(142.06)	(203.52)	(243.07)	320.79)	(387.33)
S-C	0.1	38.733	71.228	105.88	111.94	157.63	162.32
	1	50.614	112.43	117.47	197.44	205.56	219.62
	10	97.854	177.43	244.61	279.24	372.56	419.82
C-C	0.1	41.293	76.413	107.99	119.72	162.29	171.83
	1	61.374	128.14	129.54	219.48	226.39	228.57
	10	127.90	218.32	289.12	327.85	428.87	479.33

Table 6.6

Frequency parameters $(\omega^2 \rho h a^4/D)$ for uniform, isotropic, sectorial plates with simply supported radial edges and with or without intermediate arc supports; $b/a = 0.2$, $\alpha = \pi/3$, $\nu = 0.3$;

(A) no intermediate suport,
(B) one intermediate support at $r/a = 0.6$,
(C) two intermediate supports at $r/a = 0.5$, 0.8.

Periphery conditions	Case	Mode sequence number 1	2	3	4	5	6
F-F	(A)	12.40	47.43	52.80	102.3	111.3	123.6
	(B)	21.52	51.42	103.8	110.4	156.3	177.0
	(C)	59.04	90.06	140.5	159.3	210.3	258.6
F-S	(A)	39.66	93.12	98.07	164.6	177.7	184.9
	(B)	85.22	131.4	131.9	197.7	258.9	288.1
	(C)	152.5	244.4	209.7	336.6	340.7	377.8
F-C	(A)	50.51	108.5	114.2	184.0	198.9	207.0
	(B)	108.4	145.0	164.3	228.6	267.1	297.2
	(C)	155.0	215.7	251.1	347.7	388.6	423.1
S-F	(A)	12.47	47.38	53.70	102.2	118.7	123.2
	(B)	21.57	51.41	103.6	115.6	168.9	176.6
	(C)	58.85	88.83	137.9	177.0	206.8	266.1
S-S	(A)	40.31	97.52	98.00	177.7	181.8	184.4
	(B)	85.75	128.7	144.5	195.0	286.8	287.0
	(C)	166.5	235.0	237.7	326.2	356.6	374.5
S-C	(A)	51.70	114.2	115.4	198.8	205.6	206.3
	(B)	114.5	155.6	163.3	228.1	297.7	319.5
	(C)	171.5	240.6	242.7	340.8	429.3	448.7

Table 6.6 (continued)

Frequency parameters $(\omega^2 \rho h a^4/D)^{\frac{1}{2}}$ for uniform, isotropic, sectorial plates with simply supported radial edges and with or without intermediate arc supports; $b/a = 0.2$, $\alpha = \pi/3$, $\nu = 0.3$;

(A) no intermediate suport,
(B) one intermediate support at $r/a = 0.6$,
(C) two intermediate supports at $r/a = 0.5$, 0.8.

Periphery conditions	Case	Mode sequence number 1	2	3	4	5	
C-F	(A)	12.62	47.38	55.42	102.1	122.7	123.2
	(B)	21.56	51.25	103.6	119.3	171.3	176.0
	(C)	58.92	88.77	137.4	184.0	205.4	250.6
C-S	(A)	41.33	98.00	102.4	177.6	184.2	192.0
	(B)	86.61	128.7	159.8	194.8	286.5	286.7
	(C)	171.4	234.4	267.1	326.2	350.4	369.6
C-C	(A)	53.39	114.2	121.7	198.8	206.4	218.6
	(B)	118.2	162.7	168.0	227.1	297.2	318.7
	(C)	177.7	241.8	272.8	338.5	435.6	454.3

free, simply supported and clamped boundary conditions at the inner periphery and the second those at the outer periphery.

In Table 6.7, the results obtained with equation (6.7) are presented for plates clamped at $r = b$ and $\theta = 0$, and the other two boundaries simply supported. Three cases of support conditions are considered for plates with $b/a = 0.2$, $\alpha = \pi/3$ and $\nu = 0.3$;

(A) a plate with no intermediate support,

(B) a plate with one intermediate support in each direction ($r = 0.6a$ and $\theta = 0.5\alpha$), and

(C) a plate with two intermediate supports in each direction.

The results may be of interest to other workers in the field.

The last problem is that of isotropic, fully-clamped, sectorial plates with linearly and parabolically varying thickness. The first six frequency parameters for plates with $b/a = 0.2$, $\alpha = \pi/3$ and $\nu = 0.3$ are presented in Table 6.8. The thickness at the outer periphery is taken as one half of that at the inner periphery and the thickness at the edge $\theta = \alpha$ is one half of that at $\theta = 0$. The values for the thickness variation given in equations (6.4) and (6.5) are $p = 1$ and/or $q = 1$ for linear variation, and $p = 2$ and/or $q = 2$ for parabolical variation.

Table 6.7

Frequency parameters $(\omega^2 \rho h a^4/D)^{\frac{1}{2}}$ for uniform, isotropic, sectorial plates clamped at $r = b$, $\theta = 0$, simply supported at $r = a$, $\theta = \alpha$, and with or without intermediate supports; $b/a = 0.2$, $\alpha = \pi/3$, $\nu = 0.3$;

(A) no intermediate suports,
(B) intermediate support at $r/a = 0.6$, $\theta/\alpha = 0.5$,
(C) intermediate supports at $r/a = 0.5$, 0.8 and $\theta/\alpha = 0.4$, 0.7.

Case	Mode sequence number					
	1	2	3	4	5	
(A)	50.52	111.1	115.1	197.0	201.0	207.2
(B)	134.5	169.2	305.5	306.4	366.3	384.4
(C)	335.5	384.9	447.1	492.3	507.2	638.03

Table 6.8

Frequency parameters $(\omega^2 \rho h_{ao} a^4/D)^{\frac{1}{2}}$ for isotropic, fully-clamped sectorial plates with linearly and parabolically varying thickness ($b/a = 0.2$, $\alpha = \pi/3$, $\nu = 0.3$)

$\frac{h_b}{h_a}$	$\frac{h_\alpha}{h_o}$	Mode sequence number 1	2	3	4	5	6
(1) Linearly varying thickness							
2	1	102.1	191.4	209.2	304.0	345.1	351.6
1	0.5	55.26	104.2	111.1	169.5	177.6	189.5
2	0.5	74.49	138.0	153.8	219.8	243.1	265.7
(2) Parabolically varying thickness							
2	1	109.9	297.3	225.1	329.0	374.8	377.3
1	0.5	60.45	115.4	122.6	188.7	197.8	209.9
2	0.5	87.90	164.8	183.9	262.9	293.0	319.6

CHAPTER 7

CONCLUDING REMARKS

It has been demonstrated that the use of the beam characteristic orthogonal polynomials (BCOP), generalized by the author, in the Rayleigh-Ritz method (in conjunction with Lagrangian multipliers for plates with point supports) permits the study of vibration problems of various slender beams or thin plates subject to several complicating effects. Numerous illustrative examples have been examined and numerical results generated both for new problems and for problems for which comparison results are available in the literature. The approach can be adopted for any dynamic and static problem where the energy expressions are known and the coordinates are separable in the formulation of the approximate solution. Though only the Rayleigh-Ritz method is used in this thesis, the BCOP can be used as admissible functions for other methods such as the Galerkin method, the Kantorovich method, etc.

The approach presented in this thesis is simple but more general than most of the other approaches presented previously in the literature. Numerous problems have been treated in this work, but many more problems could be treated using the approach described. Some further plate problems which may easily be tackled are:

(1) plates subject to elastic springs or having elastically restrained boundaries, which requires simply adding the energy stored in the springs to the strain energy expression given, in a manner similar to that used for the elastically restrained beams in Chapter 3;

(2) plates with concentrated masses, which requires the addition of the effect of the masses to the kinetic energy expression given, as for the beams with concentrated masses; and

(3) plates subject to inplane force, which require the subtraction or addition (depending upon the direction) of the effect of the force to the strain energy expression given, as for the beams subject to axial load.

Though the effect of point supports was considered only for rectangular plates, their inclusion is straightforward for other plates such as circular, annular and sectorial plates. Tapered plates could also be analyzed.

The approach for the box-like structure treated is applicable to those structures which can be folded out to form a multi-span beam or plane plate.

It is believed that the present approach may be used to study various shell problems, such as cylindrical shells, shallow shells of rectangular plan form, etc.. These may again involve various complicating factors.

REFERENCES

1. D. Young and R.P. Felgar, Jr., 1949. Engineering Research Series No. 44, Tables of Characteristic Functions Representing Normal Modes of Vibration of a Beam. Austin, Texas: Bureau of Engineering Research, The University of Texas.

2. R.E.D. Bishop and D.C. Johnson, 1979. The Mechanics of Vibration. Cambridge: Cambridge University Press.

3. H.P.W. Gottlieb, 1986. Applied Acoustics 19, 347-356. Vibration characteristics of a beam with sliding end.

4. R.E.D. Bishop and D.C. Johnson, 1956. Vibration Analysis Tables. Cambridge: Cambridge University Press.

5. T.C. Chang and R.R. Craig, Jr., 1969. Journal of the Engineering Mechanics Division (ASCE) 95, 1027-1031. Normal modes of uniform beams.

6. R.D. Blevins, 1979. Formulas for Natural Frequency and Mode Shape. New York: Van Nostrand Reinhold.

7. R.P. Felgar, Jr., 1950. University of Texas Circular No. 14, Formulas for Integrals Containing Characteristic Functions of a Vibrating Beam. Austin, Texas: Bureau of Engineering Research, the University of Texas.

8. C.B. Sharma, 1978. Journal of Sound and Vibration 56, 475-480. Calculation of integrals involving characteristic beam functions.

9. J.W.S. Rayleigh, baron, 1894. Theory of Sound, Vol. 1, second edition. London: Macmillan.

10. W. Ritz, 1909. Journal für reine and angewandte Mathematik 135, 1-61. Uber eine neue Methode zur Losung gewisser Variationsprobleme der Methematischen Physik.

11. G.B. Warburton, 1954. Proceedings of the Institution of Mechanical Engineers 168, 371-384. The vibration of rectangular plates.

12. R.F.S. Hearmon, 1959. Journal of Applied Mechanics 26, 537-540. The frequency of flexural vibration of rectangular orthotropic plates with clamped or supported edges.

13. S.M. Dickinson, 1978. Journal of Sound and Vibration 61, 1-8. The buckling and frequency of flexural vibration of rectangular isotropic and orthotropic plates using Rayleigh's method.

14. C.S. Kim and S.M. Dickinson, 1985. Journal of Sound and Vibration 103, 142-149. Improved approximate expressions for the natural frequencies of isotropic and orthotropic rectangular plates.

15. W. Ritz, 1909. Annalen der Physik, Vierte Folge 28, 737-786. Theorie der Transversalschwingungen einer quadratischen Platten mit frein Randern.

16. D. Young, 1950. Journal of Applied Mechanics 17, 448-453. Vibration of rectangular plates by the Ritz method.

17. A.W. Leissa, 1973. Journal of Sound and Vibration 31, 257-293. The free vibration of rectangular plates.

18. S.F. Bassily and S.M. Dickinson, 1975. Journal of Applied Mechanics 42, 858-864. On the use of beam functions for problems of plates involving free edges.

19. S.F. Bassily and S.M. Dickinson, 1978. Journal of Sound and Vibration 59, 1-14. Buckling and vibration of in-plane loaded plates treated by a unified Ritz approach.

20. K. Vijayakumar and G.K. Ramaiah, 1978. Journal of Sound and Vibration 56, 127-135. Analysis of vibration of clamped square plates by the Rayleigh-Ritz method with asymptotic solutions from a modified Bolotin method.

21. K. Vijayakumar and G.K. Ramaiah, 1978. Journal of Sound and Vibration 59, 335-347. Use of asymptotic solutions from a modified Bolotin method for obtaining natural frequencies of clamped rectangular orthotropic plates.

22. S.M. Dickinson, 1978. Journal of Sound and Vibration 59, 143-146. On the use of simply supported plate functions in Rayleigh's method applied to the flexural vibration of rectangular plates.

23. S.M. Dickinson and E.K.H. Li, 1982. Journal of Sound and Vibration 80, 292-297. On the use of simply supported plate functions in the Rayleigh-Ritz method applied to the flexural vibration of rectangular plates.

24. S.M. Dickinson, S. Ilanko and E.K.H. Li, 1983. Journal of Sound and Vibration 86, 151-157. Numerical values for integrals of products of simply supported plate functions.

25. R.B. Bhat, 1985. Journal of Sound and Vibration 102, 493-499. Natural frequencies of rectangular plates using characteristic orthogonal polynomials in Rayleigh-Ritz method.

26. R.B. Bhat, 1985. Proceedings of the Third International Modal Analysis Conference, Orlando, Florida, 28-31 January. Vibration of rectangular plates using beam characteristic orthogonal polynomials in Rayleigh-Ritz method.

27. R.B. Bhat, 1985. Proceedings of the Tenth Canadian Congress of Applied Mechanics, London, Ontario, Canada, 2-7 June, A129-A130. Vibration of structures using characteristic orthogonal polynomials in Rayleigh-Ritz method.

28. A. Kaushal and R.B. Bhat, 1985. Proceedings of the Nineteenth Midwestern Mechanics Conference, Columbus, Ohio, 9-11 September, 173-174. Vibration of plates involving free edges, using characteristic orthogonal polynomials.

29. S.M. Dickinson and A. Di Blasio, 1986. Journal of Sound and Vibration 108, 51-62. On the use of orthogonal polynomials in the Rayleigh-Ritz method for the study of the flexural vibration and buckling of isotropic and orthotropic rectangular plates.

30 R.B. Bhat, 1985. Journal of Engineering Mechanics 111, 1301-1309. Plate deflection using orthogonal polynomials.

31. A.W. Leissa, 1969. NASA SP-160, Vibration of Plates. Washington: Office of Technology Utilization, NASA.

32. A.W. Leissa, 1977. The Shock and Vibration Digest 9-10, 13-24. Recent research in plate vibrations: classical theory.

33. A.W. Leissa, 1977. The Shock and Vibration Digest 9-11, 21-35. Recent research in plate vibrations, 1973-1976: complicating effects.

34. A.W. Leissa, 1981. The Shock and Vibration Digest 13-9, 11-22. Plate vibration research, 1976-1980: classical theory.

35. A.W. Leissa, 1981. The Shock and Vibration Digest 13-10, 19-36. Plate vibration research, 1976-1980: complicating effects.

36. A.W. Leissa, 1987. The Shock and Vibration Digest 19-2, 11-18. Recent studies in plate vibrations: 1981-85 part I. classical theory.

37. A.W. Leissa, 1987. The Shock and Vibration Digest 19-3, 10-24. Recent studies in plate vibrations: 1981-85 part II. complicating effects.

38. R. Greif and S.C. Mittendorf, 1976. Journal of Sound and Vibration 48, 113-122. Structural vibrations and Fourier series.

39. D.J. Gorman, 1974. International Journal of Mechanical Sciences 16, 345-351. Free lateral vibration analysis of double-span uniform beams.

40. D.J. Gorman and R.K. Sharma, 1974. Ottawa University Report No. Conf-740330-1. Vibration frequencies and modal shapes for multi-span beams with uniformly spaced supports.

41. D.J. Gorman, 1975. Free Vibration Analysis of Beams and Shafts. New York: John Wiley and Sons.

42. P.A.A. Laura, V.H. Cortinez, L. Ercoli and V.H. Palluzzi, 1985. Journal of Sound and Vibration 102, 595-598. Analytical and experimental investigation on a vibrating beam with free ends and intermediate supports.

43. B.P. Shastry and G. Venkateswara Rao, 1985. Journal of Sound and Vibration 103, 593-595. Initially stressed vibrations of beams with two symmetrically placed intermediate supports.

44. B.P. Shastry and G. Venkateswara Rao, 1986. Journal of Sound and Vibration 104, 524-527. Dynamic stability of columns with two symmetrically placed intermediate supports.

45. P.A.A. Laura, P. Verniere de Irassar and G.M. Ficcadenti, 1983. Journal of Sound and Vibration 86, 279-284. A note on transverse vibrations of continuous beams subject to an axial force and carrying concentrated masses.

46. R.G. Jacquot, 1976. Journal of Sound and Vibration 48, 421-424. On vibration of systems with mixed boundary conditions.

47. P.A.A. Laura, J.L. Pombo and E.A. Susemihl, 1974. Journal of Sound and Vibration 37, 161-168. A note on the vibrations of a clamped-free beam with a mass at the free end.

48. C.W.S. To, 1982. Journal of Sound and Vibration 83, 445-460. Vibration of a cantilever beam with a base excitation and tip mass.

49. B. Rama Bhat and H. Wagner, 1976. Journal of Sound and Vibration 45, 304-307. Natural frequencies of a uniform cantilever with a tip mass slender in the axial direction.

50. Rama Bhat and M. Avinash Kulkarni, 1976. AIAA Journal 14, 536-537. Natural frequencies of a cantilever with slender tip mass.

51. V.H. Cortinez and P.A.A. Laura, 1985. Journal of Sound and Vibration 99, 144-148. Vibrations and buckling of a non-uniform beam elastically restrained against rotation at one end and with concentrated mass at the other.

52. N.G. Stephen, 1985. Journal of Sound and Vibration 100, 149-150. Comments on "A note on the vibrations of restrained beams and rods with point masses".

53. P.A.A. Laura and V.H. Cortinez, 1985. Journal of Sound and Vibration 103, 596-599. Transverse vibrations of a cantilever beam carrying a concentrated mass at its free end and subjected to a variable axial force.

54. R.B. Bhat, 1986. Journal of Sound and Vibration 105, 199-210. Transverse vibrations of a rotating uniform cantilever beam with tip mass as predicted by using beam characteristic orthogonal polynomials in the Rayleigh-Ritz method.

55. M. Gürgöze, 1986. Journal of Sound and Vibration 105, 443-449. On the approximate determination of the fundamental frequency of a restrained cantilever beam carrying a tip heavy body.

56. J.C. Maltbaek, 1961. International Journal of Mechanical Sciences 3, 197-21[illegible]. The influence of a concentrated mass on the free vibrations of a uniform beam.

57. Y. Chen, 1963. Journal of Applied Mechanics 30, 310-311. On the vibration of beams or rods carrying a concentrated mass.

58. W.E. Baker, 1964. Journal of Applied Mechanics 31, 335-337. Vibration of frequencies for uniform beams with central masses.

59. R.P. Goel, 1973. Journal of Applied Mechanics 40, 821-822. Vibrations of a beam carrying a concentrated mass.

60. P.A.A. Laura and R.H. Gutierrez, 1986. Journal of Sound and Vibration 108, 123-131. Vibrations of an elastically restrained cantilever beam of varying cross section with tip mass of finite length.

61. P.A.A. Laura and V.H. Cortinez, 1986. Journal of Sound and Vibration 180, 346-348. Optimization of eigenvalues in the case of vibrating beams with point masses.

62. A.N. Kounadis, 1975. Journal of the Engineering Mechanics Division (ASCE) 101, 695-706. Dynamic response of cantilevers with attached masses.

63. A.N. Kounadis, 1976. Journal of the Engineering Mechanics Division (ASCE) 102, 370. Dynamic response of cantilevers with attached masses (Errata).

64. M. Gürgöze, 1984. Journal of Sound and Vibration 96, 461-468. A note on the vibrations of restrained beams and rods with point masses.

65. M. Gürgöze, 1985. Journal of Sound and Vibration 100, 588-589. On the vibrations of restrained beams and rods with heavy masses.

66. E. Krynicki and Z. Mazurkiewicz, 1962. Journal of Applied Mechanics 84, 497-501. Free Vibration of a simply supported bar with linearly variable height of cross section.

67. A.C. Heidebrecht, 1967. Journal of the Engineering Mechanics Division (ASCE) 93, EM2, 1-15. Vibration of non-uniform simply-supported beams.

68. H.C. Wang, 1967. Journal of Applied Mechanics 34, 702-708. Generalized hypergeometric function solutions on the transverse vibration of a class of nonuniform beams.

69. D.J. Sanger, 1968. Journal of Mechanical Engineering Science 10, 111-120. Transverse vibration of a class of non-uniform beams.

70. H.H. Mabie and C.B. Rogers, 1968. Journal of the Acoustical Society of America 44, 1739-1741. Transverse vibrations of tapered cantilever beams with end support.

71. H.H. Mabie and C.B. Rogers 1972. Journal of the Acoustical Society of America 51, 1771-1774. Transverse vibrations of double-tapered cantilever beams.

72. H.H. Mabie and C.B. Rogers, 1976. Journal of Engineering for Industry 98, 1335-1341. Technology transfer in the vibration analysis of linearly tapered cantilever beams.

73. F.W. Williams and J.R. Banerjee, 1985. Journal of Sound and Vibration 99, 121-138. Flexural vibration of axially loaded beams with linear or parabolic taper.

74. J.R. Banerjee and F.W. Williams, 1985. Journal of Sound and Vibration 102, 315-327. Further flexural vibration curves for axially loaded beams with linear or parabolic taper.

75. J.R. Banerjee and F.W. Williams, 1985. International Journal of Numerical Methods in Engineering 21, 2289-2302. Exact Bernoulli-Euler dynamic stiffness matrix for a range of tapered beams.

76. N.G. Stephen, 1982. Journal of Sound and Vibration 83, 585-587. Note on the combined use of Dunkerley's and Southwell's methods.

77. J.H. Lau, 1984 Journal of Applied Mechanics 51, 182-187. Vibration frequencies and mode shapes for a constrained cantilever.

78. M Gürgöze and H. Batan, 1986. Journal of Sound and Vibration 106, 533-536. A note on the vibrations of a restrained cantilever beam carrying a heavy tip body.

79. K.R. Chun, 1972. Journal of Applied Mechanics 39, 1154-1155. Free vibration of a beam with one end spring-hinged and the other free.

80. T.W. Lee, 1973. Journal of Applied Mechanics 40, 813-815. Vibration frequencies for a uniform beam with one end spring-hinged and carrying a mass at the other free end.

81. P.A.A. Laura, M.J. Maurizi and J.L. Pombo, 1975. Journal of Sound and Vibration 41, 397-405. A note on the dynamic analysis of an elastically restrained-free beam with a mass at the free end.

82. M.J. Maurizi, R.E. Rossi and J.A. Reyes, 1976. Journal of Sound and Vibration 48, 565-568. Vibration frequencies for a uniform beam with one end spring-hinged and subjected to a translational restraint at the other end.

83. R. Gelos and P.A.A. Laura, 1982. Journal of Sound and Vibration 83, 139-142. Vibrations of an elastically restrained-free beam with an intermediate support and carrying concentrated masses.

84. S. Alvarez and P.A.A. Laura, 1983. Journal of Sound and Vibration 86, 285-287. Fundamental frequency of an elastically restrained beam with discontinuous moment of inertia and an intermediate support.

85. C.N. Bapat and C. Bapat, 1987. Journal of Sound and Vibration 112, 177-182. Natural frequencies of a beam with non-classical boundary conditions and concentrated masses.

86. P. Vernière de Irassar, G.M. Ficcadenti and P.A.A. Laura, 1983. AIAA Journal 21, 312-314. Vibrations of nonuniform beams with one end elastically restrained against rotation.

87. R.P. Goel, 1976. Journal of Sound and Vibration 47, 1-7. Transverse vibrations of tapered beams.

88. A.S. Veletsos and N.M. Newmark, 1956. Journal of Applied Mechanics 23, 97-102. Determination of natural frequencies of continuous plates hinged along two opposite edges.

89. E.E. Ungar, 1961. Journal of Engineering for Industry 83, 434-440. Free oscillations of edge-connected simply supported plate systems.

90. V.V. Bolotin, 1961. Problems of Continuous Mechanics, 56-68 (Volume dedicated to N.I. Muskhelishvili). Philadelphia: SIAM. An asymptotic method for the study of the problem of eigenvalues for rectangular regions (English edition).

91. V.V. Bolotin, 1961. Inzhenernyi Zhurnal 3, 86-92. A generalization of the asymptotic method of the eigenvalue problems for rectangular region (in Russian).

92. V.N. Moskalenko and De-Lin Chen, 1965. Prikladnaya Mekhanika 1, 59-66. On the natural vibrations of multispan plates (in Russian).

93. S.M. Dickinson and G.B. Warburton, 1967. Journal of Mechanical Engineering Science 9, 318-324. Natural frequencies of plate systems using the edge effect method.

94. K. Vijayakumar, 1971. Journal of the Aeronautical Society of India 23, 197-204. A new method for analysis of flexural vibration of rectangular orthotropic plates.

95. I.B. Elishakoff, 1974. American Institute of Aeronautics and Astronautics Journal 12, 921-924. Vibration analysis of clamped square orthotropic plate.

96. I. Elishakoff and A. Sternberg, 1979. Journal of Applied Mechanics 46, 656-662. Eigenfrequencies of continuous plates with arbitrary number of equal spans.

97. S. Azimi, J.F. Hamilton and W. Soedel, 1984. Journal of Sound and Vibration 93, 9-29. The receptance method applied to the free vibration of coninuous rectangular plates.

98. E.H. Dill and K.S. Pister, 1958. Proceedings of the Third U.S. National Congress of Applied Mechanics, 123-132. Vibration of rectangular plates and plate systems.

99. S.M. Dickinson and G.W. Warburton, 1967. Journal of Mechanical Engineering Science 9, 325-335. Vibration of box-type structures.

100. S.M. Dickinson, 1969. Journal of Applied Mechanics 36, 101-106. The flexural vibration of rectangular orthotropic plates.

101. S.M. Dickinson, 1971. Journal of Applied Mechanics 38, 699-700. The flexural vibration of rectangular orthotropic plates subject to in-plane forces.

102. K. Takahashi and T.Chishaki, 1979. Journal of Sound and Vibration 62, 455-459. Free vibrations of two-way continuous rectangular plates.

103. S.C. Fan and Y.K. Cheung, 1984. Journal of Sound and Vibration 93, 81-94. Flexural free vibrations of rectangular plates with complex support conditions.

104. H.L. Cox and J. Boxer, 1960. Aeronautical Quarterly 11, 41-50. Vibration of rectangular plates point-supported at the corners.

105. R.E. Reed, Jr., 1965. NASA TND-3030 Comparison of methods in calculating frequencies of corner supported rectangular plates.

106. H.L. Cox, 1955. Journal of the Acoustical Society of America 27, 791-792. Vibration of a square plate, point supported at midpoints of sides.

107. D.J. Johns and R. Nataraja, 1972. Journal of Sound and Vibration 25, 75-82. Vibration of square plate symmetrically supported at four points.

108. G. Venkateswara Rao, 1975. Journal of Sound and Vibration 38, 271. Fundamental frequency of a square plate with multiple point supports on edges.

109. J. Drake, C.K. Kang and E.H. Dowell, 1973. AMS Report No. 1133, Princeton University. Free vibrations of a plate with varying number of supports.

110. W.K. Tso, 1966. American Institute of Aeronautics and Astronautics Journal 4, 733-735. On the fundamental frequency of a four point supported square elastic plate.

111. D.J. Johns and V.T. Nagaraj, 1969. Journal of Sound and Vibration 10, 404-410. On the fundamental frequency of a square plate symmetrically supported at four points.

112. E.H. Dowell, 1971. Journal of Applied Mechanics 38, 595-600. Free vibrations of a linear structure with arbitrary support conditions.

113. M. Petyt and W.H. Mirza, 1972. Journal of Sound and Vibration 21, 355-364. Vibration of column-supported floor slabs.

114. G. Venkateswara Rao, I.S. Raju and C.L. Amba-Rao, 1973. Journal of Sound and Vibration 29, 387-391. Vibrations of point supported plates.

115. G. Venkateswara Rao, C.L. Amba-Rao and T.V.G.K. Murphy, 1975. Journal of Sound and Vibration 40, 561-562. On the fundamental frequency of point supported plate.

116. I.S. Raju and C.L. Amba-Rao, 1983. Journal of Sound and Vibration 90, 291-297. Free vibrations of a square plate symmetrically supported at four points on the diagonals.

117. D.J. Gorman, 1981. Journal of Sound and Vibration 79, 561-574. An analytical solution for the free vibration analysis of rectangular plates resting on symmetrically distributed point supports.

118. Y. Narita, 1984. Journal of Sound and Vibration 93, 593-597. Note on vibrations of point supported rectangular plates.

119. J.G.M. Kerstens, 1979. Journal of Sound and Vibration 65, 493-504. Vibration of a rectangular plate supported at an arbitrary number of points.

120. J.G.M. Kerstens, 1981. Journal of Sound and Vibration 76, 467-480. Vibration of complex structures: the modal constraint method.

121. H.L. Cox, 1955. Quarterly Journal of Mechanics and Applied Mathematics, 8, 454-456. Vibration of certain square plates having similar adjacent edges.

122. J.G.M. Kerstens, P.A.A. Laura, R.O. Grossi and L. Ercoli, 1983. Journal of Sound and Vibration 89, 291-293. Vibrations of rectangular plates with point supports: comparison of results.

123. P.A.A. Laura, J.C. Utjes and G. Sánchez Sarmiento, 1984. Journal of Sound and Vibration 97, 176-178. Comments on "Flexural free vibrations of rectangular plates with complex support conditions".

124 P.A.A. Laura and V.H. Cortinez, 1985. Journal of Sound and Vibration 100, 456-458. Fundamental frequency of point-supported square plates carrying concentrated masses.

125. J.C. Utjés, P.A.A. Laura, G. Sánchez Sarmiento and R. Gelos, 1986. Applied Acoustics 19, 17-24. Vibrations of thin elastic plates with point-supports: a comparative study.

126. W. Nowacki, 1963. Dynamics of Elastic Systems. New York: John Wiley and Sons.

127. W. Nowacki, 1953. Archiwum Mechaniki Stosowanej 5, 437. Vibration and buckling of rectangular plates simply-supported at the periphery and at several points inside (in Polish).

128. H.T. Saliba, 1984. Journal of Sound and Vibration 94, 381-395. Free vibration analysis of rectangular cantilever plates with symmetrically distributed point supports along the edges.

129. Y. Narita, 1985. Journal of Sound and Vibration 102, 305-313. The effect of point constraints on transverse vibration of cantilever plates.

130. H. Carrington, 1925. Philosophical Magazine 50, 1261-1264. The frequencies of vibration of flat circular plates fixed at the circumference.

131. K. Itao and S.H. Crandall, 1979. Journal of Applied Mechanics 46, 448-453. Natural modes and natural frequencies of uniform, circular, free-edge plates.

132. A.W. Leissa and Y. Narita, 1980. Journal of Sound and Vibration 70, 221-229. Natural frequencies of simply supported circular plates.

133. T. Akasaka and T. Takagishi, 1958. Bulletin of the Japanese Society of Mechanical Engineers 1, 215-221. Vibration of corrugated diaphragm.

134. J. Mossakowski and K. Borsuk, 1960. Applied Mechanics (edited by A. Rolla and N. Koiter), 266-269. Buckling and vibrations of circular plates with cylindrical orthotropy. Amsterdam: Elsevier.

135. I.A. Minkara and W.H. Hoppmann, II, 1964. The Journal of the Acoustical Society of America 36, 470-475. Flexural vibrations of cylindrically aeolotropic circular plates.

136. K.A.V. Pandalai and S.A. Patel 1965. AIAA Journal 3, 780-781. Natural frequencies of orthotropic circular plates.

137. P.G. Kirmser, C.L. Huang and H.K. Woo, 1972. AIAA Journal 10, 1690-1691. Vibration of cylindrically orthotropic circular plates.

138. K. Singa Rao, K. Ganapathi and G. Venkateswara Rao, 1974. Journal of Sound and Vibration 36, 433-434. Vibration of cylindrically orthotropic circular plates.

139. G. Prathap and T.K. Varadan, 1976. AIAA Journal 14, 1639-1640. Axisymmetric vibrations of polar orthotropic circular plates.

140. D. Avalos, H. Hack and P.A.A. Laura, 1982. AIAA Journal 20, 1626-1628. Galerkin method and axisymmetric vibrations of polar-orthotropic circular plates.

141. R.Y. Bodine, 1959. Journal of Applied Mechanics 26, 666-668. The fundamental frequency of a thin, flat, circular plate simply supported along a circle of arbitrary radius.

142. R.Y. Bodine, 1967. The Journal of Acoustical Society of America 41, 1551. Vibration of a circular plate supported by a concentric ring of arbitrary radius.

143. A.V. Singh and S. Mirza, 1976. Journal of Sound and Vibration 48, 425-429. Free axisymmetric vibration of a circular plate elastically supported along two concentric circles.

144. P.A.A. Laura, R.H. Gutierrez, V.H. Cortinez and J.C. Utjes, 1987. Journal of Sound and Vibration 113, 81-86. Transverse vibrations of circular plates and membranes with intermediate supports.

145. V.X. Kunukkasseril and A.S.J. Swamidas, 1974. International Journal of Solids and Structures 10, 603-619. Vibration of continuous circular plates.

146. P.A.A. Laura and G.M. Ficcadenti, 1981. Journal of Sound and Vibration 77, 303-310. Transverse vibrations and elastic stability of circular plates of variable thickness and with non-uniform boundary conditions.

147. G.M. Ficcadenti and P.A.A. Laura, 1981. Journal of Sound and Vibration 78, 147-153. Fundamental frequency and buckling load of circular plates with variable profile and non-uniform boundary conditions.

148. P.A.A. Laura and B. Valerga de Greco, 1981. Journal of Sound and Vibration, 79, 306-310. A note on vibrations and elastic stability of circular plates with thickness varying in a bilinear fashion.

149. P.A.A. Laura, D.R. Avalos and C.D. Galles, 1982. Journal of Sound and Vibration 82, 151-156. Vibrations and elastic stability of polar orthotropic circular plates of linearly varying thickness.

150. S.M. Vogel and D.W. Skinner, 1965. Journal of Applied Mechanics 32, 926-931. Natural frequencies of transversely vibrating annular plates.

151. K. Vijayakumar and G.K. Ramaiah, 1972. Journal of Sound and Vibration 24, 165-175. On the use of a coordinate transformation for analysis of axisymmetric vibration of polar orthotropic annular plates.

152. G.K. Ramaiah and K. Vijayakumar, 1973. Journal of Sound and Vibration 26, 517-531. Natural frequencies of polar orthotropic annular plates.

153. Y. Narita, 1984. Journal of Sound and Vibration 92, 33-38. Natural frequencies of completely free annular and circular plates having polar orthotropy.

154. A.D. Lizarev, V.I. Klenov and N.B. Rostanina, 1977. Soviet Applied Mechanics 13, 694-699. Free vibrations of cylindrically anisotropic annular plates.

155. J.B. Greenberg and Y. Stavski, 1979. Journal of the Acoustical Society of America 66, 501-508. Flexural vibrations of certain full and annular composite orthotropic plates.

156. F. Ginesu, B. Picasso and P. Priolo, 1979. Journal of Sound and Vibration 65, 97-105. Vibration analysis of polar orthotropic annular discs.

157. D.G. Gorman, 1982. Journal of Sound and Vibration 80, 145-154. Natural frequencies of polar orthotropic uniform annular plates.

158. Y. Narita, 1984. Journal of Sound and Vibration 93, 503-511. Free vibration of continuous polar orthotropic annular and circular plates.

159. I.S. Raju, B. Prakasa Rao and G. Venkateswara Rao, 1974. Journal of Sound and Vibration 32, 507-512. Axisymmetric vibrations of linearly tapered annular plates.

160. S.R. Soni and C.L. Amba-Rao, 1975. Journal of Sound and Vibration 38, 465-473. Axisymmetric vibrations of annular plates of variable thickness.

161. U.S. Gupta and R. Lal, 1979. Journal of Sound and Vibration 64, 269-276. Axisymmetric vibrations of linearly tapered annular plates under an in-plane force.

162. R. Lal and U.S. Gupta, 1982. Journal of Sound and Vibration 83, 229-240. Axisymmetric vibrations of polar orthotropic annular plates of variable thickness.

163. N. Sankaranarayanan, K. Chandrasekaran and G. Ramaiyan, 1985. Journal of Sound and Vibration 99, 351-360. Axisymmetric vibrations of layered annular plates with linear variation in thickness.

164. U.S. Gupta, R. Lal and C.P. Verma, 1986. Journal of Sound and Vibration 104, 357-369. Buckling and vibrations of polar orthotropic annular plates of variable thickness.

165. D.G. Gorman, 1983. Journal of Sound and Vibration 86, 47-60. Natural frequencies of transverse vibration of polar orthotropic variable thickness annular plates.

166. H.D. Conway, E.C.H. Becker and J.F. Dubil, 1964. Journal of Applied Mechanics 31, 329-331. Vibration frequencies of tapered bars and circular plates.

167. T.A. Lenox and H.D. Conway, 1980. Journal of Sound and Vibration 68, 231-239. An exact, closed form, solution for the flexural vibration of a thin annular plate having a parabolic thickness variation.

168. R.V. Southwell, 1922. Proceedings of the Royal Society of London 101 (series A), 133-153. On the free transverse vibrations of a uniform circular disc clamped at its centre and on the effect of rotation.

169. R.C. Colwell and H.C. Hardy, 1937. Philosophical Magazine 24 (series 7), 1041-1055. The frequencies and nodal systems of circular plates.

170. I.E. Sakharov, 1959. Izv. An SSSR, OTN, Mekh. i Mashin., no. 5, 90-98. Dynamic stiffness in the theory of axisymmetric vibrations of circular and annular plates (in Russian).

171. R.A. Westmann, 1962. Journal of the Aerospace Sciences 29, 1139-1140. A note on free vibrations of triangular and sector plates.

172. R. Ramakrishnan and V.X. Kunukkasseril, 1973. Journal of Sound and Vibration 30, 127-129. Free vibration of annular sector plates.

173. J.F. Wilson and D.P. Garg, 1978. AIAA Journal 16, 270-272. Frequencies of annular plate and curved beam elements.

174. R. Ramakrishnan and V.X. Kunukkasseril, 1976. Journal of Sound and Vibration 44, 209-221. Free vibration of stiffened circular bridge decks.

175. G.K. Ramaiah and K. Vijayakumar, 1974. Journal of Sound and Vibration 34, 53-61. Natural frequencies of circumferentially truncated sector plates with simply supported straight edges.

176. M. Bem-Amoz, 1959. Journal of Applied Mechanics 26, 136-137. Note on deflections and flexural vibrations of clamped sectorial plates.

177. C. Rubin, 1975. Journal of Sound and Vibration 39, 523-526. Nodal circles and natural frequencies for the isotropic wedge.

178. A.P. Bhattacharya and K.N. Bhowmic, 1975. Journal of Sound and Vibration 41, 503-505. Free vibration of a sectorial plate.

179. Y.K. Cheung and M.S. Cheung, 1971. Journal of the Engineering Mechanics Division 97, 291-411. Flexural vibrations of rectangular and other polygonal plates.

180. H.B. Khurasia and S. Rawtani, 1979. Journal of Sound and Vibration 67, 307-313. Vibration analysis of circular segment shaped plates.

181. M.D. Waller, 1952. Proceedings of the Royal Society of London 211 (series A), 265-276. Vibrations of free plates: line symmetry; corresponding modes.

182. K. Maruyama and O. Ichinomiya, 1981. Journal of Sound and Vibration 74, 565-573. Experimental investigation of free vibrations of clamped sector plates.

183. M. Swaminadham, J. Danielski and O. Mahrenholtz, 1984. Journal of Sound and Vibration 95, 333-340. Free vibration analysis of annular sector plates by holographic experiments.

184. C. Rubin, 1975. Journal of the acoustical Society of America 58, 841-845. Vibrating modes for simply supported polar-orthotropic sector plates.

185. G.K. Ramaiah, 1980. Journal of Sound and Vibration 70, 589-596. Flexural vibrations of polar orthotropic sector plates with simply supported straight edges.

186. T. Irie, G. Yamada and F. Itao, 1979. Journal of Sound and Vibration 67, 89-100. Free vibration of polar-orthotropic sector plates.

187. M. Mukhopadhyay, 1979. Journal of Sound and Vibration 63, 87-95. A semi-analytic solution for free vibration of annular sector plates.

188. R.S. Srinivasan and V. Thiruvenkatachari, 1983. Journal of Sound and Vibration 89, 425-432. Free vibration of annular sector plates by an integral equation technique.

189. M. Mukhopadhyay, 1982. Journal of Sound and Vibration 80, 275-279. Free vibration of annular sector plates with edges possessing different degrees of rotational restraint.

190. R.S. Srinivasan and V. Thiruvenkatachari, 1986. Journal of Sound and Vibration 109, 89-96. Free vibration analysis of laminated annular sector plates.

191. Y. Naria, 1985. Journal of Vibration , Acoustics, Stress and Reliability in Design (Trans. ASME) 107, 334-338. Free vibration of polar-orthotropic sector plates resting on point supports.

192. T.S. Chichara, 1978. An Introduction to Orthogonal Polynomials. New York: Gordon and Breach.

193. M. Abramowitz and I.A. Stegun, 1972. Handbook of mathematical functions. New York: Dover.

194. P. Beckmann, 1973. Orthogonal Polynomials for Engineers and Physicists. Boulder, Colorado: Golem.

195. C.D. Mote, Jr., 1971. Journal of the Engineering Mechanics Division (ASCE) 97, 645-656. Nonconservative stability by finite element.

196. S.P. Timoshenko and J.M. Gere, 1961. Theory of Elastic Stability. New York: McGraw Hill.

197. PAFEC, PAFEC Limited, Strelley Hall, Strelley, Nottingham, England.

198. P.A.A. Laura and R.O. Grossi, 1978. Journal of Sound and Vibration 59, 355-368. Transverse vibration of a rectangular plate elastically restrained against rotation along three edges and free on the fourth edge.

199. R.O. Grossi and P.A.A. Laura, 1979. Ocean Engineering 6, 527-539. Transverse vibrations of rectangular, orthotropic plates with one or two free edges, while the remaining are elastically restrained against rotation.

200. M.E. McIntyre and J. Woodhouse, 1985. Journal of the Catgut Acoustical Society 43, 18-24. On measuring wood properties, part 2.

201. S.G. Lekhnitskii, 1968. Anisotropic plates. New York: Gordon and Breach.

202. R.F.S. Hearmon, 1961. An Introduction to Applied Anisotropic Elasticity. Oxford: Oxford University Press.

203. N.S. Sehmi, 1985. Journal of Sound and Vibration 100, 409-421. A Newtonian procedure for the solution of the Kron characteristic value problem.

204. C.S. Kim, 1986. Journal of Sound and Vibration 108, 166-167. Comment on "Natural frequencies of rectangular plates using characteristic orthogonal polynomials in Rayleigh-Ritz method".

205. C.E.S. Ueng and R.C. Nickels, Jr., 1978. International Journal of Solids and Structures 14, 571-578. Dynamic response of a structural panel by Bolotin's method.

206. S.M. Dickinson, 1978. International Journal of Solids and structures 15, 743-746. Comment on "Dynamic response of a structural panel by Bolotin's method".

207. T. Irie, G. Yamada and Y. Kobayashi, 1985. Journal of Sound and Vibration 102, 501-513. Free vibration of an oblique rectangular prismatic shell.

208. S.M. Dickinson, 1966. Ph.D. Thesis, The University of Nottingham. Flexural vibration of rectangular plate systems.

APPENDIX A

The values for displacement, slope, bending moment and shear force for beams with one end rotationally restrained-hinged and the other end translationally restrained (S_1=1, K_1 = 1)

x/ℓ	w	$\ell dw/dx$	$\ell^2 d^2w/dx^2$	$\ell^3 d^3w/dx^3$
(1) First mode: Ω = 2.3587				
0.00	0.00000	1.45515	1.45515	-3.01191
0.10	0.15229	1.58564	1.15534	-2.97015
0.20	0.31614	1.68650	0.86406	-2.84032
0.30	0.48864	1.75904	0.59040	-2.61678
0.40	0.66708	1.80549	0.34396	-2.29551
0.50	0.84898	1.82907	0.13465	-1.87389
0.60	1.03227	1.83399	-0.02743	-1.35060
0.70	1.21533	1.82550	-0.13207	-0.72534
0.80	1.39713	1.80983	-0.16911	0.00144
0.90	1.57730	1.79427	-0.12843	0.82892
1.00	1.75626	1.78707	0.00000	1.75626
(2) Second mode: Ω = 16.371				
0.00	0.00000	4.86767	4.86767	-104.02392
0.10	0.49388	4.83982	-5.31417	-97.39916
0.20	0.93571	3.84872	-14.18412	-78.01960
0.30	1.23779	2.08596	-20.57773	-48.49845
0.40	1.33683	-0.15716	-23.69962	-13.49456
0.50	1.20185	-2.53559	-23.29129	21.05795
0.60	0.83662	-4.70909	-19.71362	48.86124
0.70	0.27611	-6.40445	-13.93757	64.15174
0.80	-0.42317	-7.47256	-7.45259	62.41943
0.90	-1.19793	-7.93311	-2.11850	40.79158
1.00	-1.99655	-8.00338	0.00000	-1.99655
(3) Third mode: Ω = 50.935				
0.00	0.00000	-9.37655	-9.37655	543.35822
0.10	-0.89601	-7.69885	40.91981	423.45912
0.20	-1.40190	-1.94999	68.83847	112.83601
0.30	-1.24923	4.88589	61.84897	-245.97341
0.40	-0.50463	9.36590	23.76397	-483.25269
0.50	0.46687	9.21242	-26.90853	-487.82088
0.60	1.17918	4.37642	-66.04191	-263.76145
0.70	1.25610	-3.00446	-75.98903	68.21679
0.80	0.59974	-9.76765	-54.96807	323.66730
0.90	-0.59373	-13.50304	-19.56515	332.52571
1.00	-1.99584	-14.20275	0.00000	-1.99621
(4) Fourth mode: Ω = 105.22				
0.00	0.00000	13.78500	13.78513	-1591.99946
0.10	1.19468	7.82817	-120.77667	-874.59385
0.20	1.28817	-6.17881	-133.82199	631.34223
0.30	0.15824	-14.42335	-16.17393	1509.42438
0.40	-1.11932	-8.85873	117.55316	925.17418
0.50	-1.32106	5.16828	137.83511	-557.39835
0.60	-0.26217	14.08128	24.14157	-1517.51149
0.70	1.01468	9.07242	-116.43630	-1054.02258
0.80	1.21726	-5.67156	-155.08556	319.62029
0.90	-0.02342	-17.73306	-72.87852	1092.96656
1.00	-1.99728	-20.46833	-0.00035	-2.08498

(S_1 = 1, K_1 = 100)

x/ℓ	w	$\ell dw/dx$	$\ell^2 d^2w/dx^2$	$\ell^3 d^3w/dx^3$
(1) First mode: Ω = 9.6625				
0.00	0.00000	3.42798	3.42798	-42.64318
0.10	0.35286	3.55892	-0.78199	-41.00613
0.20	0.69817	3.28256	-4.66312	-36.07816
0.30	0.99739	2.64795	-7.89602	-28.11346
0.40	1.21843	1.73427	-10.20384	-17.69833
0.50	1.33838	0.64495	-11.38199	-5.67775
0.60	1.34554	-0.50065	-11.31941	6.94058
0.70	1.24055	-1.57724	-10.00935	19.09686
0.80	1.03643	-2.46407	-7.54882	29.79540
0.90	0.75763	-3.05486	-4.12649	38.21650
1.00	0.43815	-3.26586	0.00000	43.81513
(2) Second mode: Ω = 27.026				
0.00	0.00000	5.05721	5.05721	-166.06197
0.10	0.50364	4.74815	-10.92801	-147.47868
0.20	0.90104	2.99291	-23.30035	-95.10492
0.30	1.07088	0.30464	-29.23182	-21.44504
0.40	0.95486	-2.59627	-27.51779	54.30988
0.50	0.56942	-4.96977	-18.99541	111.42804
0.60	-0.00255	-6.25901	-6.42871	132.91723
0.70	-0.63884	-6.25691	6.08020	109.48952
0.80	-1.21820	-5.19779	13.95901	41.01762
0.90	-1.66535	-3.76004	13.02309	-65.17765
1.00	-1.99239	-2.99708	0.00000	-199.23907
(3) Third mode: Ω = 55.378				
0.00	0.00000	-9.13686	-9.13686	572.84960
0.10	-0.86624	-7.30297	43.50602	435.27785
0.20	-1.31918	-1.29926	70.67301	84.67652
0.30	-1.09851	5.51873	59.15596	-303.63927
0.40	-0.31386	9.43881	15.43354	-530.32622
0.50	0.61723	8.29237	-37.52801	-480.85703
0.60	1.18850	2.54522	-72.50370	-189.15589
0.70	1.06450	-5.03004	-72.85307	175.83243
0.80	0.23856	-10.97405	-42.39118	390.92464
0.90	-1.00556	-13.28599	-5.69065	279.17528
1.00	-2.33234	-13.14340	0.00000	-233.23468
(4) Fourth mode: Ω = 107.22				
0.00	0.00000	13.71309	13.71328	-1612.55225
0.10	1.18412	7.66659	-122.11404	-872.69561
0.20	1.25672	-6.39971	-133.07781	667.68305
0.30	0.11477	-14.38140	-11.85626	1533.96430
0.40	-1.13511	-8.35324	121.46621	888.61965
0.50	-1.27527	5.78868	135.51576	-634.94621
0.60	-0.17822	14.11581	15.47358	-1551.75545
0.70	1.05699	8.22914	-123.63973	-989.27427
0.80	1.15318	-6.79293	-152.69874	427.46231
0.90	-0.17194	-18.17796	-63.39504	1101.72501
1.00	-2.14951	-20.25330	-0.00044	-215.06018

(S_1 = 1, K_1 = 10000)

x/ℓ	w	$\ell dw/dx$	$\ell^2 d^2w/dx^2$	$\ell^3 d^3w/dx^3$
(1) First mode: Ω = 10.704				
0.00	0.00000	3.90783	3.90783	-54.63656
0.10	0.40125	4.02733	-1.47986	-52.34944
0.20	0.78809	3.62715	-6.40926	-45.49822
0.30	1.11159	2.77545	-10.44186	-34.53485
0.40	1.33172	1.58103	-13.21089	-20.42465
0.50	1.42102	0.18388	-14.46680	-4.52256
0.60	1.36699	-1.25833	-14.10847	11.58587
0.70	1.17319	-2.58588	-12.19746	26.26370
0.80	0.85852	-3.65326	-8.95398	38.00398
0.90	0.45513	-4.34407	-4.73545	45.59504
1.00	0.00483	-4.58306	0.00000	48.25267
(2) Second mode: Ω = 40.236				
0.00	0.00000	8.22387	8.22387	-383.08450
0.10	0.80077	7.18652	-27.86237	-316.85990
0.20	1.33360	3.07610	-51.35468	-138.50280
0.30	1.37065	-2.37847	-53.93998	87.80810
0.40	0.88654	-6.98665	-35.05315	276.78051
0.50	0.06371	-8.92004	-2.28024	356.32693
0.60	-0.78108	-7.40892	31.49379	296.20605
0.70	-1.32132	-3.03437	53.04193	120.08182
0.80	-1.34873	2.50059	53.90476	-103.56893
0.90	-0.85506	7.03315	33.64989	-288.11578
1.00	-0.03626	8.77814	0.00000	-362.63639
(3) Third mode: Ω = 88.950				
0.00	0.00000	-12.52850	-12.52846	1232.54377
0.10	-1.11827	-8.02652	94.58981	759.94679
0.20	-1.36234	3.56216	119.27442	-298.99200
0.30	-0.50090	12.38932	43.80066	-1095.19230
0.40	0.76646	11.05776	-68.50273	-981.22844
0.50	1.39785	0.62176	-124.54848	-55.16806
0.60	0.87323	-10.32611	-77.96776	916.55552
0.70	-0.37519	-12.76944	32.71223	1129.93272
0.80	-1.32051	-4.73095	115.79981	405.29547
0.90	-1.19239	7.05733	101.81689	-667.74679
1.00	-0.12252	12.61900	0.00002	-1225.22123
(4) Fourth mode: Ω = 156.18				
0.00	0.00000	16.72068	16.73626	-2824.05108
0.10	1.31883	5.93121	-201.18379	-986.26494
0.20	0.88008	-13.57986	-136.16851	2103.56947
0.30	-0.74914	-14.67594	117.38504	2287.14529
0.40	-1.34964	4.26628	210.87099	-668.12486
0.50	-0.10187	17.35106	15.85183	-2711.28614
0.60	1.28476	6.67048	-200.95659	-1045.93294
0.70	0.90972	-13.18183	-143.17588	2045.02153
0.80	-0.72160	-15.12936	108.85579	2314.74156
0.90	-1.40386	3.14875	205.85285	-659.30439
1.00	-0.29943	15.43063	-0.01606	-2998.16786

(S_1 = 100, K_1 = 1)

x/ℓ	w	$\ell dw/dx$	$\ell^2 d^2w/dx^2$	$\ell^3 d^3w/dx^3$
(1) First mode: Ω = 3.9758				
0.00	0.00000	0.07043	7.04339	-10.52190
0.10	0.04051	0.72218	5.99184	-10.49847
0.20	0.14094	1.26903	4.94748	-10.36227
0.30	0.29086	1.71243	3.92604	-10.02683
0.40	0.48009	2.05578	2.95111	-9.42203
0.50	0.69888	2.30519	2.05245	-8.49350
0.60	0.93830	2.46996	1.26453	-7.20171
0.70	1.19048	2.56304	0.62510	-5.52043
0.80	1.44907	2.60125	0.17393	-3.43473
0.90	1.70959	2.60546	-0.04815	-0.93830
1.00	1.96986	2.60063	0.00000	1.96986
(2) Second mode: Ω = 21.712				
0.00	0.00000	0.41095	41.09511	-204.28622
0.10	0.21256	3.50132	20.77148	-200.48974
0.20	0.63371	4.60028	1.53163	-180.97304
0.30	1.07265	3.90735	-14.71443	-140.47809
0.40	1.36865	1.82480	-25.96100	-82.11282
0.50	1.41039	-1.07181	-30.85669	-15.46662
0.60	1.14905	-4.12732	-29.22397	46.06549
0.70	0.59995	-6.73833	-22.28856	88.31926
0.80	-0.16970	-8.49250	-12.61208	99.15042
0.90	-1.06616	-9.28841	-3.78526	70.33101
1.00	-2.00467	-9.41740	0.00000	-2.00467
(3) Third mode: Ω = 60.603				
0.00	0.00000	-1.11643	-111.64337	935.99315
0.10	-0.51470	-7.64728	-20.14990	861.43048
0.20	-1.24687	-5.78914	51.80395	532.08857
0.30	-1.49864	1.21810	79.50322	6.20099
0.40	-1.00044	8.32469	54.53981	-474.71440
0.50	0.01309	10.93415	-5.53445	-664.10923
0.60	0.97162	7.23045	-65.29683	-471.84681
0.70	1.30626	-0.97518	-91.33705	-28.20530
0.80	0.76658	-9.49301	-72.14954	378.72045
0.90	-0.47186	-14.51038	-26.98783	448.23480
1.00	-1.99490	-15.48502	-0.00001	-1.99671
(4) Fourth mode: Ω = 118.77				
0.00	0.00000	2.12300	212.30001	-2565.90219
0.10	0.85208	10.84745	-29.82576	-2066.59659
0.20	1.50498	0.10125	-154.78478	-274.08361
0.30	0.78105	-13.38464	-84.81091	1500.51235
0.40	-0.70242	-13.38141	85.80146	1556.04934
0.50	-1.40715	0.66885	167.02838	-100.48540
0.60	-0.60063	13.78901	68.61843	-1674.11844
0.70	0.82411	11.72479	-106.78234	-1491.84099
0.80	1.27380	-3.93680	-178.03181	175.43364
0.90	0.08606	-18.30036	-89.82576	1305.80631
1.00	-1.99332	-21.70789	-0.00040	-2.09805

(S_1 = 100, K_1 = 100)

x/ℓ	w	$\ell dw/dx$	$\ell^2 d^2w/dx^2$	$\ell^3 d^3w/dx^3$
(1) First mode: Ω = 13.056				
0.00	0.00000	0.22201	22.20056	-81.44609
0.10	0.11964	2.03529	14.07687	-80.68395
0.20	0.38022	3.04458	6.17713	-76.56679
0.30	0.70312	3.29249	-1.06566	-67.36816
0.40	1.01536	2.87137	-7.11133	-52.65238
0.50	1.25992	1.92778	-11.43447	-33.11643
0.60	1.39093	0.65574	-13.62601	-10.34116
0.70	1.38764	-0.71877	-13.46573	13.53730
0.80	1.25166	-1.95893	-10.95901	36.20966
0.90	1.00787	-2.83976	-6.33409	55.59397
1.00	0.70216	-3.16866	0.00000	70.21619
(2) Second mode: Ω = 31.171				
0.00	0.00000	0.46300	46.30028	-275.83297
0.10	0.23192	3.71912	18.95709	-267.20105
0.20	0.65535	4.33262	-5.97852	-224.58660
0.30	1.02428	2.73472	-24.59319	-141.68195
0.40	1.15550	-0.25822	-33.45203	-33.34572
0.50	0.96147	-3.58681	-31.35138	72.21080
0.60	0.46163	-6.22214	-20.16000	143.49176
0.70	-0.23612	-7.47254	-4.64525	155.46154
0.80	-0.98226	-7.22842	8.53700	96.06435
0.90	-1.65095	-6.08193	12.24177	-32.80819
1.00	-2.21057	-5.31286	0.00000	-221.05683
(3) Third mode: Ω = 64.271				
0.00	0.00000	-1.12437	-112.43744	972.89067
0.10	0.51343	-7.55614	-17.52335	888.94543
0.20	-1.21997	-5.34842	55.55429	523.11711
0.30	-1.41234	1.91232	80.09223	-45.88578
0.40	-0.85149	8.77952	48.97996	-537.38375
0.50	0.17040	10.56901	-15.65971	-684.30245
0.60	1.04138	5.87154	-73.79169	-417.69578
0.70	1.20945	-2.80552	-91.39774	77.34998
0.80	0.50414	-10.80479	-62.13337	459.03500
0.90	-0.80586	-14.58047	-14.15948	409.68774
1.00	-2.28537	-14.78660	-0.00001	-228.53924
(4) Fourth mode: Ω = 120.53				
0.00	0.00000	2.12771	212.77053	-2592.38467
0.10	0.85067	10.77682	-31.56363	-2078.29463
0.20	1.48751	-0.13514	-155.64700	-244.08626
0.30	0.74181	-13.51421	-81.62821	1540.82963
0.40	-0.73357	-13.06019	90.69828	1541.31654
0.50	-1.38720	1.28680	167.01795	-176.34603
0.60	-0.53198	14.01912	61.24355	-1727.69252
0.70	0.87369	11.10338	-114.70298	-1443.59776
0.80	1.23356	-4.96132	-177.11450	285.06481
0.90	-0.03540	-18.76495	-81.06418	1324.64438
1.00	-2.12257	-21.54228	-0.00052	-212.39379

(S_1 = 100, K_1 = 10000)

x/ℓ	w	$\ell dw/dx$	$\ell^2 d^2w/dx^2$	$\ell^3 d^3w/dx^3$
(1) First mode: Ω = 15.104				
0.00	0.00000	0.28893	28.89315	-116.73043
0.10	0.15392	2.59538	17.25634	-115.41314
0.20	0.48070	3.75256	6.00351	-108.39379
0.30	0.86844	3.83287	-4.14116	-93.01887
0.40	1.21642	2.99022	-12.31231	-69.07593
0.50	1.44357	1.46245	-17.73157	-38.44199
0.60	1.49615	-0.44699	-19.89096	-4.54450
0.70	1.35264	-2.40272	-18.67463	28.32453
0.80	1.02495	-4.07976	-14.40770	55.76548
0.90	0.55512	-5.20686	-7.82968	74.00429
1.00	0.00805	-5.60378	0.00000	80.50410
(2) Second mode: Ω = 48.804				
0.00	0.00000	0.90308	90.30770	-674.99437
0.10	0.42979	6.58353	23.92921	-635.07250
0.20	1.10757	6.03975	-31.73048	-450.84452
0.30	1.48982	1.10444	-61.62208	-131.61409
0.40	1.28501	-5.12596	-57.22843	211.32700
0.50	0.53305	-9.34345	-23.34368	436.29024
0.60	-0.44192	-9.38063	22.78252	447.22123
0.70	-1.19768	-5.12886	58.82829	243.45075
0.80	-1.38855	1.45722	67.49614	-77.72882
0.90	-0.93158	7.29442	44.40894	-365.71983
1.00	-0.04871	9.61681	0.00000	-487.11418
(3) Third mode: Ω = 101.31				
0.00	0.00000	-1.81077	-181.07624	2005.96159
0.10	-0.75584	-10.09209	10.39265	1688.54369
0.20	-1.47215	-2.30354	124.95174	476.78163
0.30	-1.06137	10.06928	98.67468	-931.27546
0.40	0.24813	13.96456	-28.40546	-1382.60126
0.50	1.29401	5.18955	-132.37625	-514.86500
0.60	1.12309	-8.30466	-114.48319	842.96693
0.70	-0.09980	-14.05590	9.21264	1418.14198
0.80	-1.23885	-6.78825	123.42387	667.89668
0.90	-1.24617	6.59646	120.68222	-723.90611
1.00	-0.14987	13.28602	-0.00011	-1498.70656
(4) Fourth mode: Ω = 171.87				
0.00	0.00000	2.96032	296.05951	-4396.29422
0.10	1.06143	11.52877	-102.64537	-3027.73348
0.20	1.34980	-7.58440	-210.48584	1021.37130
0.30	-0.15113	-18.26865	31.76546	3064.01691
0.40	-1.36906	-2.56781	236.84657	420.37129
0.50	-0.53670	16.73930	92.58053	-2883.52156
0.60	1.09671	11.10123	-188.69979	-1913.84695
0.70	1.09809	-11.09349	-189.87848	1891.08106
0.80	-0.54412	-16.95949	89.16144	2857.36030
0.90	-1.42154	1.80251	228.15055	-522.10648
1.00	-0.34936	15.74608	-0.03349	-3501.60376

(S_1 = 10000, K_1 = 1)

x/ℓ	w	$\ell dw/dx$	$\ell^2 d^2w/dx^2$	$\ell^3 d^3w/dx^3$
(1) First mode: Ω = 4.0395				
0.00	0.00000	0.00073	7.31351	-10.85256
0.10	0.03483	0.67783	6.22874	-10.83335
0.20	0.13196	1.24669	5.15050	-10.70501
0.30	0.28060	1.70866	4.09449	-10.37470
0.40	0.47024	2.06712	3.08482	-9.76699
0.50	0.69078	2.32819	2.15231	-8.82332
0.60	0.93294	2.50135	1.33280	-7.50095
0.70	1.18855	2.59983	0.66570	-5.77144
0.80	1.45099	2.64095	0.19264	-3.61851
0.90	1.71555	2.64625	-0.04364	-1.03513
1.00	1.97990	2.64155	0.00000	1.97990
(2) Second mode: Ω = 22.121				
0.00	0.00000	0.00441	44.08161	-211.25985
0.10	0.18567	3.35793	23.03725	-208.08438
0.20	0.60249	4.64402	2.99553	-189.32317
0.30	1.05174	4.05557	-14.08526	-148.60535
0.40	1.36440	1.99739	-26.07609	-88.64489
0.50	1.42183	-0.93921	-31.49564	-19.27033
0.60	1.17006	-4.07237	-30.08494	45.42898
0.70	0.62217	-6.76778	-23.07045	90.38266
0.80	-0.15392	-8.58685	-13.10504	102.58220
0.90	-1.06171	-9.41497	-3.94639	73.17451
1.00	-2.01329	-9.54964	0.00000	-2.01329
(3) Third mode: Ω = 61.717				
0.00	0.00000	-0.01233	-123.28295	968.52217
0.10	-0.45681	-7.53221	-28.08795	905.36389
0.20	-1.20930	-6.22802	48.79685	583.74008
0.30	-1.51170	0.72202	81.11955	43.17159
0.40	-1.05004	8.12716	58.37572	-468.49527
0.50	-0.03734	11.10042	-2.55340	-685.14256
0.60	0.94861	7.56742	-64.98748	-500.27703
0.70	1.31411	-0.73337	-93.31388	-42.74402
0.80	0.78721	-9.48534	-74.49500	385.46976
0.90	-0.46043	-14.67971	-28.02436	464.23595
1.00	-2.00323	-15.69287	-0.00001	-2.00536
(4) Fourth mode: Ω = 120.89				
0.00	0.00000	0.02415	241.48564	-2658.08258
0.10	0.77097	11.12354	-12.79482	-2229.18301
0.20	1.50746	1.19656	-155.49670	-439.54729
0.30	0.86643	-12.99791	-95.93683	1472.08847
0.40	-0.61225	-13.99616	79.07543	1655.76572
0.50	-1.41403	-0.07567	170.94609	-12.62742
0.60	-0.65178	13.70882	76.14993	-1693.66314
0.70	0.79561	12.15901	-105.01107	-1569.41694
0.80	1.28561	-3.66651	-182.21906	147.81854
0.90	0.10273	-18.45476	-92.97994	1345.03103
1.00	-2.00120	-21.98777	-0.00036	-2.09884

(S_1 = 10000, K_1 = 100)

x/ℓ	w	$\ell dw/dx$	$\ell^2 d^2w/dx^2$	$\ell^3 d^3w/dx^3$
(1) First mode: Ω = 13.251				
0.00	0.00000	0.00234	23.36234	-83.36503
0.10	0.10316	1.92207	15.04178	-82.74021
0.20	0.35689	3.01717	6.92439	-78.86113
0.30	0.68039	3.32804	-0.55614	-69.79898
0.40	0.99933	2.94575	-6.84264	-54.99458
0.50	1.25130	2.01781	-11.38424	-35.09762
0.60	1.39125	0.74182	-13.74508	-11.70854
0.70	1.39578	-0.65018	-13.68286	12.96612
0.80	1.26552	-1.91345	-11.18954	36.51798
0.90	1.02521	-2.81433	-6.49020	56.76306
1.00	0.72149	-3.15167	0.00000	72.14894
(2) Second mode: Ω = 31.535				
0.00	0.00000	0.00498	49.82727	-282.85242
0.10	0.20256	3.57721	21.72589	-275.74003
0.20	0.62411	4.42092	-4.18048	-235.32829
0.30	1.00902	2.94733	-23.91309	-152.88939
0.40	1.16310	-0.03114	-33.80656	-42.39871
0.50	0.98865	-3.43398	-32.41018	67.43080
0.60	0.49821	-6.19078	-21.44770	143.65932
0.70	-0.20264	-7.56190	-5.70697	159.49504
0.80	-0.96225	-7.40030	7.97071	101.42985
0.90	-1.65011	-6.28545	12.14236	-29.40997
1.00	-2.23019	-5.51688	0.00000	-223.01874
(3) Third mode: Ω = 65.341				
0.00	0.00000	-0.01244	-124.41629	1005.76463
0.10	-0.45635	-7.46376	-25.70431	934.82291
0.20	-1.18630	-5.82138	52.58625	578.11034
0.30	-1.43197	1.40180	82.04040	-6.86098
0.40	-0.90723	8.60617	53.20511	-532.15764
0.50	0.11791	10.78892	-12.51589	-708.52500
0.60	1.02194	6.26197	-73.64229	-448.93935
0.70	1.22504	-2.53686	-93.70711	62.33530
0.80	0.53355	-10.80187	-64.74300	467.39107
0.90	-0.78715	-14.77183	-15.27653	427.35901
1.00	-2.28880	-14.98883	-0.00001	-228.88349
(4) Fourth mode: Ω = 122.63				
0.00	0.00000	0.02422	242.19107	-2684.92663
0.10	0.77016	11.06729	-14.42848	-2243.50436
0.20	1.49204	0.96972	-156.55972	-412.14679
0.30	0.82891	-13.14493	-93.02265	1513.93928
0.40	-0.66436	-13.70564	84.01695	1644.96738
0.50	-1.39728	0.53301	171.27224	-87.30547
0.60	-0.58558	13.96180	69.01336	-1750.04383
0.70	0.84570	11.56822	-113.01493	-1523.97576
0.80	1.24817	-4.67786	-181.51349	257.79596
0.90	-0.01552	-18.92190	-84.29830	1365.53412
1.00	-2.12766	-21.82686	-0.00049	-212.89708

(S_1 = 10000, K_1 = 10000)

x/ℓ	w	$\ell dw/dx$	$\ell^2 d^2w/dx^2$	$\ell^3 d^3w/dx^3$
(1) First mode: Ω = 15.393				
0.00	0.00000	0.00307	30.73794	-120.71736
0.10	0.13389	2.47385	18.69429	-119.61906
0.20	0.45499	3.75324	7.00479	-112.89517
0.30	0.84705	3.91102	-3.59277	-97.50090
0.40	1.20485	3.10145	-12.19035	-73.03203
0.50	1.44312	1.56763	-17.95711	-41.35850
0.60	1.50465	-0.37671	-20.33987	-6.05715
0.70	1.36574	-2.38231	-19.19753	28.34965
0.80	1.03755	-4.10910	-14.85698	57.16256
0.90	0.56282	-5.27235	-8.08730	76.35185
1.00	0.00832	-5.68243	0.00000	83.19912
(2) Second mode: Ω = 49.703				
0.00	0.00000	0.00989	98.94791	-698.10625
0.10	0.37969	6.43223	30.01624	-864.41980
0.20	1.06756	6.33824	-28.91146	-485.40565
0.30	1.48809	1.51737	-62.04402	-159.70178
0.40	1.31841	-4.87038	-59.66773	200.22396
0.50	0.57877	-9.35479	-25.92847	443.87447
0.60	-0.40840	-9.59002	21.58448	465.41003
0.70	-1.18800	-5.36540	59.44597	259.45904
0.80	-1.39718	1.34512	69.16370	-73.78466
0.90	-0.94302	7.34497	45.76662	-375.29576
1.00	-0.05030	9.74053	0.00000	-502.96292
(3) Third mode: Ω = 103.10				
0.00	0.00000	-0.02042	-204.24155	2075.87966
0.10	-0.67985	-10.21604	-3.89449	1804.56495
0.20	-1.45903	-3.21828	123.62373	603.91991
0.30	-1.12765	9.55127	106.54226	-886.30884
0.40	0.17234	14.27818	-21.32217	-1436.78151
0.50	1.[illegible]7376	5.86049	-132.70224	-592.30719
0.60	1.15714	-7.97828	-120.04111	824.48653
0.70	-0.06086	-14.25503	5.35032	1463.74913
0.80	-1.23060	-7.11467	124.72687	712.92422
0.90	-1.25847	6.54533	123.95661	-733.24973
1.00	-0.15466	13.43139	-0.00015	-1546.60763
(4) Fourth mode: Ω = 174.78				
0.00	0.00000	0.03435	343.50442	-4553.98096
0.10	0.97490	12.33381	-78.83819	-3366.42414
0.20	1.40343	-6.16978	-220.88[illegible]	755.42802
0.30	-0.03773	-18.62664	13.09479	3169.72254
0.40	-1.35645	-3.86929	238.79699	652.85413
0.50	-0.61287	16.48663	107.49628	-2888.62246
0.60	1.05850	11.91442	-185.20163	-2088.48293
0.70	1.13208	-10.67984	-199.02817	1850.67775
0.80	-0.51281	-17.33578	85.15710	2970.42193
0.90	-1.42964	1.54581	233.09201	-492.34580
1.00	-0.36045	15.85745	-0.03782	-3613.63813

APPENDIX B

EQUATIONS FOR POLAR ORTHOTROPIC PLATES

Though several researchers have used the strain energy expression for polar orthotropic plates, the full derivation of the expression is not readily available in the literature, while that for rectangular orthotropic plates is present in various books treating thin plate theory. In this appendix, a reasonably rigorous derivation in terms of the cylindrical coordinates (r, θ, z) is presented for the energy and related bending moments, shear force, etc..

The assumptions involved in the classical thin plate theory are [quoted from reference B1]:

(i) points which lie on a normal to the mid-plane of the undeflected plate lie on a normal to the mid-plane of the deflected plate;

(ii) the stresses normal to the mid-plane of the plate, arising from the applied loading, are negligible in comparison with the stresses in the plane of the plate;

(iii) the slope of the deflected plate in any direction is small so that its square may be neglected in comparison with unity;

(iv) the mid-plane of the plate is a 'neutral plane', i.e. any mid-plane stresses arising from the deflection of the plate into a non-developable surface may be ignored.

It may be noted that, the assumptions have, as mentioned in reference [B1], their counterparts in the slender beam theory; for example, assumption (i) corresponds to the dual assumptions in the beam theory that 'plane cross sections remain plane' and 'deflections due to shear may be neglected'.

Now consider an annular sectorial element cut out of the plate by two adjacent axial planes forming an angle $d\theta$ and by two cylindrical surfaces of radii r and r+dr, respectively, and of uniform thickness h in z-direction, as shown in Figure B1(a). The bending moments and shear forces per unit length acting on the element are also shown in the figure.

Applying the assumption (ii), the strain-stress relationships (Hooke's law) in terms of plane polar coordinates are given by the equations

$$\varepsilon_r = (\sigma_r - \nu_{r\theta}\sigma_\theta)/E_r,$$

$$\varepsilon_\theta = (\sigma_\theta - \nu_{\theta r}\sigma_r)/E_\theta, \qquad \text{(B1)}$$

$$\gamma_{r\theta} = \tau_{r\theta}/G_{r\theta}.$$

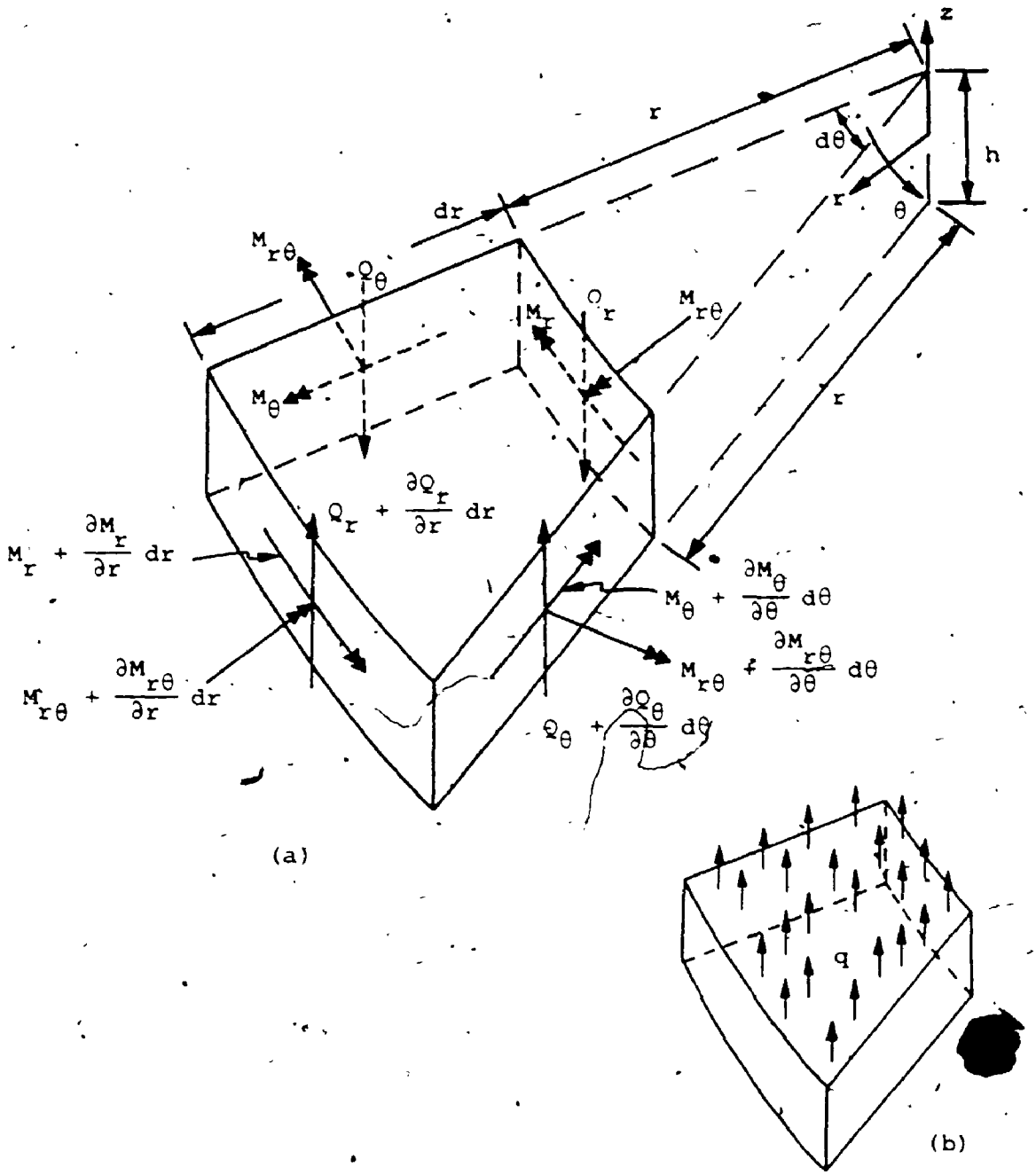

Figure B1. An annular sectional element. The direction of the moments (double head arrows) are defined by the conventional 'right-hand rule'.

Here, σ_r and σ_θ are normal stresses in radial r- and tangential θ-directions, respectively, $\tau_{r\theta}$ shear stress, ϵ_r and ϵ_θ normal strains, $\gamma_{r\theta}$ shear strain, E_r and E_θ Young's moduli, $G_{r\theta}$ shear modulus, and $\nu_{r\theta}$ and $\nu_{\theta r}$ Poisson's ratios ($E_r \nu_{\theta r} = E_\theta \nu_{r\theta}$).

On the basis of the assumption (i), the deflections u and v in r- and θ-directions at a distance z from the mid-plane (From assumption (iv), the mid-plane is a neutral plane) are given [B2]

$$u = - z \frac{\partial w}{\partial r}, \qquad v = - \frac{z}{r} \frac{\partial w}{\partial \theta}, \tag{B2}$$

where $w = w(r, \theta)$ denotes an arbitrary small deflection of the mid-plane in z-direction.

Applying the assumption (iii), the linearized strain-displacement equations are given as [B3]:

$$\begin{aligned} \epsilon_r &= \frac{\partial u}{\partial r}, \\ \epsilon_\theta &= \frac{1}{r} \frac{\partial v}{\partial \theta} + \frac{u}{r}, \\ \gamma_{r\theta} &= \frac{1}{r} \frac{\partial u}{\partial \theta} + \frac{\partial v}{\partial r} - \frac{v}{r}. \end{aligned} \tag{B3}$$

Utilizing the strain-stress relationships (B1), kinematic relationships (B2) and strain-displacement relationships (B3), which are based on the assumptions for thin plate theory, the equations for strain energy, bending

moments, shear forces etc. are derived.

Equations (B1) can be rewritten as

$$\sigma_r = E_r'\varepsilon_r + E_\theta'\nu_{r\theta}\varepsilon_\theta,$$

$$\sigma_\theta = E_\theta'\varepsilon_\theta + E_r'\nu_{\theta r}\varepsilon_r, \qquad \text{(B4)}$$

$$\tau_{r\theta} = G_{r\theta}\gamma_{r\theta},$$

where $E_r' = E_r/(1-\nu_{r\theta}\nu_{\theta r})$ and $E_\theta' = E_\theta/(1-\nu_{r\theta}\nu_{\theta r})$.

Substitution of equations (B2) into (B3) yields

$$\varepsilon_r = -z\frac{\partial^2 w}{\partial r^2},$$

$$\varepsilon_\theta = -z\left(\frac{1}{r^2}\frac{\partial^2 w}{\partial\theta^2} + \frac{1}{r}\frac{\partial w}{\partial r}\right), \qquad \text{(B5)}$$

$$\gamma_{r\theta} = -2z\frac{\partial}{\partial r}\left(\frac{1}{r}\frac{\partial w}{\partial\theta}\right).$$

The strain energy stored in the plate during elastic deformation is given by

$$V = \tfrac{1}{2}\int_{Vol}(\sigma_r\varepsilon_r + \sigma_\theta\varepsilon_\theta + \tau_{r\theta}\gamma_{r\theta})d(Vol), \qquad \text{(B6)}$$

where the integral is taken over the volume of the plate. Substituting equations (B4) into (B6), recalling $E_r\nu_{\theta r} = E_\theta\nu_{r\theta}$, yields

$$V = \tfrac{1}{2}\int_{Vol}(E_r'\varepsilon_r^2 + 2E_r'\nu_{\theta r}\varepsilon_r\varepsilon_\theta + E_\theta'\varepsilon_\theta^2 + G_{r\theta}\gamma_{r\theta}^2)d(Vol). \qquad \text{(B7)}$$

Further, substituting equations (B5) into (B7), the strain energy can be expressed as

$$V = \tfrac{1}{2}\int_{Vol}[E_r' z^2(\frac{\partial^2 w}{\partial r^2})^2 + 2E_r' \nu_{\theta r} z^2(\frac{\partial^2 w}{\partial r^2})(\frac{1}{r^2}\frac{\partial^2 w}{\partial \theta^2} + \frac{1}{r}\frac{\partial w}{\partial r})$$

$$+ E_\theta' z^2(\frac{1}{r^2}\frac{\partial^2 w}{\partial \theta^2} + \frac{1}{r}\frac{\partial w}{\partial r})^2 + G_{r\theta}(4z^2)\{\frac{\partial}{\partial r}(\frac{1}{r}\frac{\partial w}{\partial \theta})\}^2]d(Vol)$$

$$= \tfrac{1}{2}\int_{Area}[D_r(\frac{\partial^2 w}{\partial r^2})^2 + 2D_r\nu_{\theta r}(\frac{\partial^2 w}{\partial r^2})(\frac{1}{r}\frac{\partial w}{\partial r} + \frac{1}{r^2}\frac{\partial^2 w}{\partial \theta^2}) \qquad \text{(B8)}$$

$$+ D_\theta(\frac{1}{r}\frac{\partial w}{\partial r} + \frac{1}{r^2}\frac{\partial^2 w}{\partial \theta^2})^2 + 4D_{r\theta}\{\frac{\partial}{\partial r}(\frac{1}{r}\frac{\partial w}{\partial \theta})\}^2]d(Area),$$

where $D_r = E_r h^3/12(1-\nu_{r\theta}\nu_{\theta r})$, $D_\theta = E_\theta h^3/12(1-\nu_{r\theta}\nu_{\theta r})$ and $D_{r\theta} = G_{r\theta}h^3/12$. Here, the integration

$$\int_{-h/2}^{h/2} z^2 dz = \frac{h^3}{12}$$

is used.

The moment-curvature relations are obtained by integrating the inplane stresses over the plate thickness, using equations (B4) and (B5):

$$M_r = \int_{-h/2}^{h/2}\sigma_r z dz = -D_r\{\frac{\partial^2 w}{\partial r^2} + \nu_{\theta r}(\frac{1}{r}\frac{\partial w}{\partial r} + \frac{1}{r^2}\frac{\partial^2 w}{\partial \theta^2})\},$$

$$M_\theta = \int_{-h/2}^{h/2}\sigma_\theta z dz = -D_\theta(\frac{1}{r}\frac{\partial w}{\partial r} + \frac{1}{r^2}\frac{\partial^2 w}{\partial \theta^2} + \nu_{r\theta}\frac{\partial^2 w}{\partial r^2}),$$

$$M_{r\theta} = \int_{-h/2}^{h/2}\tau_{r\theta} z dz = -2D_{r\theta}\frac{\partial}{\partial r}(\frac{1}{r}\frac{\partial w}{\partial \theta}). \qquad \text{(B9)}$$

The transverse shearing force expressions are obtained by taking the moment about point 0 (see Figure B2); Figure B2 is the top view of Figure B1(a). The summation of moment in θ-direction, in Figure B2, yields

$$(M_r + \frac{\partial M_r}{\partial r} dr)(r + dr)d\theta - M_r r d\theta - (Q_r + \frac{\partial Q_r}{\partial r})(r + dr)d\theta \frac{dr}{2}$$

$$-Q_r r d\theta \frac{dr}{2} - (M_\theta + \frac{\partial M_\theta}{\partial \theta} d\theta)dr \sin\frac{d\theta}{2} - M_\theta dr \sin\frac{d\theta}{2}$$

$$+(Q_\theta + \frac{\partial Q_\theta}{\partial \theta} d\theta)dr(r+\frac{dr}{2}) \frac{d\theta}{2} \sin\frac{d\theta}{2} - Q_\theta dr(r+\frac{dr}{2})(\frac{d\theta}{2})\sin\frac{d\theta}{2}$$

$$+ (M_{r\theta} + \frac{\partial M_{r\theta}}{\partial \theta} d\theta)dr \cos\frac{d\theta}{2} - M_{r\theta} dr \cos\frac{d\theta}{2}$$

$$= M_r dr d\theta + \frac{\partial M_r}{\partial r} dr(r+dr)d\theta - Q_r r d\theta dr - Q_r dr d\theta \frac{dr}{2} + \frac{\partial Q_r}{\partial r}(r+dr)d\theta \frac{dr}{2}$$

$$-2 M_\theta dr \sin\frac{d\theta}{2} - \frac{\partial M_\theta}{\partial \theta} d\theta dr \sin\frac{d\theta}{2} + \frac{\partial Q_\theta}{\partial \theta} d\theta dr(r + \frac{dr}{2})\frac{d\theta}{2} \sin\frac{d\theta}{2}$$

$$+ \frac{\partial M_{r\theta}}{\partial \theta} d\theta dr \cos\frac{d\theta}{2} = 0.$$

Since $d\theta << 1$, $\sin d\theta/2 \approx d\theta/2$ and $\cos d\theta/2 \approx 1$. Dividing by $r dr d\theta$ and neglecting the terms including smaller quantities, Q_r is given in terms of the moments;

$$Q_r = \frac{1}{r} M_r + \frac{\partial M_r}{\partial r} - \frac{1}{r} M_\theta + \frac{1}{r} \frac{\partial M_{r\theta}}{\partial \theta}. \qquad \text{(B10)}$$

Similarly, taking the summation of moments in the r-direction gives

$$Q_\theta = \frac{1}{r}\frac{\partial M_\theta}{\partial \theta} + \frac{2}{r} M_{r\theta} + \frac{\partial M_{r\theta}}{\partial r}. \tag{B11}$$

Then, substitution of equations (B9) into (B10) and (B11) yields

$$Q_r = -\{D_r(\frac{1}{r}\frac{\partial^2 w}{\partial r^2} + \frac{\partial^3 w}{\partial r^3}) - \frac{D_\theta}{r^2}(\frac{\partial w}{\partial r} + \frac{1}{r}\frac{\partial^2 w}{\partial \theta^2}) + \frac{H}{r}\frac{\partial^2}{\partial r\,\partial \theta}(\frac{1}{r}\frac{\partial w}{\partial \theta})\},$$

$$Q_\theta = -\{\frac{D_\theta}{r^2}\frac{\partial}{\partial \theta}(\frac{\partial w}{\partial r} + \frac{1}{r}\frac{\partial^2 w}{\partial \theta^2}) + \frac{H}{r}\frac{\partial^3 w}{\partial r^2\,\partial \theta}\}, \tag{B12}$$

where $H = D_r \nu_{\theta r} + 2D_{r\theta}$.

Finally, the governing differential equation of motion is obtained from the transverse force equilibrium equation (see Figure B1):

$$(Q_r + \frac{\partial Q_r}{\partial r} dr)(r + dr)d\theta - Q_r r d\theta$$

$$+ (Q_\theta + \frac{\partial Q_\theta}{\partial \theta} d\theta)dr - Q_\theta dr + q(r + \frac{dr}{2})d\theta dr$$

$$= Q_r dr d\theta + \frac{\partial Q_r}{\partial r} dr(r + dr)d\theta + \frac{\partial Q_\theta}{\partial \theta} d\theta dr + q(r + \frac{dr}{2})d\theta dr = 0.$$

Since $dr << r$, this equation yields, after dividing by $r d\theta dr$ and neglecting the terms including smaller quantities,

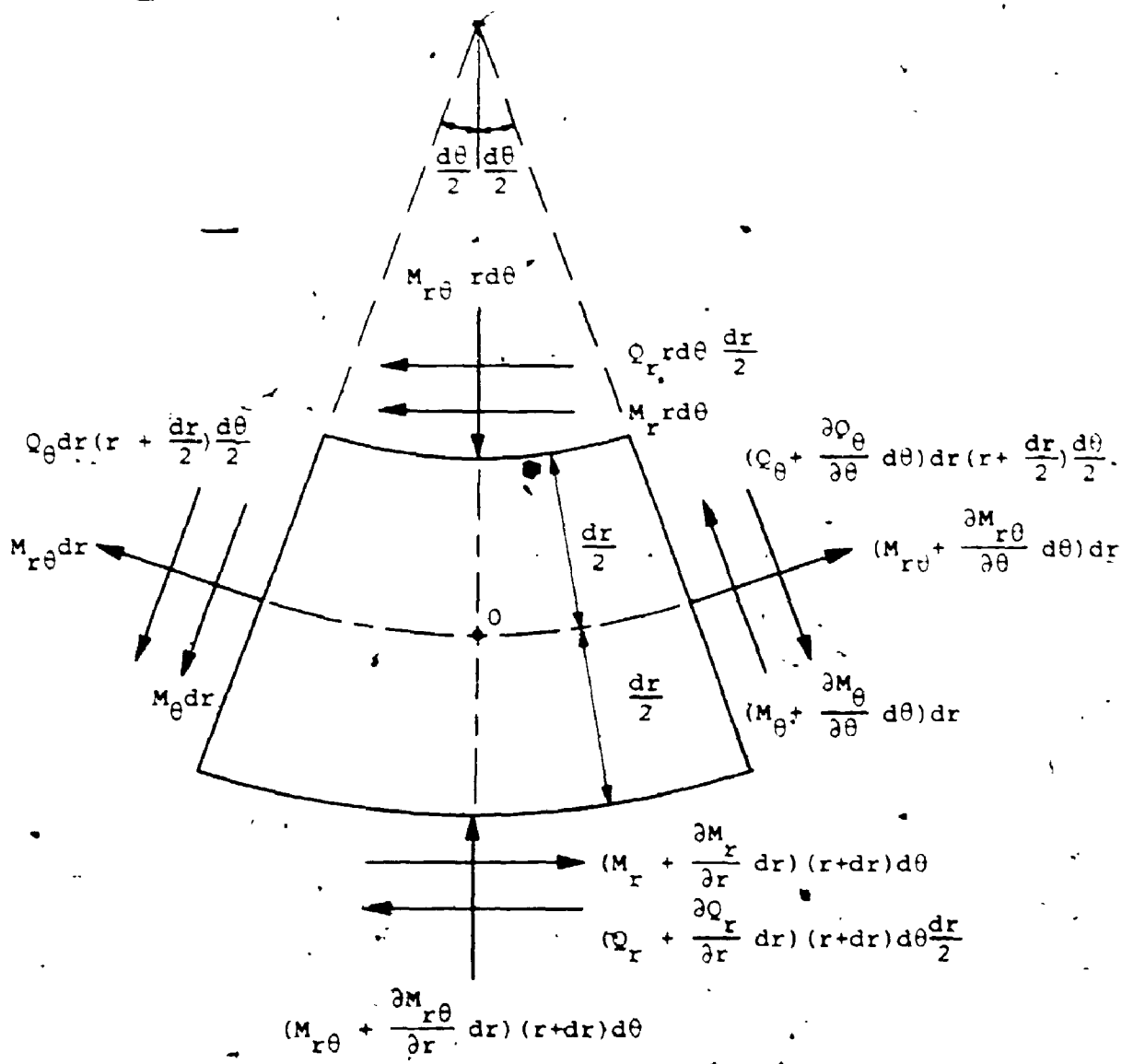

Figure B2. The top view of the plane element. The direction of the moment vectors is defined by the conventional 'right-hand rule'.

$$\frac{Q_r}{r} + \frac{\partial Q_r}{\partial r} + \frac{1}{r}\frac{\partial Q_\theta}{\partial \theta} + q = 0, \tag{B13}$$

where q is the force per unit area.

Substituting equations (B12) and $q = -\rho(\partial^2 w/\partial t^2)$ into equation (B13), the governing equation of motion can be expressed as

$$D_r\left(\frac{\partial^4 w}{\partial r^4} + \frac{2}{r}\frac{\partial^3 w}{\partial r^3}\right) + \frac{D_\theta}{r^2}\left(\frac{1}{r^2}\frac{\partial^4 w}{\partial \theta^4} + \frac{2}{r^2}\frac{\partial^2 w}{\partial \theta^2} + \frac{1}{r}\frac{\partial w}{\partial r} - \frac{\partial^2 w}{\partial r^2}\right)$$

$$+ \frac{2H}{r^2}\left(\frac{\partial^4 w}{\partial r^2 \partial \theta^2} - \frac{1}{r}\frac{\partial^3 w}{\partial r \partial \theta^2} + \frac{1}{r^2}\frac{\partial^2 w}{\partial \theta^2}\right) + \rho\frac{\partial^2 w}{\partial t^2} = 0. \tag{B14}$$

REFERENCES

B1. E.H. Mansfield 1964. The Bending and Stretching of Plates. Oxford: Pergamon Press.

B2. S.G. Lekhnitskii 1968. Anisotropic Plates. New York: Gordon and Breach.

B3. S.P. Timoshenko and J.N. Goodier 1970. Theory of Elasticity. New York: McGraw-Hill.